PB86-244639

EPA (Environmental Protection Agency) Workshop on Global Atmospheric Change and EPA Planning

North Carolina Univ. at Chapel Hill

Prepared for

Environmental Protection Agency
Research Triangle Park, NC

Jul 86

U.S. Department of Commerce
National Technical Information Service
NTIS

PB86-244639
EPA/600/9-86/016
July 1986

EPA WORKSHOP ON GLOBAL ATMOSPHERIC CHANGE AND EPA PLANNING

Final Report

Professor Harvey Jeffries, Workshop Chairman
Department of Environmental Sciences and Engineering
The University of North Carolina at Chapel Hill
Chapel Hill, NC 27514

Contract No. 68-02-3839

Project Officer

Basil Dimitriades
Atmospheric Chemistry and Physics Division
Atmospheric Sciences Research Laboratory
Research Triangle Park, NC 27711

Atmospheric Sciences Research Laboratory
Office of Research and Development
U.S. Environmental Protection Agency
Research Triangle Park, NC 27711

REPRODUCED BY
U.S. DEPARTMENT OF COMMERCE
NATIONAL TECHNICAL
INFORMATION SERVICE
SPRINGFIELD, VA. 22161

TECHNICAL REPORT DATA

(Please read Instructions on the reverse before completing)

1. REPORT NO. EPA/600/9-86/016	2.	3. RECIPIENT'S ACCESSION NO. PB86 244639/AS
4. TITLE AND SUBTITLE EPA WORKSHOP ON GLOBAL ATMOSPHERIC CHANGE AND EPA PLANNING Final Report		5. REPORT DATE July 1986
		6. PERFORMING ORGANIZATION CODE
7. AUTHOR(S) Harvey E. Jeffries		8. PERFORMING ORGANIZATION REPORT NO.
9. PERFORMING ORGANIZATION NAME AND ADDRESS University of North Carolina Chapel Hill, NC 27514		10. PROGRAM ELEMENT NO. CDWA1A/01 - 5163 (FY-85 & 86)
		11. CONTRACT/GRANT NO. 68-02-3839
12. SPONSORING AGENCY NAME AND ADDRESS Atmospheric Sciences Research Laboratory--RTP, NC Office of Research and Development U. S. Environmental Protection Agency Research Triangle Park, N. C. 27711		13. TYPE OF REPORT AND PERIOD COVERED Final (7/1/85-6/30/86)
		14. SPONSORING AGENCY CODE EPA/600/09
15. SUPPLEMENTARY NOTES		

16. ABSTRACT

Expanding industrial and agricultural growth are leading to greater and greater emissions of many compounds that are changing the earth's atmosphere and climate. The changes are warming of the climate caused by greenhouse gases, stratospheric ozone modifications caused by chlorofluorocarbons, and tropospheric chemistry modifications caused by carbon monoxide and methane. Consensus among scientific researchers as to the causes, probable magnitudes, and timing of the changes has led to a call for assessment of policy options and impacts.

This workshop was organized to begin a collaborative process among EPA research and policy personnel, and climate researchers. EPA policy makers described their needs and working methods. Eight technical papers, presenting the state of the science, were given by non-EPA climate researchers. In addition to typical discussion and dialogue, a panel of policy makers and scientists discussed the impact of the projected global climate change on EPA planning. EPA responses to climate problems were suggested.

17. KEY WORDS AND DOCUMENT ANALYSIS

a. DESCRIPTORS	b. IDENTIFIERS/OPEN ENDED TERMS	c. COSATI Field/Group

18. DISTRIBUTION STATEMENT RELEASE TO PUBLIC	19. SECURITY CLASS *(This Report)* UNCLASSIFIED	21. NO. OF PAGES 275
	20. SECURITY CLASS *(This page)* UNCLASSIFIED	22. PRICE

EPA Form 2220-1 (Rev. 4-77) PREVIOUS EDITION IS OBSOLETE

CORRECTIONS

Executive Summary, page 9 and Chapter 9, page 9-1:

EPA has delayed approval of the test demonstration originally scheduled for late August. This delay is due to EPA's consideration of several issues raised by the public related to approval of the test demonstration permit. The testing period will now begin September 22, 1986.

Chapter 5, page 5-92:

The first line under Flooding should read Section 5.2.1.5 rather than 5.2.2.5.

The first line under Tornado should read Section 5.2.1.6 rather than 5.2.2.6

Chapter 5, 5-94:

The first line under Airplane crash involving the facility should read Section 5.2.1.7 rather than 5.2.2.7.

NOTICE

This document has been reviewed in accordance with U.S. Environmental Protection Agency policy and approved for publication. Mention of trade names or commercial products does not constitute endorsement or recommendation for use.

ABSTRACT

Expanding industrial and agricultural growth are leading to greater and greater emissions of many compounds that are changing the earth's atmosphere and climate. The changes are warming of the climate caused by greenhouse gases, stratospheric ozone modifications caused by chlorofluorocarbons, and tropospheric chemistry modifications caused by carbon monoxide and methane. Consensus among scientific researchers as to the causes, probable magnitudes, and timing of the changes has led to a call for assessment of policy options and impacts.

This workshop was organized to begin a collaborative process among EPA research and policy personnel, and climate researchers. EPA policy makers described their needs and working methods. Eight technical papers, presenting the state of the science, were given by non-EPA climate researchers. In addition to typical discussion and dialogue, a panel of policy makers and scientists discussed the impact of the projected global climate change on EPA planning. EPA repsonses to climate problems were suggested.

ACKNOWLEDGEMENTS

We appreciate the time and effort given by the presenters at this workshop. Their contributions made the workshop possible.

Dennis Tirpak and John Hoffman at the Office of Policy, Planning, and Evaluation orginated the concept of this workshop. Basil Dimitriades and Joseph Buffalini at the Atmospheric Sciences Research Laboratory; Larry Zaragoza at the Office of Air Quality, Planning, and Standards; Bill Keith at the Office of Research and Development; and Dwain Winters at the Office of Program Development were instrumental in defining elements of the workshop.

The efforts of Jaynee Allen, Northrop Services, Inc., in managing the actual meeting are gratefully acknowledged. Linda Cooper, Workshop Coordinator, Northrop Services, Inc., provided assistance in planning the workshop and making arrangements with the presenters. Her editorial assistance in assembling this final report was essential and is appreciated.

CONTENTS

Abstract ---------- iii

Acknowledgements ---------- iv

Executive Summary ---------- 1
  Workshop Purpose ---------- 1
  Summary of Scientific Information ---------- 2
  EPA's Planning Needs ---------- 12
  Panel Discussion ---------- 14
  Recommendations ---------- 15

Panel Discussion 17

Papers

1. Emissions and Atmospheric Concentrations
   Ralph Cicerone

2. Evidence for a Greenhouse Effect
   John Perry

3. Past and Future Changes in Climate
   David Rind

4. Abstract of Depletion of Stratospheric Ozone
   Richard Stolarski and Donald Wuebbles

   Nimbus 7 SBUV/TOMS Measurements of the Springtime Antarctic Ozone Hole
   Richard Stolarski et al.

5. Relationships among CO, NO_X, CH_4, and $HO^\cdot$
   Anne Thompson

6. Tropospheric Ozone
   Jennifer Logan

7. Effects of Increased UV Radiation on Urban Ozone
   Gary Whitten

8. Linkages between Global Climate Change and Acid Rain
   Dennis Tirpak

Appendices

A. Workshop Agenda
B. Workshop Attendees

Executive Summary

Workshop on Global Atmospheric Change and EPA Planning

Harvey E. Jeffries
Workshop Chairman

Workshop Purpose

Expanding industrial and agricultural growth are leading to greater and greater emissions of many compounds that are changing the earth's atmosphere and climate. The changes are broadly classified as:

- warming of the climate caused by increasing concentrations of "greenhouse" gases;
- modifications of stratospheric composition and ozone chemistry caused by the introduction of compounds, especially the chlorofluorocarbon gases, that contribute to ozone depletion; and
- modifications of tropospheric chemistry mainly caused by increasing levels of carbon monoxide and methane.

The emissions include carbon dioxide from fossil fuel combustion, carbon monoxide from automobile and combustion sources, methane from agricultural sources, nitrous oxide from fertilizers, and Freons from industrial processes.

The World Meteorological Organization, United Nations Environment Programme, and the International Council of Scientific Unions sponsored a conference on assessment of global climate change. The meeting was held at Villach, Austria in October 1985 and was attended by some 80 scientists from 29 countries. The participants concluded that our understanding of the implications of rising concentrations of trace gases is "sufficiently developed that scientists and policymakers should begin immediately to work together to assess policy options and impacts."

The Global Atmospheric Change and EPA Planning workshop was designed to begin this active collaboration process among EPA research and policy personnel and non-EPA climate researchers. The workshop served as a forum for scientific leaders in the climate research field to impress upon the decision makers the extent to which they understand the problems and believe that actions are needed. EPA decision makers had the opportunity to begin an on-going dialogue with climate researchers and to develop a better understanding of the relevance of this field to EPA control policies and methodologies.

Scientific presenters at the workshop were from the National Center for Atmospheric Research, National Academy of Sciences, Goddard Space Flight Center, Goddard Institute for Space Studies, Lawrence Livermore National Laboratory, System Applications, Inc., and Center for Earth and Planetary Physics at Harvard University. In addition, collected papers and abstracts from research being done at the Geophysical Fluid Dynamics Laboratory at Princeton University, the Department of Chemical Engineering at Washington State University, the Center for Meteorology and Physical Oceanography at MIT, the Department of Chemical, Biological, and Environmental Sciences at Oregon Graduate Center, and the British Antarctic Survey from Cambridge, U.K. were supplied to all participants in the form of a Background Information Notebook. The notebook also included information from the National Climate Program and the whole text of the Villach conference statement.

Summary of Scientific Information

Climate Modification Processes

There is reliable evidence that the climate of the earth is far from constant.

The most fundamental factors influencing climate are: the solar constant (*i.e.*, the energy flux at the earth's orbit) and orbital variations (*i.e.*, changes in the earth's axis tilt) that influence the latitudinal distribution of the energy input. There is evidence that suggests that major climate swings between glacial and interglacial periods have occurred every 120,000 years, and it is believed that orbital variations may have been the triggers for these large changes in climate although changes in CO_2 concentrations are also implicated (see paper by John Perry).

The composition of a planet's atmosphere influences its global temperature. The earth's climate is maintained by a balance between incoming short wavelength radiation (*e.g.*, the sun's spectrum peaks in the yellow visible region) and outgoing long wavelength radiation (*e.g.*, infrared (IR) region). Gases that absorb radiation in the IR-region can influence the global temperature by intercepting some of the outgoing energy and re-radiating it back to the surface, thus warming the surface. This is called the "greenhouse" process and the gases are described as greenhouse gases (see papers by John Perry, Ralph Cicerone, and David Rind). Our knowledge of atmospheric compositions from Venus and Mars and their mean global temperatures are consistent with this simple model of the greenhouse effect. (see John Perry's paper and the Hanson, *et al.* paper in Background Information Notebook).

Water vapor is one of the major naturally occurring greenhouse gases. The greenhouse effect caused by the earth's pre-industrial atmosphere is responsible for raising the earth's average global temperature by about 30°C. The earth's global temperature would be about -18°C without an IR-absorbing atmosphere.

In addition to the direct greenhouse effect of IR-absorbing gases, there are major positive feedback processes that determine climate sensitivity to long-term changes. Examples of these feedback processes are:

- Air temperature controls how much water vapor is present in the air, which determines how much water vapor contributes to the greenhouse effect. Cold air holds less water, which leads to less greenhouse effect, which leads to more cooling, which lowers air temperature, leading to lower water vapor. Likewise, warmer air holds more water vapor, which leads to more greenhouse effect, which leads to more warming and still warmer air.
- Ice reflects incoming solar radiation back to space, and therefore, energy to warm the earth is lost. Warming of the earth caused by some other process, however, can lead to less ice, which reflects less solar radiation (more is absorbed by bare earth), leading to more warming and still less ice. The converse is also true.

Climate change is, therefore, discussed in terms of an initial forcing function (the factor that caused the change to occur) and the positive and negative feedback processes that increase or decrease the initial change. Thus, the direct effect of doubling the carbon dioxide (CO_2) over pre-industrial concentrations is estimated to be a temperature rise of 1.2°C because of increased IR-radiation absorption (the direct effect); currently the total multiplicative feedback processes are estimated to increase the initial effect by factors of 3 to 4, leading to a total temperature rise at equilibrium of 3.2–4.8°C (the total direct and indirect effect).

The Atmosphere Is Dynamic

The atmosphere is in continuous motion and is coupled to the oceans and the biosphere; in addition, the atmosphere's composition is a result of both long-term and short-term chemical cycles.

The troposphere is coupled (from presentation by McElroy):

- pole-to-pole with a time constant of 1–1.5 years;
- to the stratosphere with a time constant of 5 years;
- to the ocean with a time constant of 10 years;
- to the biosphere with a time constant of 10 years.

The oceans have a large heat capacity, and thus, they introduce large lags in response time for temperature changes. Oceans are the dominant sink for atmospheric CO_2.

The abundance of trace gases in the global atmosphere is the result of the interaction between sources and sinks; estimates of atmospheric lifetimes for important trace gases are given in the Cicerone paper.

For the majority of the trace gases, the two major sink processes are reaction with hydroxyl radicals ($HO^{\cdot}$) in the troposphere and photolysis by short wavelength ultraviolet (UV) radiation in the stratosphere.

Hydroxyl radicals are produced in the troposphere by a chemical cycle involving the oxidation of methane (CH_4), carbon monoxide (CO), other hydrocarbons, and aldehydes. Its primary source in the troposphere is the photolysis of ozone (O_3), as well as the reaction of hydroperoxy radicals ($HO_2^{\cdot}$) with nitric oxide (NO). A major source of $HO_2^{\cdot}$ radicals is the photolysis of aldehydes (such as formaldehyde), which are products of all organic oxidation including methane. Methane and CO are the primary consumers of $HO^{\cdot}$ in the troposphere (see paper by Anne Thompson).

Outside the earth's atmosphere, the solar spectrum is rich in high-energy short wavelength UV-radiation. As light passes through the atmosphere, most of the shortest wavelength UV-radiation is absorbed by various gases that photolyze into reactive radicals. Absorption of UV-radiation is a dominant sink process for many trace chemicals. These chemicals are relatively inert in the troposphere: they do not wash out, do not react rapidly with $HO^{\cdot}$, and do not photolyze at the longer UV wavelengths found in the troposphere. Their photolysis in the stratosphere, however, can introduce materials not normally found there, and thus, influence major chemical cycles (see paper by Richard Stolarski).

The most common stratospheric photolysis process is for molecular oxygen (O_2) to photolyze into atomic oxygen (O). The O atom most often reacts with O_2 to produce ozone (O_3). Ozone also absorbs UV-radiation and photolyzes to produce O and O_2 again. This cycle recurs many times and converts light energy into heat in the upper stratosphere. Sometimes O reacts with O_3 to produce two O_2, thereby ending a long cycle. This absorption of UV radiation limits the amount of short wavelength, high-energy light that reaches the earth's surface. Such wavelengths can cause skin cancer and promote rapid smog formation (see paper by Gary Whitten).

The dynamic processes and chemistry of the atmosphere are so complex and interactive that mathematical simulation models are the only tools available to comprehend the processes. Thompson said, "We are not dealing with independent gases whose sources and sinks can be isolated from one another, but we are dealing with a series of compounds that are linked by photochemical reactions. The causes and effects of processes, therefore, are not so clear." For example, Stolarski, in his presentation, said that stratospheric O_3 concentration determines how much UV-radiation is available; the available UV-radiation determines how rapidly other compounds are decomposed, which interact with the O_3 cycle to determine how much O_3 would be present. Furthermore, reactions and UV absorption give rise to heat, which results in winds that transport material that influences the concentrations of the reactants; in addition, temperature feeds back on the rates of chemical reaction producing the material that is absorbing the UV-radiation to cause the heating, and so on.

Because of the complexity, models must often simulate only one aspect of the problem, using simple or average descriptions for the other aspects. For example, one-dimensional models tend to have complex chemistry and no horizontal atmospheric transport. Still, these models predict the *average* concentrations in the hemisphere fairly well. More complex and costly two-dimensional models also predict concentrations as a function of latitude as well. These models have to make assumptions about how transport occurs and different assumptions lead to somewhat different predictions of the temporal and spatial distributions of the O_3.

The amount of O_3 in the atmosphere is most conveniently measured as the "total column" of O_3 in Dobson Units (DU). Ozone, however, has tropospheric sources as well as the stratospheric source, and thus, its vertical concentration profile varies significantly. The peak O_3 concentration is usually in the stratosphere at 20–30 km. Likewise, because of atmospheric dynamics, total column O_3 varies greatly, much like weather patterns, over the surface of the earth. Values are usually between 250–500 DU.

Emissions Are Increasing

Cicerone stated that although it is difficult to believe that "global conditions can be changed by these small concentrations of little known gases, in fact, there is a 10 year record of research that gives some confidence that change is under way. In many cases, research has progressed to process and mechanistic understanding as well."

Carbon dioxide concentrations have increased from 315 ppm in 1958 to more than 340 ppm in 1985, a very considerable increase. Researchers, using samples from ice cores, have determined that pre-industrial CO_2 concentrations were about 225 ppm, and in the last glacial period, the values were even lower (see Paper 4 in the Background Information Notebook.)

Part of the source of this increase in CO_2 is from the combustion of fossil fuel. Man's activities are injecting about 5 gigitons per year into the atmosphere; about 50% of this material appears to remain in the atmosphere, the rest going into the oceans and the biosphere (see paper by John Perry). In his presentation, McElroy estimated that "In terms of the global natural carbon cycle, we are lifting carbon from the sediments 20-30 times faster than nature. It is not surprising that we are seeing a steady rise in CO_2."

Chlorofluorocarbons (CFC) have been measured precisely and accurately over the last decade, and the evidence clearly shows that their atmospheric concentrations are increasing at about 3% per year. The two most abundant Freons, F12 and F11 (CCl_2F_2 and CCl_3F), have long atmospheric lifetimes (65 and 110 years) and are ultimately destroyed by UV-radiation in the upper stratosphere.

Nitrous oxide (N_2O), which had a northern hemispheric concentration of 301 ppb in 1980, has an estimated atmospheric lifetime of more than 120 years. Careful measurements over the last four years show that its concentration is increasing at about 0.5 ppb per year. McElroy, in his presentation, estimated that production now exceeds loss by 40%. Considerable uncertainty exists in the source of this increase; the two most likely sources are coal combustion and microbial production through nitrification and denitrification of inorganic nitrogen fertilizers applied to soils. Estimates of atmospheric concentrations in the year 2030 give a range of 350–450 ppb.

Methane (CH_4) is the most abundant atmospheric hydrocarbon, and in 1980 its concentration was 1.65 ppm in the northern hemisphere. Its concentration has also been shown to be increasing at rates between 0.5 and 2% per year, and the rate itself has been increasing. By using measurements from ice cores, it has been estimated that the CH_4 concentrations have approximately doubled in the last 350 years, with most of the increase occurring in the last 150 years (see Paper 6 in the Background Information Notebook). At least 80–90% of CH_4 sources could be biogenic, the major sources being enteric fermentation in ruminant animals, release from organic-rich sediments below shallow water bodies (*e.g.*, rice paddies), and biomass burning. As indicated above, reaction with $HO^{\cdot}$ is the dominant sink for CH_4.

Near the surface, in rural areas of Europe and the central and eastern U.S., the summertime concentration of O_3 may have increased by 6–12 ppb since the 1940s. There is reliable evidence for an increase in ozone in the middle troposphere over Europe during the past 15 years, and weaker evidence for a similar increase over North America and Japan. It is argued that these increases are due to photochemical production associated with anthropogenic emissions of nitrogen oxides (NO_x), hydrocarbons, and CO from combustion of fossil fuels (see paper by Jennifer Logan).

Implications For Climate and Atmosphere

Increasing the concentrations of IR-absorbing gases can cause an increase in the earth's average global temperature. Three independently developed global climate models predict a total climate sensitivity of about 4°C for a doubling of CO_2 concentrations over pre-industrial times or for a combination of some increase in CO_2 and increases in other greenhouse gases such as methane, ozone, chlorofluorocarbons, and nitrous oxide (see paper by David Rind).

Although CO_2 is the greenhouse gas that is increasing the most, other trace gases (Freons, N_2O, CH_4, and O_3) also have a major greenhouse effect. If present trends continue, their combined concentrations will lead to an equivalent effect of doubling the CO_2 concentration by the 2030s instead of the actual doubling of the CO_2 concentration that was predicted to occur sometime around 2070 (see Paper 1 in Background Information Notebook).

Analysis of observations over the last 100 years suggests that the average global temperature has increased 0.3–0.5°C. Model simulations of the changes in emissions and concentrations over this same period also predict similar increases. Because of uncertainties in the model inputs and formulations, however, it is not possible to ascribe, in a scientifically rigorous manner, the increase in global temperature to the increases in the greenhouse gases (see paper by David Rind, and Paper 1 in Background Information Notebook).

To put a 4°C change in average global temperature in perspective, during the last Ice Age, 18,000 years ago, the average global temperature was 3.7°C cooler than now; ice extended over Long Island; some northern areas had temperatures 25°C cooler than present day temperatures, primarily because there were large ice sheets 3 km thick. At the same time, however, there was very little temperature change in the low latitudes. Simulating these Ice Age conditions has been used as a validation test for many of the global climate models.

Such studies show that small initial changes can be greatly amplified by positive feedback processes. Because of large lag times in the feedback processes, however, the system requires sustained initial perturbations so the feedback processes can build. For example, the oceans have a very large heat capacity and the deep water turnover time may be hundreds of years, so it would require a long period to heat up or cool down the oceans. The surface layers of the ocean may reach equilibrium more rapidly.

Although agreeing on the ultimate climate sensitivity, the climate model predictions by different groups differ in the spatial details of the temperature changes, some giving 25°C warmings occurring throughout the southwestern U.S. and extreme northeast and others predicting less dramatic changes. In all cases, the lower latitudes have a smaller change than the higher latitudes.

In a time-dependent model for the period 1956 to 2010, Rind and his co-workers found that temperature changes on the order of 0.3–0.5°C occur with no specific forcing whatever, just due to the natural variability and dynamics of the model. Therefore, if we wanted to be sure that we were seeing a clear indication of the warming trend, a rise of 1°C would have to be observed. Rind's model, using current emissions trends, suggests that this will occur in the 1990s.

The photolysis of chlorofluorocarbons in the stratosphere results in the release of chloride that acts as a catalyst in shortening the O_3 formation chain reaction and ultimately lowering the stratospheric O_3. Stratospheric O_3 absorbs short wavelength UV-radiation and thus filters such radiation from the earth's surface. Lower O_3 results in more UV-radiation in the troposphere and at the surface, as well as cooler stratospheric and warmer tropospheric temperatures. At the same time, the increase in tropospheric gases such as CH_4 and NO_x results in increases in O_3 in the troposphere.

In their presentations, Stolarski and Wuebbles described model calculations of global O_3 production that have been made from pre-industrial times to 2050.

These models predict that the total column O_3 increased during the 1970s. This, however, was the result of the cancellation of substantial, but opposing changes in O_3 with altitude. A maximum decrease of 4.4% was predicted at 40 km, largely due to CFC emissions (it was noted that increasing CO_2 emissions reduced the CFC impact!), while an increase of 1% was predicted at 30 km and an increase of 6.7% was predicted at 8–9 km due to aircraft and increased CH_4 emissions.

As indicated above, based on monitoring data, there is reliable evidence that O_3 did increase in the middle troposphere in Europe over the past 15 years and supporting evidence for a similar increase in North America and Japan. This increase is estimated to contribute significantly to the total column O_3, and may have compensated for a 20–30% decrease in O_3 in the stratosphere over middle and high latitudes of the northern hemisphere (see paper by Jennifer Logan).

In future scenarios, most models predict either a small decrease or increase in total column O_3 mainly due to increasing CH_4 in the troposphere. The vertical distributions of O_3, however, are dramatically modified. For example, one model predicts up to a 36% O_3 increase below 26 km and a 22% O_3 decrease above 26 km.

The British have been measuring total column O_3 at Halley, Antarctica (76°S) since the International Geophysical Year in 1956. In 1957, the values were 310–320 DU in the springtime. Now values are 40% lower in October (antarctic spring). In the winter at Halley, there is no sunlight; in the spring, the sun returns. It is speculated that during the dark, very cold winter, CFCs accumulate, and when the sun does reach the upper stratosphere for the first time in the spring, the CFCs undergo rapid reaction and destroy the O_3. As the CFCs are consumed, O_3 levels gradually increase to higher values, but by autumn the level is still 5–10% lower than it was 10 years ago. (see Paper 9 in Background Information Notebook)

NASA has made a color movie from the Nimbus-7 satellite's TOMS instrument that can measure total O_3. The movie, which was shown at the EPA workshop, shows the pole view of O_3 concentrations on each day in October for the years 1980 to 1985. The images are dramatic: in the beginning of each year the O_3 is reasonably uniform, and then the depletion process starts. It appears as if a large hole—thousands of kilometers wide—is being eaten in the atmosphere. The O_3 begins to recover near the end of the month. Each year, however, the area of O_3 depletion increases as does the depth of the central depletion. In 1984, the pole O_3 values were down to about 190 DU, and in 1985, they were down to about 180 DU (see paper by Richard Stolarski).

Increased emissions of CO and CH_4 can, through complex photochemical interactions, result in a decrease in the average tropospheric $HO^\cdot$ concentration. Estimates suggest that $HO^\cdot$ concentrations were as much as 30% higher in 1860 than now. Projections of emissions patterns suggest that in 2035, $HO^\cdot$ concentrations will have decreased another 20–30%. Not only will many trace gases (including some toxics) survive longer in such conditions, so will CH_4, which contributes to the greenhouse effect. In addition, O_3 production increases as a result of the increased organic oxidation, and O_3 is a greenhouse gas that also can contribute to the global warming (see paper by Anne Thompson). Longer survival in the troposphere also means a greater concentration in the stratosphere through tropospheric–stratospheric coupling and transport. McElroy, in his presentation, indicated that CH_4 oxidation is now a major source of water vapor in the stratosphere; low temperatures and atmospheric stability prevent water vapor from being directly transported into the stratosphere.

Preliminary modeling studies of urban smog formation have shown the effects of increased UV-radiation caused by stratospheric O_3 depletion combined with an increase in global temperature. These suggest a significantly enhanced potential for smog formation. In the simulations, the warming always increased the production of O_3 and decreased the production of peroxyacyl nitrate (PAN). The direct effect of raising temperatures by 4°C was to increase O_3 by 10–20 ppb for typical urban scenarios. More complex was the effect of increasing UV-radiation, in that different results occurred in differ city simulations, with the maximum change being a 26% increase in O_3 for a 16% decrease in stratospheric O_3. The combined effects appear to be additive in some scenarios, resulting in a 40% increase in O_3 in the Nashville case, increasing the O_3 from its current 130 ppb to 184 ppb in the future, keeping the emissions the same as current values.

Climate changes may have a variety of impacts on the acid rain problem (see paper by Dennis Tirpak):

- Increased air temperatures will lead to a larger demand for electricity for air conditioning in summertime, which most likely will lead to increased sulfur dioxide (SO_2) atmospheric loadings; in addition, the higher air temperatures will lead to a more rapid oxidation of the SO_2 and NO_X, particularly in northern latitudes, which will decrease the importance of long-range transport of sulfate and nitrate ions.
- Altered precipitation patterns can potentially change both the importance of some long-range sources and the impacts on aquatic systems and forests (over the past 50 years, increased precipitation has been associated with increased temperatures in the Adirondack Mountain area of New York); the forests may

undergo significant ecological changes due to altered microclimates; a changed winter snow pack can lead to altered vulnerability of aquatic life during spring snow melt; altered frequency of wet days can lead to changed degradation rates for materials.

- Changed cloud cover at different altitudes may lead to changes in aqueous-phase oxidation rates for SO_2 and NO_x, thereby altering the significance of long-range transport; in addition, increased cloud cover may increase natural NO_x formation from increased lightning.

EPA's Planning Needs

At the workshop, many EPA policy makers discussed the problems of balancing today's apparently pressing needs against problems that are long-range, global in scale, and multi-component in nature.

Hoffman, from the Office of Policy Analysis, described the basic EPA approach as "setting air quality goals and then making plans to achieve these goals." He stressed that present EPA planning relies heavily on historical trends. The time dimension for major climate change is shortening, however, and thus the predicted global changes have a large potential to impact current decisions.

Emisson, Director of the Office of Air Quality Planning and Standards (OAQPS), stressed that his organization must make numerous trade-off decisions. This results in a need to have a clear understanding of the problems, especially the uncertainties associated with the problem, not only to make better decisions, but also to convince the public when there is a need to change. In addition, the public health implications of the problem must be recognized and methods for risk management and risk assessment must be developed and applied before regulations can be put forth that might affect the problem.

Weigold, head of Strategic Planning Programs in OAQPS, stressed that OAQPS has been in the mode of dealing with "known conventional problems" and functions, for the most part, in a reactionary mode. Furthermore, EPA tends to be constrained by the realities of the enabling legislation. Efforts are under way, however, to broaden OAQPS's viewpoint, to improve information flow in the organization, to be less single pollutant oriented, and to deal with more complex cross-media problems. One such action in OAQPS has been the organization of the Strategic Planning Program to identify emerging issues and problems and to formulate responses.

Hoffman ended his presentation by posing a series of questions for consideration by presenters and attendees. These were:

- How might EPA programs be affected?
- When might current programs be affected?
- How significant might changes be?
- How could EPA programs be used to limit change, if needed?
- Are current science efforts going to provide EPA with answers in time?
- Is EPA building its own intellectual infrastructure rapidly enough?

Weigold presented another set of questions that reflected OAQPS's needs; these were:

- What is happening or may be happening?
- When will serious problems become manifest?
- What kind of research may be needed?
- What will EPA get for that research?
- Will this research be worth the required trade-offs?
- What kinds of changes in present operations are needed?
- What solutions are there to these problems, if any?
- What are the institutional and legislative barriers to solutions?
- How should the problem best be presented to the public and to lawmakers?

Panel Discussion

A discussion panel that included policy planners and researchers held a lively discussion.

The basic position of many OAQPS staff members was that the linkages between the global climate and atmospheric change issues and the regulatory program had not been built. EPA was described as basically a regulatory agency, and research is done in support of regulation. The limited research resources of EPA are already overextended in dealing with immediate issues and it was hard for many to determine what needed to be done.

The Office of Policy, Planning, and Evaluation staff members suggested that the global climate change issue did add a long-range perspective to many daily issues at EPA, for example, the O_3 attainment issue. Global climate change would likely make it much more difficult to move near-attainment areas into attainment and to keep those who are in attainment still in attainment in the future. Some discussion suggested that regulations could be designed to prevent further deterioration of stratospheric O_3 and these could be beneficial in helping marginal locations meet O_3 attainment.

Improving awareness of staff making regulatory decisions every day in the Agency was another major point made. Taking into account the impact of global atmospheric changes on these current regulatory activities might lead to more optimal decisions. In addition, EPA should expend more effort to inform outside climate researchers of Agency informational needs in the climate change area.

It was suggested that the global climate change issue would have a gradual and incremental effect on the Agency and would eventually be incorporated into the Agency, that is, the issue would be "institutionalized" and the Agency would therefore deal with global climate change as part of its normal activities.

Some of the scientists suggested that many of the major effects of global atmospheric change would occur while this "institutionalization" of the problem was occurring. This is because so much of the problem was linked to our use of fossil fuel, and changes of the magnitude needed to delay the changes would require more than 30 years to implement. During this time, major changes in climate would occur.

Recommendations

Four general types of responses to these problems were described by Hoffman:

- Understanding—We can continue to develop the basic science and measurement programs needed to determine the magnitude and timing of environmental effects. We can modify current policy development (one suggestion raised in discussion was to include global climate effects in environmental impact statement development).
- Preventing—Many scientists believe that climate change can not be prevented: too much material is already in the air and only lags in the system (such as ocean turnover) are delaying the changes; the changes will happen eventually. Furthermore, the problems are global in scale and other industrially developed countries make major contributions to the problems.
- Limiting—There are questions about the quasi-irreversibility of the systems that suggest that options to limit the changes are difficult. The long lifetimes of some of the species mean that if emissions stopped now, it would require 30–50 years for conditions to be restored to those of pre-industrial times. On the other hand, a "wait and see" approach implies very significant changes will occur when the system lags catch up with the emissions input. Actions can be taken to limit the emissions of some of the critical species, for example, non-critical uses of Freons.
- Adjusting—We can adjust to the existence of the situation by accounting for its existence in our activities. This means that decision makers at all levels should begin to consider the impact of the probable changes in their policies and strategies. There have been very few policy impact analyses comparable with the level of scientific modeling work done in the last few years.

McElroy said, "One of the challenges that EPA should address is the problem of devising an observational strategy and supporting validating studies that would give the policy and scientific community a good model for the continental U.S."

Tirpak, from OPPE, stressed that in the short term, EPA can build understanding and institutional capability. Furthermore, EPA should undertake additional analyses to assure that agency actions do not inadvertently speed up the rate of change by EPA actions. In the long term, Tirpak suggested that EPA should use climate scenarios in long-range transport models; conduct synergistic experiments for the world of 2020 (*e.g.*, CO_2, increased UV-radiation, and acid rain) on forests, crops, lakes, and materials; and we should begin the process of developing a risk methodology for the global environment.

Panel Discussion

Transcribed and Edited by
Harvey Jeffries
Workshop Chairman

A panel consisting of EPA policy, headquarters, and research staff and of invited scientists was assembled under the leadership of Dr. Michael McElroy, Harvard University, to discuss the topics and issues that had been raised. Dr. McElroy asked each panel member to make initial comments.

B. Steigerwald, OAQPS/EPA

"I have been disappointed. I have a concern about not only how this issue affects EPA but also how it specifically affects the Air Program and there has not been as much said about EPA Planning as I had hoped. I am able to concede a lot of what the scientific consensus is, but I do not have a good sense of what it means to EPA. That is, putting this information in the context of EPA and what EPA does.

"EPA is a regulatory agency and we put up with research because it helps us support policy decisions, keeps us from doing dumb things, and helps define regulatory issues. If we expect more than that from EPA we are going to be disappointed. We fight the budget fights on a year-to-year basis looking at the current issues. After the FY86 budget was fixed, for example, the air research group had to change the current budget and operational plans for such things as: a million dollars for the radon problem; $900,000 to non-ionizing radiation; a million dollars for low lead gasoline effects on agricultural vehicles; accident prevention; and indoor air quality and toxics required an additional $800,000. So it appears that we are constantly dropping a million here, a million there, until 10% of the research program is reprogrammed after the start of the fiscal year.

"Although I can see how this issue might fit with the ozone problem in Nashville 40 years from now, I do not see what it means to us now. We did not ask ourselves tough enough questions."

M. McElroy

"While I am sympathetic to the day-to-day pressures that a manager like you has, I think that perhaps the promise to solve the management problems of EPA as well as addressing the science problems, would not be possible in a day and a half. I am distressed by your statement—and I hope that you really did not mean it—that EPA is a regulatory agency and that you are obliged to put up with research. EPA, under those circumstances, will always make decisions in ignorance."

B. Steigerwald

"We do have research programs, for example, five-year, sizable programs to attempt to understand what is involved in say the context of a ten-year regulatory program, in which the first five years are an attempt to understand it and the last five years are when the regulations are passed and we attempt to meet the requirements. This is a focused, narrow program, however, and we have very little money to attempt to define problems. We often are pushed to move into regulatory programs early and need immediate research support for these. There is little left over to attempt to define problems and attempt to study things."

D. Rind, Goddard Institute for Space Studies

"There is a lot of research going on that can be of benefit to EPA. These researchers do not always know EPA needs. Without pre-consultation, it is very hard to know what small incremental work could be done. You need to develop such communications: 'What programs might be affected by global atmospheric change and what are the informational needs in these programs that might be supplied by outside-funded researchers?' And we need communication established as a on going situation."

R. Cicerone, NCAR

"I see tremendous opportunities here for exchange of information and to identify needs. A good example of how EPA can have an impact on the total research community is the EPA funding of Rand to do emissions scenarios. This was not being done by other research agencies. There are another 15-20 such focused opportunities where EPA can do things to contribute to total effort.

"We must also, however, be building towards programs at EPA about the systems that are just coming into view. We should remember that we have only thought about the earth as a system in very recent years. This idea is not very old and we should not be ashamed of this. It has only been since WWII that we have had much disposable income, education, and time to make these types of questions meaningful. But they are coming into view and we will be helping each in many ways, and EPA will be taking a major responsibility in this area."

R. Morgenstern, OPPE/EPA

"I would like to echo a sentiment somewhere between Steigerwald and the scientists. EPA has a responsibility to study this issue very seriously. The challenge is to make a link between the global importance and the everyday budget constraints and problems.

"In the policy area, for example, the global atmospheric change adds a long-range perspective. The ozone strategy will be impacted by global atmospheric change in the long range. A second way that global atmospheric change information can enter the policy debate is in selected issues where a decision is to be made and where knowledge of the future of the sort discussed here is very important.

"In the air area, for example, where banning of a particular hazardous material may be under consideration, the question of substitutes is raised. What kinds of substitutes are available and will they have deleterious effects on the atmosphere?

"In terms of the research issue, it is easy to get bogged down in your budget, my budget type questions, but this is an important area and it does need support, and if nothing else the international community is likely to pick this up and it will be an area of international debate in the next decade. EPA must play a leadership role in that debate."

J. Hoffman, OPPE/EPA

"This meeting is to initiate the process and the process will be years in the making.

"There are immediate applications, however. For example, for air issues, Whitten's work suggests that we may need modification of the treatment of photolytic radiation in models, and that current treatment may not reflect the existing situation.

"EPA recently re-budgeted a lot of money to go after small hydrocarbon sources, who are difficult and expensive to control, and in which we do not get a lot out of. If Whitten's results are correct, this effort might not be doing the job. Are we making an error in going after these small sources?

"Another example, is in the EPA mobile sources group. They put out standards for CO emissions. We have found that the rest of the world tends to follow U.S. technology. Because of our reduction, the world has followed, leading to a more rapid decrease in CO globally than had been estimated. What other types of activities is EPA involved in like this?

"We need to consider the wisdom of our investments. For example, we are making a big investment in trying to bring all the areas that are not in attainment into attainment and to hold the ones in attainment where they are. Bromine is leaking into the stratosphere, which will cause a more rapid depletion of O_3. According to Whitten's work, small changes in global temperature and in stratospheric O_3 can be as important in helping Nashville meet and sustain attainment as hydrocarbon controls. In fact, it may be that the most important strategy for keeping Nashville in attainment is to control bromine emissions. This might be done at a cost of 1/10,000 the cost of hydrocarbon controls in Nashville. But at present there are no regulations on bromine. A lot of it comes from practice in fire fighting and thus a simple modification of practice rules might significantly decrease bromine emissions.

"Other examples of the possible effects of EPA decisions are: biotechnology areas–can we find different bugs that decrease methane production in cows?; toxics decisions–are there tradeoffs between PERC and CFC 113? We may have a major impact on global atmospheric change for getting rid of a small toxic risk like PERC. We are in the process of regulating a whole bunch of solvents and nobody is analyzing how all these solvents are interrelated and what various tradeoffs in solvent regulations may do to the stratosphere.

"We should be concerned about short-term vs. long-term planning and the U.S. economy. For example, we spend a lot of time bringing all the locations that are marginally outside of attainment into attainment. If, at the same time, we ignore the areas that are in attainment, but that may slip out of attainment because of long-term global changes, then we are going to find that we are very unproductive as an agency and in marshaling the nation's resources.

"We have to justify the Agency's regulation expenditures to the nation. We can not regulate anymore without good cause. Some scientists are telling us that it is oxidants and not just acid rain that are killing the trees, or that a 1°C warming and 3% ozone depletion means that ozone attainment is going to be difficult."

B. Dimitriades, ASRL/EPA

"EPA research is, rightly or wrongly, dictated by priorities and we *[the research group]* do not set them, the regulatory part of EPA sets them. The priorities are based on impressions that they build about the relative importance of various issues. I personally have a concern as to whether there was enough of an impression made on EPA policy makers. Is this a new program to replace something else, or is it a new program in itself?"

M. McElroy

"The EPA decision maker must take the long view. EPA can not maintain a responsible view of the environment while ignoring that oxidants are going to change, weather systems may change, and regulatory standards that are set on the basis of historical data may be inadequate and outdated. The target is a moving target."

B. Steigerwald

"I may have possibly overstated it—as everyone has said—but a key point is that the linkages to the regulatory program must be built better than they have been. It is not enough to say that 'Aren't you being irresponsible not considering...' Somehow the linkages have to built in a 'harder' way than they have been. You are going to have to compete with existing problems. You have to say: 'Here is an action. Here is what happens if it does or does not happen. Here is why it is more important than something else'. "

D. Tirpak, OPPE/EPA

"I agree. We have only turned over a few stones in the course of this meeting, and we have only looked at a few issues; we do not have money, or people, or time to examine the issue in an adequate manner. We are in a chicken and egg sort of situation. You are right, all those linkages have not been built. What we are trying to do with this conference is to get enough recognition that there are a lot of things to be looked at. How do we begin that process today? This is a historic meeting. We have not had this type of dialogue about what kind of future we want to look towards. People should not either feel invested or bad about where they find themselves and where EPA stands. It happens to be where we are and the question is 'How do we allow this issue to unfold as time goes on?'."

Audience Comment

Public understanding about this issue is very poor. How do we make these issues a lot better known?

J. Hoffman

"What I would expect to see happen at EPA is that before we make decisions, people examine the effect of the decision on the global issue. For example, people working on methylene chloride regulations could ask 'What is going to happen when we regulate? What will be the effects of the substitutes?' It is easy to ask this, because in figuring out the costs of the action, they have to figure out what the costs of the substitutes are. What is lacking is not that they do not have information, but that they do not consider the effect that a proposed regulation may have on the stratosphere. So the first thing we have to do in the Agency is to identify the decisions that might be changed, not by spending more money, but by accounting for global atmospheric issues in making these decisions. A priority of the Agency then, should be to identify five or six regulatory programs that might be affected by global atmospheric changes and to begin examining the decisions in light of existing information."

R. Morgenstern

"We must focus on specific problems. What specific problems are underway at EPA or are on the horizon at EPA that will be affected by global atmospheric change? That is the way change occurs in the kind of political and bureaucratic situation in which EPA operates."

M. McElroy

"Most of the issues we are discussing here are related to the use of fossil fuel. And accepting the climate impacts we have heard discussed here might underestimate as well as overestimate what is actually going to happen, it could be worse. What is the response of the 'future thinker,' the gentleman at the top with the long-range view? If we judge that the climate change that may occur is undesirable to disastrous, how are we going to deal with it? Are we going to make an instantaneous decision to switch from fossil fuel to nuclear? How do you build into that fact that there is a minimum time to make the switch—not less than 30 years—with an impact that is going to occur on a shorter time scale. There are some very serious potential problems that lie ahead. At the very least then let us understand as well as we can what might happen because maybe there is someone with enough wisdom to respond to the issue."

D. Winters, OPD/EPA

"I think the way we respond as an institution is not through a process of revolution, that is, it is not through a process of making a major institutional change: 'Gee, we have a major societal problem, we have to drop what we are doing and do something else.' Instead, it comes through a series of incremental changes that build momentum in terms of ways in which the institution begins to focus its direction. That process is already under way at EPA and other agencies. The very fact that we are having this meeting is evidence that the process is under way. We now have the question of stratospheric change and chlorofluorocarbons fully institutionalized and recognized as an issue in EPA. It exists not because there are particular groups of managers within the Agency that want to support the work, but because the institution has now blessed it as a piece of work that can go forward in a planned time line. These things are the indications of that incremental change that lead to a new focus.

"The discussion we have had here today relative to the full interrelated nature of the atmosphere, as opposed to simply looking at acid rain or looking at it on a regional scale, are things that most of the people who are working on these problems are already aware of. Some of us are aware of this on a daily basis. But the ways in which we begin to accommodate the complexity of the global atmosphere will be incremental and gradual changes. I came to this meeting with most of the basic convictions I have now, I come away a little supercharged. I go away with a little better sense of targets of opportunity, a little greater drive—yes, I think I am going to push a little harder here, I think I am going to shake things a little harder there. This, I think, is the way the institution will respond and we will end up with a greater and greater percentage of the movers and shakers in the Agency and outside the Agency adopting these views. That is the best chance we have for success. If we try to go for the fundamental revolutionary change, that, at best, happens if one individual adopts that and it lasts as long as that individual is around. What we are moving for is an institutional change. That will be difficult, because we operate an institution that is ultimately making intuitive decisions. Sometimes, we make intuitive decisions on counterintuitive problems. The accountability of all the decision makers, in terms of their success or failure at making decisions, is in the short term. That is a fundamental problem our society has: 'How do people who are accountable in the short term, making intuitive decisions, deal with a counterintuitive problem?' The main way we attempt to deal with this issue is to institutionalize the problem so that it is spread over more individuals and several different time lines.

"For the global atmospheric change problem, we are moving in that direction. Are we moving there fast enough? The answer is probably no. Can we move faster? The answer is probably yes. Can we move a lot faster. My own view is probably not. The main value that comes from the exercise we have today and from the times that we redo that exercise is that it helps refocus us on where it is we are trying to get to, because we get lost in the day-to-day battles.

"So it is the gradual progress and when it is going in the right direction, to recognize it and when it is going in the wrong direction, identify what direction it should be going and help it move on through."

M. McElroy

"That is very useful. We need to distinguish, however, between the easy problems and the really tough ones. When you pick the stratospheric problem, for example, I think you pick a very easy one. That it was easy explains why the public, political, and the regulatory response to the ozone issue was so positive from the very beginning. It was basically because here was one of these complicated global problems in which the answer was relatively simple: you regulate a few chemicals, and impose alternatives, the public would not have to spend very much money, a few industrialists would have to make adjustments. But it was really basically a simple thing to do.

"I think it is important to tackle the tropospheric oxidant issue, because that is a lot more complicated. And then, if you really want to go for the big one, take on the climate issue because that is really a powerful challenge. Given what you said, and I believe that what you described is the way in which we will proceed—in a stepwise fashion, then maybe the people on the cutting edge in the scientific area should be thinking about, in a worst case, how would we intervene to change the climate, because we may actually have to. Maybe it is time we should give a little thought about how you might do that, because the time scales involved here—the time scales of global atmospheric change—are really becoming quite short compared to natural rates of change *[and while we wait to see what to do, the change may already have taken place]*."

M. McElroy

"Thank you for attending. The meeting is adjourned."

Paper 1

Emissions and Atmospheric Concentrations

by

Ralph Cicerone
National Center for Atmospheric Research

This presentation was based upon the following published paper, which has been reproduced with permission of the American Geophysical Union. The authors' consent has been obtained.

Trace Gas Trends and Their Potential Role in Climate Change

by

V. Ramanathan
R.J. Cicerone
H.B. Singh
J.T. Kiehl

V. Ramanathan, R.J. Cicerone, H.B. Singh, and J.T. Kiehl, *Journal of Geophysical Research*, Vol. 90, No. D3, Pages 5547-5566, June 20, 1985, copyright by the American Geophysical Union.

NTIS is authorized to reproduce and sell this report. Permission for further reproduction must be obtained from the copyright owner.

JOURNAL OF GEOPHYSICAL RESEARCH, VOL. 90, NO. D3, PAGES 5547–5566, JUNE 20, 1985

Trace Gas Trends and Their Potential Role in Climate Change

V. RAMANATHAN, R. J. CICERONE, H. B. SINGH,[1] AND J. T. KIEHL

National Center for Atmospheric Research, Boulder, Colorado

This study examines the potential climatic effects of the radiatively active trace gases that have been detected in the atmosphere including chlorofluorocarbons, chlorocarbons, hydrocarbons, fluorinated and brominated species, and other compounds of nitrogen and sulfur, in addition to CO_2 and O_3. A one-dimensional radiative-convective model is used to estimate trace gas effects on atmospheric and surface temperatures for three cases: (1) modern day (1980) observed concentrations are adopted and their present trends are extrapolated 50 years into the future. These projections are based on analyses of observed trends and atmospheric residence times; (2) the preindustrial to present increase in CO_2 and other trace gases are inferred from available observations; (3) a hypothetical increase of 0–1 ppbv is considered to provide insights into the radiative processes. Trace gases other than CO_2 are shown to be potentially as important as CO_2 for long-term climate trends. The relative importance of the 30 or so trace gases included in this study depends on the problem under consideration. The inferred CO_2 increase from preindustrial to the present causes an equilibrium warming of the model surface by 0.5 K, which is amplified by 50% by CH_4, $CFCl_3$ (F11), CF_2Cl_2 (F12), and tropospheric ozone. For the projected increase from year 1980 to 2030, the other trace gases amplify the estimated CO_2 warming of 0.7 K by about 110%: $CFCl_3$, CF_2Cl_2, ozone, and CH_4 each contribute in the 0.1–0.2 K range followed by N_2O, $CHClF_2$ (F22), CH_3CCl_3, and CCl_4 in the 0.03–0.1 K range. Finally, on a per ppb basis, about 12 trace gases are identified to be important: $CBrF_3$, C_2F_6 (F116), CHF_3, and CF_3Cl (F13) have greenhouse effects comparable to those of $CFCl_3$ (F11) and CF_2Cl_2 (F12). The narrow-band overlap treatment and the accurate spectral and angular integration techniques employed in the present radiation model enable quantitative interpretation of the differences between various published estimates for the greenhouse effects of $CFCl_3$ and CF_2Cl_2. For the projected trace gas increase, we compute the stratospheric O_3 change by employing a photochemical model coupled to the radiative-convective model. The O_3 change cools the stratosphere and the magnitude of the cooling is as large as that due to the projected CO_2 increase. Because of the O_3-induced stratospheric cooling and the surface warming due to the greenhouse effect, the trace gas effects on climate are virtually indistinguishable from those of CO_2.

1. INTRODUCTION

The release of chemicals into the atmosphere has grown greatly over the last 50 years. Increased reliance on synthetic chemicals, deforestation, biomass burning, and fossil fuel combustion have all contributed to the observed perturbations of trace chemicals in the atmosphere. One of the important potential consequences of this chemical change is an alteration of the earth's climate because trace chemicals modify the radiation energy balance of the earth-atmosphere system. To date, the climatic effects of future levels of CO_2 have received the most attention [e.g., see *National Research Council*, 1982, 1983; *World Meteorological Organization*, 1983]. However, from the studies summarized by the *World Meteorological Organization* [1982*a*] as well as subsequent publications [*Chamberlain et al.*, 1982; *Alexandrov et al.*, 1981; *Ramanathan*, 1982; *Hansen et al.*, 1982; *Wuebbles*, 1983*a*], it can be inferred that the combined effects of the other trace gases is to warm the surface-troposphere system and the magnitude of this warming in the future can potentially be as large as the warming due to projected increases in CO_2.

The study of climatic effects of other trace gases poses certain special problems. The difficulty encountered in examining the effects of trace gases other than CO [illegible]ses because they perturb the radiation energy balance [illegible] the earth/troposphere/stratosphere system in a number of ways: (1) some of the trace gases (e.g., $CFCl_3$, CF_2Cl_2, and CH_4) have strong infrared bands in the 5- to 20-μm wavelength region, which enhance the atmospheric opacity and contribute to the greenhouse effect [e.g., *Ramanathan*, 1975; *Wang et al.*, 1976]; (2) addition of chemicals, such as CO and NO, even if by themselves they are not radiatively important, can alter the chemistry of the background troposphere, which in turn can perturb the radiatively important gases, such as O_3 and CH_4 [*Hameed et al.*, 1980]; (3) the IR cooling due to the increase in several of the gases perturbs the stratospheric temperature, so that the middle stratospheric chemistry is altered appreciably through temperature-dependent reaction rates [*Boughner and Ramanathan*, 1975]. The net effect of these chemical-radiative interactions is a substantial perturbation of the stratospheric ozone concentrations, which in turn modulates the solar and IR fluxes to the troposphere. A summary of our current understanding of the above issues can be found by the *World Meteorological Organization* [1982*a*], which also gives a lengthy compilation of published studies on the problem; hence these earlier studies will not be reviewed here.

The potential importance of the other trace gases provides the primary motivation for the present study, which attempts to examine the climatic effects of most (if not all) of the anthropogenic trace gases. The major objectives of the present study are given below in the order in which they are discussed.

1. Characterize the trace gases, their observed abundances, known sources, and sinks in the present-day atmosphere.
2. Based on current understanding of the observed trends, estimate the future concentrations of trace gases, including stratospheric ozone. This step, while it has numerous pitfalls,

---

[1] Also at SRI International, Menlo Park, California.

Copyright 1985 by the American Geophysical Union.

Paper number 5D0059.
0148-0227/85/005D-0059$05.00

TABLE 1*a*. Estimates of the Abundance of Trace Chemicals in the Global Atmosphere of 1980 and 2030

Chemical Group	Chemical Formula	Dominant Source*	Dominant Sink*	Estimated Average Residence Time (τ_i), years	Year 1980 Global Average Mixing Ratio, ppb†	Year 2030 Probable Global Average Concentration, ppb		Remarks (also see text for details)
						Best Estimate	Possible Range	
Carbon dioxide	CO_2	N,A	O	2	339×10^3	450×10^3		Based on a 2.4% increase over the next 50 years
Nitrogen compounds	N_2O	N,A	S(UV)	120	300	375	350-450	Combustion and fertilizer sources
	NH_3	N,A	T	0.01	< 1	< 1		Concentration variable and poorly characterized
	$(NO + NO_2)$	N,A	T(OH)	0.001	0.05	0.05	0.05-0.1	Concentration variable and poorly characterized
Sulfur compounds	CSO	N,A	T(O,OH)?	1(?)	0.52	0.52		Sources and sinks largely unknown
	CS_2	N,A	T	1(?)	< 0.005	< 0.005		Sources uncharacterized
	SO_2	A(?)	T(OH)	0.001	0.1	0.1	0.1–0.2	Given the short lifetime the global presence of SO_2 is unexplained
	H_2S	N	T(OH)	0.001	< 0.05	< 0.05		
Fully fluorinated species	CF_4 (F14)	A	I	> 500	0.07	0.24	0.2-0.31	Aluminum industry a major source
	C_2F_6 (F116)	A	I	> 500	0.004	0.02	0.01–0.04	Aluminum industry a major source
	SF_6	A	I	> 500	0.001	0.003	0.002-0.05	
Chlorofluorocarbons	$CClF_3$ (F13)	A	S(UV),I	400	0.007	0.06	0.04–0.1	All chlorofluorocarbons are of exclusive man-made origin. A number of regulatory actions are pending. The nature of regulations and their effectiveness would greatly affect the growth of these chemicals over the next 50 years.
	CCl_2F_2 (F12)		S(UV)	110	0.28	1.8	0.9–3.5	
	$CHClF_2$ (F22)	A	T(OH)	20	0.06	0.9	0.4–1.9	
	CCl_3F (F11)	A	S(UV)	65	0.18	1.1	0.5–2.0	
	CF_3CF_2Cl (F115)	A	S(UV)	380	0.005	0.04	0.02-0.1	
	$CClF_2CClF_2$ (F114)	A	S(UV)	180	0.015	0.14	0.06–0.3	
	CCl_2FCClF_2 (F113)	A	S(UV)	90	0.025	0.17	0.08-0.3	
Chlorocarbons	CH_3Cl	N(O)	T(OH)	1.5	0.6	0.6	0.6–0.7	Dominant natural chlorine carrier of oceanic origin
	CH_2Cl_2	A	T(OH)	0.6	0.03	0.2	0.1–0.3	A popular reactive but nontoxic solvent
	$CHCl_3$	A	T(OH)	0.7	0.01	0.03	0.02–0.1	Used for manufacture of F22; many secondary sources also exist
	CCl_4	A	S(UV)	25-50	0.13	0.3	0.2–0.4	Used in manufacture of fluorocarbons; many other applications as well
	CH_2ClCH_2Cl	A	T(OH)	0.4	0.03	0.1	0.06–0.3	A major chemical intermediate (global production = 10 tg/yr); possibly toxic
	CH_3CCl_3	A	T(OH)	8.0	0.14	1.5	0.7–3.7	Nontoxic, largely uncontrolled degreasing solvent
	C_2HCl_3	A	T(OH)	0.02	0.005	0.01	0.005-0.02	Possibly toxic, declining markets because of substitution to CH_3CCl_3
	C_2Cl_4	A	T(OH)	0.5	0.03	0.07	0.03-0.2	Possibly toxic, moderate growth due to substitution to CH_3CCl_3
Brominated and iodated species	CH_3Br	N	T(OH)	1.7	0.01	0.01	0.01-0.02	Major natural bromine carrier
	$CBrF_3$ (F13B1)	A	S(UV)	110	0.001	0.005	0.003–0.01	Fire extinguisher
	CH_2BrCH_2Br	A	T(OH)	0.4	0.002	0.002	0.001–0.01	Major gasoline additive for lead scavenging; also a fumigant
	CH_3I	N	T(UV)	0.02	0.002	0.002		Exclusively of oceanic origin
Hydrocarbons, CO, H_2	CH_4	N	T(OH)	5–10	1650	2340	1850–3300	A trend showing increase over the last 2 years has been identified
	C_2H_6	N	T(OH)	0.3	0.8	0.8	0.8–1.2	Predominantly of auto exhaust origin
	C_2H_2	A	T(OH)	0.3	0.06	0.1	0.06–0.16	No trend has been identified to date
	C_3H_8	N,	T(OH)	0.03	0.05	0.05	0.05-0.1	No trend has been identified to date
	CO	N,A	T(OH)	0.3	90	115	90–160	No trend has been identified to date
	H_2	N,A	T(SL,OH)	2	560	760	560–1140	
Ozone	O_3 (Tropospheric)	N	T(UV, SL,O)	0.1–0.3	F(Z)‡	12.5%		A small trend appears to exist but data are insufficient
Aldehydes	HCHO	N	T(OH,UV)	0.001	0.2	0.2		Secondary products of hydrocarbon oxidation
	CH_3CHO	N	T(OH,UV)	0.001	0.02	0.02		1980 concentration estimated from theory

*N, natural; A, anthropogenic; O, oceanic; S, stratosphere; UV, ultraviolet photolysis; T, troposphere; OH, hydroxyl radical removal; I, ionospheric and extreme UV and electron capture removal; SL, soil sink.

†These concentrations are integrated averages; for chemicals with lifetimes of 10 years or less, significant latitudinal gradients can be expected in the troposphere; for chemicals with extremely short lifetimes (0.001–0.3 years) vertical gradients may also be encountered.

‡Varies from 25 ppbv at the surface to about 70 ppbv at 9 km. The concentration was increased uniformly by the same percentage from the surface to 9 km.

is necessary for the discussions concerning the relative importance of the various trace gases.

3. From observational records and other considerations, infer the preindustrial concentrations of trace gases.

4. Estimate the radiative effects of the trace gases and their potentials for climate changes.

5. Clarify the sources for differences and discrepancies between published estimates for the trace gas radiative effects.

First, some comments are in order on the scientific necessity of this study because several papers have been published on the trace gas effects. None of the previous studies have included all of the trace gases included in this study. The present study uses new laboratory spectroscopic data made available subsequent to the earlier studies; the present study relies heavily on observed concentrations and trends for the trace gases as opposed to the hypothetical concentrations and increases assumed in most of the earlier studies. The *Lacis et al.* [1981] study did use observed trends but was restricted to only the effects of chlorofluorocarbons (CFC's), CH_4, and N_2O. *Chamberlain et al.* [1982] included the direct effects of most of the trace gases considered in this study, but inferred the temperature changes from the radiative flux change at the surface instead of the changes to the surface-troposphere system. It is the radiative flux change to the surface-troposphere system that governs the surface temperature change [*Manabe and Wetherald*, 1967; *Ramanathan*, 1981, 1982; *Hansen et al.*, 1982]. Furthermore, all of the above studies ignore stratospheric ozone changes due to CFC's.

For estimating their present-day radiative effects, we adopt the observed concentrations as of 1980. With respect to projected increases, we extrapolate the present-day trends to 50 years into the future. This procedure enables us to determine the relative importance of the various trace gases. Furthermore, we examine quantitatively the validity of the optically thin approximation, an important issue because this approximation is employed by all studies to treat the radiative effects of trace gases other than CO_2, O_3, N_2O, and CH_4.

For the purposes of this study, the word "climate" refers to surface/troposphere/stratospheric temperatures. The temperature changes are computed from a one-dimensional radiative-convective model described by *Ramanathan* [1981]. The radiative-convective model provides a convenient framework for examining the other trace gas effects, even though it ignores several important feedback processes arising from atmospheric circulation, oceans, and the cryosphere (e.g., ice-albedo feedback). Numerous one-, two-, and three-dimensional climate model calculations have estimated the surface warming due to doubled CO_2 (see summaries by the *National Research Council* [1982, 1983], among several others). Furthermore, the radiative effects of the other trace gases (with the exception of stratospheric ozone changes) are very similar to that of CO_2. Hence one-dimensional model estimates for the surface warming effects of the other trace gases and that of CO_2 (provided both are performed with the same model) can be used to scale the effects for the more realistic general circulation models (GCM), since numerous GCM estimates for the CO_2 effects are currently available.

2. OBSERVED AND PROJECTED CONCENTRATIONS OF TRACE GASES

The earth's atmosphere currently contains trace gases with atmospheric lifetimes that vary from much less than an hour to several hundred years. The abundance of trace gases is therefore dictated as much by their removal rates as by the growth in sources. From a viewpoint of global climate effects, species with extremely short lifetimes are unlikely to play an important direct role. To project the concentration of each species to year 2030, we have used a knowledge of the following: (1) recent (1980) atmospheric concentration and recent trend data if any; (2) nature of sources (man-made, natural, etc.), relative strengths or budget for each gas; (3) growth in natural as well as man-made sources due to projected human activities over the next 50 years; and (4) atmospheric lifetimes of each species.

TABLE 1*b*. Assumed Preindustrial (Year 1880) Concentrations of the Trace Gases

Trace Gas	Concentration
CO_2	270 ppm
CH_4	1.15 ppm
N_2O	0.285 ppm
Tropospheric O_3	−12.5%*
Stratospheric O_3	Same as present-day values
CFC11 and 12	0.
CCl_4	0.
All others	0.

*O_3 concentration is altitude dependent. Uniformly smaller at all altitudes from 0 to 12 km by 12.5%.

In what follows, we emphasize radiatively important gases. Table 1*a* briefly describes the lifetimes, dominant sources, and sinks of trace chemicals that have been identified in the global atmosphere. Many of these properties were listed earlier in an extensive review of scientific literature [*World Meteorological Organization*, 1982*b*]. For a large number of species where reaction with hydroxyl radical (OH) is the principal removal mechanism, lifetimes are estimated using an average OH concentration of 7×10^5 molecules/cm^3 and an average global atmospheric temperature of 265 K. While uncertain, this OH average is consistent with the budgets of CH_3CCl_3, CO, and ^{14}CO [*Volz et al.*, 1981]. For species with lifetimes greater than 20 years in Table 1*a*, removal is largely due to photolytic decomposition in the stratosphere. For all of the chlorofluorocarbons in Table 1*a*, lifetimes are determined based only on stratospheric photolysis from the computations of *Wuebbles* [1981] and those summarized by the *World Meteorological Organization* [1982*b*]. Only oxygenated species (O_3, aldehydes) and CH_3I absorb UV light in the troposphere ($\lambda > 290$ nm). The fully fluorinated species are not decomposed by UV light even in the stratosphere. Their destruction by and large would occur in the mesosphere and ionosphere from absorption of Lyman alpha and Lyman beta radiation at altitudes above 70 km [*Cicerone*, 1979]. The lifetime of fully fluorinated organics (Table 1*a*) can be in the 500- to 1000-year range. Hydrogen is the only species in Table 1*a* where microbial action at soil surfaces provides the major removal process. Ozone destruction also occurs on all surfaces (e.g., soil, water, and snow), but the mechanism of this destruction process is not known.

In addition to providing source, sink, and lifetime information, Table 1*a* also presents global average concentrations of species for the atmosphere of year 1980. These data are based on actual measurements that have already been summarized in some detail [*World Meteorological Organization*, 1982*b*].

It must be remembered that for species with lifetimes of less than 10 years, significant horizontal (latitudinal) gradients can exist. As an example, the ratio of northern to southern hemispheric average concentration is about 1.4 for CH_3CCl_3 ($\tau_l = 8$ years) and >2 for C_2Cl_4 ($\tau_l = 0.5$ year). For short-lived species ($\tau_l < 0.3$ year), vertical gradients can also be expected. These gradients have been taken into consideration, based on available information, in developing the global averages shown in Table 1*a*.

The year 2030 concentrations are projected to develop a standard set of conditions, but a probable range is also included. The year 2030 "best estimates" in Table 1*a* thus constitute the "standard set." The range of likely variability associated with this standard set is also presented in Table 1*a*.

In the following sections we discuss the information that was utilized in developing the year 2030 projections. The year 1980 characterization is based exclusively on atmospheric measurements.

2.1. *Carbon Dioxide*

The CO_2 concentrations in the atmosphere have been measured to be increasing at a rate of approximately 1.5 ppm/yr (see Figure 1.2 of the *National Research Council* [1983]). Fossil fuel combustion is believed to be a major contributor to this increase. Over the past decades, CO_2 release rates due to combustion have increased at a rate of about 4.3%/yr. A recent analysis [*Rotty and Marland*, 1980] supports a 2.4%/yr increase in CO_2 emissions over the next 50 years. Only a fraction ($\approx 50\%$) of this input is expected to remain airborne. Based on this analysis, *Wuebbles* [1981] described the CO_2 concentration in ppm empirically.

$$[CO_2] = 330.0e^{0.0056(t-1975)} \qquad 1975 \le t \le 2100$$

The CO_2 concentration of year 2030 is computed to be 450 ppm. This projected concentration is consistent with available scenarios based on more detailed considerations of energy policies and the sources and sinks for CO_2 [e.g., *Smagorinsky*, 1983, p. 278].

2.2. *Chlorofluorocarbons (CFC's)*

These chemicals came into major use in the 1960's and initially exhibited a rapid growth (10–15%/yr). The most important CFC's to date have been CF_2Cl_2 (F12 or CFC12) and $CFCl_3$ (F11 or CFC11). The global emissions of the major CFC's (F12 and F11) actually declined somewhat from the mid-1970's through 1982 [*Chemical Manufacturer's Association*, 1983]. Part of this decline may be attributed to a ban on some nonessential usages (e.g., spray cans) of CFC's and due to adverse economic conditions that have prevailed in several industrial nations during this time. CFC emissions increased sharply in 1983. Data for $CFCl_3$ and CF_2Cl_2 have been presented by *Logan et al.* [1981] and *Cunnold et al.* [1983*a*, *b*]. The use of CFC's in other more essential industries and in previously less industrialized nations (e.g., refrigeration) is expected to grow. We estimate that a 3%/yr growth rate for all of the relatively inert CFC's, i.e., F11, F12, and $C_2Cl_3F_3$ (F113), $C_2Cl_2F_4$ (F114), C_2ClF_5 (F115), and C_2F_6 (F116), is a reasonable scenario. The range of concentrations shown in Table 1*a* is established based on a 0–5%/yr growth. For $CHClF_2$ (F22), less severe controls are anticipated, since 60% of the emitted amount could be removed in the troposphere. A 5% growth rate with a 3–7%/yr range is used for computations presented in Table 1*a*.

2.3. *Chlorocarbons*

All chemicals (except carbon tetrachloride) in this category have atmospheric residence times of less than 10 years. Because of the toxic nature of many of these chemicals [*Surgeon General*, 1980], a rapid growth of emissions cannot be expected. Also, because of relatively fast removal rates, a dramatic buildup of these in the global atmosphere is not likely.

Methyl chloride (CH_3Cl) is the most abundant natural chlorine carrier; it appears to arise mostly from the world's oceans [*Lovelock*, 1975; *Rasmussen et al.*, 1980; *Singh et al.*, 1983*b*], although relatively small man-made sources are known to exist [*National Academy of Sciences/National Research Council*, 1976] and inadvertent release is possible due to biomass burning and/or reactions between organic matter and chlorinated water, as in rivers. Thus it is unlikely that the sources of atmospheric CH_3Cl will increase substantially, and we indicate in Table 1*a* little or no growth in its atmospheric concentration by the year 2030. It is worth noting, however, that if tropospheric OH (dominant sink for CH_3Cl) levels decrease, CH_3Cl concentrations could increase; see methane discussion below.

Methylene chloride (CH_2Cl_2), a relatively short-lived chemical, is a popular solvent which is expected to undergo rapid growth unless found to be toxic in the future. Its virtual noninvolvement in the stratosphere and its lack of toxicity assures it an excellent growth potential. On the average, a 5%/yr (range of 3–7%/yr) growth rate appears a reasonable projection. This growth rate is also consistent with the growth in the last decade [*Bauer*, 1979].

Over the last decade, the methyl chloroform (CH_3CCl_3) market has grown at a rate of about 15%/yr. Although it may make an increasing contribution to stratospheric ozone depletion, its market is expected to grow rapidly and a growth rate similar to that of CH_2Cl_2 is projected. Methylene chloride along with CH_3CCl_3 are the most likely chemicals to be used for substitution as other more toxic chemicals (e.g., C_2HCl_3, C_2Cl_4) are more severely controlled.

Carbon tetrachloride (CCl_4) is the longest lived atmospheric chlorocarbon, and its historical emission pattern is more complicated [*Singh et al.*, 1976]. Since the early 1960's, when the toxic effects of CCl_4 became evident, direct emissions virtually ceased. The present atmospheric CCl_4 concentration growth rate is between 2%/yr [*Simmonds et al.*, 1983] and 5%/yr [*Singh et al.*, 1983*a*]. Current emission levels of CCl_4 could grow at a rate of about 2% (0–3%/yr) over the next 50 years, in a manner similar to those of fluorocarbons because a large fraction of CCl_4 emitted is during its use in fluorocarbon production.

2.4. *Fully Fluorinated Species*

Three chemicals in this cateogry have been measured at enough locations to characterize global concentrations: CF_4 (F14), C_2F_6 (F116), and sulfur hexafluoride (SF_6). These three man-made species are relatively stable chemicals with atmospheric residence times over 500 years. These species are not chemically involved in atmospheric processes below about 50 km. The sources of CF_4 and C_2F_6 are not at all clear. Inadvertent emissions from carbon-electrode processing of minerals [*Cicerone*, 1979] are likely, specifically from aluminum processing [*Penkett et al.*, 1981]. Assuming a 2–3% steady growth rate of the aluminum industry over the next 50 years, the year 2030 concentrations of CF_4 and C_2F_6 are shown in Table 1*a*. Indeed, a temporal increase of about 2%/yr in CF_4 concentrations has been measured recently (R. J. Cicerone et al., unpublished manuscript, 1985). This rate of increase is less than that deduced by *Cicerone* [1979]. SF_6 is a dielectric agent used in electrical equipment. Its concentrations are also estimated based on a 2–3%/yr growth rate.

2.5. *Nitrogen Compounds*

The most important nitrogen-containing chemical from a climatic viewpoint is N_2O. The 1980 atmospheric concentration is 301 ppb (0.8 ppb less in the southern hemisphere) as measured by *Weiss* [1981]. Contrary to many previous estimates, it is now accepted that N_2O has a very long atmospheric lifetime (> 100 years) with stratospheric photolysis the only known removal process. Microbial production in soils and oceans has been found to be a source as well as a sink of N_2O. The net contribution of soils and oceanic microbes to the atmospheric budget of N_2O is not yet clear; *Weiss* [1981] calculated that the total annual source of atmospheric N_2O is about 3×10^{12} g. Over a 4-year period (1976–1980), Weiss measured a rate of increase of 0.2%/yr for N_2O concentrations. Further, he constructed a mathematical model which used an exponentially increasing N_2O source function to fit his measurement data. More recent data (R. F. Weiss, private communication, 1984) continue to fit Weiss' mathematical model. The recent record shows more uniformity among data from measurement locations than was apparent in the 1976–1980 record. From the *Weiss* [1981] mathematical model, we estimate the year 2030 concentration to be 375 ppb and a likely range of 350–450 ppb. This range reflects the considerable existing uncertainty as to the identity of the N_2O sources most responsible for the observed N_2O concentration trend, e.g., coal combustion and microbial production of N_2O through nitrification and denitrification of inorganic nitrogen fertilizers applied to soils. Even with the recent expansion of Weiss's data base, the record is still not adequate to distinguish between these two sources (R. F. Weiss, private communication, 1984). In the future, the atmospheric residence time of N_2O could decrease if ozone concentrations decrease above 30-km altitude (Table 2); increased UV light levels just below 30 km would increase the rate of N_2O photolysis. Also, while we have adopted *Weiss*'s [1981] semiempirical method for projecting future N_2O concentrations, we note that there remain many questions about sources of atmospheric N_2O. For example, if we employ a slower rate of increase of fossil fuel combustion than did Weiss, we arrive at a reduced lower limit for N_2O in that year, i.e., 350 ppb. Further, while many studies suggest that only 1–2% of all fertilizer N is released as N_2O in the year following fertilization, much higher release rates are possible especially from fertilized organic-rich soils [*Duxbury et al.*, 1982].

Two other nitrogen-containing gases, hydrogen cyanide (HCN) and peroxyacetyl nitrate (PAN), have now been observed in the nonurban troposphere. Infrared absorption measurements with the sun as the source have shown that HCN is present in the northern hemisphere (NH), midlatitude troposphere, and the entire NH stratosphere at about 160 ppt, with little, if any, altitude gradient up to the midstratosphere. These measurements, the atmospheric chemistry and possible sources of HCN, have been discussed by *Cicerone and Zellner* [1983]. In Table 1*a* we show no increase in HCN concentration by 2030, but only because there are no data on its temporal trends and because the identities of its sources are uncertain. Similarly for PAN, we can do little more than note that it has been detected recently in the nonurban troposphere, occasionally at concentrations of 400 ppt. While there is reason to believe that its global concentrations are nonnegligible [*Singh and Salas*, 1983] and that its precursors (NO_x, ethane, and propane) might increase in the future, there is too little information to permit an estimate of PAN's future concentrations.

TABLE 2. Computed Stratospheric Ozone Changes From 1980 to 2030

Altitude	Percent Ozone Change
10	3.8
16	4.1
22	4.5
26	2.0
28	−1.2
30	−6.1
32	−13.4
34	−22.6
36	−31.1
38	−36.7
40	−37.9
44	−27.4
50	−5.4

The calculations account for the feedback between temperature and chemistry within the model stratosphere (above 10 km) and employ the chemistry model of *Cicerone et al.* [1983] and the radiative-convective model used in this study.

The other nitrogen species (NH_3 and NO_x) have extremely short lifetimes (0.5–5 days). The global distribution of these species, even for the 1980 atmosphere, is poorly characterized [*Kley et al.*, 1981]. As expected with species of such short lifetime, a great deal of variability in atmospheric levels is evident. Although anthropogenic sources of NO_x in the troposphere (auto and aircraft exhaust, high-temperature combustion, soil emissions) may double over the next 50 years, it is unclear if this change would increase the atmospheric abundance of NO_x outside the range of present uncertainty.

2.6. *Ozone*

The climatic effects of ozone change depend very strongly on whether tropospheric or stratospheric ozone is being altered [*Ramanathan and Dickinson*, 1979; *Wang*, 1982]. Hence we discuss separately the tropospheric and stratospheric O_3 trends.

Focusing first on ozone in the free troposphere (above the planetary boundary layer), there are data and theories that suggest that ozone concentrations are increasing with time. A number of investigators [*Logan*, 1982; *Angell and Korshover*, 1983; *Bojkov*, 1983] have reviewed and analyzed data from many ozone-measuring stations supported by Umkehr data. Logan finds that at Uccle (Belgium) at 500- and 700-mbar levels, ozone increased by about 1%/yr between 1969 and 1980. Similarly, at Hohenpeissenberg (Germany) at the 500- and 700-mbar levels, ozone increased by 15% from 1967 to 1981. However, at Payerne (only 500 km away) at these same altitudes, no such trend was observed. A preliminary analysis of data from nine NH ozonesonde stations has been performed by *Liu et al.* [1980]. Eight of nine stations show ozone increases (8 ± 4%) from 1969 to 1977 in the middle troposphere, a result consistent with that reported by the *National Aeronautics and Space Administration* [1979] for the 2- to 8-km region. These ozone increases are not mirrored in surface measurements where no trends have been observed or in the southern hemisphere (SH), where one station, Aspendale, shows a decrease in tropospheric ozone 1965–1978 [*Liu et al.*, 1980]. Based on available data, one cannot distinguish a clear trend, but an upward trend in tropospheric ozone (2–8 km) seems to have occurred [*Angell and Korshover*, 1983].

Other considerations suggest that tropospheric ozone is increasing in the northern hemispheric troposphere. First, *Fishman et al.* [1979*b*] presented evidence that there is appreciable in situ photochemical production of ozone. This evidence includes the fact that ozone is more concentrated in the NH even though there should be faster uptake at the earth's surface in the NH. Also, Fishman et al. noted that there are much stronger seasonal variations in the NH production of ozone. Recent models of tropospheric chemistry that embody this theory predict that tropospheric ozone has already increased and will continue to do so, especially in the NH. Due to increases in combustion releases of NO_x, CO, H_2, and increased CH_4, *Logan et al.* [1978] calculated that tropospheric O_3 can increase greatly, even 100% in the next century, especially in the middle and upper troposphere. *Liu et al.* [1980] focused on the consequences of NO_x injections from high flying aircraft. In their view, most photochemical production of ozone occurs above the boundary layer, so direct injections by aircraft are especially effective and ground-level NO_x sources may not lead to much photochemical ozone in the free troposphere. Liu et al. calculated that a 14–30% ozone increase should have occurred in the NH middle and upper troposphere between 1970 and 1980. A more recent analysis of tropospheric ozone production by human activities is given by *Crutzen and Gidel* [1983].

To summarize the two paragraphs above, there is some observational evidence that NH tropospheric ozone has increased by 0.8–1.5%/yr since about 1967; this evidence is compelling but not conclusive. Photochemical theory applied to emission histories and projections of combustion NO_x suggests that a 1%/yr increase in NH tropospheric ozone is possible. In the SH, given the smaller anthropogenic influences, O_3 might not change at all (NH anthropogenic NO_x, a key ingredient for photochemical production of O_3, should not influence the SH). For our globally averaged radiative calculations, we will adopt an annual growth rate for tropospheric ozone of 0.25%/yr, although values from zero to 1.5%/yr appear possible, at least for the NH. A nominal 40 ppb of tropospheric ozone, for example, becomes 45 ppb in the year 2030 with a 0.25%/yr growth rate; a 1%/yr growth rate would result in 64 ppb in 2030. Note that we do not assume a constant mixing ratio with altitude in our calculations. Table 1*a* provides the adopted altitude variation in the model calculations which are based on the hemispherical, annual mean ozone data described by *Ramanathan and Dickinson* [1979].

Stratospheric ozone is also thought to be susceptible to perturbing influences, including man-made chloro- and chlorofluorocarbons, increasing CH_4 and N_2O concentrations (see below) and decreases in stratospheric temperature due to increasing CO_2. For our stratospheric ozone profile for the year 2030, we have taken the computed ozone perturbations listed in Table 2. These ozone changes were calculated with the basic chemistry model of *Cicerone et al.* [1983] with fixed-flux lower boundary conditions for N_2O, CH_3Cl, and CCl_4 but a fixed mixing ratio (1.6 ppm) for CH_4. As discussed later, the present computations account for the feedback between temperature and chemistry. A refined diurnal averaging scheme was employed; it led to less nonlinearity in the ozone-chlorine response curve than reported by Cicerone et al. The ozone change shown in Table 2 was obtained by increasing the flux of $CFCl_3$ (F11) and CF_2Cl_2 (F12) till the stratospheric mixing ratio of inorganic chlorine (ClX) reached a value of 9.4 ppb for the year 2030. A ClX value of 9.4 ppb for year 2030 results from a 3%/yr increase (1980–2030) in emissions of CF_2Cl_2, $CFCl_3$, CH_3CCl_3, $C_2Cl_3F_3$, $C_2Cl_2F_4$, CCl_4, and $CHClF_2$ (D. J. Wuebbles, private communication, 1984; also see *Wuebbles* [1983*b*]). This uniform 3% growth rate is consistent with those adopted in Table 1*a*, except that Table 1*a* shows a 2% growth rate for CCl_4 and a 5% rate for $C_2H_3Cl_3$. In order to place this slight inconsistency in proper perspective, we note that the calculated future stratospheric ClX mixing ratios depend, not only on future emissions, but also on the vertical eddy-mixing coefficient in the (one-dimensional) model. For the 1980 reference atmosphere, we took ClX = 2.5 ppb.

The ozone changes shown in Table 2 account for the feedback between temperature and chemistry. For this purpose, we iterated the temperature changes computed by the climate model (described later) with the ozone change resulting from the chemistry model. The temperature change calculations include not only the ozone changes but also the increase in all other trace gases shown in Table 1*a* (see the "Best Estimate" column). This temperature feedback reduced the computed ozone changes by a nonnegligible amount. For example, without the temperature feedback, the computed ozone change at a few of the levels are +4.2% (10 km), +5.1% (20 km), −7.3% (30 km), −45% (40 km), and −36% (44 km); these changes can be compared with those in Table 2.

Our usage of a fixed mixing-ratio lower boundary condition for CH_4 actually assumes an increasing flux of CH_4 (to maintain the fixed mixing ratio as ClX increases). A fixed-flux boundary condition for CH_4 would have led to larger ozone changes than those shown in Table 2. Beyond the year 2030, even larger ozone changes are possible [*Prather et al.*, 1984]. In the present paper, we have neglected stratospheric ozone changes due to the projected CH_4 and N_2O increases shown in Table 1*a*. It should also be stated that model calculations of ozone changes below 30 km are plagued with uncertainties. Accordingly, model results have fluctuated over the past 10 years or so [see, e.g., *National Academy of Sciences/National Research Council*, 1982].

2.7. *Methane* (CH_4) *and Carbon Monoxide* (*CO*)

The most abundant atmospheric hydrocarbon, methane, was present at about 1.65 ppm in the NH in 1980; a concentration about 6% lower characterized the SH. More relevant for our present purposes, atmospheric CH_4 concentrations are known to be increasing globally. Between early 1978 and early 1981, concentrations increased by (2 ± 0.5)%/yr as measured by *Rasmussen and Khalil* [1981] and by 1–1.5%/yr as measured by *Blake et al.* [1982]. *Ehhalt et al.* [1983] have reviewed these and other data on atmospheric methane and conclude that its concentration increased by about 0.5%/yr between 1965 and 1975 and by 1–2%/yr between 1978 and late 1980. Further, from trapped air in dated ice cores, *Craig and Chou* [1982] have deduced that CH_4 concentrations have approximately doubled in the last 350 years with a greater rate of increase in the last century. It is not clear why these increases have occurred, i.e., which of the methane sources have increased or even if the atmospheric sink of methane (oxidation by OH reaction) has decreased. Arguments for increasing sources of methane are favored by ^{13}C data [*Craig and Chou*, 1982]. Principal sources of atmospheric methane appear to be enteric fermentation in ruminant animals, release from organic-rich sediments below shallow water bodies and rice paddies, and quite possibly, production by termites and biomass burning. Also, methane release in mineral, oil, and gas exploration and gas transmission is growing. Clearly, to be able to predict future levels of atmospheric methane, it is necessary to know the relative importance of the various methane sources and their trends. If, for example, rice agriculture is a dominant source, then trends in cultivated area, plant-strain proportions, irrigation, and multiple cropping and fertilization practices must be discerned as they affect methane release.

The dominant sink of atmospheric methane, tropospheric gaseous OH, may not be unchanging. Increased levels of tropospheric CO or of CH_4 itself can suppress OH concentrations, as has been noted by several authors. CO exhibits large hemispheric differences; these patterns and our knowledge of CO sources are reviewed by *Logan et al.* [1981]. Recently, Khalil and Rasmussen have reported evidence from measurement (in Oregon) of dramatic (6%/yr) increases of atmospheric CO between 1979 and 1983. On the other hand, W. Seiler (private communication, 1984) has measured little or no change (≤ 1%/yr) in CO at several stations in both hemispheres. For a clean, background troposphere a CO increase of x% leads to a depletion of tropospheric OH of $x/(4 \pm 1)$%, depending on altitude and various model assumptions, according to A. M. Thompson and R. J. Cicerone (unpublished manuscript, 1984). Combining the (1) source analysis by *Logan et al.* [1981], (2) information on trends of these sources (e.g., fossil fuel usage, oxidation of anthropogenic hydrocarbons), and (3) the CO data mentioned above, it is clearly possible that CO will increase by 1–2%/yr through 2030 A.D. Such an increase could cause CH_4 concentrations to increase faster (through OH suppression) than if only CH_4 source increases were considered. Because of the spectral locations of the absorption of CO, the CO increase itself is not of interest here. Its effects on the atmospheric levels of OH, CH_4, and O_3 could be very important.

Lacking all the detailed information necessary to understand the presently documented rate of increase of atmospheric CH_4 concentrations and to predict the future, we estimate that CH_4 will increase by 0.75%/yr between now and 2030; this would lead to a globally averaged CH_4 concentration of 2.34 ppm in 2030. Rates of increase of 1.5% and 0.25%/yr would lead to 3.30 and 1.85 ppm in 2030, respectively, as listed in Table 1*a*. Beyond the year 2030, when the release of continental-slope sediment methane clathrates might occur due to oceanic warming [*Revelle*, 1983], faster methane increases are possible.

2.8. *Nomethane Hydrocarbons*

In this category we include alkanes, alkenes, alkynes, aldehydes, ketones, and H_2. We pay little attention to simple aromatic compounds. By contrast with the situation for methane, there is too little information available on the concentrations, distributions, and sources of these compounds (except for C_2H_2 and H_2) to justify projections of future concentrations. For acetylene (C_2H_2), fossil fuel burning (e.g., internal combustion engines, oil-fired heaters) is a known source; its atmospheric residence time is about 4 months, and no significant biological sources are known yet [*Rudolph and Ehhalt*, 1981]. If its sources are wholly anthropogenic, an annual increase of 1–2% would be a reasonable guess. For ethane (C_2H_6), ethylene (C_2H_4), propane (C_3H_8), and propene (C_3H_6) the existing atmospheric and oceanic surface water data suggest that there are natural as well as anthropogenic sources [see, e.g., *Rudolph and Ehhalt*, 1981, and references therein]. Fugitive emissions from oil and gas wells and transmission lines are likely, of course. The state of our measurement data base for higher hydrocarbons, aldehydes (present as oxidation products of hydrocarbons), and acetone is discussed by *Penkett* [1982].

2.9. *Sulfur Compounds*

Carbonyl sulfide (OCS) is the most abundant gaseous sulfur carrier in the atmosphere. It is nearly uniformly distributed with a measured average concentration of 0.52 ppb. *Turco et al.* [1980] have examined the sources and sinks of OCS. While there are many remaining questions, they propose that up to 50% of the total source is anthropogenic. If so, OCS concentration could increase in the future, but our present understanding of OCS sinks and its atmospheric residence time is not very complete. No measured trend in OCS concentration is available at this time. Considering the lack of such data and the uncertainties about OCS sources and sinks, we cannot project other than a constant OCS abundance in Table 1*a*.

Sulfur dioxide (SO_2) is a notorious atmospheric constituent because of its role in acid deposition. In continental boundary layers where its principal source is combustion of S-containing fuels, its concentrations are often 10 ppb. Above the boundary layer its concentration is of order 100 ppt [*Maroulis et al.*, 1980]; its presence there is probably due to escape from the boundary layer below, and to oxidation of other species, e.g., OCS, CS_2, and CH_3SCH_3. Similar concentrations have been measured in the marine boundary layer [*Herrmann and Jaeschke*, 1984]. Near major anthropogenic SO_2 sources its atmospheric residence time is about 1 day (due largely to gas-to-particle conversion); in the higher troposphere in clear air its residence time is up to 1 week. Because of its very short lifetime and the uncertain future of SO_2 emission, it is not at all clear that SO_2 concentration will increase in the future. Dimethyl sulfide (DMS) is now known to exist in the oceanic boundary layer; it appears to have microbial sources in oceans that provide a significant DMS flux to the marine atmosphere [*Andreae and Raemdonck*, 1983]. Because this natural source appears to be the major DMS source and because of the short (~ 2 days) atmospheric residence time of DMS, we project no growth in its atmospheric concentrations.

Carbon disulfide (CS_2) is known to be present in background surface air at concentrations that vary from 0.03 to 0.08 ppb. However, it is virtually undetectable in the free troposphere. Excited-state oxidation [*Wine et al.*, 1981] can be an important removal process. Oceans may be a major source. No growth projection in CS_2 concentrations can be proposed reliably at this time.

2.10. *Brominated and Iodated Species*

Only a handful of species in this class have been measured in the nonurban atmosphere. The species of interest are brominated and iodated methane- and ethane-series molecules: methyl bromide (CH_3Br), methylene bromide (CH_2Br_2), bromoform ($CHBr_3$), bromotrifluoromethane or (F13B1, $CBrF_3$), methyl iodide (CH_3I), and dibromoethane ($C_2H_4Br_2$, or ethylenedibromide, EDB). CH_3Br is apparently a natural species [*Lovelock*, 1975; *Singh et al.*, 1983*b*]. Man-made emissions have the potential to perturb its global background, but only slightly. Methyl iodide is essentially all natural and, given its concentration, is predicted to remain unchanged. $CHBr_3$ and CH_2Br_2 have been measured only recently [*Berg et al.*, 1984], and too little is known about their sources to permit reasonable future projections. $CBrF_3$ (F13B1) and ethylene dibromide are exclusively anthropogenic. A continued shift toward nonleaded gasoline could offset growth that may occur in fumigation applications of ethylene dibromide. Because of its high carcinogenic potential, a rapid growth is not likely to be permitted in any case. $CBrF_3$ (used as a fire extinguisher) is the only brominated organic whose sink is primarily in the stratosphere (where bromine atoms can be efficient ozone destroyers). Despite its very low present abundance it can become an important carrier of organic bromine within the next 50 years. Inorganic species such as HBr, HI, BrO, IO, and NOBr are not discussed here because they are as yet undetected in the atmosphere. Their residence times are probably 5 days or less, and future trends are difficult to predict.

3. PREINDUSTRIAL ERA CONCENTRATIONS OF GREENHOUSE GASES

It is important to ask if CO_2 and the other trace gases should already have caused a global warming. It is very difficult, if not impossible, to answer this question for at least two reasons: (1) there are no direct data on the trace gases of interest from, say, the 1850–1940 time period, and (2) there should be a significant time lag between any increased atmospheric radiative forcing and increased global temperatures, due to oceanic heat capacity. To allow at least a rough estimate of the size of the effect due to increased trace gas concentrations from about 1880 until 1980, we will attempt to estimate the 1880 concentrations of methane, nitrous oxide, chlorofluorocarbons, CCl_4, and tropospheric ozone. The proposed preindustrial concentrations of the trace gases are shown in Table 1*b*.

For CO_2, the *National Research Council* [1983] study suggests that the most likely preindustrial value is between 260 and 290 ppm. For this study, the preindustrial concentration of CO_2 is assumed to be 275 ppm.

For CH_4, the data of *Craig and Chou* [1982] show that CH_4 has increased monotonically for the past 400 years; these data are CH_4 concentrations in air trapped in dated Greenland ice cores. Craig and Chou noted that there is as much as a 90 year uncertainty in the age of this air, depending on whether air moved freely throught the firn phase of the snow above the firn-closure depth. If the air at the 90-year firn level was zero years old, then the CH_4 concentration in the year 1880 was about 1.05 ppm. If the air there was not so young, the Craig and Chou data show that the CH_4 concentration in 1880 had to be over 1.05 ppm. If, for example, the air in 90-year old ice at this site were 50 years old instead of zero years old, the implied 1880 CH_4 concentration would be 1.10–1.15 ppm in 1880. We assume that the 1880 CH_4 level was 1.15 ppm.

For nitrous oxide, there are no direct data from pre-1900; indeed, N_2O was discovered in the atmosphere only in 1938. Modern data from 1976–1980 and from 1961–1974 have been used by *Weiss* [1981] to estimate a preindustrial atmosphere N_2O concentration of 281–291 ppb. Accordingly, we assign a value of 285 ppb to N_2O for the year 1880.

The chlorofluorocarbons and fluorocarbons (CCl_2F_2, CCl_3F, and the other compounds listed in Table 1 are almost certainly of exclusive and post-1940 anthropogenic origin [*National Academy of Sciences/National Research Council*, 1979]. Therefore we estimate that each of them was absent from the 1880 atmosphere.

Carbontetrachloride is more interesting. It is known to be produced by marine organisms [see, e.g., *Fenical*, 1982], yet its mid-1970's (and present) concentration can be explained by anthropogenic emissions [*Singh et al.*, 1976]. Because of the apparent unimportance of current natural sources, we will assume that it was essentially absent from the 1880 atmosphere.

Of the important greenhouse gases, tropospheric ozone is most difficult for which to estimate differences between present-day concentrations and those of one century ago. The surplus of NH over SH ozone, the more pronounced seasonal cycle in the NH ozone data, the strong theoretical case for excess ozone production in the industrialized NH and the hints of a positive trend since 1967, all imply that there was less O_3 in the 1880 NH troposphere. Detailed examination of these and other factors [see *Levy et al.*, 1985] does not allow one to state with confidence that the hemispheric or global background tropospheric ozone is strongly controlled by photochemical reactions (such as those between hydrocarbons and nitrogen oxides to produce ozone). For example, there is evidence that the NH troposphere receives perhaps 3 times as much ozone from the stratosphere as does the SH troposphere. One would predict higher NH concentrations from this meteorological input of ozone, although the higher surface-destruction rates in the NH would offset some of the additional input. Perhaps 50% more ozone is observed in the NH tropics than in the SH tropics (0- to 12-km altitude; *Fishman et al.* [1979*b*]) and 25–50% more in the midlatitudes of the NH at 800-mbar pressure levels than at corresponding SH locations. Another feature of ozone in the NH midtroposphere, the east-west gradient over North America [*Chatfield and Harrison*, 1977], appears to be evidence for photochemical production over continents. We assume that half of the difference between NH and SH is due to anthropogenic emissions (and that 1880 emission of NO_x and hydrocarbons was negligible compared with those in 1980). Even with these assumptions, one is left with uncertainty about vertical profiles. In the upper troposphere, there is more influence from the stratosphere, but there is also significant existing potential for human impact by direct injections from aircraft [*Liu et al.*, 1980]. As a very rough estimate, we will guess that there was 25% less ozone in the 1880 NH troposphere than in 1980 NH troposphere and that SH tropospheric ozone did not change during that century.

4. DESCRIPTION OF THE CLIMATE MODEL

The direct radiative effects of trace gases are included in this study. The effects due to altered chemistry are included explicitly as far as stratospheric O_3 perturbation is considered and implicitly with respect to tropospheric O_3, i.e., projected O_3 increases can be considered to arise from the projected increases in hydrocarbons, CO, and NO. With respect to the feedback effects, this study accounts for troposphere/stratosphere radiative interactions and the feedback between temperature and chemistry within the stratosphere. The climate-chemistry interactions in the troposphere and the possible effects of temperature changes on stratospheric H_2O are ignored. Both of these feedback effects, while they may be relatively smaller than the direct radiative effects would require coupled photochemical climate models [*Callis et al.*, 1983].

A brief description follows of the radiative-convective model and the source for the spectroscopic data used for the computations.

4.1. *Radiative-Convective Model*

The one-dimensional radiative-convective model described by *Ramanathan* [1981] is adopted. This model, hereafter referred to as model R, has a surface boundary layer which explicitly allows for the surface-atmosphere exchange of latent and sensible heat and also solves for the boundary layer moisture [*Ramanathan*, 1981, equations 17–20, Figure 7]. The standard radiative-convective models [e.g., *Manabe and Wetherald*, 1967; *Ramanathan and Coakley*, 1978] ignore these processes and do not treat explicitly the exchange of latent heat flux between the surface and the free atmosphere.

The boundary layer moisture and hence the relative humidity are explicitly computed in the model, but the tropospheric relative humidity is prescribed as discussed by *Ramanathan* [1981]. The mass mixing ratio of H_2O above 12 km is prescribed to be 2.5 ppm. Because of the explicit treatment of the boundary layer, the model R computes the surface temperature and the surface air temperature. Standard radiative-convective models compute only one temperature for the lower boundary which can be interpreted as an average of the surface and surface air temperature. In model R the surface air temperature change is larger than that of the surface temperature change by about 10–13%. This point should be noted when comparing the present calculations with the published results.

4.2. *Radiation Model and Spectroscopic Data*

The trace gases, their longwave band centers, and the adopted band strengths are shown in Table 4. The treatment of H_2O, O_3, CO_2, and CH_4 are as described in model R. For CO_2, one of us (J.T.K.) incorporated the more detailed band model of *Kiehl and Ramanathan* [1983] in model R. The surface warming due to doubled CO_2 estimated with the detailed CO_2 scheme was in excellent agreement (within 5%) with that estimated from the somewhat simpler scheme in model R. For CH_4, model R employs the *Donner and Ramanathan* [1980] band model. Although the band strength adopted in model R is stronger than the current accepted value by about 35%, the band model parameters were fit to give agreement with laboratory absorptances. Hence the CH_4 radiative forcing estimated by this band model agrees within 5–10% of that estimated from a 5 cm^{-1} spectral resolution narrow band model which employs recent [*Rothman et al.*, 1983] line data. Numerous modifications were incorporated in model R to treat the effects of the minor trace gases included in this study and these modifications are described below.

N_2O. The R scheme used the *Donner and Ramanathan* [1980] band model scheme. We have retained this scheme, but included the following N_2O bands that were ignored by *Donner and Ramanathan* [1980]: the two-band systems centered at 1168 cm^{-1}, one of which is the $2v_4$ band of the four isotopes with bandstrength 8.5 cm^{-1} (cm atm)$^{-1}$ STP and the hot bands of the four isotopes with band strength 1.5 cm^{-1} (cm atm^{-1}) STP. Although these bands are considerably weaker than the fundamental v_1 band system centered at 1285 cm^{-1}, they contribute as much as 20% of the v_1 band system to the surface warming due to N_2O. This disproportionately large contribution by the weak bands arises because N_2O is almost in the strong line limit, and hence the opacity scales as the square root of the band strength. Hence for gases whose concentration are large and their band strengths are sufficiently strong that they are in the strong line limit, great care must be exercised in including all the bands whose strengths are smaller by as much as 2 orders of magnitude than the strong fundamental band. This is the reason why the present model incorporates many isotopic and hot bands of trace gases such as CO_2, N_2O, and CH_4.

Other trace gases. The band absorption A is expressed as

$$A = \Delta\omega\left[1 - \sum_{i=1}^{N} f_i e^{-\tau_i/\bar{\mu}}\right] \tag{1}$$

$$\tau_i = \left(\frac{k_i}{f_i}\right)\left(\frac{Sw}{\Delta\omega}\right) \tag{2}$$

$$\sum_{i=1}^{N} f_i = 1 \tag{3}$$

$$\sum_{i=1}^{N} k_i = 1 \tag{4}$$

where $\Delta\omega$ is the band width in cm^{-1}, S is the band strength in cm^{-1} (cm atm)$^{-1}$, w is the absorber amount in cm atm. The above procedure of expressing the band transmission as a sum of transmission functions averaged over pseudo-spectral intervals i with weighting functions f_i and k_i is essentially the exponential-sum fitting method described by *Wiscombe and Evans* [1977]. The procedure of employing $\bar{\mu}$ to approximate the solid angle integration of the transmission is referred to as the exponential kernel approximation [*Sparrow and Cess*, 1970, p. 226]. However, instead of adopting the standard procedure of employing one value for $\bar{\mu}$, we obtain exact values of $\bar{\mu}$ as a function of the optical depth from tabulated values of the E_3 exponential kernel function [see *Sparrow and Cess*, 1970, pp. 200, 312]. The values of $\bar{\mu}$ as a function of τ is fit by the following smooth expression:

$$(\bar{\mu})^{-1} = 1.5 + \frac{0.5}{1 + 4\tau + 10\tau^2} \tag{5}$$

In (5), the optical depth τ is the total optical depth, i.e., the sum of the optical depths of all gases in the interval. The above set of equations is mathematically and conceptually rigorous if one of the two following asymptotic limits are satisfied.

1. The optically thin limit, i.e., $\tau_i \ll 1$. In this limit, (1)–(5) reduce to

$$A = 2Sw \tag{6}$$

It can be easily shown that (6) is the exact expression for the band absorption in the optically thin limit. *Ramanathan* [1975] used this expression to treat the $CFCl_3$ and CF_2Cl_2 bands.

2. The smeared out line structure limit. In this limit, the line spacing between neighboring lines is much smaller when compared with the line half-width. Consequently, the lines are smeared out and the absorption coefficient follows a smooth variation with wavelength. This limit is adequately satisfied for the $CFCl_3$ and CF_2Cl_2 bands, as can be inferred from the

TABLE 3. Band Parameters for Trace Gases that Employ Equation (1) for the Band Absorption

Species	$\Delta\omega$, cm^{-1}	N	i	f_i	k_i
$CFCl_3$ (CFC11)	60	3	1	0.25	0.72
			2	0.25	0.22
			3	0.5	0.06
CF_2Cl_2 (CFC12)	60	2	1	0.25	0.52
			2	0.75	0.48
CF_4	20	1	1	1	1
All others	60	1	1	1	1

TABLE 4. Band Locations and Strengths

Trace Gas	Band Center, cm^{-1}	Band Strengths, cm^{-1} (atm cm)$^{-1}$ STP: Range of Measurements	Band Strengths, cm^{-1} (atm cm)$^{-1}$ STP: Value Adopted[2]	Reference[1]
CO_2	667	[3]	44 bands incl.	M
N_2O	589	20.7–40.3	27(F, 1H, 4I)	M
	1168	8.5–12	10(F, 1H, 4I)[4]	
	1285	242–384	234.5(F, 1H, 4I)	
CF_4 (F14)	632	42–62	54.7	P
	1261($2\nu_4$) 1285(ν_3)	4175–5934	4175	
C_2F_6 (F116)	714		146	P
	1116		1057	
	1250		3658	
CF_3Cl (F13)	783		157	P
	1102		2505	
	1210		3000	
CF_2Cl_2 (F12)	915	1370–1568	1567.5	K
	1095	1237–1330	1236.8	
	1152	789–893	835.8	
$CHClF_2$ (F22)	810		237	N
	1110		691	
	1310		109	
$CFCl_3$ (F11)	846	1670–1965	1965	K
	1085	576–781	736	
CH_2Cl_2	717	35	35	P
	758	424–548	424	
	898	4.3–5.4	5.4	
	1268	119–147	118.7	
$CHCl_3$	774	864–1201	1009	P
	1220	140–206	140	
CCl_4	776	1317–2026	1437	P
CH_3CCl_3	725		299.8	N
	1080		167	
	1385		14.2	
CH_4	1306	148–185	185	P
	1534	2–3		P
C_2H_2	730	724–804	801	P
	1328	95.6–101.1	95.6	P
SO_2	518	116–125		P
	1151	96–106.8	106.8	
	1362	844–857	857	
Ozone	1041	356–382	376	M
	1103	10–11	11	
	590		78	
	790		321	N
PAN	1160		326	
	1300		272	
	1730		576	
CHF_3	1117–1152		3838.5	P
CH_2F_2	1090		1314	P
$CBrF_3$	1085		2069.3	P
	1209		2074.7	

[1] The reference is for the value adopted in this study: M, *McClatchey et al.* [1973]; N, H. Niki (personal communication, 1983); P, *Pugh and Rao* [1976]; and K, *Kagann et al.* [1983].

[2] F, fundamental band; 1H, first hot band; I, isotopic band. 4I denotes four isotopic bands.

[3] Minimum of 44 isotopic, fundamental, and hot bands are required.

[4] Treated as two band systems: one for the $2\nu_4$ band and one for the hot band, and each system has four isotope bands.

line parameters given by *Goldman et al.* [1976*a*]. Inspection of published spectra reveals that this limit is more than adequately satisfied for most other polyatomic trace gases considered here.

The values of the band parameters and band strengths are given in Tables 3 and 4, respectively. In order to examine the validity of the present approach (i.e., (1)), we computed the surface-troposphere heating due to the strongest band of $CFCl_3$ (F11) with a fine spectral resolution model which computes transmittances at 1 cm^{-1} intervals employing line parameters given by *Goldman et al.* [1976*a*] and performs angular integration with a 12-point Gaussian quadrature scheme. As shown in the next section, the surface-troposphere heating estimated by employing (1) agrees within 4% with that obtained from the detailed computations. The procedure adopted in the present study for the various trace gases is summarized below.

1. For all trace gases except H_2O, CO_2, CH_4, N_2O, and O_3, (1)–(5) are adopted.
2. The parameter, $\Delta\omega$, is assumed to be 60 cm^{-1} for all of

the bands, except CF_4, for which $\Delta\omega = 20$ cm^{-1}. These values are chosen by inspection of the published spectra. For example, *Goldman et al.* [1976*a*, *b*] have shown the spectra for the strongest bands of $CFCl_3$ and CF_2Cl_2. For the $CFCl_3$ band at 846 cm^{-1}, the line strengths in the band wings around 810 and 869 cm^{-1} are smaller by 2 orders of magnitude than their values near the band center. For the CF_2Cl_2 band, the $\Delta\omega$ can be as large as 100 cm^{-1}, but our calculations are rather insensitive to $\Delta\omega$ for $\Delta\omega > 40$ cm^{-1}. The CF_4 band at 1285 cm^{-1} appears to be extremely narrow [*Goldman et al.*, 1979]. Although we have chosen 20 cm^{-1}, we have examined values as low as 5 cm^{-1}, and these results will be discussed subsequently.

3. For $CFCl_3$ and CF_2Cl_2, the exponential-sum fit parameters N, f_i, and k_i are obtained from the random model line parameters published by *Goldman et al.* [1976*a*, *b*]. Note however, as mentioned later, the band strengths are obtained from *Kagann et al.* [1983]. For all other gases, the relevant line parameters are not available, and hence we let $N = 1$. This in turn forces $k_i = 1$ and $f_i = 1$ because of the consistency relationship expressed in (3) and (4).

4. We employ an accurate procedure for evaluating the Planck function. For $\omega > 1000$ cm^{-1}, the Planck variation with ω is so strong that, the Planck function evaluated at the band center (a commonly adopted procedure in climate models) can differ from the mean value for the band by as much as 10–15%. To avoid such errors, the Planck function is evaluated at 10 cm^{-1} intervals within the band, and a mean value for the band is obtained by averaging the narrow band values.

5. Band strengths: Except for $CFCl_3$, CF_2Cl_2, CH_3CCl_3, CFC22, and PAN, we have relied heavily on the published summary by *Pugh and Rao* [1976], denoted as P in Table 4. These authors give a range of measured values, which are reproduced in Table 4. For this study, we have chosen the values measured after the 1970's, and if these were not available, we adopted the middle value of the range given in P. For $CFCl_3$ and CF_2Cl_2 we have adopted the most recent values of *Kagann et al.* [1983]. For the CF_4 ν_3 band at 1285 cm^{-1}, *Wang et al.* [1980] have employed a value of 5934 cm^{-1} (cm atm)$^{-1}$ based on *Saeki et al.*'s [1976] measurements. This value is beyond the range given by *Pugh and Rao* [1976], and furthermore, the recent measurements by *Goldman et al.* [1979] yield a value of 4500 cm^{-2} atm^{-1}. The band strengths for CH_3CCl_3, $CHClF_2$ (F22), and PAN are not available in the open literature. High-resolution spectral data for these bands and integrated band strengths were kindly supplied to us by H. Niki (personal communication, 1983), whose values are shown in Table 4 as N.

TABLE 5. Surface-Troposphere Heating due to CFC11 846-cm^{-1} Band

Model*	F, W m^{-2}	Comment
Reference	0.51	Narrow-band model with 1-cm^{-1} resolution; 12-point Gauss quadrature for angular integration.
Present scheme	0.525	Equations (1)–(5). Parameters from Table 3.
Optically thin approximation	0.59	Equation (6)

Atmosphere: midlatitude clear-sky conditions. *F*: surface-troposphere heating due to increase of CFC11 from 0 to 2 ppb.

*For comparison purposes, all the three models adopt the spectroscopic parameters from *Goldman et al.* [1976*a*].

6. The CFC's and other trace gases besides CO_2 are assumed to be mixed uniformly from the surface up to 12 km, above which the mixing ratio is assumed to decrease with a scale height of 3 km. However, as shown by *Fabian et al.* [1984], the mixing ratios of long-lived species such as CF_4, C_2F_6, and CF_3Cl are nearly constant from the surface to the middle stratosphere (~30 km). In the next section we will examine the sensitivity of the greenhouse effect to the mixing-ratio profile. CH_4, N_2O, and CO_2 are assumed to be uniformly mixed throughout the atmosphere. The observed mixing ratio of CH_4 and N_2O decreases with height above 12 km. However, as shown in the next section, the computed surface warming due to CH_4 and N_2O increase is insensitive to their mixing-ratio profile in the stratosphere. The O_3 profile is taken from the hemispherical, annual data given by *Ramanathan and Dickinson* [1979].

7. We have allowed for the overlap of all of the minor trace gas bands with H_2O, CO_2, O_3, CH_4, N_2O, and CFC's and the mutual overlap of these gases. In certain spectral locations, e.g., 1285 cm^{-1}, as many as four gases have strong overlapping bands, and such effects are included in the calculations. For all of the trace gases with band centers shortward of 8 μm and longwave of 12 μm, the overlap with CH_4, N_2O, CO_2, or H_2O is treated by adopting the Malkmus narrow-band model. The transmission is computed with a spectral resolution of 20 cm^{-1}. The line parameters are derived from the 1982 Air Force Geophysics Laboratory (AFGL) line tape [*Rothman et al.*, 1983]. Hence the overlap treatment does not follow the broadband model approach.

In summary, the number of trace gases included in this study, together with the treatment of the overlap between the various gases and the details of the various fundamental, hot, and isotopic bands, make the present study the most comprehensive climate model calculations that have been performed so far for the trace gas climate effects.

4.3. *Accuracy of the Trace Gas Radiative Treatment*

The accuracy of the treatment as given by (1)–(5) is examined by performing detailed narrow-band calculations for the $CFCl_3$ band at 11.8 μm. This band is chosen because it is the strongest of the CFC bands and hence provides a stringent test of the present scheme. Furthermore, random-band model parameters, with a spectral resolution of 1 cm^{-1}, for this band have been provided by *Goldman et al.* [1976*a*]. For the reference calculations, a Malkmus random-band model with a spectral resolution of 1 cm^{-1} is employed. The details of this model are given by *Kiehl and Ramanathan* [1983]. The angular integration within each spectral interval is performed with a 12-point Gaussian quadrature. The model atmosphere represents midlatitude summer condition with no clouds. In Table 5, the change in the net (down-up) flux at the tropopause, i.e., the surface-troposphere heating, due to increase of CFC11 from 0 to 2 ppb as computed by the reference model is compared with that obtained from the present scheme, i.e., (1)–(5). Also shown in this table, for comparison purposes, is the result obtained from (6), which is the form of the optically thin limit equation employed by *Ramanathan* [1975]. It is seen that the present scheme is in excellent agreement with the more detailed calculations. The equation for the optically thin assumption employed by *Ramanathan* [1975] overestimates the heating by about 16%. However as shown later, the sur-

TABLE 6. Examples of the Effect of Overlapping of Absorption Bands on the Computed Surface Warming

Constituent	Change	With Overlap* ΔT_s	With Overlap* ΔT_g	Without Overlap ΔT_g
CH_4†	1.25X	0.09	0.08	0.19
N_2O†	1.25X	0.12	0.1	0.2
CF_2Cl_2 (F12)‡	0–1 ppb	0.16	0.15	0.19
$CFCl_3$ (F11)	0–1 ppb	0.14	0.13	0.16
CF_4 (F14)	0–1 ppb	≈0.06	≈0.05	0.12
CF_3Cl (F13)	0–1 ppb	0.22	0.2	0.25
CH_2Cl_2	0–1 ppb	≈0.03	≈0.02	0.04
$CHCl_3$	0–1 ppb	≈0.06	≈0.06	0.09
CCl_4	0–1 ppb	≈0.08	≈0.07	0.11
C_2H_2	0–1 ppb	≈0.02	≈0.02	0.07
C_2F_6 (F116)	0–1 ppb	0.13	0.12	0.2
CH_3CCl_3	0–1 ppb	≈0.02	≈0.01	0.04
PAN	0–1 ppb	≈0.04	≈0.03	0.06

ΔT_s is surface-air temperature change, and ΔT_g is surface (or ground) temperature change.

*Numbers have been rounded off; when ΔT is less than about 0.02 K, because of the convergence criterion, the result may be uncertain by as much as ±30%.

†CH_4 and N_2O are assumed to be uniformly mixed from the surface to the top of the atmosphere. However, these calculations, when repeated with observed profiles which show a decrease in the mixing ratio above 12 km, yield ΔT results identical to those shown in this table.

‡For this gas and for all the others following it, the mixing ratio decreases above 12 km with a scale height of 3 km. The computed surface warming is larger by about 15% when the mixing ratio above 12 km is held constant at the surface value.

face warming due to increase of CFC's computed with the present accurate scheme is in excellent agreement with that estimated by *Ramanathan* [1975]. The agreement is because of the following compensating effects: (1) the band strengths used in *Ramanathan* [1975] are smaller by about 10% than the recent values used in this study; (2) the 16% error shown in Table 5 is reduced somewhat with the inclusion of clouds; (3) the error in the optically thin approximation is smaller for the other bands of CFC11 and 12 whose strengths are considerably smaller than the 11.8-μm CFC11 band.

Cess [1982] has also performed similar narrow-band calculations for $CFCl_3$ and showed that the smeared-out line structure assumption, which is invoked in arriving at (1), is an excellent approximation for CFC bands. In summary, we conclude that the present scheme is very accurate. The only source of remaining error is the neglect of the temperature dependence of the hot bands of CFC's that have been detected, in the vicinity of the strong $CFCl_3$ and CF_2Cl_2 bands, by *Varanasi and Ko* [1977] and *Nanes et al.* [1980]. While the effects of the hot bands are included in this study, the temperature dependence of their band strengths arising from the temperature dependence of the excited vibrational states is ignored. *Nanes et al.* [1980], however, suggest only a weak temperature dependence. As a note of caution, we add that the temperature dependence mentioned above should not be confused with the temperature correction that is needed to convert band strengths, S, measured at temperature T to STP conditions. Recall that in (1), the path length w is in cm atm, STP, and hence S measured at a temperature T in the units of cm^{-1} $(cm\ atm)^{-1}$ should be multiplied by $(T/273)$ to convert to the units of cm^{-1} $(cm\ atm)^{-1}$, STP. In some instances in the literature, this correction factor has been confused for the temperature dependence of S. The procedure of employing the correction factor $(T/273)$ is rigorous for the fundamental CFC bands. For the hot bands, however, we need an additional term to account for the temperature dependence of the excited vibrational state [e.g., see *Kiehl and Ramanathan*, 1983, equation 12].

5. RESULTS

5.1. *Uniform Increase in Certain Trace Gases*

Before presenting the results for the trace gas scenario shown in Table 1*a*, we will discuss results for a hypothetical case of 0–1 ppb increase for several of the trace gases. The purpose of this exercise is twofold: to elucidate the processes that determine the magnitude of the trace gas effects and to identify the most important trace gases from a climate viewpoint. For these two objectives, we avoid specific scenarios to assure that conclusions are not scenario dependent.

The computed surface warming due to a 0–1 ppb increase in 15 different trace gases is shown in Figure 1. The tropospheric O_3, CH_4, and N_2O effects are relatively better known and are shown merely for comparison purposes. Several interesting and rather surprising features of the results shown in Figure 1 are noted below.

TABLE 7. Computed Surface Temperature Change Resulting From Increasing CFC's From 0 to 2 ppbv[1]

Item	Model	FCA,[2] K	FCT,[3] K	Empirical,[4] K
1	*Ramanathan* [1975]	0.56[5]	0.9	0.9
2	*Reck and Fry* [1978]	0.76[6]		
3	*Chamberlain et al.* [1982]			1.42
4	*Wang et al.* [1976]	0.38	0.56	
5	*Wang et al.* [1980]		0.69	
6	*Hansen et al.* [1982]		0.50	
7	*Lacis et al.* [1981]		0.65	
8	*Karol et al.* [1981]	0.8		
9	*Hummel and Reck* [1981]	0.76		
10	This study[7]	0.55–0.6[8]		
11	This study (uniformly mixed)[9]	0.63–0.7[8]		
12	This study: CFC band strengths from *Ramanathan* [1975]	0.51–0.56[8]		
13	This study: CFC band strengths from *Varanasi and Ko* [1977]	0.50–0.55[8]		

Comparison of various model results. $CFCl_3$ and CF_2Cl_2 are each increased from 0 to 2 ppbv.

[1] *Ramanathan* [1975], this study, and the GISS models (items 4–6) assume a constant CFC mixing ratio from the ground to 12 km, and above 12 km the mixing ratio decreases exponentially with a scale height of 3 km. *Reck and Fry* [1978], *Karol et al.* [1981], and *Hummel and Reck* [1981] assume a constant CFC mixing ratio from the ground to the top of the atmosphere.

[2] One-dimensional radiative-convective model with fixed relative humidity and with fixed-cloud altitude (FCA).

[3] Same as footnote 2, but with fixed-cloud temperature (FCT) instead of fixed-cloud altitude.

[4] Estimated from an empirical expression for the surface temperature sensitivity parameter.

[5] The FCA model results were not mentioned by *Ramanathan* [1975] but were obtained for the purposes of the present comparison.

[6] Reck and Fry gave ΔT results for 1-ppbv increase, which was linearly scaled for the 2-ppbv increase.

[7] CFC mixing ratio as described by *Ramanathan* [1975]. See footnote 1 above.

[8] The lower value is surface temperature change, and upper value is surface air temperature change.

[9] CFC mixing ratio is constant from surface to top of the atmosphere.

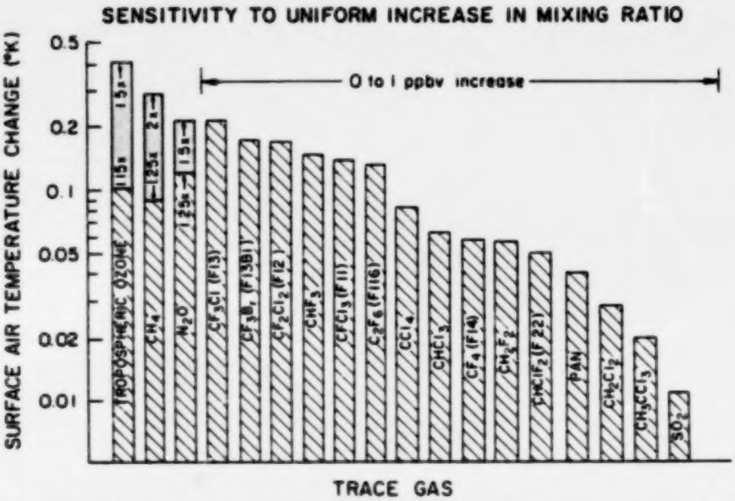

Fig. 1. Surface temperature increase due to a 0–1 ppbv increase in trace gas concentration. Tropospheric O_3, CH_4, and N_2O increases are also shown for comparison.

1. Among the other trace gases, $CFCl_3$, CF_2Cl_2, CF_3Cl, C_2F_6, CHF_3, and $CBrF_3$ exert the largest surface warming effect. The contribution by CF_3Cl, C_2F_6, CHF_3, and $CBrF_3$ has not been discussed before and is a surprising and new aspect of the present results. The primary reason is the strength of their bands, and as shown in Table 4, the strongest bands of these gases are stronger than the strongest bands of $CFCl_3$ and CF_2Cl_2 by more than a factor of 2. The location of the band center, however, plays a crucial role because of the overlap effect. For example, in the 1295-cm^{-1} region, the absorption by N_2O, CH_4, and H_2O bands saturates this region, and hence trace gases in this spectral region have relatively lesser impact on climate. This is the primary reason why CF_4, although possessing a band in the 1285-cm^{-1} region which is stronger than any other bands in the 8- to 20-μm region, produces a surface warming of only 0.06 K.

2. The sensitivity of surface temperature to tropospheric ozone has been anticipated earlier [*Ramanathan and Dickinson*, 1979] but has not received much consideration elsewhere in the literature.

3. Although PAN has several moderately strong bands, its strongest band is in the middle of the strong 6.3-μm H_2O bands. Similarly, although CCl_4 and $CHCl_3$ have moderately strong bands, their strongest bands are located in the 774-cm^{-1} region, where they are overlapped by CO_2, H_2O rotation bands, and the H_2O continuum.

4. To illustrate the importance of the overlap problem, we show in Table 6 the surface temperature increase with and without the overlap effects. Such results, besides illustrating the contribution from various radiative processes, also facilitate model intercomparison study by enabling the identification of the sources for model differences. We also show in this table, the surface and surface air temperature change for one of the two cases. In general, surface air temperature is larger than the surface temperature change by about 10%. It is clear from Table 6 that for several trace gases, e.g., CF_4, $CHCl_3$, CH_3CCl_3, C_2F_6, the overlap effect ameliorates ΔT_s by factors of 1.5–2.

We will now compare the present estimates of ΔT_s with other published estimates for a few of the trace gases. Consider first $CFCl_3$ and CF_2Cl_2 for which the differences between the various model estimates of the global surface temperature change are disturbingly large as illustrated in Table 7. The differences shown in Table 7 can arise from differences in the radiative treatment and (or) from differences in the model sensitivity. In order to isolate these two sources, the climate sensitivity parameter, λ, as estimated from various models is shown in Table 8. As explained by *Dickinson* [1982] and *Ramanathan* [1982], λ and ΔT_s are approximately related by

$$\Delta T_s \approx \lambda \Delta F \tag{7}$$

where ΔF is the radiative forcing of the surface-troposphere system due solely to trace gas increase, i.e., CFC increase in the present example. As described below, Tables 7 and 8 provide the answers for all of the differences in the computed ΔT_s.

1. There is a wide spread in the measured band strengths. For example, Figure 2 shows the measured band strengths by various investigators for the strongest CFC bands. The present study uses the recent measurements of *Kagann et al.* [1983], whereas all of the other studies employ the earlier measurements. The values used by *Ramanathan* [1975] underestimate (compare item 12 with item 10) ΔT_s by 8% while Varanasi and Ko's values employed in the Goddard Institute for Space Studies (GISS) models underestimate (compare item 13 with item 10) ΔT_s by 10%.

2. With respect to the radiative treatment, *Ramanathan* [1975] and *Chamberlain et al.* [1982] employ (6), which is one form of the optically thin approximation. By comparing item 12 with 1, both of which use the same band strengths, it is seen that (6) overestimates ΔT_s by about 5%. However, the present study which uses an accurate procedure is in excellent agreement with *Ramanathan* [1975] because of the compensating effects of the smaller band strengths used in that study. The other models cited in Table 7, unfortunately, do not give the equation or the details of their radiative treatment. However, all of these models rely primarily on integrated band strengths and hence must employ the optically thin approximation, but not necessarily (6).

3. The unrealistically large value obtained by *Chamberlain et al.* [1982] results primarily from their approach of esti-

TABLE 8. Comparison of Model Climate Sensitivity Parameter

Model	λ, K/W m^{-2}	f^*	f (empirical)
Manabe and Wetherald [1967]	0.53		
Ramanathan [1975]	0.52	1.6	1.6
Reck and Fry [1978]	0.53		
Wang et al. [1976]	0.47	1.5	
Wang et al. [1980]	0.47	1.23	
Hansen et al. [1982]	0.47	1.4	
Lacis et al. [1981]	0.47	1.4	
This study	0.52		

Here, $f^* = \lambda(\text{FCT})/\lambda(\text{FCA})$; $f(\text{empirical}) = \lambda(\text{empirical})/\lambda(\text{FCA})$. See Table 7 (footnotes 2 and 3) for explanation of FCA and FCT.

mating the CFC heating from the change in the net flux at the surface rather than at the tropopause (see *Ramanathan* [1982] for more details on this topic).

4. *Hummel and Reck* [1981], *Karol et al.* [1981], and *Reck and Fry* [1978] assume the CFC mixing ratio to be uniform from the surface to the model top, whereas *Ramanathan* [1975], the present study, and the GISS models assume an exponentially decaying mixing ratio (see footnote 1 in Table 7) in the stratosphere. Our model calculations, when repeated with a constant mixing ratio, show that the constant mixing ratio overestimates (compare items 10 and 11) ΔT_s by about 15%. Reducing these constant mixing-ratio model estimates by 15% would bring them closer to the present values.

5. This brings us to the GISS models. First note from Table 7, the estimates from the various versions of these models have undergone substantial change. We will adopt the latest result of *Lacis et al.* [1981] as their best estimate and compare this with that of the present study. Lacis et al. have not given the result for the fixed-cloud altitude (FCA) model, but using the factor $f^*(= 1.4)$ in Table 8, we infer from Table 7 that the Lacis et al. result for the FCA version is 0.46 K (= 0.65/1.4). The sensitivity of their model is smaller than that of the present model by 11% (= 0.52/0.47). Furthermore, Varanasi and Ko's band strengths used in their study underestimates ΔT_s by 10% (compare items 10 and 13 in Table 7). Their model result of 0.46 K when corrected for the above differences increases to 0.56 (0.46 × 1.11 × 1.1), which is in close agreement with the present estimate of 0.55–0.6 K.

In summary, we can account for almost all of the differences between the various model estimates. The analyses lead to the conclusion that, in view of the accurate treatment of the CFC radiative effects and in view of the detailed and up-to-date spectroscopic information incorporated in this study, the present estimates of 0.55–0.6 K for CFC increase from 0 to 2 ppb should be considered as the state-of-the art estimates for a radiative-convective model with fixed cloud top altitude.

For CF_4, the only available calculation is that of *Wang et al.* [1980], who compute a surface temperature change, for 0–1 ppbv change in CF_4, of 0.07 K to be compared with the present value of 0.06 K. Although the close agreement is reassuring, there are substantial differences in the CF_4 treatment between the two models. Wang et al.'s band strength is larger than the present study value by 40% and also they assume a 5-cm^{-1} bandwidth. Decreasing the bandwidth from 20 to 5 cm^{-1} in the present model leads to about 20% reduction in ΔT_s, while increasing the band strength to Wang et al.'s value of 5934 cm^{-2} atm^{-1} leads to abut 25% increase in ΔT_s. It is not clear how the overlap of CF_4 with H_2O, N_2O, and CH_4 is treated in Wang et al.'s model calculations.

Hummel and Reck [1981] have computed the effects of $CHClF_2$ (CFC22), CH_3CCl_3, and CH_2Cl_2. Their surface warming for $CHClF_2$, CH_3CCL_3, and CH_2Cl_2 are, respectively, (for 0–1 ppb increase) 0.04, 0.02, and 0.01, and the respective results of the present study are 0.05, 0.02, and 0.01 K. The two models seem to be in good agreement. Since *Hummel and Reck* [1981] have given neither the quantitative details of their radiation model nor the band strengths, it is difficult to rule out the possibility of a fortuitous agreement.

Sensitivity to vertical distribution. The sensitivity of the computed surface temperature change to vertical O_3 distribution is discussed in the next section. The discussion here is restricted to those gases that are uniformly mixed in the troposphere, i.e., all of the gases, other than O_3, shown in Figure 1.

Observed profiles of CH_4 and N_2O reveal a decrease in the mixing ratio above about 12 km as opposed to the constant mixing-ratio profile assumed in this study. The scale height for the mixing ratio depends strongly on latitude [*World Meteorological Organization*, 1982*b*]. Midlatitude profiles show a sharper decrease (scale height ≈8 km) with altitude than tropical profiles (scale height >15 km). We repeated the surface temperature calculations with the observed midlatitude profiles [*World Meteorological Organization*, 1982*b*, Figures 1-43 and 1-44]. For a doubling of CH_4, both the uniform mixing-ratio profile and the midlatitude profile yielded a ΔT_s of 0.31 K. Similarly, for a doubling of N_2O, both mixing ratio profiles yielded a ΔT_s of 0.4 K. The scale height of the mixing ratio for CH_4 and N_2O is sufficiently large (≥8 km) that the stratospheric column abundance (of CH_4 and N_2O) for the uniform mixing-ratio profile and the observed profile is nearly the same, and hence both profiles yield the same surface warming.

For all of the other trace gases shown in Figure 1, the computed ΔT_s is about 15% larger for the uniform mixing-ratio profile than for the reference profile (assumed in this study) in which the mixing ratio decreases (above 12 km) with

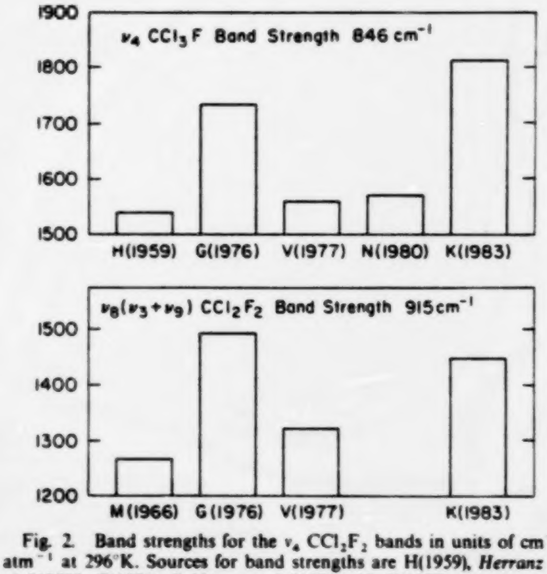

Fig. 2. Band strengths for the ν_4 CCl_2F_2 bands in units of cm^{-2} atm^{-1} at 296°K. Sources for band strengths are H(1959), *Herranz et al.* [1959]; G(1976), *Goldman et al.* [1976*a*, *b*]; V(1977), *Varanasi and Ko* [1977]; N(1980), *Nanes et al.* [1980]; and K(1983), *Kagann et al.* [1983].

a scale height of 3 km. This nonnegligible sensitivity in the computed surface warming for these trace gases is largely because of the substantial difference in the stratospheric abundance between the uniform mixing-ratio profile and the profile with a 3-km scale height.

5.2. *Climatic Effects of the Projected Increases*

Figure 3 shows the results of the radiative-convective model calculations employing the projected increases shown in Tables 1*a* and 2. Our results basically confirm the suggestions by earlier calculations (see *World Meteorological Organization*, [1982*a*] for a summary) that the other trace gases can amplify the CO_2 surface warming by factors ranging from 1.5 to 3. But our results reveal several new features. We will summarize these features by considering the "best estimate" curve in Figure 3.

1. The surface warming (ΔT_s) due to all the trace gases (shown in Figure 3) is 1.54 K. The increase in CO_2 contributes about 0.71 K.
2. The CFC's, $CFCl_3$ (F11) and CF_2Cl_2 (F12), have the largest warming effect of all the trace gases besides CO_2. The direct radiative effect of $CFCl_3$ and CF_2Cl_2 (increase) contributes about 0.36 K to the surface warming. Furthermore, the stratospheric O_3 change, resulting largely from the projected increase in CFC's, leads to an additional warming of about 0.08 K. Hence the combined effect of 0.44 K due to CFC's is roughly 60% of the CO_2 effect.
3. Somewhat smaller, but nonnegligible, surface warming results from the increases in CH_4 (0.14 K), N_2O (0.1 K) and tropospheric O_3 (0.06 K).
4. Increases in $CHClF_2$ (F22), CH_3CCl_3, and CF_3Cl contribute, respectively, about 0.04 K, 0.02 K, and 0.01 K. All others shown in Figure 3 have negligible (<0.005 K) impact.

The warming we compute due to stratospheric ozone is at variance with *Wang et al.* [1980] results, who compute a surface cooling due to CFM-induced ozone perturbations. The major source of discrepancy is in the adopted stratospheric O_3 perturbation profile. The present profile is based on the most recent chemistry and reaction rates, and it shows that large decreases in middle and upper stratospheric O_3 profile are accompanied by somewhat smaller percentage increases in the lower stratosphere. Additional calculations were performed to examine the sensitivity of the computed surface warming to vertical distribution of O_3 change, which lead to the following inferences. The profile shown in Table 2 leads to a surface warming of 0.08 K. Roughly, 0.06 K is due to the O_3 decrease above 30 km, and the remainder of 0.02 K is due to the O_3 increase below 30 km. Thus the O_3 decrease above 30 km as well as the O_3 increase below 30 km contribute to a warming. The perplexing nature of this result can be understood from the detail analyses given by *Ramanathan et al.* [1976] and *Ramanathan and Dickinson* [1979], and hence only a brief discussion is given below.

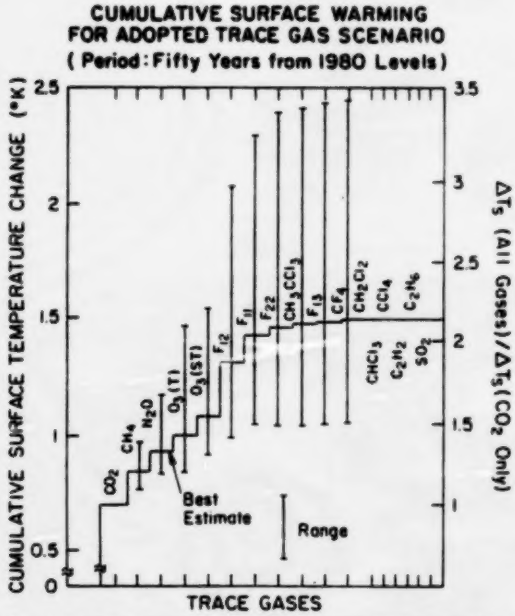

Fig. 3. Cumulative equilibrium surface temperature warming due to increase in CO_2 and other trace gases. Increases in gas amounts from 1980 values to 2030.

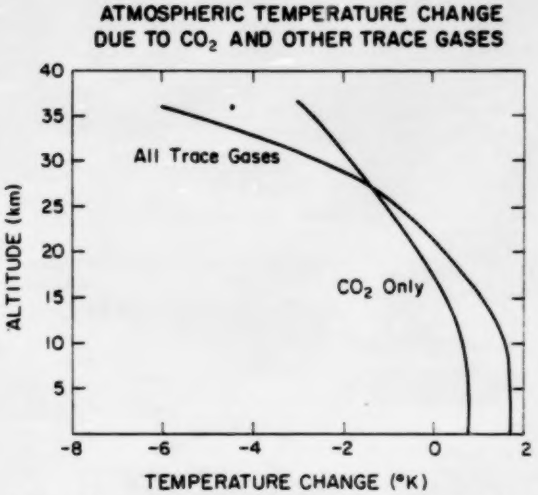

Fig. 4. Change in the vertical distribution of temperature due to an increase in CO_2 alone, and CO_2 along with all other trace gases listed in Figure 3. The trace gas increase scenario is as given by the "best estimate" values in Table 1*a*.

A decrease in stratospheric O_3, irrespective of the altitude of the decrease, would lead to an increase in the solar radiation reaching the troposphere, and this solar effect would tend to warm the surface. However, O_3 also alters the IR (longwave) emission from the stratosphere in two ways: first, the decreased solar absorption (due to O_3 decrease) cools the stratosphere; the cooler stratosphere emits less downward to the troposphere. Second, a decrease in O_3 reduces the absorption (by the O_3 9.6-μm band) of the surface-troposphere emission. This reduction causes an additional cooling of the stratosphere, which in turn, causes an additional reduction in the downward IR emission by the stratosphere. Thus the IR effects of O_3 decrease tend to cool the surface. However, the IR opacity of stratospheric CO_2, H_2O, and O_3 is sufficiently strong that the impact of the reduction in IR emission (by the stratosphere) on the surface diminishes with an increase in the altitude of O_3 perturbation. On the other hand, the surface warming induced by the solar effect is independent of the altitude of O_3 perturbation. Consequently, for a decrease in O_3 in the upper stratosphere, the solar effect dominates (leading to a surface warming), while for a decrease in the lower

TABLE 9. Gases Not Shown in Figure 3

Gas	7- to 13-μm Absorption Feature	Predicted Concentration Increase	Potential Role
$CHCl_2F$	band intensities unavailable	yes	yes
$C_2Cl_3F_3$	band intensities unavailable	yes	yes
$C_2Cl_2F_4$	band intensities unavailable	yes	yes
C_2ClF_5	band intensities unavailable	yes	yes
SO_2; CS_2; H_2S	strong	uncertain	no
COS; CS_2; H_2S	weak	no	no
CH_2ClCH_2Cl	strong	small	no
CH_3Cl	weak	no	no
C_2H_6; C_2H_4; C_3H_8	weak	uncertain	no
HCHO; CH_3CHO	weak	uncertain	no
CH_3F; CH_3Br; CH_3I	weak	uncertain	no
CH_2F_2	strong	uncertain	yes
CHF_3	very strong	uncertain	yes
$CBrF_3$	very strong	small	no
HNO_3	strong	small but uncertain	no
NO_x(NO, NO_2, NO_3, N_2O_5)	weak	uncertain	no
HCN	weak absorption	uncertain	no

The first four chlorofluorocarbon gases here could contribute significantly to future global warming because of the spectral positions of their absorption bands in the 7–13 μm atmospheric window region if their band-absorption intensities are large enough. For other gases, e.g., HCN and SO_2, their absorption bands are not strong enough to be significant at present or near-present atmospheric concentrations. For other gases such as C_2H_6 and CH_3F, we have too little information to be able to estimate future trends.

stratospheric O_3, the IR effect dominates (leading to a surface cooling).

The uncertainty in our computed surface warming due to stratospheric O_3 change is best illustrated by the following examples. The profile of O_3 change in Table 2 for altitude above 30 km when combined with 10% uniform O_3 decrease between 12 and 30 km leads to a surface warming of 0.02 K; whereas the same profile (as in Table 2) above 30 km when combined with a 10% uniform O_3 increase between 12 and 30 km leads to a surface warming of 0.1 K. In view of the high sensitivity of the computed temperature change to the vertical O_3 profile, our computed estimates for stratospheric O_3 change should be viewed with caution because such distributions would be influenced by atmospheric dynamics (whose effects are ignored in this analysis) and of course by remaining uncertainties in model chemistry.

The vertical distribution of the computed atmospheric temperature change is shown in Figure 4. It is clear from this figure that other trace gas effects on temperatures are comparable to CO_2 effects, not only for surface warming, but also for stratospheric cooling. The stratospheric cooling, to a large extent, results from the stratospheric O_3 reduction. The potential climatic effect of gases that are not explicitly discussed in Figure 3 is summarized in Table 9.

5.3. *Effects of the Inferred Trace Gas Increases From the Preindustrial to the Present Levels*

For the sake of discussion, the concentrations for the year 1880 are associated with the preindustrial levels, and these concentrations have been shown in Table 1*b*, while the observed 1980 concentrations are shown in Table 1*a*. The computed equilibrium temperature changes are shown in Table 10. The CO_2 increase causes a surface warming of 0.52 K, which is enhanced by 50% due to the increase in the other trace gases. The computed stratospheric cooling due to CO_2 increase is substantial, but that due to other gases is negligible. The computed stratospheric cooling would be larger had we included the effects of stratospheric O_3 decrease due to increases in CFC's. From Table 10*b*, which shows the contribution of the individual gases, it is seen that CH_4, tropospheric O_3, and CFC's are the largest contributors, next to CO_2, to the surface warming computed for the period 1880–1980.

6. SUMMARY

The basic conclusion that can be derived from the present study is that the radiative effects of increases in trace gases (other than CO_2) are as important as that of CO_2 increase in determining the climate change of the future or the past 100 years. Several tens of man-made chemicals have been detected in the troposphere and about 20 of these have strong absorption features in the 7- to 13-μm regions of the longwave spectrum. The present-day, taken as the year 1980, concentrations are taken from in situ observations. A careful analysis of the measured trends from early 1970's to 1980 form the basis for the concentrations projected 50 years into the future. Published ice-core CH_4 observations, surface-based O_3 observations, and other studies are used to infer the trace gas concentrations for the preindustrial era. The equilibrium surface and atmospheric temperature changes estimated with the aid of a radiative-convective model reveal the following features.

1. The preindustrial to present-day increase in CO_2 causes an equilibrium surface warming of 0.5 K in the model, which is enhanced by a factor of 1.5 by the increases in the other trace gases. CH_4, tropospheric O_3, and CFC's are the largest contributors to this enhancement. The upper stratospheric cooling due to the CO_2 increase is as large as about 3 K.

2. The projected CO_2 increase from 339 ppm in the year 1980 to 450 ppm in 2030 warms the model surface by 0.7 K, which is enhanced by a factor of about 2.1 by the other trace

gases. The factor of trace gas enhancement varies from about 1.5 to 3 depending on the assumed scenario. The trace gases that contribute to this significant enhancement are $CFCl_3$ (F11), CF_2Cl_2 (F12), CH_4, N_2O, stratospheric and tropospheric O_3. Somewhat smaller but nonnegligible contributions arise from $CHClF_2$ (F22), CH_3CCl_3, and $CFCl_3$.

3. The stratospheric O_3 changes resulting from the assumed increase in CFC's and other chlorine compounds by year 2030 are a large decrease in middle stratospheric O_3 accompanied by a slight increase in lower stratospheric O_3. Hence although CFC's are estimated to cause only a slight reduction in the column ozone, the significant perturbation to the shape of the O_3 profile leads to a nonnegligible surface warming of 0.08 K. Thus the O_3 change due to CFC's adds to the surface warming of 0.36 K resulting from the CFC direct radiative effects. These two effects when considered together make CFC's the largest contributors (next to CO_2) to the overall surface warming computed in this study. However, because of the strong sensitivity of the computed surface warming to the vertical profile of O_3 change, the magnitude of the potential surface warming due to stratospheric O_3 change is highly uncertain.

4. All of the other trace gases perturb the vertical atmospheric profile in the same manner as CO_2 in the following sense: they warm the surface and the troposphere while cooling the stratosphere (above 20 km) significantly. However, there is one important difference between the radiative effects of CO_2 and the other trace gases: as pointed out by *Dickinson et al.* [1978], CFC's have a strong warming on the tropical tropopause. Also the studies by *Ramanathan and Dickinson* [1979] and *Fels et al.* [1980] reveal the significant sensitivity of tropical tropopause to O_3 perturbations. Warming of the tropical tropopause by 2-3 K could lead to large changes in stratospheric water vapor.

5. On a ppb basis, CF_3Cl has the strongest greenhouse effect (exceeding very slightly even that of CFC12) followed closely by $CBrF_3$, CF_2Cl_2 (F12), CHF_3, $CFCl_3$ (F11), and C_2F_6 (F116), all of which have effects comparable to that of $CFCl_3$ or CF_2Cl_2. Gases such as CF_4, CCl_4, and PAN have strong absorption features, but due to the overlap with CH_4, N_2O, CO_2, and H_2O bands, these gases are not very effective in enhancing the atmospheric greenhouse effect. However, our conclusion concerning the overlap effects should be considered as tentative. Measurements of narrowband spectroscopic parameters for these other trace gases are currently not available, and such measurements are needed for improving the accuracy of the estimates for the overlap effects. For important species such as $C_2Cl_3F_3$ (F113), $C_2Cl_2F_4$ (F114), and C_2ClF_5 (F115) even band strengths are not available.

6. The accurate radiation model developed here for $CFCl_3$ (F11) and CF_2Cl_2 (F12) helped sort out the differences between the various published studies for the estimated surface warming.

The important implication of this study is that the preindustrial to the present increase in CO_2 and the other trace gases might, very likely, have caused a significant perturbation to the radiative heating of the climate system. This perturbation radiative heating induces a warming of about 0.8 K in the present model, whereas it might have induced a warming twice as large in recent GCM's [*Washington and Meehl*, 1984; *Hansen et al.*, 1984]. These GCM's compute a 4 K global warming due to CO_2 doubling as opposed to the 2 K yielded by the radiative-convective model. The 0.8–1.6 K global warming, had it indeed occurred from the preindustrial to the present, should have been detectable above the statistical fluctuations of the climate. This is a controversial issue, and the published papers have contradictory results. *Hansen et al.* [1982] suggest that the CO_2 warming is discernible from observed records of global or hemispherical average temperatures. The statistical analysis of the 70-year homogeneous (in time and in longitude) temperatures for 50–70°N by *Madden and Ramanathan* [1980] has failed to reveal the CO_2 effect. Before we can attempt to verify the greenhouse theories of preindustrial to present warming by comparing model results with the observations, the following important issues must be dealt with.

1. The one-dimensional and GCM results pertain only to the equilibrium warming of the surface to a step-function increase in the trace gases. The quantity of interest, for the purpose of verification, is the transient climate response to a time-varying distribution of trace gases. Even assuming that time-dependent trace gas distribution is known (for the past 100 years), our understanding of the ocean mixed layer interactions with the atmosphere and the thermocline as well as the lateral ocean heat transport is too imprecise to estimate reliably the transient response of the climate system.

2. Other climate forcing terms, e.g., solar irradiance, volcanic aerosols, surface radiative properties, can also change on the time scales of interest to this study, and we do not have adequate data bases to estimate their contributions to past climates. Major volcanic events, such as El Chichon, can cause an equilibrium global cooling of 0.5–1 K, but the aerosol residence time is about 2 years or less, and as yet, we have not come to grips with the tough issue of estimating the transient response to an episodic forcing.

3. The last issue concerns the source of errors in observations of temperatures, humidities, and other trace gases arising from instrumental and sampling biases. There are no reliable global measurements for key components like lower stratospheric H_2O and tropospheric O_3.

It is hoped this study will provide more scientific justification for making some key measurements on a long-term

TABLE 10. Computed Temperature Changes due to Inferred Trace Gases for the Period 1880–1980

Constituent	Temperature Change, K Surface*	Stratosphere, km 26–30	 38–42
a. Surface and Stratospheric Temperature Change			
CO_2	0.52	−0.77	−2.78
CO_2 plus all other gases	0.79	−0.8	−2.85

Constituent	Concentration Change	Temperature Change
b. Itemized Contribution to Surface Warming		
CO_2	275–339 ppm	0.52
CH_4	1.15–1.65 ppm	0.12
N_2O	0.285–0.3 ppm	0.02
Troposphere O_3	12.5%	0.04
CFC11	0–0.18 ppb	0.025
CFC12	0–0.28 ppb	0.04
All others in Table 1*a*	0 to 1980 values	0.02

Possible changes in stratospheric O_3 are ignored.

*Surface air temperature change is larger than the surface temperature change by about 10–13%.

basis of trace gas trends (at least the top 12 gases identified here), stratospheric aerosols, stratospheric humidity, and tropical tropopause temperatures. Of equal importance, accurate measurements of narrow-band spectroscopic parameters and band strengths for the trace gases are urgently needed.

Acknowledgments. We are indebted to Dr. Niki for providing unpublished data. One of us (V.R.) thanks the Atmospheric Sciences Division, NASA Langley for the hospitality extended during the sabbatical visit. L. B. Callis of NASA Langley provided a careful review of an earlier version of this manuscript. We thank Gretchen Escobar for typing several versions of this manuscript. We also thank M. Coffey of NCAR for providing the routines and data tapes for inferring narrow-band model parameters. NCAR is sponsored by the National Science Foundation.

REFERENCES

Alexandrov, E. L., J. L. Konol, A. Ch. Khrgian, L. R. Rakipova, and Yu. S. Sedonov, Contribution of ozone and other minor trace gases to atmospheric radiation regime and their possible effect on global climate change, WMO Global Ozone Res. and Monitoring Proj. Rep. 10, 79 pp., World Meteorol. Organ., Geneva, 1981.

Andreae, M. O., and H. Raemdonck, Dimethyl sulfide in the surface ocean and the marine atmosphere: A global view, *Science, 221*, 744–747, 1983.

Angell, J. K., and J. Korshover, Global variation in total ozone and layer-mean ozone: An update through 1981, *J. Climate Appl. Meteorol., 22*, 1611–1627, 1983.

Bauer, E., A catalog of perturbing influences on stratospheric ozone 1955–1975, *J. Geophys. Res., 84*, 6929–6940, 1979.

Berg, W. W., L. E. Heidt, W. Pollock, P. D. Sperry, R. J. Cicerone, and E. S. Gladney, Brominated organic species in the Arctic atmosphere, *Geophys. Res. Lett., 11*, 429–432, 1984.

Blake, D. R., E. W. Mayer, S. C. Tyler, Y. Makide, D. C. Montague, and F. S. Rowland, Global increase in atmospheric methane concentrations between 1978 and 1980, *Geophys. Res. Lett., 9*, 477–480, 1982.

Bojkov, R. D., Tropospheric ozone, its changes and possible radiative effect, *WMO Spec. Environ. Rep. 16*, World Meteorol. Organ., Geneva, 1983.

Boughner, R. E., and V. Ramanathan, Climatic consequences of increasing CO_2: A study of the feedback mechanisms between increased CO_2 concentrations and the atmospheric ozone, water vapor, and thermal structure and balance, paper presented at the Second Conference on Atmospheric Radiation, Am. Meteorol. Soc., Arlington, Va., Oct. 29–31, 1975.

Callis, L. B., M. Natarajan, and R. E. Boughner, On the relationship between the greenhouse effect, atmospheric photochemistry, and species distributions, *J. Geophys. Res., 88*, 1401–1426, 1983.

Cess, R. D., The optically thin approximation, Meeting of Experts on Potential Climatic Effects of Ozone and Other Trace Gases, *WMO Rep. 14*, pp. 27–28, World Meteorol. Organ., Geneva, 1982.

Chamberlain, J. W., H. M. Foley, G. J. MacDonald, and M. A. Rudenman, Climatic effects of minor atmospheric constituents, in *Carbon Dioxide Review: 1982*, edited by W. C. Clark, pp. 253–278, Clarendon Press, New York, 1982.

Chatfield, R. B., and H. Harrison, Tropospheric ozone, 2, Variations along a meridional band, *J. Geophys. Res., 82*, 5969–5976, 1977.

Chemical Manufacturers Association, 1982 world production and sales of fluorocarbons FC-11 and FC-12, 29 pp., Washington, D. C., 1983.

Cicerone, R. J., Atmospheric carbon tetrafluoride: A nearly inert gas, *Science, 206*, 59–61, 1979.

Cicerone, R. J., and R. Zellner, The atmospheric chemistry of hydrogen cyanide, *J. Geophys. Res., 88*, 10689–10696, 1983.

Cicerone, R. J., S. Walters, and S. C. Liu, Nonlinear response of stratospheric ozone column to chlorine injections, *J. Geophys. Res., 88*, 3647–3661, 1983.

Craig, H., and C. C. Chou, Methane: The record in polar ice cores, *Geophys. Res. Lett., 9*, 1221–1224, 1982.

Crutzen, P. J., and L. T. Gidel, A two-dimensional photochemical model of the atmosphere, 2, The tropospheric budgets of the anthropogenic chlorocarbons, CO, CH_4, CH_3Cl and the effect of various NO_x sources on tropospheric ozone, *J. Geophys. Res., 88*, 6641–6661, 1983.

Cunnold, D., R. Prinn, R. Rasmussen, P. Simmonds, F. Alyea, C. Cardelino, A. Crawford, P. Fraser, and R. Rosen, The Atmospheric Lifetime Experiment, 3, Lifetime methodology and application to 3 years of $CFCl_3$ data, *J. Geophys. Res., 88*, 8379–8400, 1983*a*.

Cunnold, D., R. Prinn, R. Rasmussen, P. Simmonds, F. Alyea, C. Cardelino, and A. Crawford, The Atmospheric Lifetime Experiment, 4, Results for $CFCl_2$ based on 3 years of data, *J. Geophys. Res., 88*, 8401–8414, 1983*b*.

Dickinson, R. E., Modeling climatic changes due to carbon dioxide increases, in *Carbon Dioxide Review*, edited by W. C. Clark, pp. 101–133, Clarendon Press, New York, 1982.

Dickinson, R. E., S. C. Liu, and T. M. Donahue, Effect of clorofluoromethane infrared radiation on zonal atmospheric temperature, *J. Atmos. Sci., 35*, 2142–2152, 1978.

Donner, L., and V. Ramanathan, Methane and nitrous oxide: Their effects on the terrestrial climate, *J. Atmos. Sci., 37*, 119–124, 1980.

Duxbury, J. M., D. R. Baldwin, R. E. Terry, and R. L. Tate, Emissions of nitrous oxide from soils, *Nature, 298*, 462–464, 1982.

Ehhalt, D. H., R. J. Zander, and R. A. Lamontagne, On the temporal increase of tropospheric CH_4, *J. Geophys. Res., 88*, 8442–8446, 1983.

Fabian, P., R. Borchers, D. Gomer, and S. A. Penkett, The vertical distribution of halocarbons in the stratosphere, Quadrennial Ozone Symposium, IAMAP Programs and Abstracts, pp. 3–6, Int. Assoc. of Meteorol. and Atmos. Phys., 1984.

Fels, S. B., J. D. Mahlman, M. D. Schwarzkopf, and R. W. Sinclair, Stratospheric sensitivity to perturbations in ozone and carbon dioxide: Radiative and dynamical response, *J. Atmos. Sci., 37*, 2265–2297, 1980.

Fenical, W., Natural products chemistry in the marine environment, *Science, 215*, 923–928, 1982.

Fishman, J., V. Ramanathan, P. J. Crutzen, and S. C. Liu, Tropospheric ozone and climate, *Nature, 282*, 818–820, 1979*a*.

Fishman, J., S. Solomon, and P. J. Crutzen, Observational and theoretical evidence in support of a significant in-situ photochemical source of tropospheric ozone, *Tellus, 31*, 432–446, 1979*b*.

Goldman, A., F. S. Bonomo, and D. G. Murray, Statistical band model analysis and integrated intensity for the 11.8 μm band of $CFCl_3$, *Appl. Opt., 15*, 2305–2307, 1976*a*.

Goldman, A., F. S. Bonomo, and D. G. Murray, Statistical band model analysis and integrated intensity for the 10.8 μm band of CF_2Cl_2, *Geophys. Res. Lett., 3*, 309–312, 1976*b*.

Goldman, A., D. G. Murray, F. J. Murray, G. R. Cook, J. W. Van Allen, F. S. Bonomo, and R. D. Blatherwick, identification of the ν_3 vibration-rotation band of CF_4 in balloon-borne infrared solar spectra, *Geophys. Res. Lett., 6*, 609–612, 1979.

Hameed, S., R. D. Cess, and J. Hogan, Response of the global climate to changes in atmospheric chemical composition due to fossil fuel burning, *J. Geophys. Res., 85*, 7537–7545, 1980.

Hansen, J. E., A. Lacis, and S. A. Lebedeff, Commentary on climatic effects of minor atmospheric constituents, in *Carbon Dioxide Review: 1982*, edited by W. C. Clark, pp. 284–286, Clarendon Press, New York, 1982.

Hansen, J. E., A. Lacis, D. Rind, G. Russell, P. Stone, I. Fung, R. Ruedy, and J. Lerner, Climate sensitivity: Analysis of feedback mechanisms, in *Climate Processes and Climate Sensitivity, Maurice Ewing Ser. 5*, edited by J. E. Hansen and T. Takahashi, AGU, Washington, D. C., 1984.

Herranz, J. R. de la Cierva, and J. Morcillo, Intensidades absolutas en infrarrojo de bandes fundamentales del fluoroformo, chloroformo, trifluorclorometano y trichlorofluormetano, *An. R. Soc. Esp. Fis. Quim. Madrid, A55*, 69–76, 1959.

Herrmann, J., and W. Jaeschke, Measurements of H_2S and SO_2 over the Atlantic Ocean, *J. Atmos. Chem., 1*, 111–124, 1984.

Hummel, J. R., and R. A. Reck, The direct thermal effects of $CHClF_2$, CH_3CCl_3 and CH_2Cl_2 on atmospheric surface temperatures, *Atmos. Environ., 15*, 379–382, 1981.

Kagann, R. H., J. W. Elkins, and R. L. Sams, Absolute band strengths of halocarbons F-11 and F-12 in the 8- to 16-μm region, *J. Geophys. Res., 88*, 1427–1432, 1983.

Karol, I., et al., Atmospheric ozone and global climate, Report of U.S./USSR Workshop on the Climatic Effects of Increased Atmospheric Carbon Dioxide, Leningrad, 1981.

Kiehl, J. T., and V. Ramanathan, CO_2 radiative parameterization used in climate models: Comparison with narrow band models and with laboratory data, *J. Geophys. Res., 88*, 5191–5202, 1983.

Kley, D., J. W. Drummond, M. McFarland, and S. C. Liu, Tropospheric profiles of NO_x, *J. Geophys. Res., 86*, 3153–3161, 1981.

Lacis, A., J. Hansen, P. Lee, T. Mitchell, and S. Lebedeff, Greenhouse effect of trace gases, 1970–1980, *Geophys. Res. Lett.*, *8*, 1035–1038, 1981.

Levy, H., J. D. Mahlman, W. J. Moxim, and S. C. Liu, Tropospheric ozone: The role of transport, *J. Geophys. Res.*, in press, 1985.

Liu, S. C., D. Kley, M. McFarland, J. D. Mahlman, and H. Levy II, On the origin of tropospheric ozone, *J. Geophys. Rev.*, *85*, 7546–7552, 1980.

Logan, J. A., Trends in tropospheric ozone, paper presented at Second Symposium on the Composition of the Nonurban Troposphere, Williamsburg, Va., May 1982.

Logan, J. A., M. J. Prather, S. C. Wofsy, and M. A. McElroy, Atmospheric chemistry: Response of human influence, *Philos. Trans. R. Soc. London*, *290*, 187–234, 1978.

Logan, J. A., M. J. Prather, S. C. Wofsy, and M. B. McElroy, Tropospheric chemistry: A global perspective, *J. Geophys. Res.*, *86*, 7210–7254, 1981.

Lovelock, J. E., Natural halocarbons in air and in sea, *Nature*, *256*, 193–194, 1975.

Madden, R. A., and V. Ramanathan, Detecting climate change due to increasing carbon dioxide, *Science*, *209*, 763–768, 1980.

Manabe, S., and R. T. Wetherald, Thermal equilibrium of the atmosphere with a given distribution of relative humidity, *J. Atmos. Sci.*, *24*, 241–259, 1967.

Maroulis, P. J., A. L. Torres, A. B. Goldberg, and A. R. Bandy, Atmospheric SO_2 measurements on Project Gametag, *J. Geophys. Res.*, *85*, 7345–7349, 1980.

McClatchey, R. A., et al., AFCRL atmospheric absorbtion line parameters compilation, *AFCRL-TR-73-0096*, 77 pp., Air Force Cambridge Res. Lab., Hanscom Field, Bedford, Mass., 1973.

Nanes, R., P. M. Silvaggio, and R. W. Boese, Temperature dependence of intensities of the 8-12 μm bands of $CFCl_3$, *J. Quant. Spectros. Radiat. Transfer*, *23*, 211–220, 1980.

National Academy of Sciences/National Research Council, Halocarbons: Effects on stratospheric ozone, Washington, D. C., 1976.

National Academy of Sciences/National Research Council, Stratospheric ozone depletion by halocarbons: Chemistry and transport, Washington, D. C., 1979.

National Academy of Sciences/National Research Council, Causes and effects of stratospheric ozone reduction: An update, National Academy Press, Washington, D. C., 1982.

National Aeronautics and Space Administration, The stratosphere: Present and future, *NASA Ref. Publ. 1049*, 1979.

National Research Council, Carbon dioxide and climate: A second assessment, Report of the CO_2/Climate Review Panel, National Academy Press, Washington, D. C., 1982.

National Research Council, Changing climate, Report of the Carbon Dioxide Assessment Committee, National Academy Press, Washington, D. C., 1983.

Penkett, S. A., Nonmethane organics in the remote troposphere, in *Atmospheric Chemistry*, pp. 329–355, Springer, New York, 1982.

Penkett, S. A., N. J. D. Prosser, R. A. Rasmussen, and M. A. K. Khalil, Atmospheric measurements of CF_4 and other fluorocarbons containing the CF_3 grouping, *J. Geophys. Res.*, *86*, 5172–5178, 1981.

Prather, M. J., M. B. McElroy, S. C. Wofsy, Reductions in ozone at high concentrations of stratospheric halogens, *Nature*, *312*, 227–231, 1984.

Pugh, L. A., and K. N. Rao, Intensities from infrared spectra, *Mol. Spectros., Mod. Res.*, *2*, 165–225, 1976.

Ramanathan, V., Greenhouse effect due to chlorofluorocarbons: Climatic implications, *Science*, *190*, 50-52, 1975.

Ramanathan, V., The role of ocean-atmospheric interactions in the CO_2 climate problem, *J. Atmos. Sci.*, *38*, 918–930, 1981.

Ramanathan, V., Commentary on climatic effects of minor atmospheric constituents, in *Carbon Dioxide Review: 1982*, edited by W. C. Clark, Clarendon Press, New York, 1982.

Ramanathan, V., and J. A. Coakley, Climate modeling through radiative-convective models, *Rev. Geophys. Space Phys.*, *16*, 465–489, 1978.

Ramanathan, V., and R. E. Dickinson, The role of stratospheric ozone in the zonal and sesonal radiative energy balance of the earth-troposphere system, *J. Atmos. Sci.*, *36*, 1084–1104, 1979.

Ramanathan, V., L. B. Callis and R. E. Boughner, Sensitivity of atmospheric and surface temperature to perturbations in stratospheric concentration of ozone and nitrogen-dioxide, *J. Atmos. Sci.*, *33*, 1092-1112, 1976.

Rasmussen, R. A., and M. A. K. Khalil, Atmospheric methane: Trends and seasonal cycles, *J. Geophys. Res.*, *86*, 9826–9832, 1981.

Rasmussen, R. A., L. E. Rasmussen, M. A. K. Khalil, and R. W. Dalluge, Concentration distribution of methyl chloride in the atmosphere, *J. Geophys. Res.*, *85*, 7350–7356, 1980.

Reck, R. A., and D. L. Fry, The direct effects of chlorofluoromethanes on the atmospheric surface temperature, *Atmos. Environ.*, *12*, 2501–2503, 1978.

Revelle, R. R., Methane hydrates in continental slope sediments and increasing atmospheric carbon dioxide, in *Changing Climate*, sect. 3.5, pp. 252–261, National Academy of Sciences, Washington, D. C., 1983.

Rothman, L. S., and R. R. Gamache, A. Barbe, A. Goldman, J. R. Gillis, L. R. Brown, R. A. Toth, J. M. Flaud, and C. Camy-Peyret, AFGL atmospheric absorption line parameters compilation: 1982 edition, *Appl. Opt.*, *15*, 2247-2256, 1983.

Rotty, R. M., and G. Marland, Constraints on carbon dioxide production from fossil fuel use, paper presented at the Energy/Climate Interactions Workshop, Munster, Germany, March 3–8, 1980.

Rudolph, J., and D. H. Ehhalt, Measurements, of C_2-C_5, hydrocarbons over the North Atlantic, *J. Geophys. Res.*, *86*, 11959-11964, 1981.

Saeki, S., M. Mizumo, and S. Kondo, Infrared absorption intensities of methane and fluoromethanes, *Spectrochim. Acta Part A*, *32*, 403–413, 1976.

Simmonds, P. G., F. N. Alyea, C. A. Cardelino, A. J. Crawford, D. M. Cunnold, B. C. Lane, J. E. Lovelock, R. G. Prinn, and R. A. Rasmussen, The Atmospheric Lifetime Experiment, 6, Results for carbon tetrachloride based on three years data, *J. Geophys. Res.*, *88*, 8427–8441, 1983.

Singh, H. B., and L. J. Salas, Peroxyacetyl nitrate in the free troposphere, *Nature*, *302*, 326–328, 1983.

Singh, H. B., D. P. Fowler, and T. O. Peyton, Atmospheric carbon tetrachloride: Another manmade pollutant, *Science*, *192*, 1231–1234, 1976.

Singh, H. B., L. J. Salas, and R. E. Stiles, Selected man-made halogenated chemicals in the air and oceanic environment, *J. Geophys. Res.*, *88*, 3675–3683, 1983*a*.

Singh, H. B., L. J. Salas, and R. E. Stiles, Methyl halides in and over the eastern Pacific (40°N–32°S), *J. Geophys. Res.*, *88*, 3684–3690, 1983*b*.

Smagorinsky, J., Effects of carbon dioxide, chap. 4, sect. 4.1, in *Changing Climate*, pp. 266–284, Report of the Carbon Dioxide Assessment Committee, National Research Council, 1983.

Sparrow, E. M., and R. D. Cess, *Radiation Heat Transfer*, 366 pp., McGraw-Hill, New York, 1970.

Surgeon General, Health effects of toxic pollutants: A report from the Surgeon General, Report prepared for U.S. Senate, Department of Health and Human Services, *Serial 96-15*, Washington, D. C., 1980.

Turco, R. P., R. C. Whitten, O. B. Toon, J. B. Pollack, and P. Hamill, OCS, Stratospheric aerosols and climate, *Nature*, *283*, 283–286, 1980.

Varanasi, P., and F. K. Ko, Intensity measurements in freon bands of atmospheric interest, *J. Quant. Spectros. Radiat. Transfer*, *17*, 385–389, 1977.

Volz, A., D. H. Ehhalt, and R. G. Derwent, Seasonal and latitudinal variation of ^{14}CO and the tropospheric concentrations of OH radicals, *J. Geophys. Res.*, *86*, 5163–5171, 1981.

Wang, W. C., Ozone changes: Climatological effects, in *Stratospheric Ozone and Man*, edited by F. A. Bower and R. B. Ward, pp. 123–135, CRC Press, Cleveland, Ohio, 1982.

Wang, W. C., Y. L. Yung, A. A. Lacis, T. Mo, and J. E. Hansen, Greenhouse effect due to manmade perturbations of trace gases, *Science*, *194*, 685–690, 1976.

Wang, W. C., J. P. Pinto, and Y. L. Yung, Climatic effects due to halogenated compounds in the earth's atmosphere, *J. Atmos. Sci.*, *37*, 333–338, 1980.

Washington, W. M., and G. A. Meehl, Seasonal cycle experiment on the climate sensitivity due to a doubling of CO_2 with an atmospheric general circulation model coupled to a simple mixed layer model, *J. Geophys. Res.*, *89*, 9475, 1984.

Weiss, R. F., The temporal and spatial distribution of tropospheric nitrous oxide, *J. Geophys. Res.*, *86*, 7185–7195, 1981.

Wine, P. H., W. L. Chameides, and A. R. Ravishankara, Potential role of CS_2 oxidation in tropospheric sulfur chemistry, *Geophys. Res. Lett.*, *8*, 543–546, 1981.

Wiscombe, W., and J. Evans, Exponential-sum fitting of radiative transmission functions, *J. Comp. Physiol.*, *24*, 416–444, 1977.

World Meteorological Organization, Report of the meeting of experts on potential climatic effects of ozone and other minor trace gases, *WMO Global Ozone Res. and Monitoring Proj. Rep. 14*, 35 pp., Geneva, 1982*a*.

World Meteorological Organization, The stratosphere 1981—Theory and measurements, *WMO Rep. 11*, Geneva, 1982*b*.

World Meteorological Organization, The world climate research program report on the meeting of experts on detection of possible climate change, *WCP 29*, edited by W. W. Kellogg and R. D. Bojkov, p. 42, Geneva, 1983.

Wuebbles, D. J., Scenarios for future anthropogenic emissions of trace gases in the atmosphere, *UCID-18997*, Lawrence Livermore Lab., Berkeley, Calif., 1981.

Wuebbles, D. J., A theoretical analysis of the past variations in global atmospheric composition and temperature structure, Ph.D. thesis, *UCRL-53423*, Univ. of Calif., Davis, 1983*a*.

Wuebbles, D. J., Chlorocarbon emission scenarios: Potential impact on stratospheric ozone, *J. Geophys. Res., 88*, 1433–1440, 1983*b*.

R. J. Cicerone, J. T. Kiehl, and V. Ramanathan, National Center for Atmospheric Research, P. O. Box 3000, Boulder, CO 80307.

H. B. Singh, SRI International, Menlo Park, CA 94025.

(Received August 15, 1984;
revised January 14, 1985;
accepted January 18, 1985.)

Paper 2

Evidence for a Greenhouse Effect

by

John Perry
National Academy of Sciences – National Research Council

This paper was based upon the presentation made at the workshop.

Trace Gas Trends and Climate Change

by

John Perry

DRAFT 01/29/86

Presentation at Raleigh EPA Meeting

TRACE GASES AND CLIMATIC CHANGE

In contrast to the polished presentation made by Dr. Cicerone, mine will be a more conventional sort of scientific talk with messy slides, lots of wiggly lines, and at least one equation. As a card-carrying meteorologist, I feel compelled to give you at the outset a weather forecast. (Slide 1) This type of forecast that winter will follow fall and summer will follow spring is in fact the most reliable type of prediction we can make. This type of "prediction," the expectation of future weather, is known as "climate." We think of the climate of the globe, including its annual cycle and its distribution across the face of the planet, as being a fixed part of geography. For example (Slide 2), we find charts of various climatic parameters plotted on maps with the same degree of authority and permanence as if they were state boundaries or the distributions of geological or mineral resources.

In fact, however, there is much evidence that the climate of the earth is far from constant. Even a parameter such as the globally averaged mean temperature of the planet is observed to change quite a bit in the long term, and exhibit rather puzzling fluctuations even over short periods. For example, here (Slide 3) is a century-long record of one estimate of the global mean temperature. It shows an irregular increase over the period of record, and also some peculiar shorter-term features such as the rise in temperature in the 1940s.

If we look a bit further back into history, I am sure we all recall the tales in our schoolbooks about the great ice ages. About 18,000 years ago, great ice sheets extended over much of the northern hemisphere and well down into North America and Europe. Much research in recent years has focused on elucidating the details of these climatic changes of the past. Here (Slide 4) is a reconstruction of global sea-surface temperatures derived from deep sea sediment cores by the CLIMAP group of researchers. The boundaries of sea ice coverage derived in this way match very well with what we know of the land ice cover in the same period.

Thus, by digging into the past, we have established quite a good chronology of climate change in the relatively recent history of the earth. Ice ages such as the one which culminated 18,000 years ago have been duplicated many times in the Quaternary period in which we live. The climate of this geological epoch has been characterized by swings between glacial and interglacial conditions with a periodicity of about 120,000 years. The precise pacing of this oscillation seems to be triggered by the characteristics of the earth's orbit, but the mechanisms are not clear. Going back still further into mists of time (Slides 5 and 6), we find that the earth has gone through a variety of different climatic regimes. By and large, however, it has stayed in range in which life is possible. Our own period with its rapid fluctuations between glacial and interglacial conditions is a bit cooler than the period in which the great masses of fossil coal were formed.

For these reasons, the title of a report issued a few years ago by the National Academy of Sciences (Slide 7), Changing Climate, is quite appropriate. We have to think of climate as a constantly changing and perhaps a fragile element of our global environment. Such a viewpoint leads us to another question: What determines our climate? The fundamental governing factor, of course, is the relationship between the earth and its parent sun that provides virtually all our energy. It is relatively easy to estimate the temperature, that is the climate, of an inert lump of rock located at the same distance as the earth from the sun (Slide 9). The rock would receive about 340 w/m^2 of energy from the sun and would thus slowly warm. Elementary physics tells us that the rock would radiate thermal energy back to space at a rate proportional to the fourth power of its absolute temperature. Eventually, it would warm to the point where it would be radiating as much energy as it absorbed from the sun. A lump of rock with the same reflectivity as our present earth would thus warm to a temperature of about $-18^{o}C$, significantly less comfortable than the real earth on which we find ourselves.

The curves in the upper right hand corner of the slide show another fundamental property of the energy balance. The energy coming in from the sun is primarily in the shorter wavelengths of light, around the yellow part of the spectrum in which our own eyes are the most sensitive. On the other hand, the rock, like any other warm body, emits most of its energy in thermal radiation at a considerable longer wavelength in the infrared. Thus, the balance of energy that maintains its temperature is composed of two streams of radiant energy in very different wavelengths.

The real earth, however, (Slide 10) is not a naked lump of rock like the moon. Instead, it has a very peculiar sort of atmosphere that, on the one hand, is essential for life and, on the other hand, was largely made by life. Its components are nitrogen, oxygen, and a small collection of trace gases. Among the most important of the latter in the radiation balance of the earth are water vapor, which varies widely in concentration, and carbon dioxide. These gases have interesting effects on the way radiation is handled by the earth's atmosphere (Slide 11). At the top of this illustration, we see again the two curves showing the emission of energy by the sun and the earth, respectively. Below, we see the absorption of energy in the atmosphere in various wavelengths. One large open window of transmission neatly underlies the visible input from the sun. Thus, solar energy is admitted to the surface of the earth quite effectively. However, under the peak of radiation from the earth, there is considerable absorption by the atmosphere, indeed, almost total absorption.

The effects of the atmosphere can be readily discerned from satellite observations. Here (Slide 12) is a series of measurements taken from a satellite flying over the Sahara and looking down at the earth in different wavelengths in the infrared. The topmost dotted line shows approximately the radiation one would expect to receive from the earth's surface at the temperature of the Sahara. But what the satellite actually saw was the lower trace, from which we see that large portions of that radiation have been taken out by the atmosphere. What one sees instead of the surface radiation is much lower amounts of radiation from a much colder source up in the higher atmosphere. Each of the dips in this curve, the slices taken out of the energy coming from the earth, can be associated with individual absorbing gases in the atmospehre. For example, large amounts are taken out by water vapor, carbon dioxide, ozone, and methane.

If we now consider an earth surrounded by an atmosphere with these properties, we find a very different type of energy balance (Slide 13). Solar energy still comes in largely unabated, but the radiation leaving the earth now is absorbed by the atmosphere in major parts of the infrared spectrum. The energy balance with space is achieved in quite a different fashion. Only a small part of the energy leaving the earth goes directly to space. The remainder of the energy needed to balance the earth's accounts with the cosmos is provided by the atmosphere running at a much cooler temperature. The balance that eventually evolves involves a warm earth's surface, about 15°C on the average, and a cooler atmosphere acting as a filter or blanket between the earth and space. Largely for traditional reasons, this is called the "greenhouse effect," but actually it would be more appropriate to call it the "blanket" effect. Indeed, the situation is not unlike sleeping in a chilly bedroom with a wool blanket.

This type of elementary physical reasoning may be tested very easily by calculating what the greenhouse effect should be for the different planets of the solar system given current understanding of the nature of their atmospheres. With no atmosphere, calculation for the moon is quite simple, and agreement with observations is excellent. More impressively, for climates as different as Venus, the Earth, and Mars, the arithmetic still works out quite well (Slide 14). We find, for example, that Mars without an atmosphere would be quite chilly at -56°C, but its puny atmosphere gives it about 3° worth of greenhouse warming. On the other hand, the dense atmosphere of Venus provides a massive greenhouse effect leading to truly torrid surface temperatures. The major greenhouse gas on Venus is carbon dioxide, and we have seen that CO_2 is also present in small amounts in our own atmosphere. Moreover (Slide 15), measurements of CO_2 carried out by Charles Keeling from 1958 to the present show steadily increasing concentrations. Indeed, the data are sufficiently accurate for us to perceive the annual respiration of the biosphere reflecting the fact that the vast mass of forest lies primarily in the northern hemisphere. Still further back, recent Swiss work on glacial ice has permitted quite a consistent reconstruction of past trends in carbon dioxide concentration (Slide 16).

The principal reason for this increase in recent times is easy to infer. Our modern society is taking vast reserves of fossil carbon

(Slide 17) that were entombed many millions of years ago and bit by bit returning them to the atmosphere at the rate of 5 gigatons per year. Historically, it appears that about 50% of the emissions in each year from fossil fuel combustion has stayed in the atmosphere. The remainder has been partitioned between the oceans and the terrestrial biosphere. The global carbon cycle that has been in operation since the dawn of life on the planet is thus being perturbed on a major scale by human activities. The magnitude of this human influence can be assessed by looking at world figures on energy consumption and fossil fuel use (Slide 18). Until quite recent times, the rate of increase in fossil fuel use was virtually exponential with no end in sight.

But what about the future? As is well known, prediction is a difficult exercise, particularly when it concerns the future. Nevertheless, a number of attempts have been made by various analysis groups. The task is not easy. Fuel is consumed by society for some purpose of society. To estimate future fuel consumption, one must look ahead 25, 50, or 100 years to determine what sort of society we will have, make some guesses as to what it will want to do in the world, and how it will get its energy. Despite these difficulties, a number of scholars have made valiant attempts to predict future energy and fossil fuel consumption. Not surprisingly, their estimates of energy use, fuel consumption, and carbon dioxide emissions diverge widely as one goes out into the future (Slide 19). Some postulate a rapidly growing and industrializing world society that burrows out of the ground every last scrap of carbon. Others visualize a frugal future society relying largely on renewable energy resources. Thus there is a widening band of uncertainty in future carbon use. A recent international conference held in Villach, Austria, developed estimates of future carbon emissions that were in a somewhat lower range than previous studies. Their conclusions were heavily biased by recent experiences in energy conservation in response to rising energy prices.

One can employ these emission estimates together with a carbon cycle model of some type to make projections of future atmospheric CO_2 concentrations (Slide 20). Here the background chart shows a range of estimates developed in the National Academy of Sciences study referred to earlier. For comparison, I have crudely indicated the estimates developed in connection with the Villach conference. The lower band of estimates shows the range for CO_2 alone. The higher band shows the equivalent effect on the radiation budget that would be produced by CO_2 plus the other trace gases considered in their survey. That is, this upper chart shows the amount of CO_2 that would be required to produce the same effect on the radiation budget as the mixture of gases that are estimated to be present. Thus, in terms of the total effect on climate, the other trace gases roughly double the impact of CO_2, and completely wipe out the beneficial effects of the expected decreases in the rate of growth of energy demand. We are essentially back to where we started. Indeed, the Villach estimates would support the equivalent of a CO_2 doubling effect on climate by as early as the year 2030.

Once we have an estimate of the future course of concentration of CO_2 and other perturbing gases in the radiation budget, how can we turn this into an estimate of future climate? The atmosphere is, after all, but one element of the complex global climate system (Slide 21). To predict future climate, we must consider the ocean that not only acts as a chemical buffer but also exchanges heat and momentum with the atmosphere. We must consider clouds whose distribution over the earth and effects on the radiation budget are by no means well understood. We must deal with the variations of ice and snow masses on an annual basis and over long periods of time. Later presentations at this conference will deal with this challenging task.

By looking at the results of climate model simulations and the projections of future atmospheric trends, the Villach conference developed a number of conclusions of considerable significance (Slide 22). First, they confirmed strongly that it is time to move out of the purely scientific arena in discussion of the issue of greenhouse gas trends. Implications of changes in atmospheric composition and global climate should be taken account of in practical policy development, not necessarily from the standpoint of taking immediate action but certainly in laying the groundwork for future actions should they become necessary. To support this effort, the conference recommended stronger public information activities and, of course, continued research. They believed that this research should be pursued with equal vigor on both the scientific front to elucidate the details of climate change, and on the policy front to examine policy and economic options. The conference believed that it was high time to arrange for more frequent and more intense interactions between scientists and policy people in the study of the implications of greenhouse gas increase. They suggested a number of specific scientific and policy research topics and the establishment of a standing international task force sponsored by the three major sponsoring agencies of the assessment-- the World Meteorological Organization, the International Council of Scientific Unions, and the United Nations Environment Program. This task force would arrange for future assessments of the issue at appropriate intervals and would provide advice to governments and international organizations. The group would also begin the consideration of a global convention to attempt regulation of all the greenhouse gases. The most important conclusion of the conference, I believe, was that "our understanding... is sufficiently developed that scientists and policymakers should begin an active collaboration to explore the effectiveness of alternative policies and adjustments."

In conclusion, the true message of the greenhouse gas problem was most clearly stated a long time ago and not by an atmospheric scientist but by a distinguished Soviet mineralogist (Slide 23). Vernadsky saw that in this century mankind has colonized the geographical map of the planet earth and its whole surface to become a large-scale geological force. Our challenge is to learn how to control and focus that force.

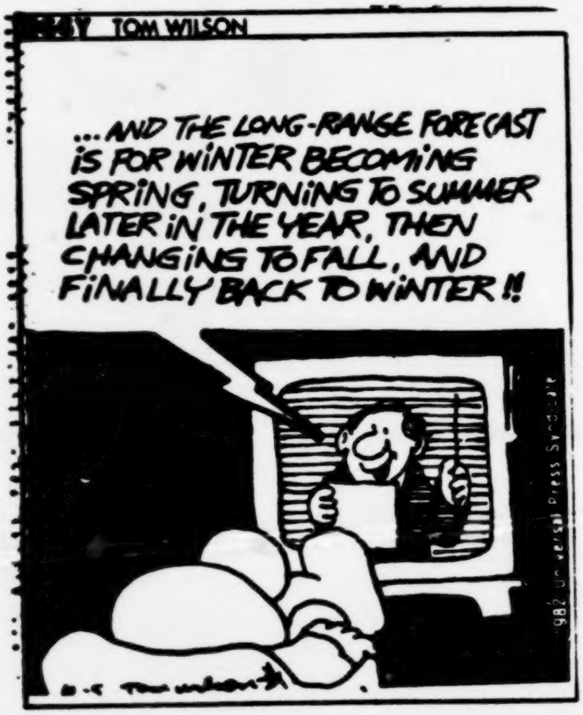
TOM WILSON
...AND THE LONG-RANGE FORECAST IS FOR WINTER BECOMING SPRING, TURNING TO SUMMER LATER IN THE YEAR, THEN CHANGING TO FALL, AND FINALLY BACK TO WINTER!!
1982 Universal Press Syndicate

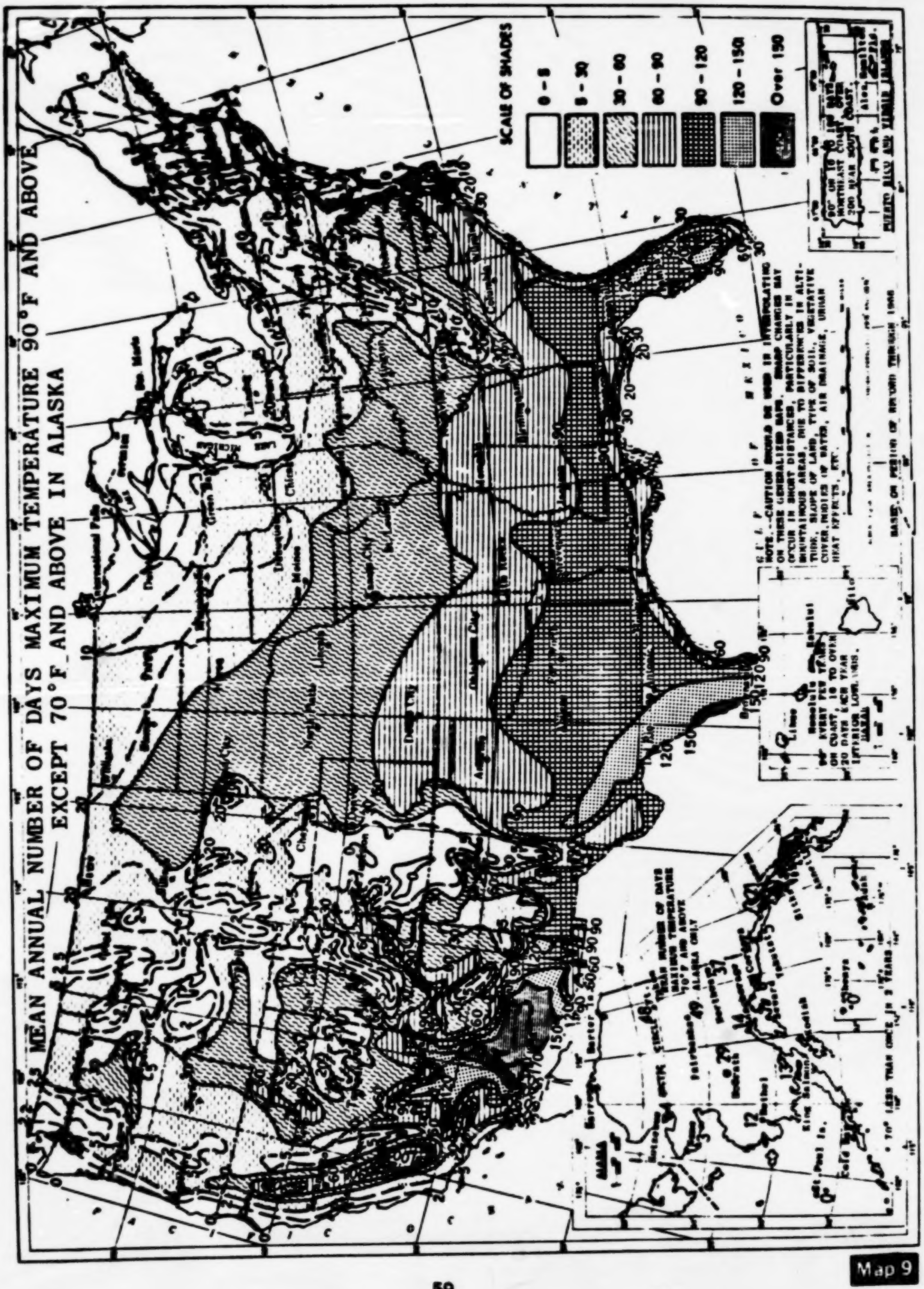
MEAN ANNUAL NUMBER OF DAYS MAXIMUM TEMPERATURE 90°F AND ABOVE
EXCEPT 70°F AND ABOVE IN ALASKA
SCALE OF SHADES
0 – 8
8 – 30
30 – 60
60 – 90
90 – 120
120 – 150
Over 150
NOTE.—CAUTION SHOULD BE USED IN INTERPOLATING ON THESE GENERALIZED MAPS. SHARP CHANGES MAY OCCUR IN SHORT DISTANCES, PARTICULARLY IN MOUNTAINOUS AREAS, DUE TO DIFFERENCES IN ALTITUDE, SLOPE OF LAND, TYPE OF SOIL, VEGETATIVE COVER, BODIES OF WATER, AIR DRAINAGE, URBAN HEAT EFFECTS, ETC.
BASED ON PERIOD OF RECORD THROUGH 1960
PUERTO RICO AND VIRGIN ISLANDS
LAKE MICHIGAN
Chicago
Des Moines
Green Bay
Sault Ste. Marie
GULF OF MEXICO
PACIFIC OCEAN
ALASKA ONLY

Map 9

Reproduced from best available copy.

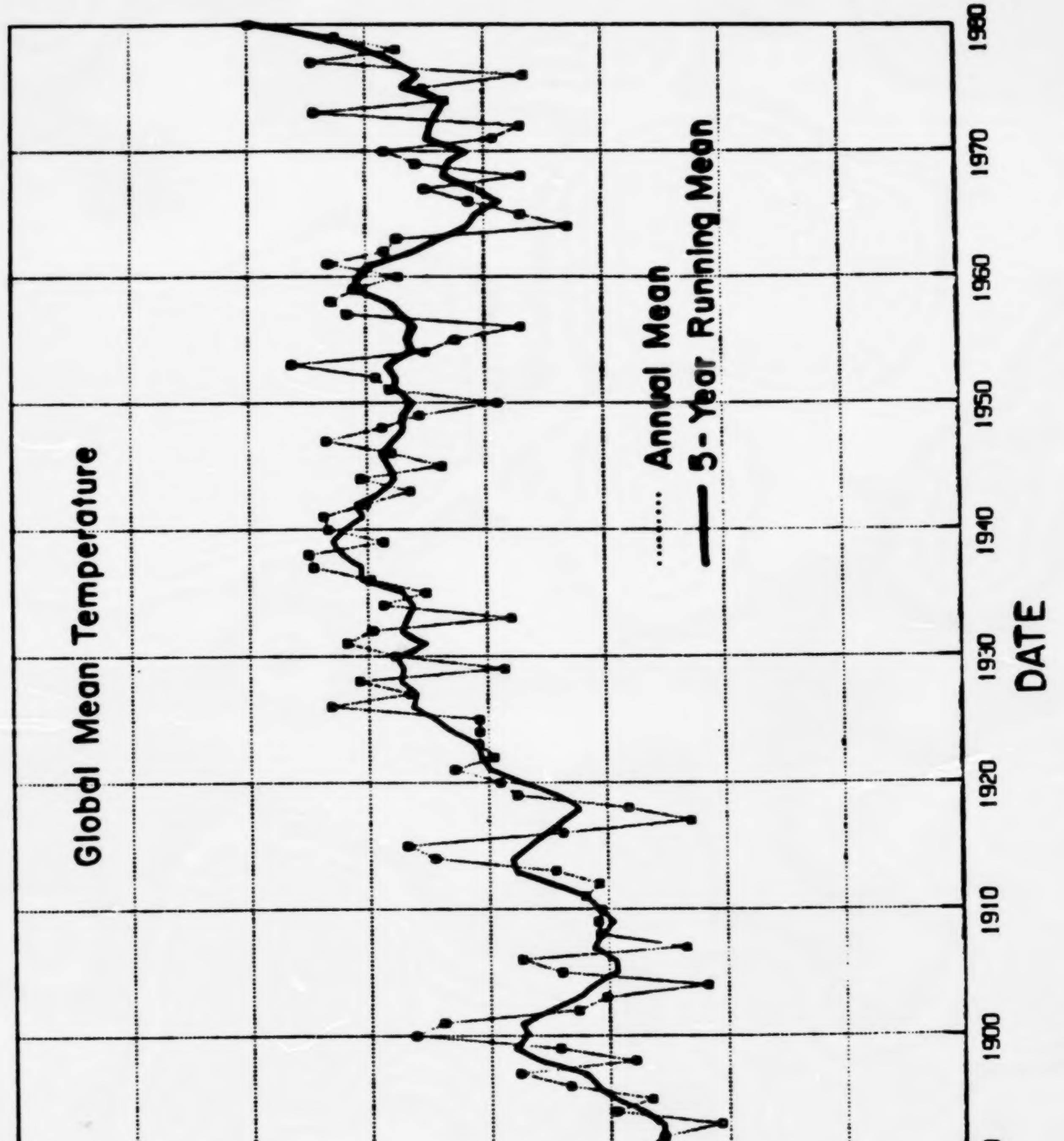
Global Mean Temperature
ΔT(°C)
0.8
0.6
0.4
0.2
0
-0.2
-0.4
-0.6
-0.8
1880
1890
1900
1910
1920
1930
1940
1950
1960
1970
1980
DATE
Annual Mean
5-Year Running Mean

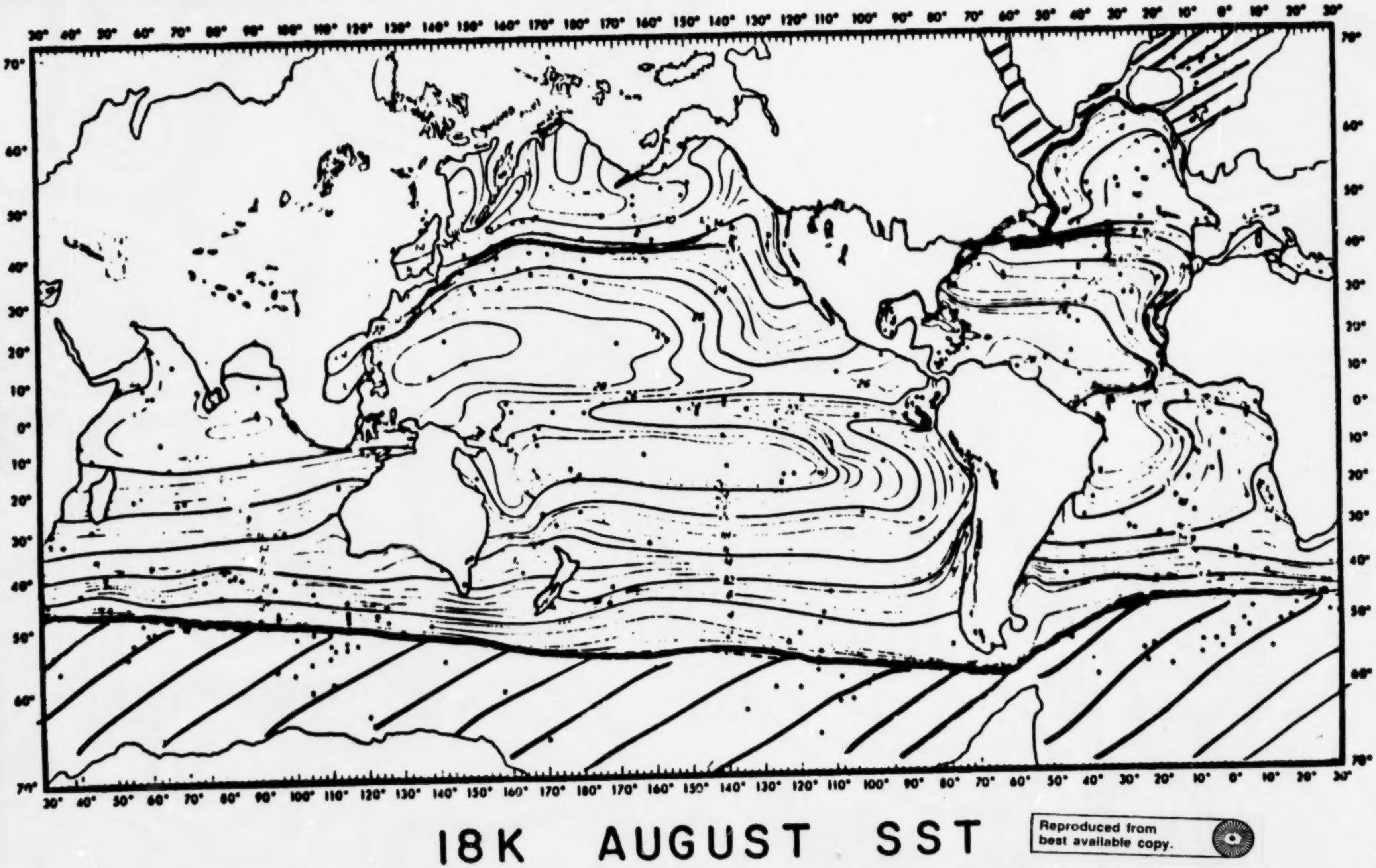
18K AUGUST SST
30° 40° 50° 60° 70° 80° 90° 100° 110° 120° 130° 140° 150° 160° 170° 180° 170° 160° 150° 140° 130° 120° 110° 100° 90° 80° 70° 60° 50° 40° 30° 20° 10° 0° 10° 20° 30°
70° 60° 50° 40° 30° 20° 10° 0° 10° 20° 30° 40° 50° 60° 70°

Reproduced from best available copy.

Figure 7. Transfer-function estimates of sea-surface temperature at the glacial maximum 18,000 years ago (from ref. 60).

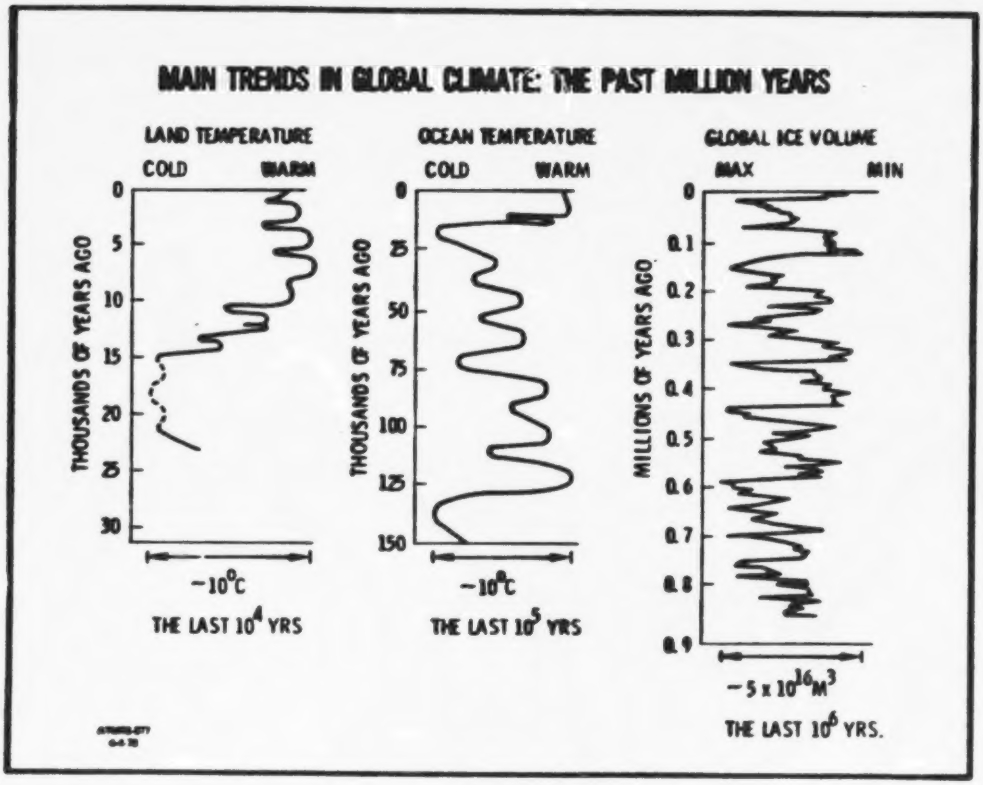

Fig. 51

Here we see climatic variations characteristic of the major components of the climate system, the land, sea, and ice. A major challenge remains in integrating these complex histories into one coherent picture.

The information in Figure 51 shows climatic variations on three different time scales. For the last 30,000 years we see the major change between a glacial world and an interglacial one. Over the last 150,000 years, some details of the change between one interglacial and another are identified. And, on a time scale of 1 million years we can see that such glacial-interglacial changes are part of a repeating cycle. While there is much to infer about the dynamics of climate from time histories, let us highlight one aspect of these data. Notice, for the period about 6,000 years ago, the Earth's climate was warmer (by several degrees) than today. This interval of time may be of particular importance in providing a perspective on the current CO_2 problem. Let me explain this, and at the same time illustrate a second part of our work in the area of global climatic record namely that of climatic reconstructions on a regional scale.

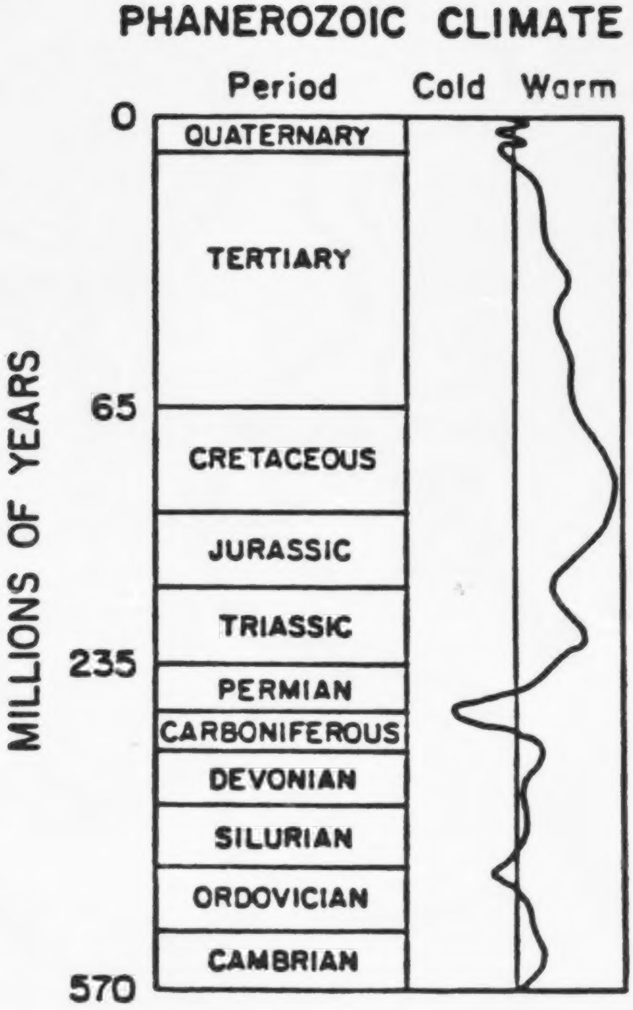

Figure 1. A schematic global temperature history of the earth for the Phanerozoic.[36]

Paper 2

Changing Climate

Report of the Carbon Dioxide Assessment Committee

NRC

"THE NAKED EARTH"

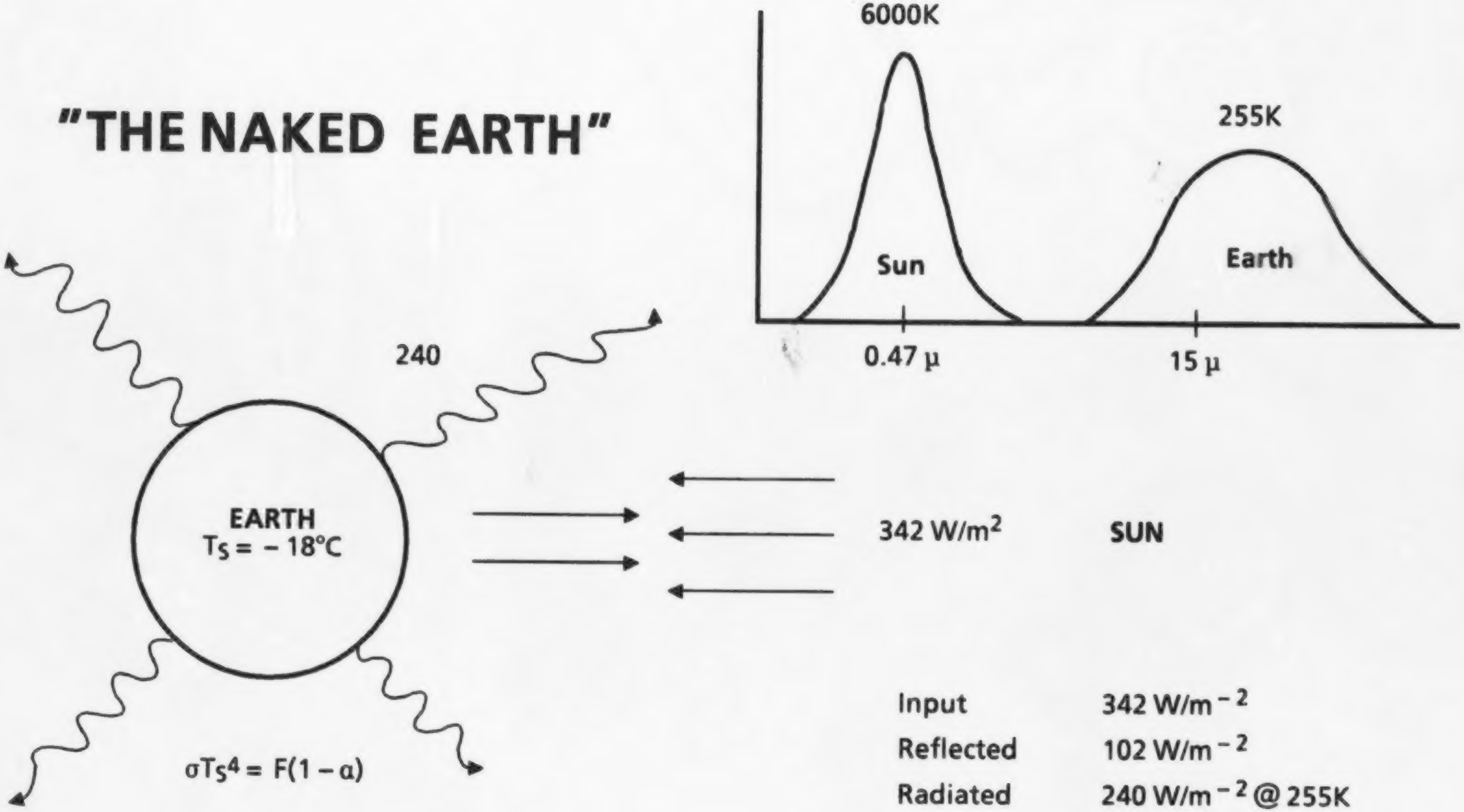
6000K
255K
Sun
Earth
0.47 µ
15 µ
240
EARTH
$T_S = -18°C$
342 W/m²
SUN
$\sigma T_S^4 = F(1-\alpha)$

Input	342 W/m^{-2}
Reflected	102 W/m^{-2}
Radiated	240 W/m^{-2} @ 255K

COMPOSITION OF THE ATMOSPHERE

Nitrogen (N)	78%
Oxygen (O)	21%
Argon, Hydrogen, etc.	$<1\%$
Water Vapor (H_2O)	0-4%
Carbon Dioxide (CO_2)	$\sim$0.3% ($\sim$300 ppm)

CO_2 ABSORBS AND EMITS INFRARED RADIATION

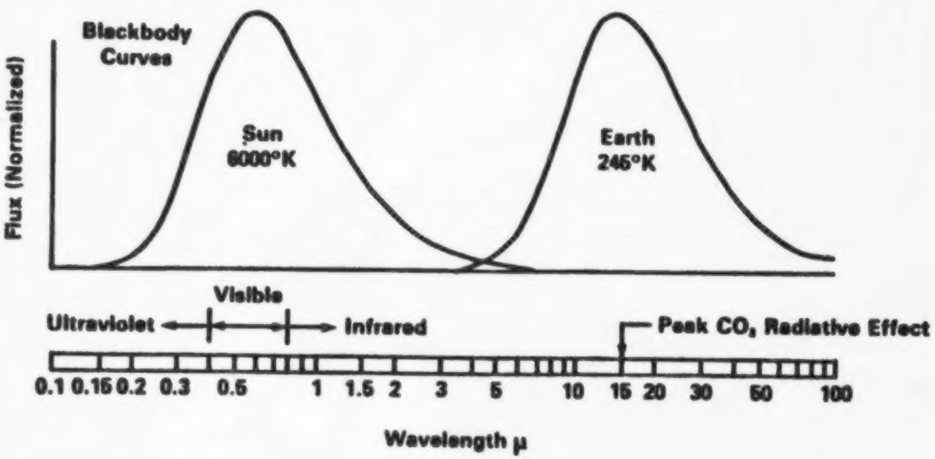

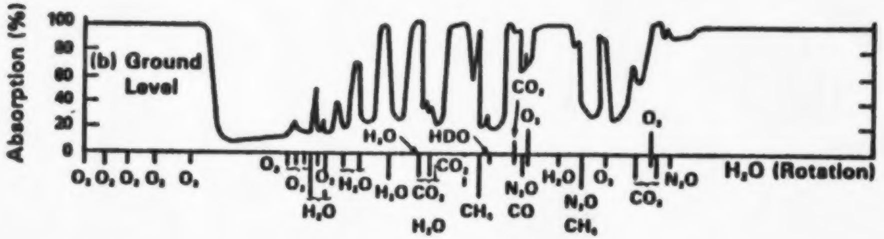

Many Other Gases Also Interact With Atmospheric Radiation, Including Methane, Water Vapor, Ozone, Fluorocarbons, Etc.

The Greenhouse

Looking
Up

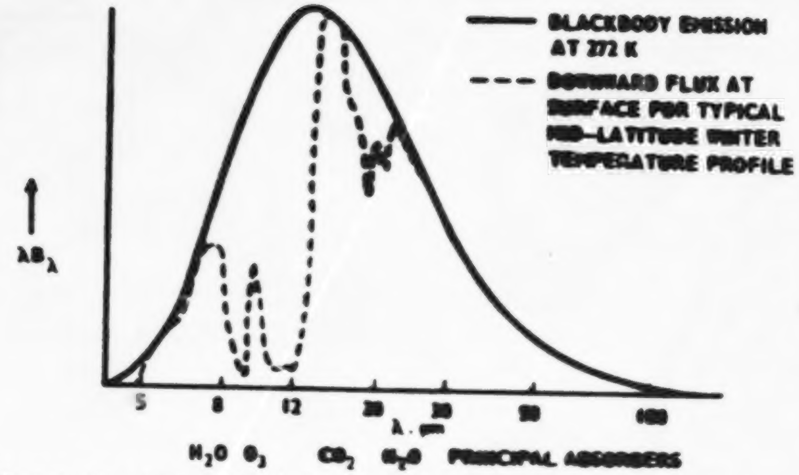

Figure 17. The Earth's black-body emission spectrum at 272 K and the downward flux at the surface for a typical mid-latitude winter temperature profile. The principal absorbers in different wavelength intervals are indicated. (Adapted from Roach and Slingo, 1979).

Looking
Down

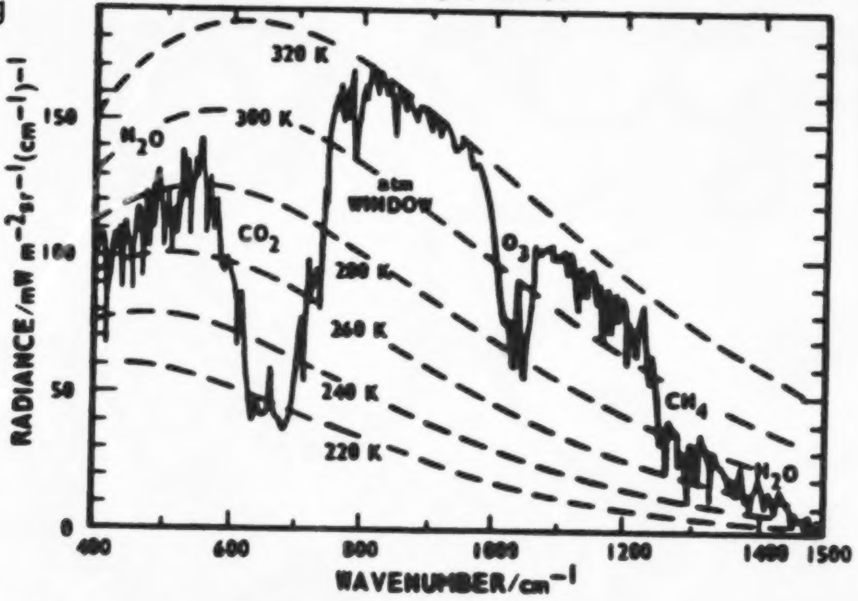

Figure 18. Thermal emission from the Earth plus atmosphere emitted vertically upwards as measured by the Michelson interferometer spectrometer on Nimbus 4 over the Sahara. The radiances of black-bodies at various temperatures are superimposed. (From Hanel et al., 1971).

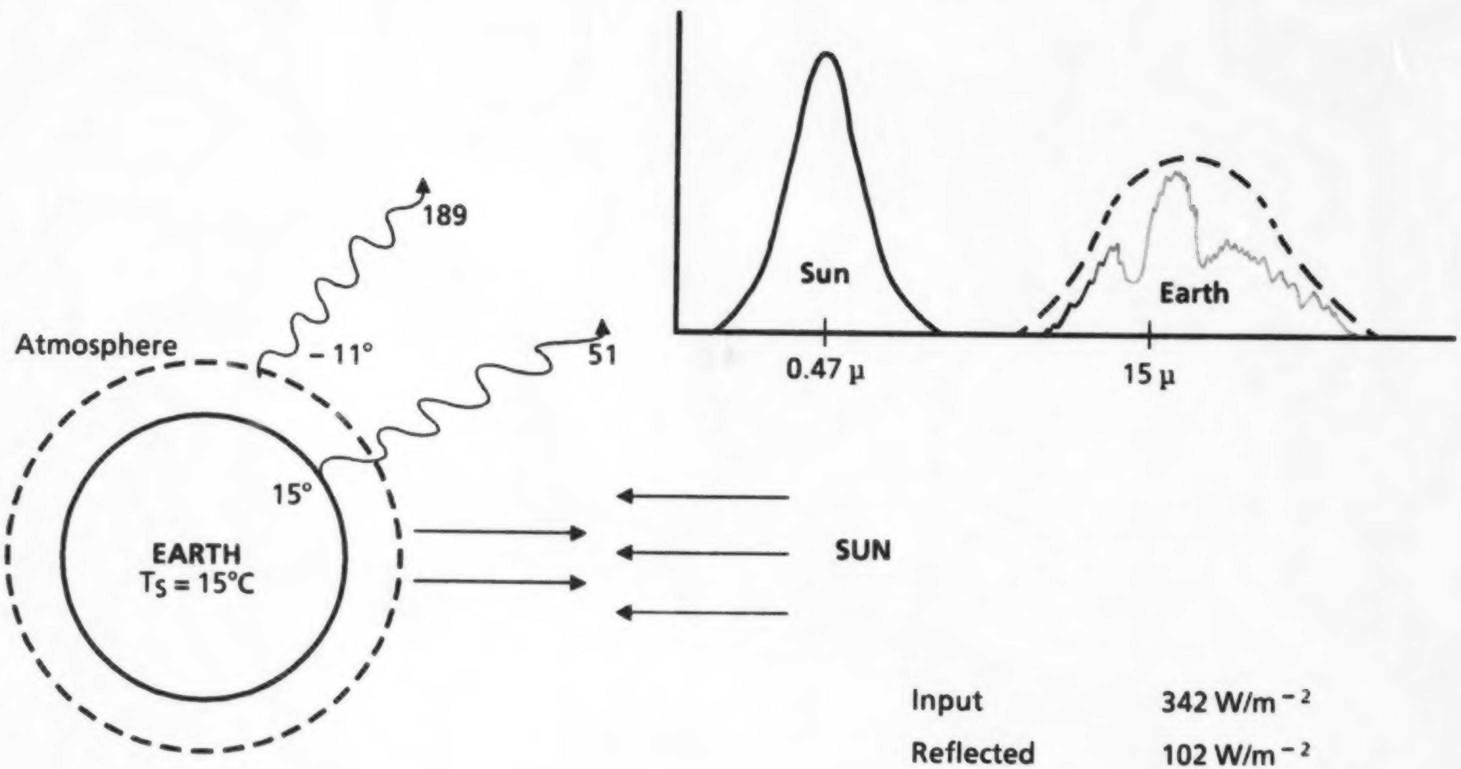
189
Atmosphere
- 11°
51
15°
EARTH
Ts = 15°C
SUN
Sun
Earth
0.47 μ
15 μ

"THE GREENHOUSE"

Input		342 W/m⁻²
Reflected		102 W/m⁻²
Radiated	ATM	189 W/m⁻² @ 262K
	Earth	51 W/m⁻² @ 288K

THE GREENHOUSE EFFECT ON THE INNER PLANETS:

PREDICTION AND OBSERVATIONS

	Sunlight Received (watts per square meter)	Sunlight Reflected (percentage)	Temperature Without An Atmosphere	Predicted Temperature With Simple Models	Actual Temperature
Venus	2613	75	-40°C	429°C	427°C
Earth	1367	30	-18°C	17°C	15°C
Mars	589	15	-56°C	-52°C	-53°C

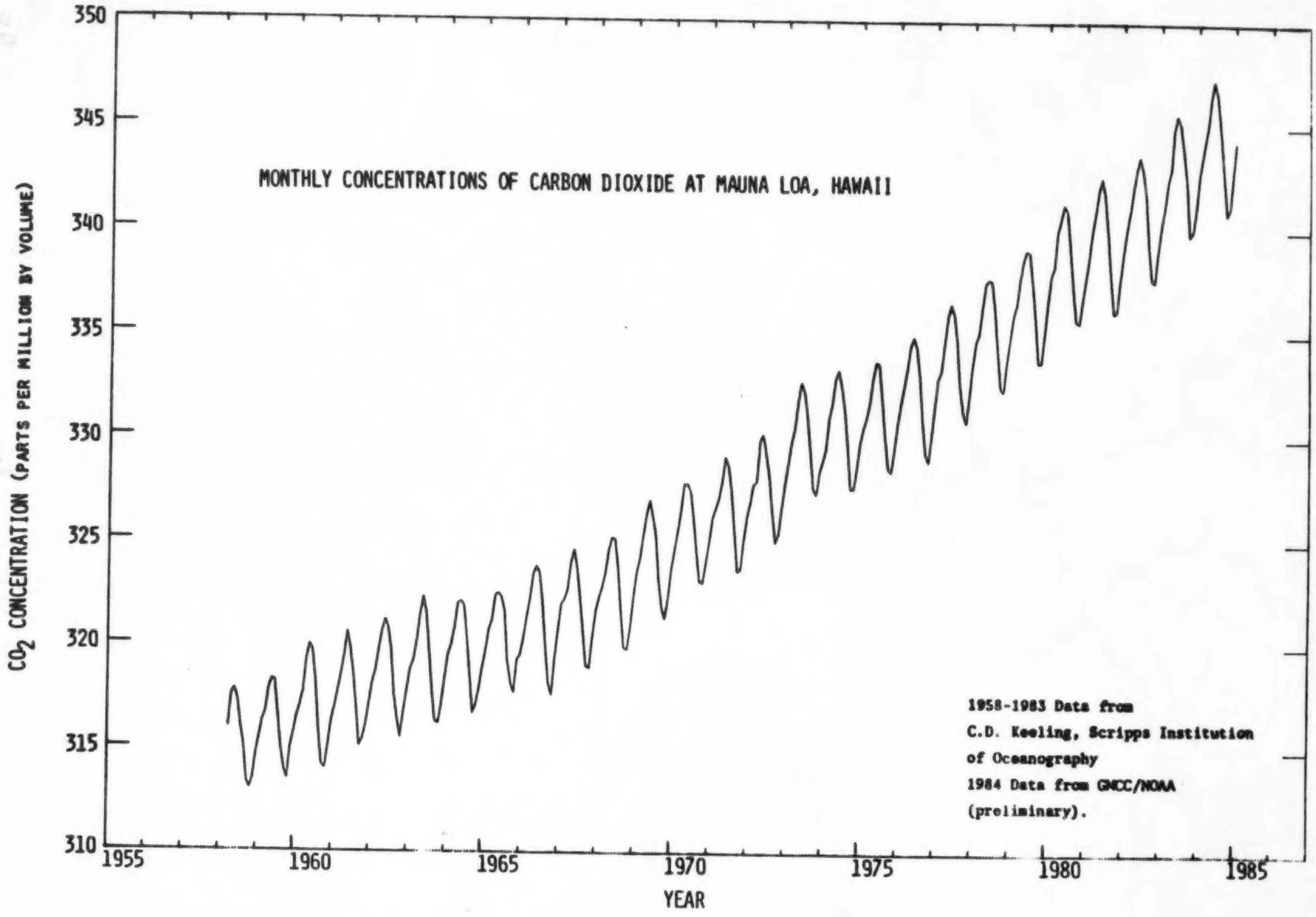

MONTHLY CONCENTRATIONS OF CARBON DIOXIDE AT MAUNA LOA, HAWAII

1958-1983 Data from
C.D. Keeling, Scripps Institution
of Oceanography
1984 Data from GMCC/NOAA
(preliminary).

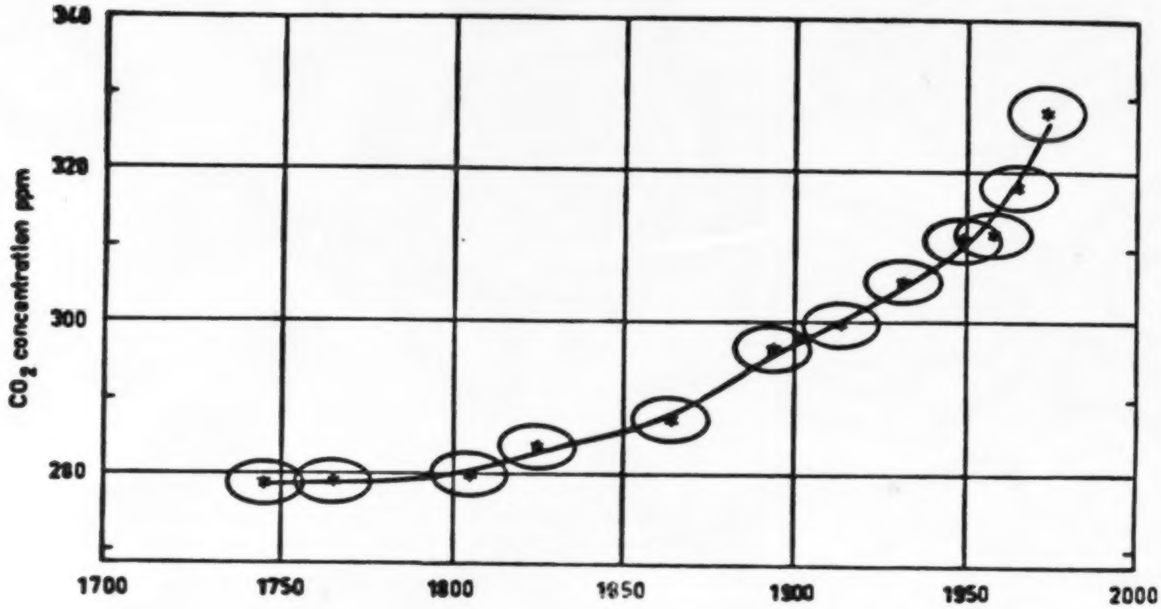

Figure 3.3 Atmospheric CO_2 concentrations measured in glacier ice formed during the last 200 years (Neftel et al, 1985).

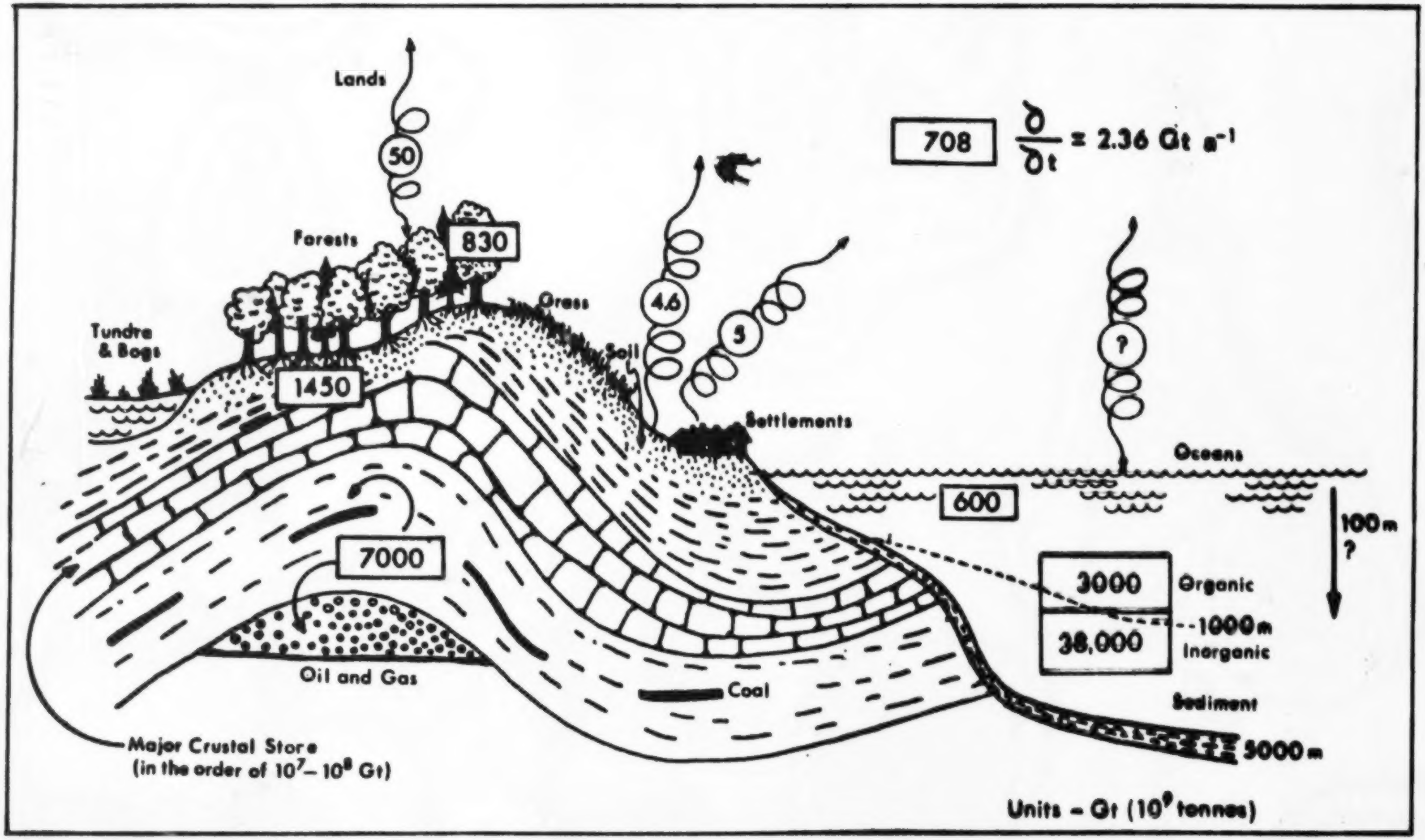
Lands
50
708
$\frac{\partial}{\partial t} = 2.36\ \mathrm{Gt\ a^{-1}}$
Forests
830
Tundra & Bogs
1450
Grass
Soil
4.6
5
?
Settlements
Oceans
600
100m ?
3000
Organic
-1000m
38,000
Inorganic
Sediment
5000m
7000
Oil and Gas
Coal
Major Crustal Store (in the order of 10^7– 10^8 Gt)
Units – Gt (10^9 tonnes)

Figure 1 Sketch of the principal reservoirs and exchange routes for the carbon cycle. Storages in rectangular boxes; annual exchanges in circles.

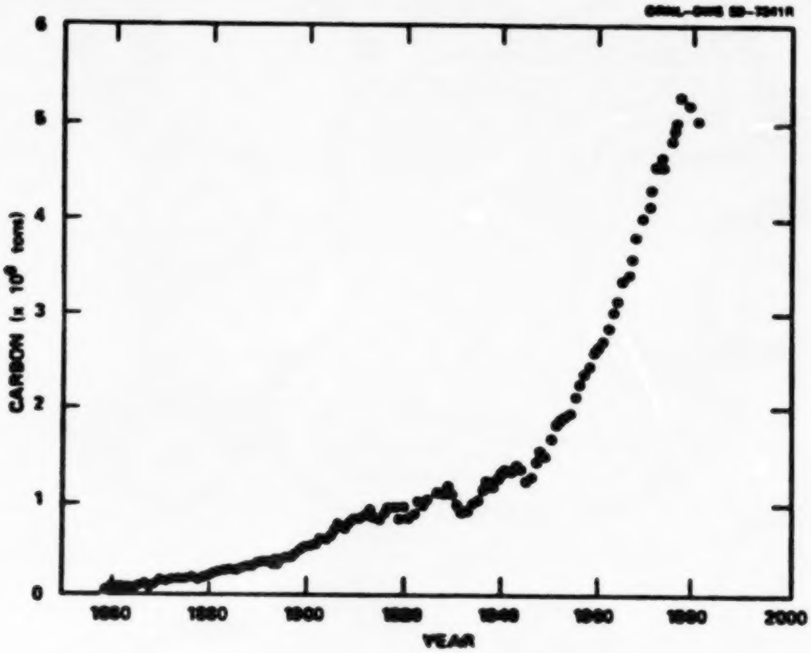

FIGURE 5. Fossil CO_2 emission: Historical, 1860-present

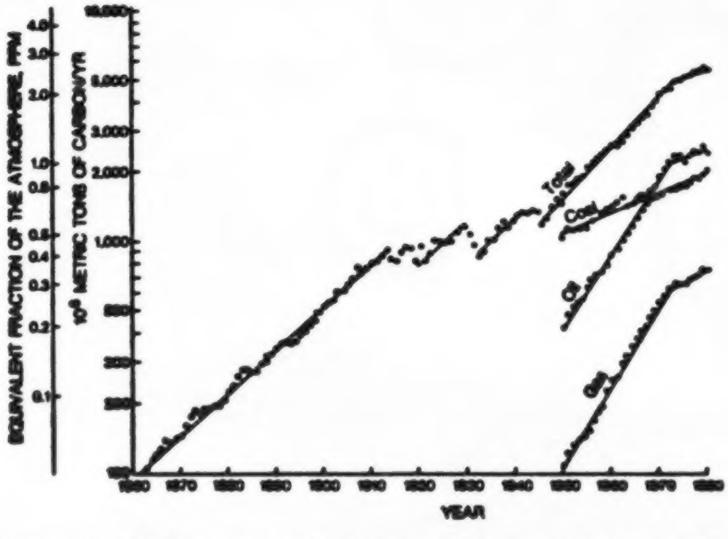

Fig. IV.4 : Global CO_2 production from fossil fuels, cement and gas flaring, 1860-1980.
Sources: Keeling (1973 for 1860-1949) and Rotty (1980, 1981 for 1950-1980).

Reproduced from
best available copy.

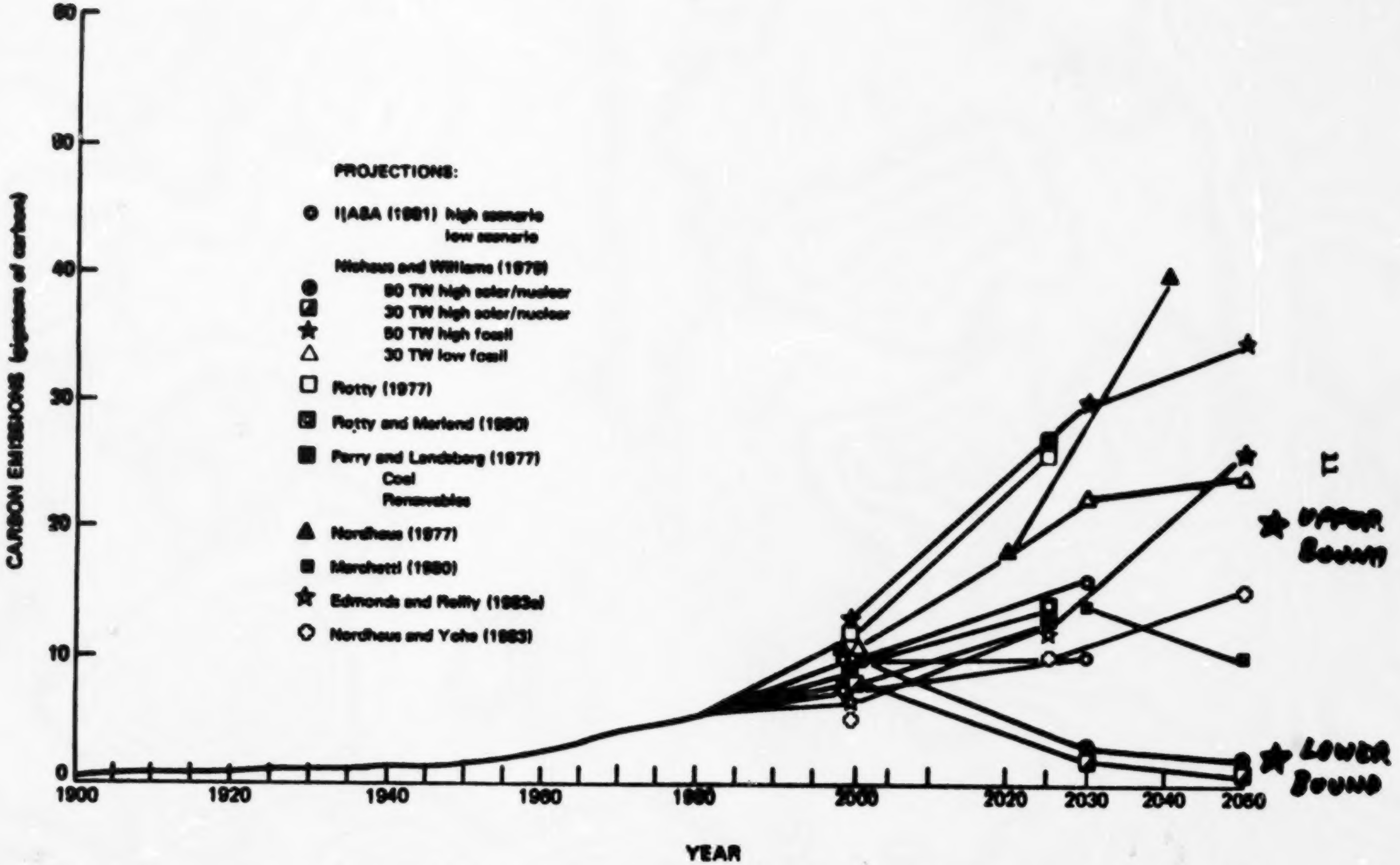

FIGURE 1.5 CO_2 emissions derived from long-range energy projections and historic production from fossil fuels. See Chapter 2, Section 2.2 for discussion of projections included here.

(Villach, 1985)

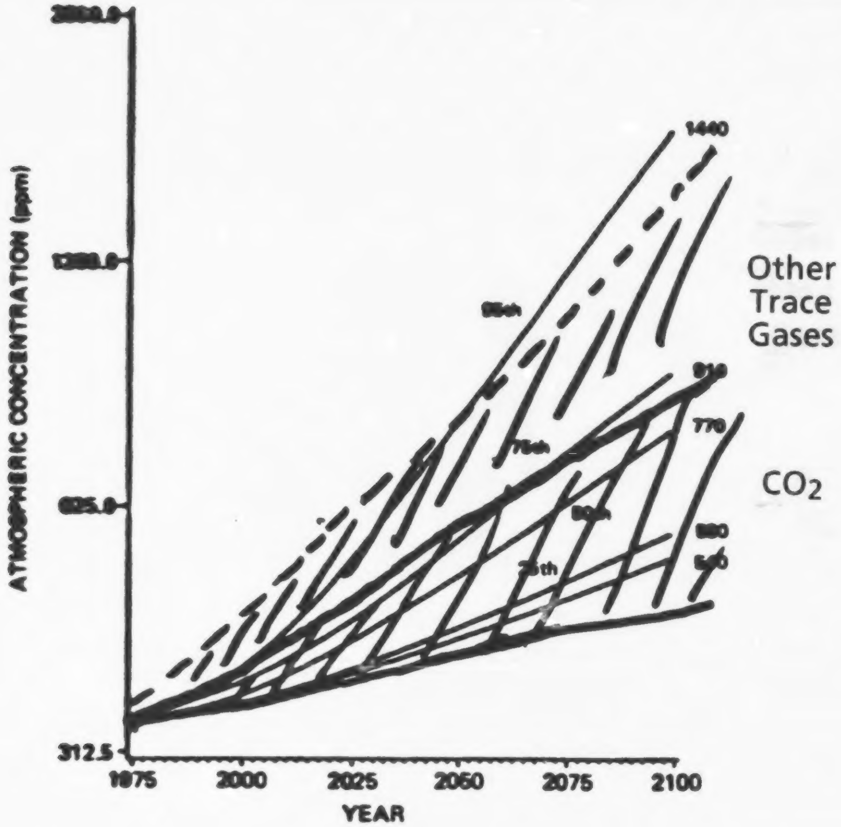

FIGURE 2.4 Atmospheric concentration of carbon dioxide (5th, 25th, 50th, 75th, and 95th percentiles; parts per million). The indicated percentile runs for concentrations; the numbers on the right-hand side indicate concentrations in the year 2100 for each run.

(Villach, 1985)

TABLE 1.2 Indices of Sensitivity of Atmospheric Concentration in 2100 to Uncertainty about Key Parameters[a] (100 = Level of Effect of Most Important Parameter[b])

	Marginal Variance from Most Likely Outcome
Ease of substitution between fossil and nonfossil fuels	100
General productivity growth	79
Trends in real costs of producing energy	73
Ease of substitution between energy and labor	70
Airborne fraction for CO_2 emission	62
Extraction costs for fossil fuels	56
Population growth	36
Fuel mix among fossil fuels	24
Trends in relative costs of fossil and nonfossil fuels	21
Total resources of fossil fuels	5

BES

Carbon Dioxide Research Program | United States Department of Energy

THE CLIMATE SYSTEM IS MADE UP OF MANY COMPONENTS AND PROCESSES

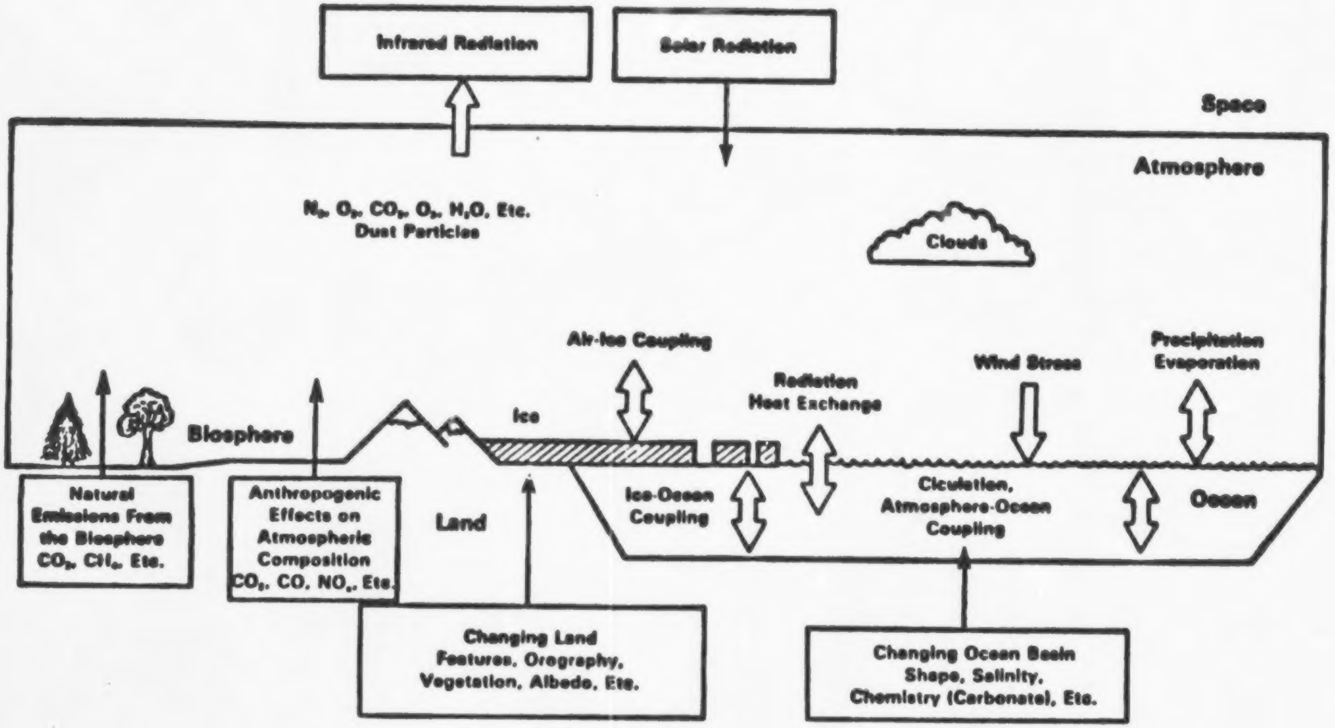
Infrared Radiation
Solar Radiation
Space
Atmosphere
N_2, O_2, CO_2, O_3, H_2O, Etc.
Dust Particles
Clouds
Air-Ice Coupling
Radiation Heat Exchange
Wind Stress
Precipitation Evaporation
Biosphere
Ice
Land
Ice-Ocean Coupling
Ciculation, Atmosphere-Ocean Coupling
Ocean
Natural Emissions From the Biosphere CO_2, CH_4, Etc.
Anthropogenic Effects on Atmospheric Composition CO_2, CO, NO_x, Etc.
Changing Land Features, Orography, Vegetation, Albedo, Etc.
Changing Ocean Basin Shape, Salinity, Chemistry (Carbonate), Etc.

CO_2 Is Present In the Atmosphere, Ocean, and Biosphere and Buried In the Land.

Paper 2

UNEP/WMO/ICSU CONFERENCE
VILLACH, OCTOBER 1985

- It Is Time To Take Greenhouse Cases Into Account In Policy Development
- Public Information Efforts Are Needed
- Research Is Needed On Both Scientific And Policy Fronts
- – Climate (Global Change, WCRP)
  - Analysis Of Policy And Economic Options
- Specific Research Topics
- International (WMO/ICSU/UNEP) Task Force
  - Assessments
  - Advice
  - Consideration Of A Global Convention

"...(U)nderstanding... is sufficiently developed that scientists and policy-makers should begin an active collaboration to explore the effectiveness of alternative policies and adjustments."

Paper 2

"In the twentieth century, man, for the first time in the history of the earth, knew and embraced the whole biosphere, completed the geographic map of the plant Earth, and colonized its whole surface. Mankind has become a single totality in the life of the earth....(F)or the first time man becomes a large-scale geological force. He can and must rebuild the province of his life by his work and thought....Wider and wider creative possibilities open before him. It may be that the generation of our grandchildren will approach their blossoming."

W.I. Vernadsky
The Biosphere and the Noösphere,
American Scientist, 33, No.1.,
January 1945

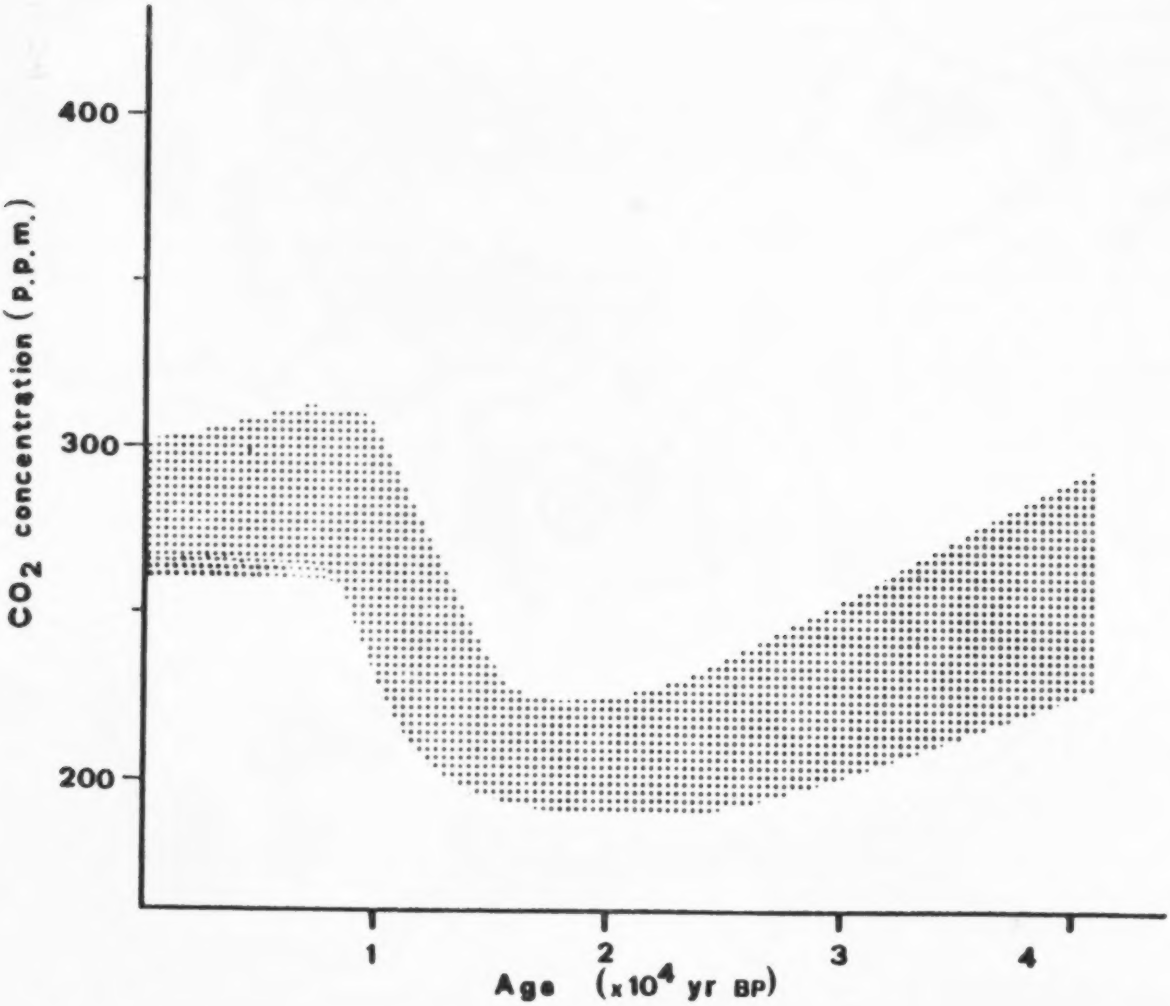
400
300
200
CO$_2$ concentration (p.p.m.)
1
2
3
4
Age (x10^4 yr BP)

Paper 3

Past and Future Changes in Climate

by

David Rind
NASA/Goddard Institute for Space Studies

This paper was based upon the presentation made at the workshop.

Climate Modeling and Climate Change

by

David Rind

CLIMATE MODELING AND CLIMATE CHANGE

D. Rind
Goddard Space Flight Center
Institute for Space Studies
2880 Broadway
New York, N.Y. 10025

The following represents an edited version of a talk given at the EPA Workshop on Global Atmospheric Changes, November 5, 1985.

Introduction

The focus of this talk will be on what climate change we may expect in the next 35 years. To put the conclusions in the proper perspective, however, it is necessary to understand the uncertainties that go into the models that are being used to provide this estimate. Thus we will first discuss how climate models are constructed, and what problems are involved. We will then review the physics of the climate system, to explain why climate is expected to change. At the end we will show preliminary results of an experiment made to assess future climate changes.

Climate Modeling

The word climate means different things to different people. Scientifically it refers to the time-averaged weather, but in practice each individual extracts from the concept that which is most appropriate to his needs. For people concerned with air pollution, climate refers to the normal wind velocity responsible for dispersal. To the "man in the street" climate probably refers to the mean temperature, primarily. For ski resort owners, it will be snowfall amounts, for farmers, rainfall and growing season degree days. The climate system is very diverse. If one wants to model the system fully, it is necessary to include all the elements that interact and whose change could be of importance to the general community.

The physics of climate modeling is, on the surface, straightforward. There are only a few conservation laws, i.e., fundamental equations, which require solution. These equations represent the conservation of momentum, energy, mass and moisture (Fig. 1). A representative application of these equations provides an answer to the question of why temperature will change in a given area with time. For this, one uses the equation for the conservation of energy. The change with time of energy (or temperature) (on the left-hand side of the equation) results from the occurrence of heating or cooling processes (on the right-hand side). For example, the sun's radiation warms the air during the daytime, while at night the only radiative process involves energy being lost back to space ("long-wave" radiation). The change of temperature or energy will be positive during the day from the radiative processes, and negative at night. The actual change depends upon the sum of all the heating and cooling processes; the air can warm when there is a flux of heat from the ground, when water vapor condenses, or when wind brings in air with a higher temperature. To know what the wind direction will be requires solution of the conservation of momentum equation, and to know if water vapor will condense in the atmosphere requires the solution of the equation for conservation of moisture. The equations are thus coupled together, and must be solved simultaneously. This brings up the first of the problems : these "non-linear, partial differential" equations cannot be solved analytically. One has to obtain an approximate solution via the computer using numerical techniques.

The method of solution involves "discretization". The differential equation indicates the instantaneous change with time of temperature, wind or humidity; the numerical solution solves for the change over a finite length of time, generally ranging from five minutes to an hour. Similarly, the advection of air with a different temperature into a region in the fundamental equation involves an infinitely small spatial change; the numerical equation calculates gradients on much coarser scales, dividing the earth into finite "grid boxes" (e.g., Fig. 2). It is important to realize that this procedure has changed the equation. We have departed from the full differential equation, which is exact, to an

P9

approximation of this equation in "finite difference" form. The closer one approaches the differential equation, i.e., the smaller the temporal and spatial scales employed, the more accurate the solution. In practice, these equations must be solved over the entire earth for a number of years when making climate projections, thus relatively large finite distance grids have to be employed. So the first problem is that we are only obtaining an approximate solution to the fundamental equations.

The grid boxes shown in Fig. 2 emphasize another limitation of climate modeling. The size of this grid is often very coarse compared to the usual scales of concern. For example, if one is interested in the pollution of a lake in a specific area, the lake will likely represent an extremely small portion of the grid box. Due to the increase in computer time needed to produce calculations on very small spatial grids, it is not practical to attempt to solve for climate change on the scale of the lake. The natural variation within the grid box provides some estimate for how representative the grid box solution is to that particular locale.

The second problem involves the calculation of the "source" terms of energy, momentum and moisture on the right-hand side of the equations. How are processes such as absorption or emission of radiation, fluxes from the surface or condensation of moisture to be calculated? For computing purposes it is necessary to find some numerical formulation for each of these physical events; however, in many cases, the precise mechanisms involved are imperfectly known. We thus use approximate equations to model these processes, often relating occurrences which take place on very small scales to the large grids used in climate models. We are "parameterizing" the physical process, and to the extent that the parameterization is not an accurate representation of reality, we are introducing additional errors into the model.

The types of processes which need to be parameterized in each grid box are shown in Fig. 2 (bottom). Included are calculations of variables as diverse as cloud cover, the radiative effect of atmospheric aerosols, and fluxes of heat and moisture within the ground. The physics of each of these tends to be quite complicated, and many involve interdisciplinary research areas. For example, moisture is drawn from the ground by plants. Understanding the exact mechanism is the goal of botanists, plant physiologists and soil scientists. How deep do the roots go into the ground, and what is their rooting density? Exactly when and under what conditions are plants activated in the spring? Atmospheric scientists who have developed the climate models need to work in conjunction with researchers from these disciplines, who are often used to viewing the problems on a much smaller spatial scale and with a different perspective. In the climate model developed at GISS (NASA Goddard Institute for Space Studies) we have incorporated a 1°

representation of the vegetation over the surface of the earth; the distribution over North America is shown in Fig. 3. The impact this vegetative cover has on the climate model is most apparent over desert regions, where there is little vegetation present to draw moisture out of the ground. A truly proper representation would include concepts such as crusting of the desert surface which inhibits infiltration. The future of climate model development involves interaction with many different disciplines to help quantify these effects.

Climate Model Output

There are essentially three climate models being used for long-term climate simulations in the United States. The models are located at Princeton (the GFDL model), at NCAR (National Center for Atmospheric Research), and at GISS. The models handle the processes we have been describing in somewhat different ways, although the approaches are generally conceptually equivalent. The major task of each modeling group is to justify their parameterizations and numerical schemes by comparing the output of their model to observed climate parameters. Shown in Fig. 4 is a comparison of the GISS model simulation of precipitation, for the annual average, with observations. The model successfully reproduces many elements of the observed precipitation field, including the dryness in desert regions and off the west coast of continents, while rainforest areas are wet. Also shown is the interannual variability of rainfall. Not only must the models accurately simulate today's climate, they must have the same variability if they are to be used to assess future climate changes. The model results appear realistic except for reduced variability over the oceans. This introduces another difficulty; the oceans are an essential part of the climate system, and ocean changes will impact climate (as climate changes will impact ocean circulation). Ocean modeling is in a very primitive state, and most climate models use very simplified ocean models. The results presented here were derived with the sea surface temperatures specified from observations of their climatological norm; since no variability is introduced in the year-to-year specifications, events such as El Nino, are not introduced. This then is responsible for a major portion of the reduced rainfall variability over the ocean in the model.

Fig. 5 shows the surface air flow generated by the model for January (top) and July (bottom). At low latitudes the trade winds blow from west to east and towards the equator in the winter hemisphere. During July, the model simulates the monsoon circulation, as air is swept onto the Indian subcontinent bringing rain. These features are realistic representations of the actual flow field. All the basic models simulate the current climate in a reasonable fashion, although none are perfect. If one compares the model output with enough different types of observations, the model has to be realistic in an absolute sense to reproduce all of them.

In practice, one discovers certain aspects that are inaccurate, which then become the focus of further model development.

Fig. 6 displays the model wind at the jet stream level, where the atmospheric pressure has been reduced to about 0.2 of what it was at the surface. The jetstream is a region of strong west to east flow at that level; in the figure the circled region is where the jetstream is most intense. Again, this is a relatively realistic assessment of the actual jetstream. We have now introduced another factor: the atmosphere is three-dimensional, and therefore the discretization involves not only the horizontal grids but also vertical levels. In addition to horizontal winds, the atmosphere also features vertical advection, most strongly concentrated in convective areas (e.g., thunderstorms). To complete the point we may also note that the ground is also divided into vertical layers for calculations of the movement of water and heat within the soil.

Elements of the Climate System

To be able to predict how climate will change in the next 35 years, we must know what the sensitivity of the climate system is. Studies of past climates (paleoclimatology) provide the major source of evidence in this regard. Therefore, modeling past climates, for example the climate of the last ice age, allows us to evaluate through the model's perspective how the various elements of the climate system change, and how they feedback to amplify or diminish initial perturbations. We utilize the estimated boundary conditions derived for the peak of the last ice age, about 18,000 years ago. This includes the sea surface temperatures, sea ice, land ice and orbital parameters for that time. These boundary conditions are established by various techniques, often involving deductions of past temperatures from fossil or geologic evidence.

In Fig. 7 we show the change in surface air temperature between the ice age climate and that of today for the annual average, as produced by the GISS climate model. Large temperature changes occur in the vicinity of the ice sheets, while at low latitudes, due to the warmth of the estimated sea surface temperatures, little cooling occurs. Whether low latitudes really were this warm during the last ice age is a matter of some debate.

The global average temperature change in the model produced in this experiment is close to 4°C; global surface air temperature changes of this magnitude were associated with the advance of ice sheets to Long Island. In the simulation, the insertion of the ice sheets and colder ocean temoperatures force the model to produce a colder climate. However, additional feedbacks arise (Fig. 7, bottom). For example, a colder atmosphere can hold less moisture; when the atmosphere cools, not as much water vapor is evaporated from the oceans. Water vapor is a very effective greenhouse gas, absorbing energy radiating from the earth, so with less moisture in the atmosphere more energy escapes, and the atmosphere cools further. The water vapor reaction is an example of a positive feedback inherent in the system - as the climate cools, there is less water vapor, which cools the climate more, which results in even less water vapor, and so on. There are other such feedbacks in the system. For example, when ice replaces vegetation as the surface land feature, it increases the reflection of solar radiation back to space. There is thus less available energy to warm the climate, and temperature is reduced. Lower temperatures allow more ice to form, and again, the cooling is accentuated.

Carbon dioxide in the atmosphere was apparently less abundant during the last ice age. If CO_2 was reduced prior to the beginning of the ice age, then it could have helped initiate the ice age. If the reduction occurred after the start of the ice age, then it is another example of a positive feedback: a reduction of CO_2 lessens the greenhouse capacity of the atmosphere, which would cool the climate further. The primary generating mechanism for ice ages is thought to be variations in the orbit of the earth, especially those changes which produce less solar radiation at upper mid-latitudes of the Northern Hemisphere during summer. Cooler summers would allow ice to remain throughout the year, and therefore to grow. This direct forcing is relatively small, especially on the global average, and the implication is that the 4°C cooling results primarily from the positive feedbacks (Fig. 7, bottom). The orbital perturbations are long lasting, with variations on the order of 20,000 to 100,000 years, so the feedbacks in this case are those applicable to long-term climate perturbations. But if the climate system can amplify initial perturbations of shorter time scales then this will effect the future climate.

Future Climates

With the current rate of atmospheric CO_2 increase, an effective doubling of the 1958 atmospheric CO_2 concentration should occur during the next century. To understand the future climate sensitivity, the climate model has been run with doubled atmospheric CO_2 concentration, allowing the ocean temperatures to adjust to the new radiative balance. The annual average surface air temperature changes which arise are shown in Fig. 8, as well as the feedbacks which have augmented the warming. Large increases in temperature are seen at high latitudes; this is partly the result of reductions in sea ice which reduce the reflectivity of the surface and allow heat from the ocean to warm the winter atmosphere. In addition, the greater natural stability of the colder regions trap the added heat near the surface, and thus exaggerate the surface air temperature change. These changes represent the model's equilibrium result; for the feedbacks to become fully involved requires allowing the ocean temperatures to respond. The ocean has a large thermal heat capacity, so its temperature changes only slowly. It was necessary to integrate the model for a simulated 35 years to arrive at the full equilibrium result. Even after the equivalent of doubled atmospheric CO_2 is achieved, some time will still elapse before the effect is felt in full.

The three different climate models all produce a warming of about 4°C when their atmospheric CO_2 concentration is doubled. However, in the GFDL model with fixed clouds (and a few other changes) the warming is only about 2°C. This underlines the importance cloud changes can have on climate sensitivity. Reduction of low level clouds, as occurs in these model runs when climate warms, reduces the reflectivity or albedo of the system, allowing more solar radiation to reach the surface. In addition, there is some tendency for upper level clouds, relatively thin cirrus clouds, to increase. Cirrus clouds act as an additional greenhouse component by absorbing the long wave radiation from the planet. Both of these cloud feedbacks are thus positive, amplifying the climatic warming in the model. There is little confidence that the models are parameterizing clouds in a realistic way, so this aspect of the climate sensitivity assessment represents a major uncertainty. A project has been organized by the World Meteorological Society to observe from satellites the present-day cloud climatology, which could then be used to determine if cloud cover is changing.

On more local levels, and for other climatic variables, there is less agreement among the models. This implies we can have less confidence in such results. The uncertainties in climate model parameterizations are probably more important when considering results at small-scales. This precaution applies, for example, to the following discussion. What are the local expressions of a 4° C global temperature change? In the model low latitudes experience less of a variation than do higher latitudes, in both the ice age and doubled CO_2 simulations. There are also seasonal variations to the global warming, with winter hemispheres more affected. The 4° C ice age cooling was associated with ice year-round in New York. To put the 4° C warming in perspective, we have looked at the impact of the model-generated temperature change on the summertime temperatures in different American cities. The procedure involved adding the mean monthly temperature difference to the observed daily summer temperatures, assuming the patterns of day-to-day variability remain unchanged.

Some results of this study are shown in Fig. 9. For example, in Omaha there are currently 3½ days during the summer in which the temperature rises above 100° F. For the doubled CO_2 climate, this number increases to 20½ days. For Washington D.C., there are currently 0.7 days of above 100° F readings; in the doubled CO_2 climate there are 11.6 days. The results for temperatures above 90° F are even more dramatic. Omaha experiences an increase from the current 36.6 days to 85.5 days above 90° F. We can also look at the nighttime temperatures : in Omaha there are now 0.2 days/year in which the temperature at night does not fall below 80°F. For the doubled CO_2 climate this occurs 9.4 days/year. In Washington D.C. the current number is 0.4 days/year, which increases to 19 days/year with doubled CO_2. It is probable that such changes would necessitate shifts in patterns of energy consumption across the country, including both seasonal and diurnal distributions.

CO_2 is only one of the atmospheric trace gases with greenhouse significance which has been increasing. In Fig. 10 we provide an assessment of the relative importance for warming or cooling of various potential forcing factors. It also provides a comparison with other components of the climate system which may affect the surface temperature. The direct effect of doubling CO_2 is similar to that of a 2% increase in the solar constant. Small fluctuations of solar input have been observed but nothing of that magnitude, although precise observations have been made for only a short time. Other trace gases whose increase effects the greenhouse capacity are methane, freons and nitrous oxide. The effect of increases in tropospheric aerosols is more complex; if the aerosol is soot (carbon particles), and if the optical thickness is increased by only a small amount, then the additional aerosols will help warm the climate. If the aerosol is made of sulfuric acid, a small increase will cause cooling of the climate. There is currently some uncertainty as to whether tropospheric aerosols are increasing away from urban areas, and, as these calculations show, the climatic impact will depend upon the nature of the aerosol.

Stratospheric aerosols associated most often with volcanoes tend to cool the climate. However, volcanic aerosols tend to fall out of the atmosphere within several years. Volcanic aerosols are thus a short-term climatic perturbation, and illustrate that the effect on this time scale is muted compared to that of longer-lived perturbations. The residence time of the volcanos is too short to allow the ocean to cool substantially, and this limits the capability of the subsequent feedbacks (such as reduced evaporation) to become involved. Again, the positive feedbacks discussed previously require that the whole system be given time to react. The potential influence of two of these feedbacks, cloud cover and land albedo, is also illustrated in this figure.

Transient Response

What has been the effect of the known climatic perturbations in recent decades? Shown in Fig. 11 are the decadal increments of greenhouse forcing that has or will occur (given reasonable projections) through the 1980s. What is most obvious is that, ignoring water vapor and ozone changes which are uncertain, the equilibrium impact of increasing trace gases other than CO_2 is cumulatively of the same order as that due to increasing CO_2. The anthropogenic impact on climate is clearly not simply a CO_2 problem. This predicted equilibrium change has not yet been fully realized, as, again, the ocean must be given time to respond. If the heat entering the ocean can diffuse below the surface mixed layer into deeper levels, then it increases the ocean heat capacity and requires that the ocean will warm even more slowly. Fig. 12 presents an estimate of how the climate would have changed between 1850 and 1980 due to the estimated CO_2 increase were the equilibrium response evident (top line), or diffusion to deeper levels in the ocean occurring. The difference, which depends on the climate sensitivity to doubled CO_2, represents the unrealized warming already built into the system due to the lag in the ocean response. If the ocean temperature change has not kept up with the atmospheric concentration change, then the system is not currently in radiative balance - more energy is coming in than is going out. This implies the oceans will continue to warm and so will the climate, even if no additional changes in atmospheric composition occur. As anthropogenically-influenced trace gases are likely to continue to increase, the system will get further out of balance, which indicates that the observed conditions will become less and less indicative of the ultimate response. The magnitude of this discrepancy will depend on the climate sensitivity and the actual heat capacity of the ocean.

To estimate what the climate change may be like over the next 35 years, we returned to the atmospheric composition prevalent in 1958 and changed CO_2, stratospheric aerosols, and other trace gases in the observed fashion through 1985. For projections into the future, in case A, we kept the growth rates for the trace gases at their current levels. The greenhouse forcing for this case, as well as for a reduced growth rate scenario (case B) is shown in Fig. 13. Note that the equivalence to a doubled CO_2 forcing occurs around 2030, although the equilibrium response will lag by at least several decades. The simple ocean model employed uses specified ocean heat transports; it allows diffusion through the bottom of the oceanic mixed layer with a diffusion coefficient calculated so as to match the vertical dispersal of oceanic transient tracers, such as tritium from atomic explosions. While several large volcanos occurred in the time period from 1958-1985, and are thus included, for the future projections for case A we simply use the mean value of the volcanic aerosol optical depth averaged over the last 100 years.

Some results of this experiment are shown in Figs. 14 and 15. The model indicates that an unambiguous warming will occur over the next several decades. The model sensitivity and simulation from 1958 to 1985 is in reasonable agreement with the observations (Fig. 14). By the mid-1990s the model indicates there will be a global average surface air temperature change of about 1° C. For the eastern United States a temperature increase approaching 2° C is reached by 2020 (Fig. 15). Warming of this magnitude is unprecedented during recorded history, and in the model simulation is occurring very rapidly. If such changes actually do take place, they would exceed the natural variability of the system, and be an unmistakable indication that the trace gas effect was proceeding as expected.

Fig. 1. Fundamental equations.

Conservation of momentum: (Newton's second law of motion)	$\frac{d\mathbf{V}}{dt} = -2\boldsymbol{\Omega} \times \mathbf{V} - \rho^{-1}\nabla p + \mathbf{g} + \mathbf{F}$	(T1)
Conservation of mass: (continuity equation)	$\frac{d\rho}{dt} = -\rho\nabla \cdot \mathbf{V} + C - D$	(T2)
Conservation of energy: (first law of thermodynamics)	$\frac{dI}{dt} = -p\,\frac{d\rho^{-1}}{dt} + Q$	(T3)
Ideal gas law: (approximate equation of state)	$p = \rho RT$	(T4)

Notation

$\mathbf{V}$	velocity relative to rotating earth
t	time
$\frac{d}{dt}$	total time derivative $\left[= \frac{\partial}{\partial t} + \mathbf{V} \cdot \nabla\right]$
$\boldsymbol{\Omega}$	planet's angular rotation vector
ρ	atmospheric density
$\mathbf{g}$	apparent gravity [=true gravity $-\ \boldsymbol{\Omega} \times (\boldsymbol{\Omega} \times \mathbf{r})$]
$\mathbf{r}$	position relative to planet's center
$\mathbf{F}$	force per unit mass
C	rate of creation of (gaseous) atmosphere
D	rate of destruction of atmosphere
I	internal energy per unit mass [$=c_v T$]
Q	heating rate per unit mass
R	gas content
c_v	specific heat at constant volume.

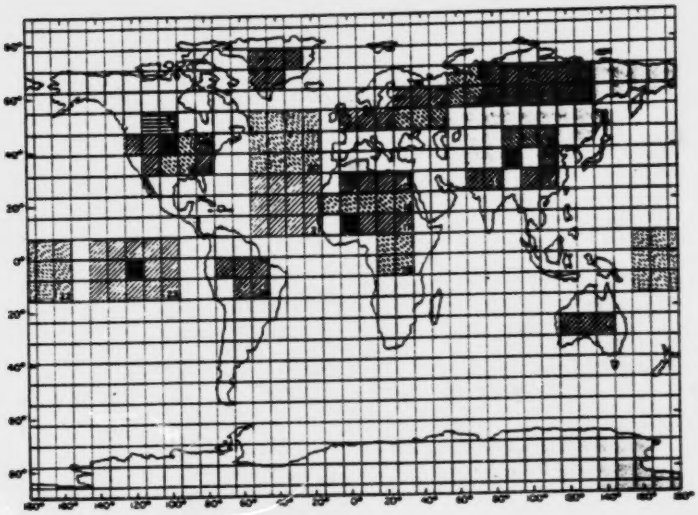
80°
60°
40°
20°
0°
20°
40°
60°
80°
180°
160°
140°
120°
100°
80°
60°
40°
20°
0°
20°
40°
60°
80°
100°
120°
140°
160°
180°

Fig. 2 .. Grid spacing for the 8 x 10° model. The shading indicates a particular choice of the regions for which special monthly diagnostics are produced. The four black regions are a particular choice of the grid-points for which special hourly diagnostics are produced.

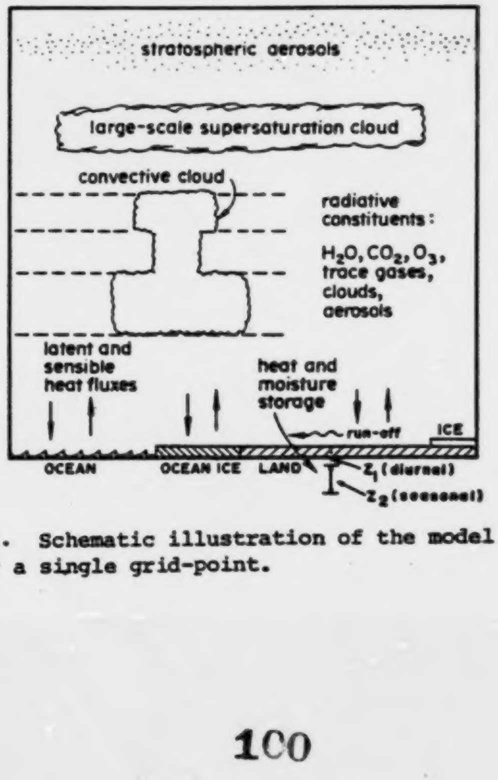
stratospheric aerosols
large-scale supersaturation cloud
convective cloud
radiative constituents:
H_2O, CO_2, O_3, trace gases, clouds, aerosols
latent and sensible heat fluxes
heat and moisture storage
run-off
ICE
OCEAN
OCEAN ICE
LAND
Z_1 (diurnal)
Z_2 (seasonal)

Fig. 3. Schematic illustration of the model structure for a single grid-point.

Reproduced from best available copy.

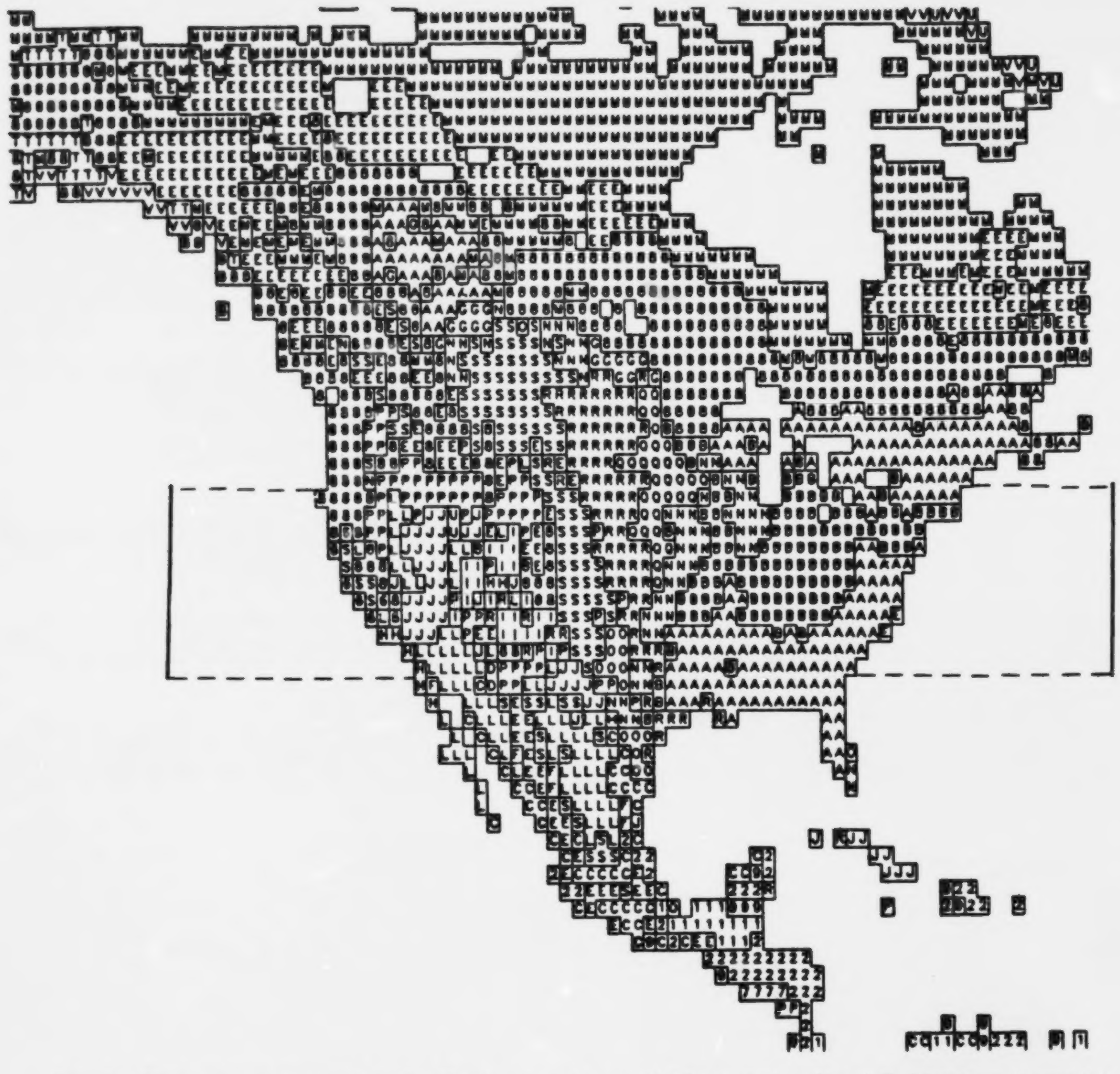

FIG. 3 . 32-component vegetation classification based on 1 × 1° vegetation file of E. Matthews. Legend: 1 = tropical rain forest, 2 = tropical/subtropical evergreen seasonal forest, 3 = subtropical rain forest, 4 = temperate rain forest, 5 = temperate evergreen seasonal forest, 6 = dry evergreen forest, 7 = subtropical evergreen needle-leaved forest, 8 = temperate evergreen needle-leaved forest, 9 = drought deciduous forest, A = cold-deciduous forest with evergreen trees, B = cold-deciduous forest without evergreen trees, C = xeromorphic woodland, D = dry evergreen woodland, E = evergreen needle-leaved woodland, F = drought-deciduous, G = cold-deciduous woodland, H = evergreen broad-leaved shrubland, I = evergreen microphyllous shrubland, J = drought-deciduous shrubland, K = cold-deciduous shrubland, L = xeromorphic shrubland, M = tundra, N = grassland: 10–40% treecover, O = grassland < 10% tree cover, P = grassland: shrub cover, Q = tall grassland, R = medium grassland, S = short grassland, T = meadow, U = desert, V = ice, W = cultivation. The different vegetation types contribute proportionally to each 8 × 10° grid. The hatched box defines the latitudinal belt encompassing most of the United States.

(after Matthews, E., J. Clim. and App. Meteor., 22, 474-483, 1983)

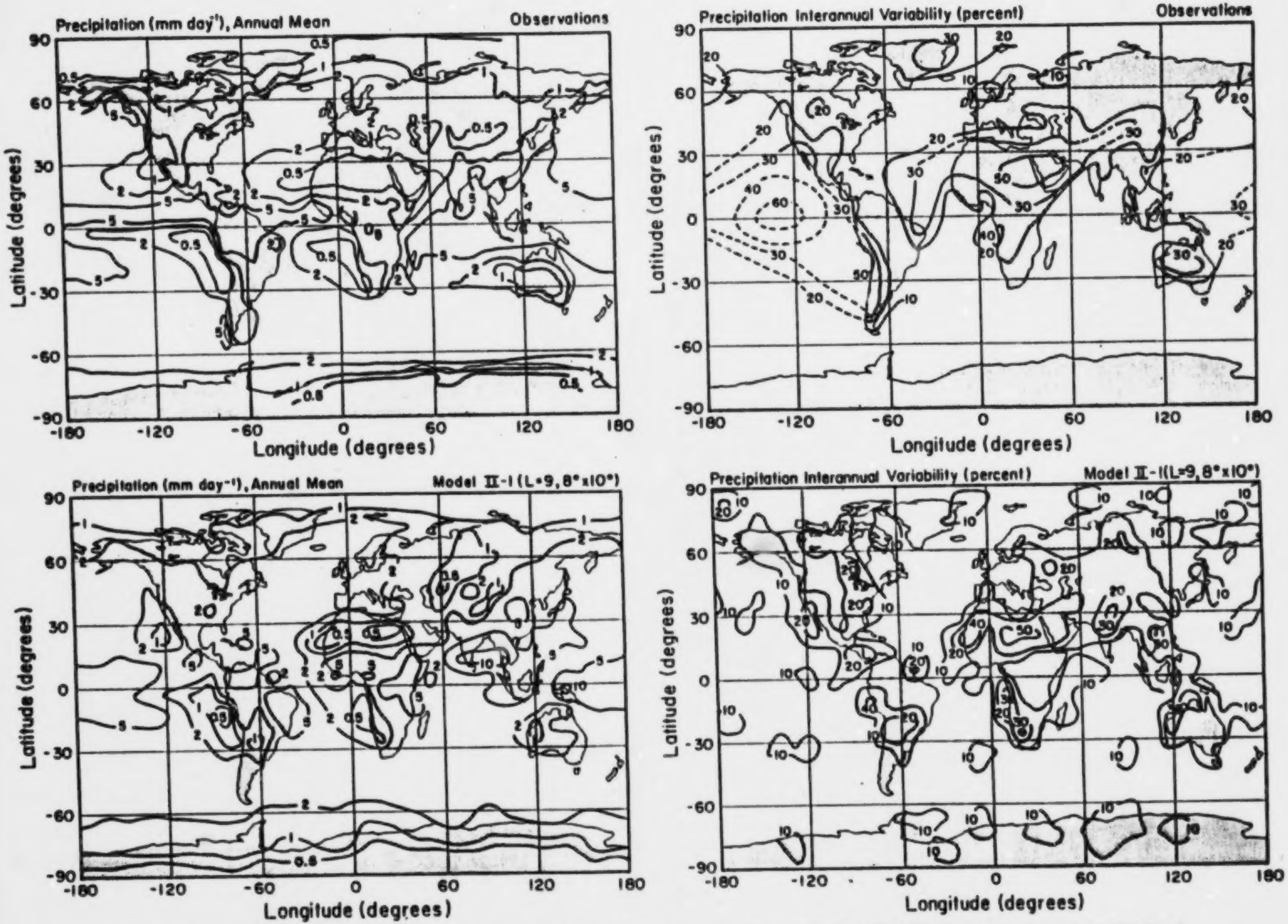
Precipitation (mm day⁻¹), Annual Mean
Observations
Precipitation Interannual Variability (percent)
Observations
Precipitation (mm day⁻¹), Annual Mean
Model II-1 (L=9, 8°x10°)
Precipitation Interannual Variability (percent)
Model II-1 (L=9, 8°x10°)
Latitude (degrees)
Longitude (degrees)
90
60
30
0
-30
-60
-90
-180
-120
-60
0
60
120
180

FIG. 4. Global distribution of annual-mean precipitation (left) and its interannual relative variability (right). Observed annual-mean precipitation is from Schutz and Gates (1971) and interannual variability from Berry *et al.* (1973).

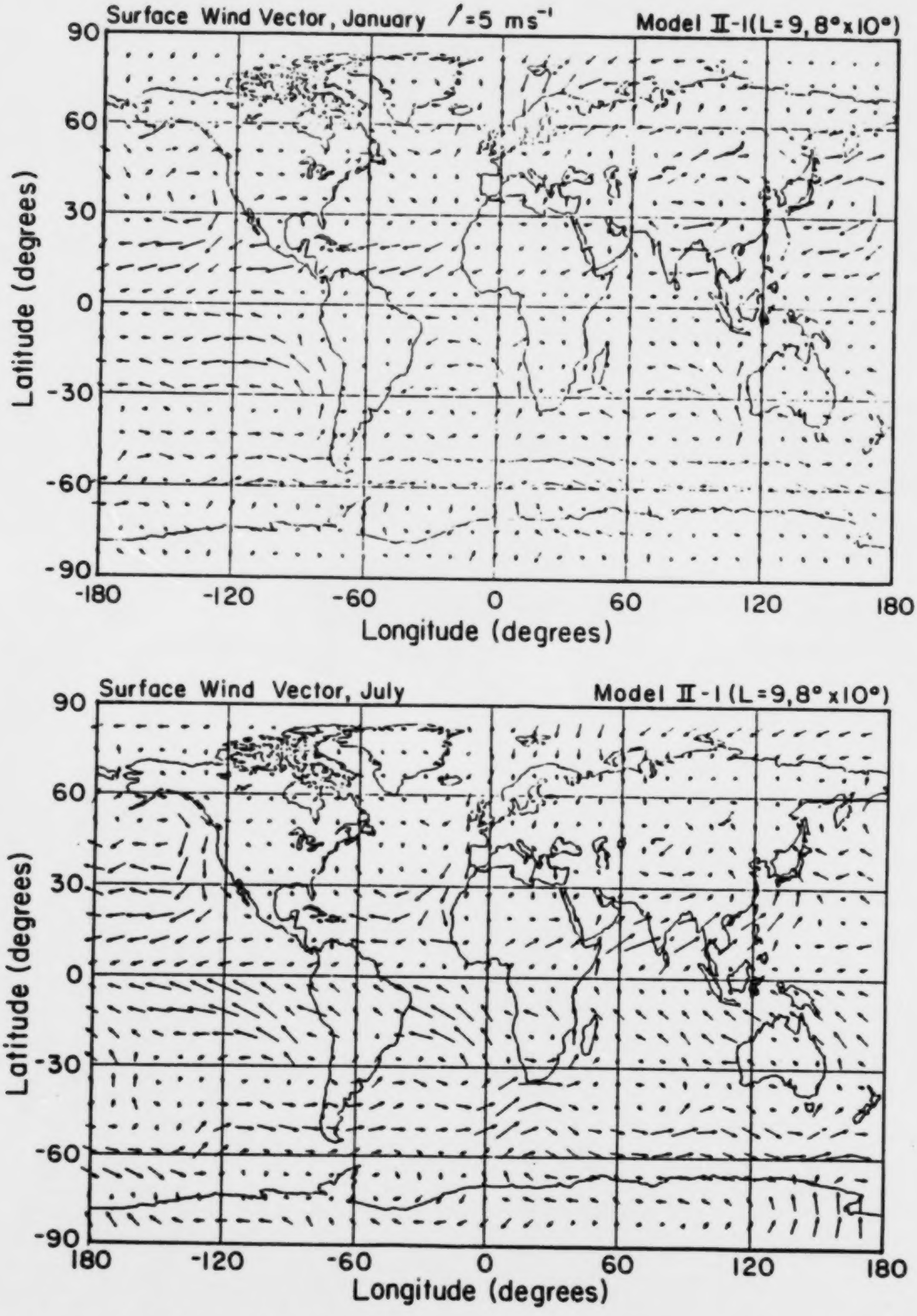
Surface Wind Vector, January /=5 ms⁻¹
Model II-1(L=9, 8°x10°)
90
60
30
0
-30
-60
-90
Latitude (degrees)
-180
-120
-60
0
60
120
180
Longitude (degrees)
Surface Wind Vector, July
Model II-1 (L=9,8° x10°)
90
60
30
0
-30
-60
-90
Latitude (degrees)
180
-120
-60
0
60
120
180
Longitude (degrees)

FIG. 5 . Surface wind field for January (top) and July (bottom) from Model II.

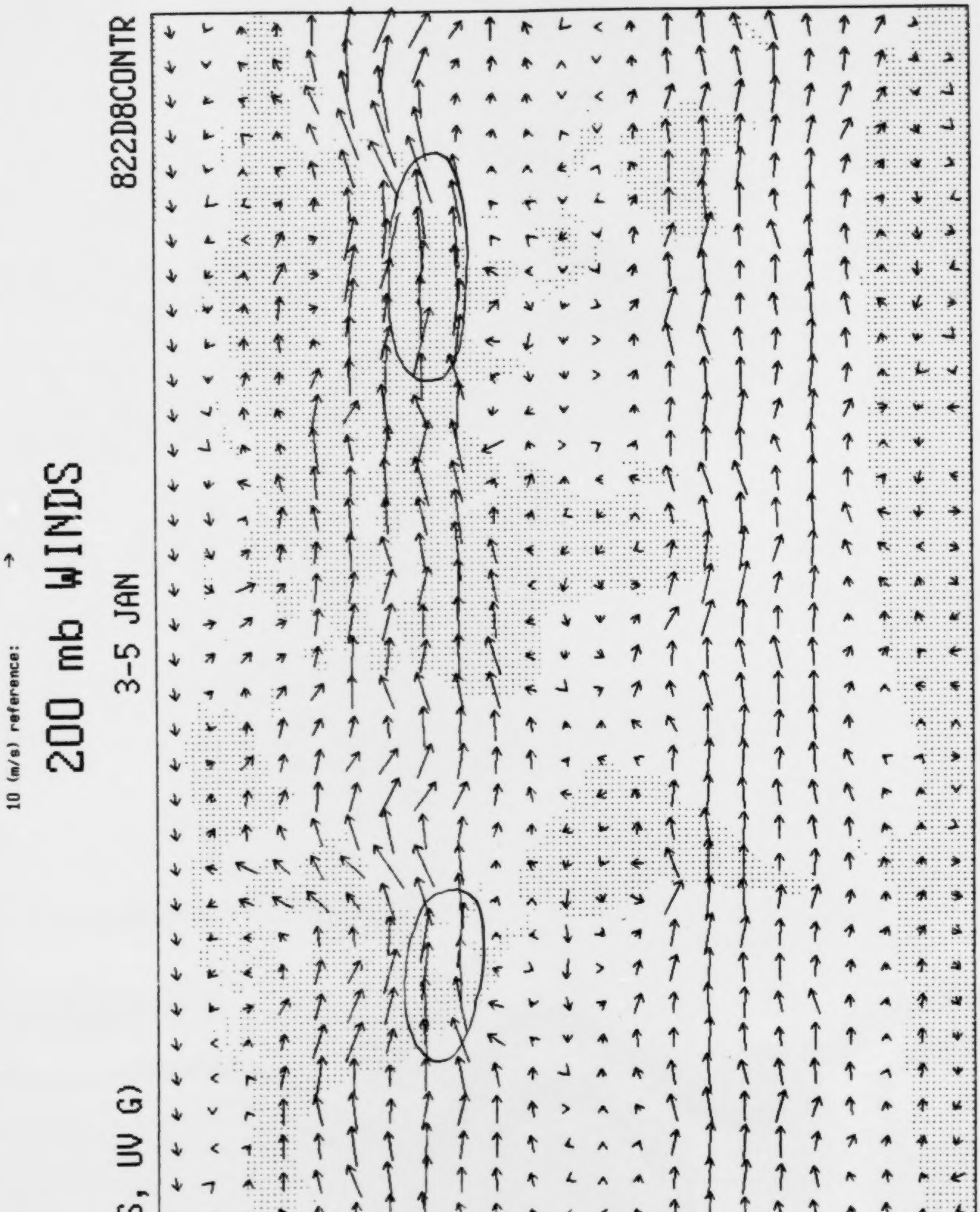

Fig. 6

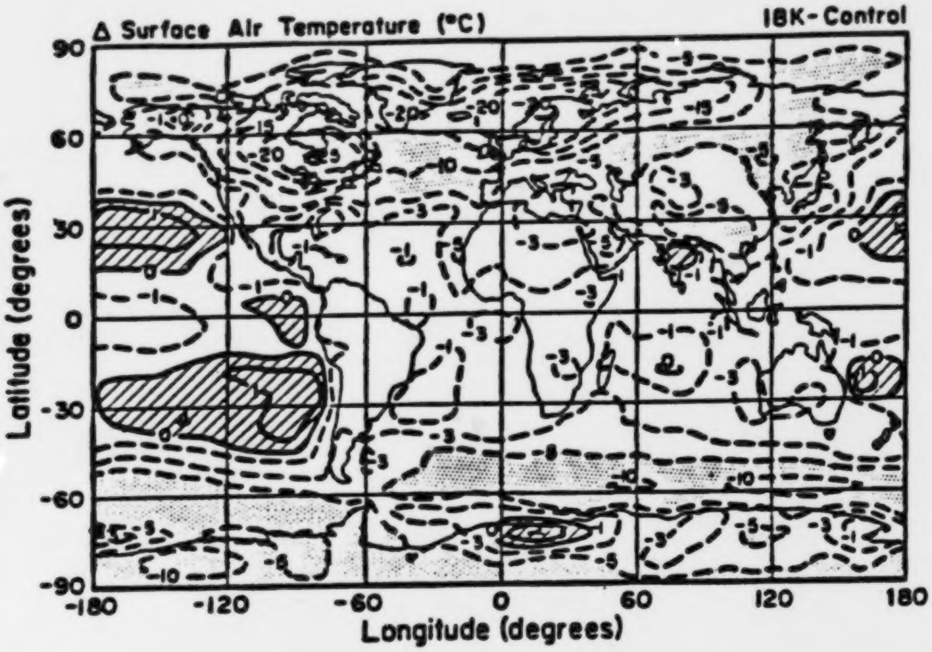
Δ Surface Air Temperature (°C)
18K-Control
Latitude (degrees)
90
60
30
0
-30
-60
-90
-180
-120
-60
0
60
120
180
Longitude (degrees)

Contributions to Cooling of Last Ice Age (18K)

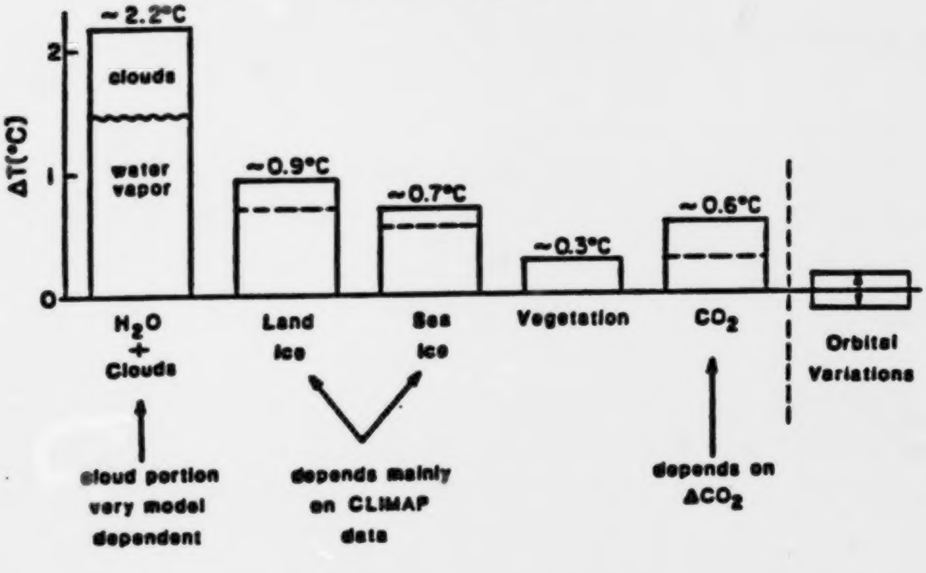

Fig. 7. Annual mean surface air temperature difference between the climates of today and the Wisconsin ice age (18,000 years ago), based on 3-D climate model simulations with the CLIMAP boundary conditions (paper 2). Areas in which the cooling exceeded 5°C are stippled, while areas with warmer temperatures at 18K are indicated by slashes. The contributions of different physical processes to the global mean cooling at 18K are shown in the lower part of the figure, as estimated by inserting individual changes of boundary conditions into the model.

(from Hansen et al., 1986, in CO_2 and Changing Climate, EPA/National Forest Products Association, in press)

GLOBAL WARMING IN 3-D MODEL FOR DOUBLED CO_2

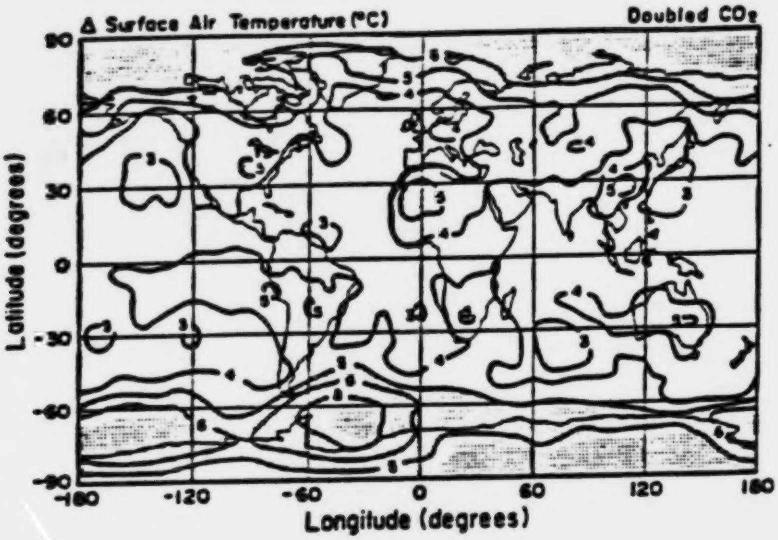
Δ Surface Air Temperature (°C)
Doubled CO_2
Latitude (degrees)
90
60
30
0
-30
-60
-90
-180
-120
-60
0
60
120
180
Longitude (degrees)

CONTRIBUTIONS TO GLOBAL WARMING IN MODEL

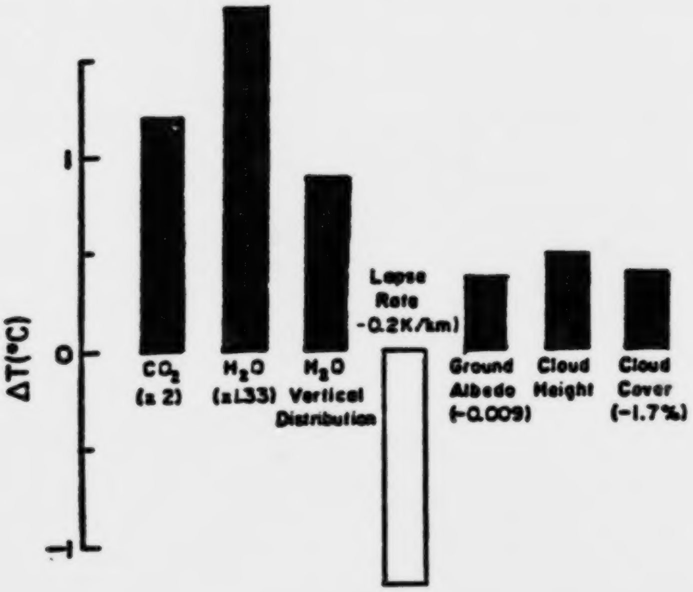

Fig.3 . Annual mean warming obtained in a 3-D global climate model (GISS model, described in papers 1 and 2) at equilibrium (t→∞) for doubled atmospheric CO_2. Lower part of figure shows contributions of different physical processes to the global warming, as estimated by inserting the changes in the 3-D model into a 1-D model.

(after Hansen et al., 1986 as in Fig. 7)

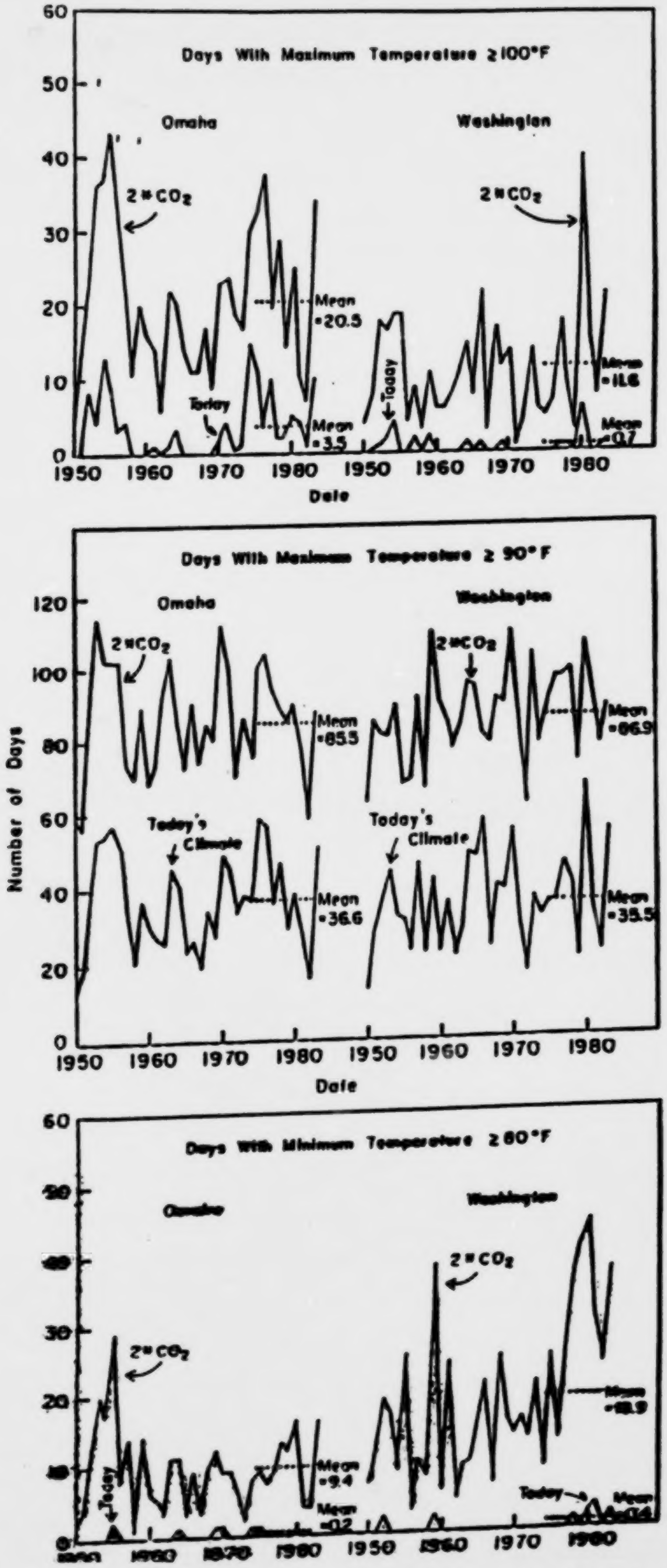

Reproduced from best available copy.

Fig. 9. (from Ashcraft and Hansen, 1986, submitted to Science)

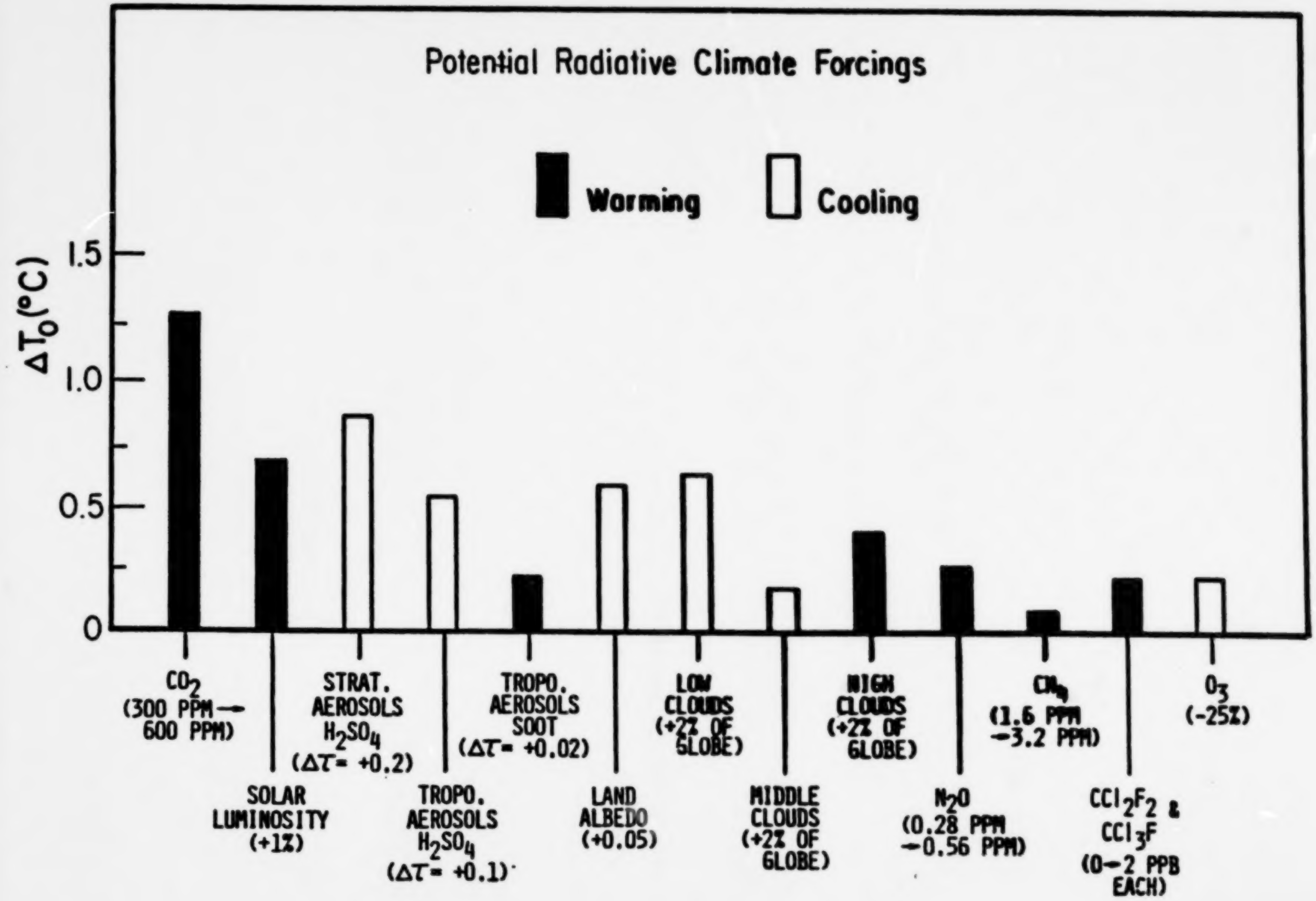

Fig. 10. (from Hansen et al., 1980, Science, 213, 957-966

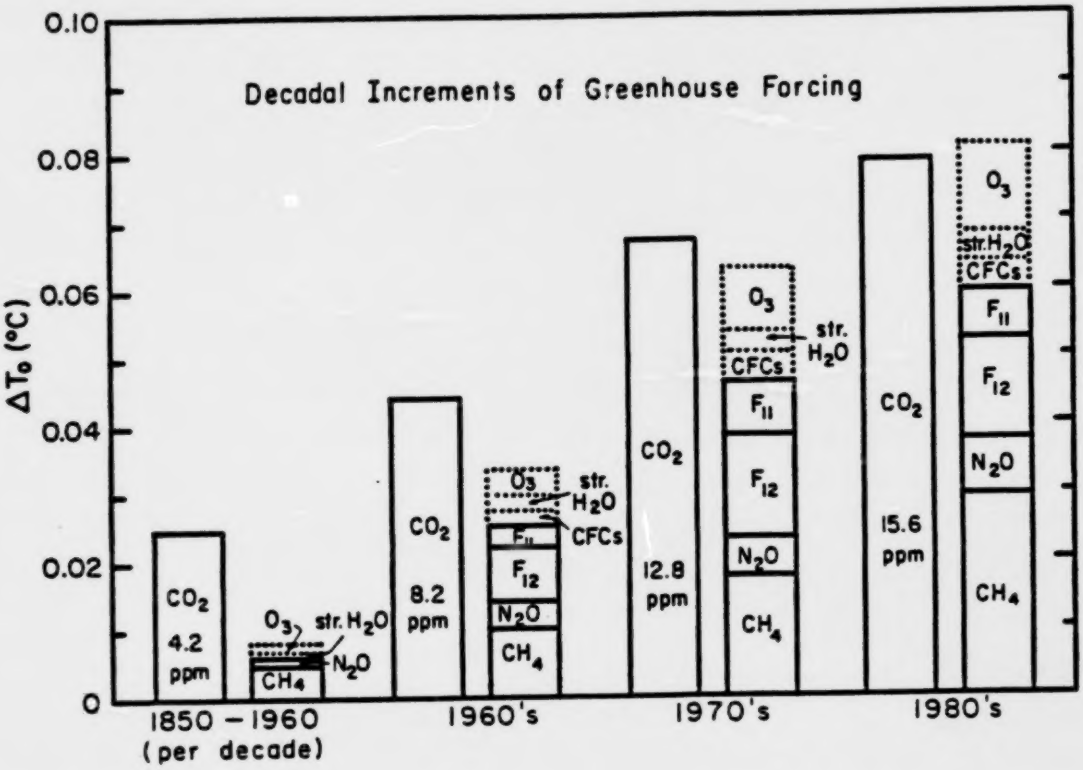

Fig 11 . Decadal additions to global mean greenhouse forcing of the climate system. ΔT_0 is the computed temperature change at equilibrium ($t \to \infty$) for the estimated decadal increases in trace gas abundances, with no climate feedbacks included. Multiply ΔT_0 by the feedback factor f to get the equilibrium surface temperature change including feedback effects. Most of the estimated trace gas increases are based on measurements, as discussed in the text. The O_3 and stratospheric H_2O trends (dotted bars) are based principally on 1-D model calculations of Wuebbles et al. (1983); however, we have decreased the ΔT_0 for O_3 by the factor 0.5 because much of the O_3 change would be confined to the hemispheric or smaller scale.

(after Hansen et al., 1986 as in Fig. 7)

24 1 15

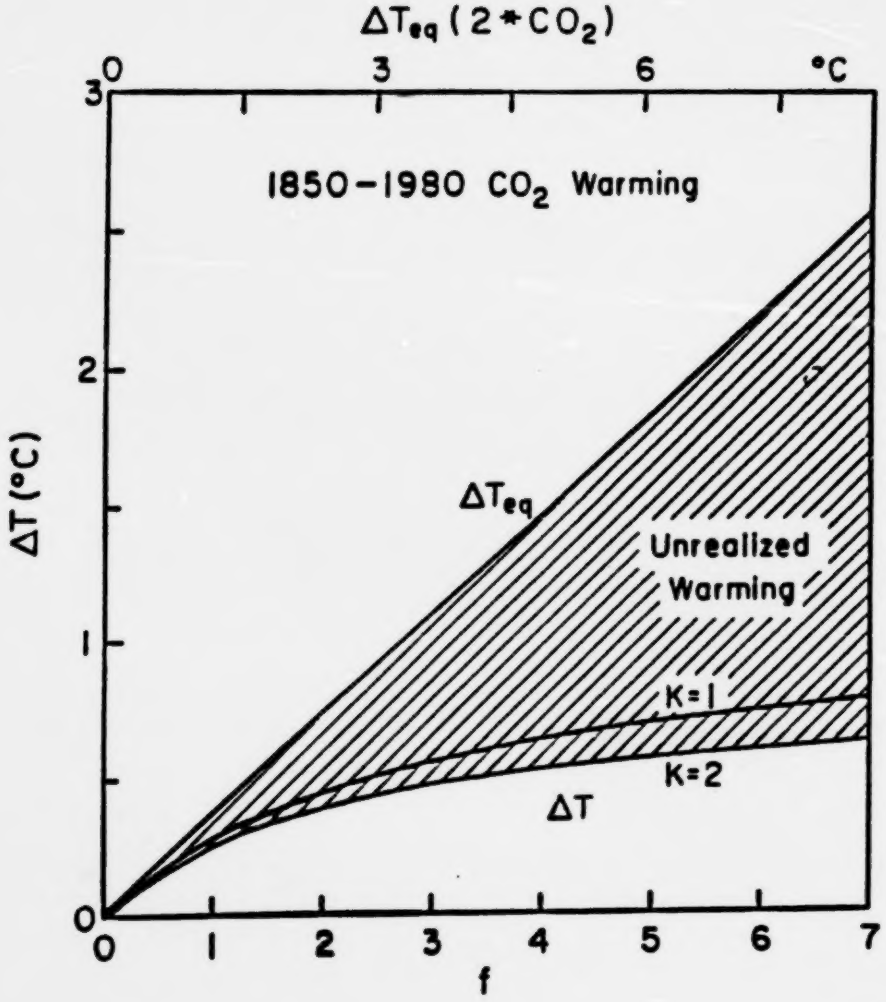

Fig.12. Ocean surface warming (ΔT) and the equilibrium warming (ΔT_{eq}) due to CO_2 added to the atmosphere in the period 1850-1980 for the 1-D box diffusion ocean model as a function of f or $\Delta T_{eq}(2 * CO_2)$.

(from Hansen et al., 1985, Science, 229, 857-859)

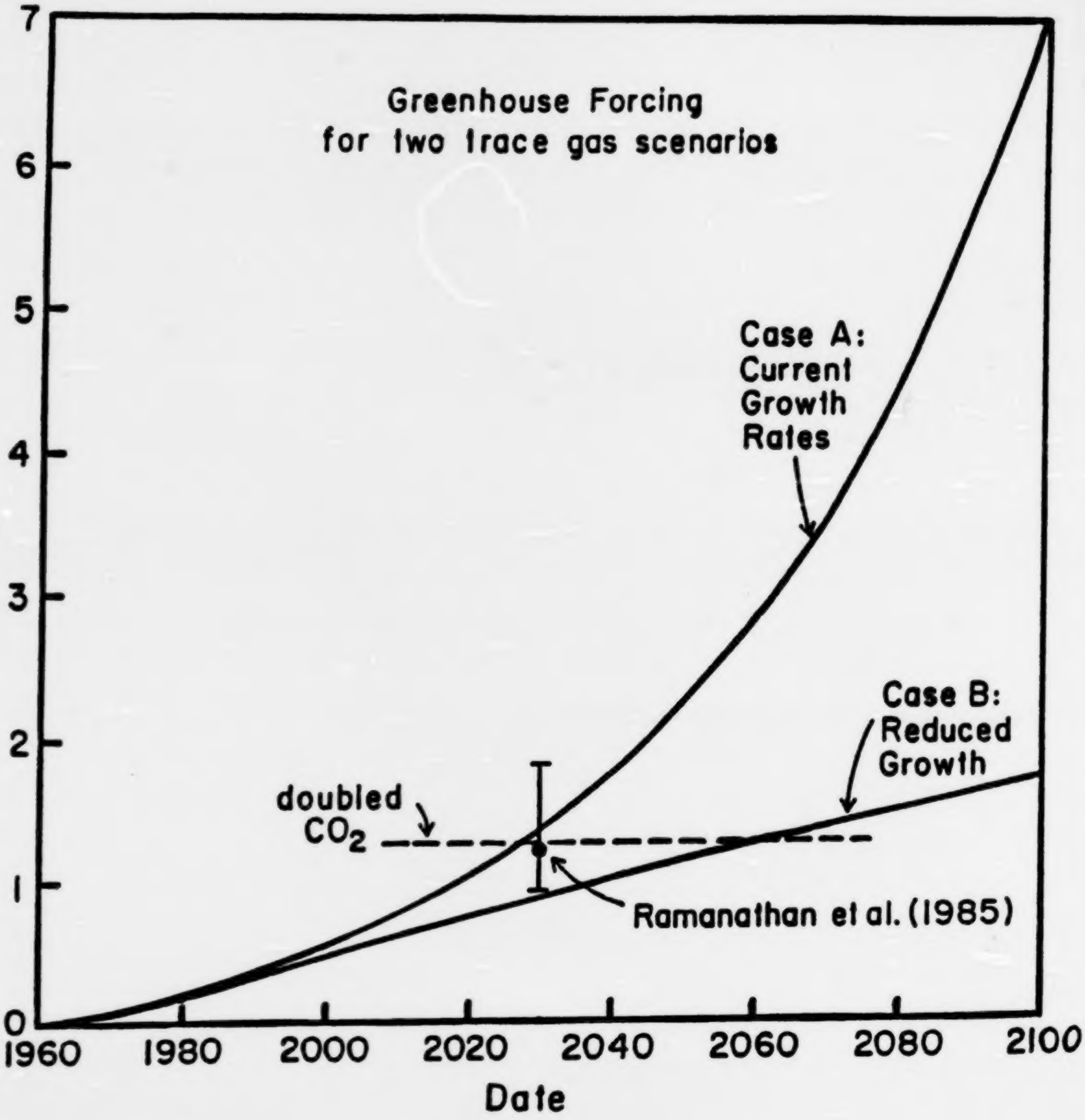

Fig. 13 (after Hansen et al., 1986, as in Fig. 7)

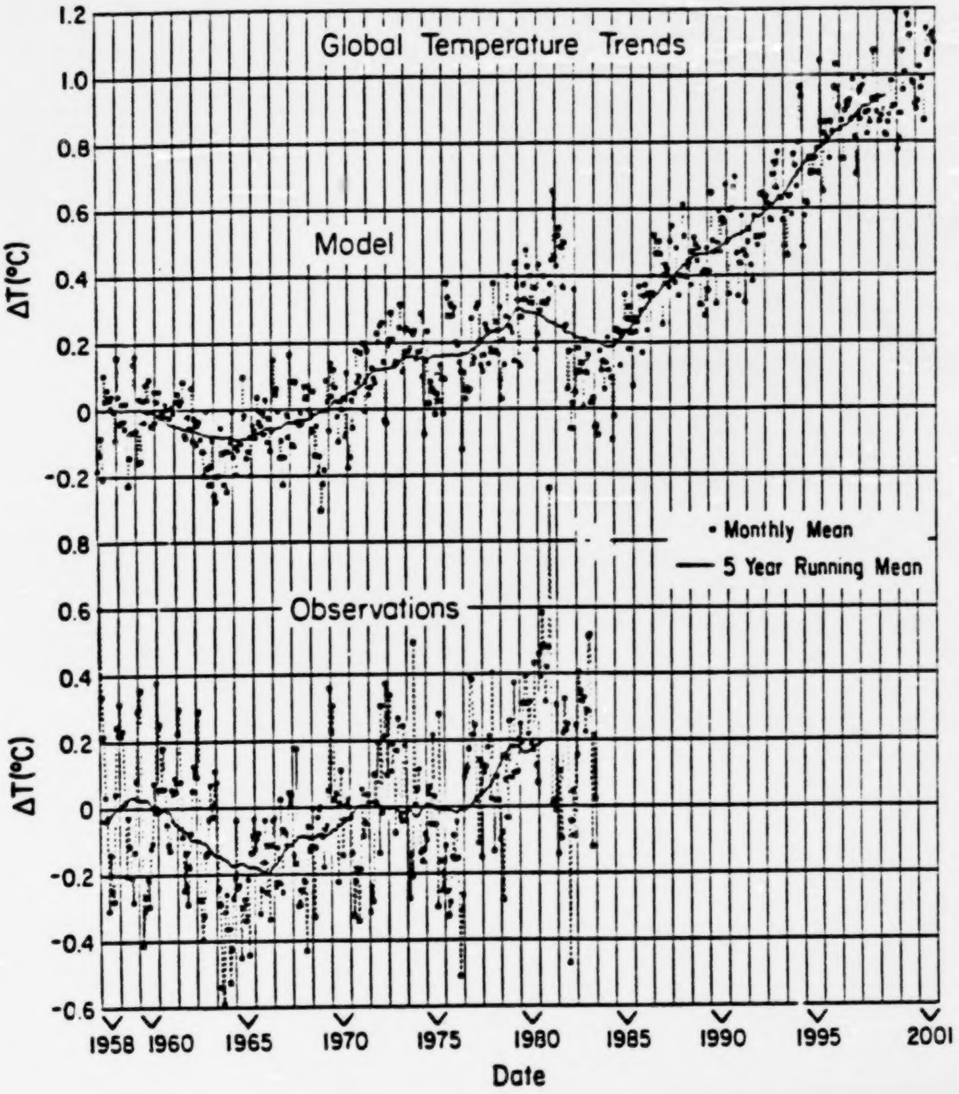

Fig.14 . Modeled and observed global mean surface air temperatures. The model climate is driven by Case A greenhouse gases and stratospheric aerosols as described in the text. The zero point for the model temperature is the mean for that month from the last 10 years of a 35 year control run with fixed January 1959 greenhouse gases and the mean 1880-1980 stratospheric aerosol optical depth. The observational data will be fully described elsewhere; the zero point for observations is the mean for that month from the period 1958-1983. Five year running means are 61 month averages for the period from 30 months before to 30 months after the indicated month.

(after Hansen et al., 1986, as in Fig. 7)

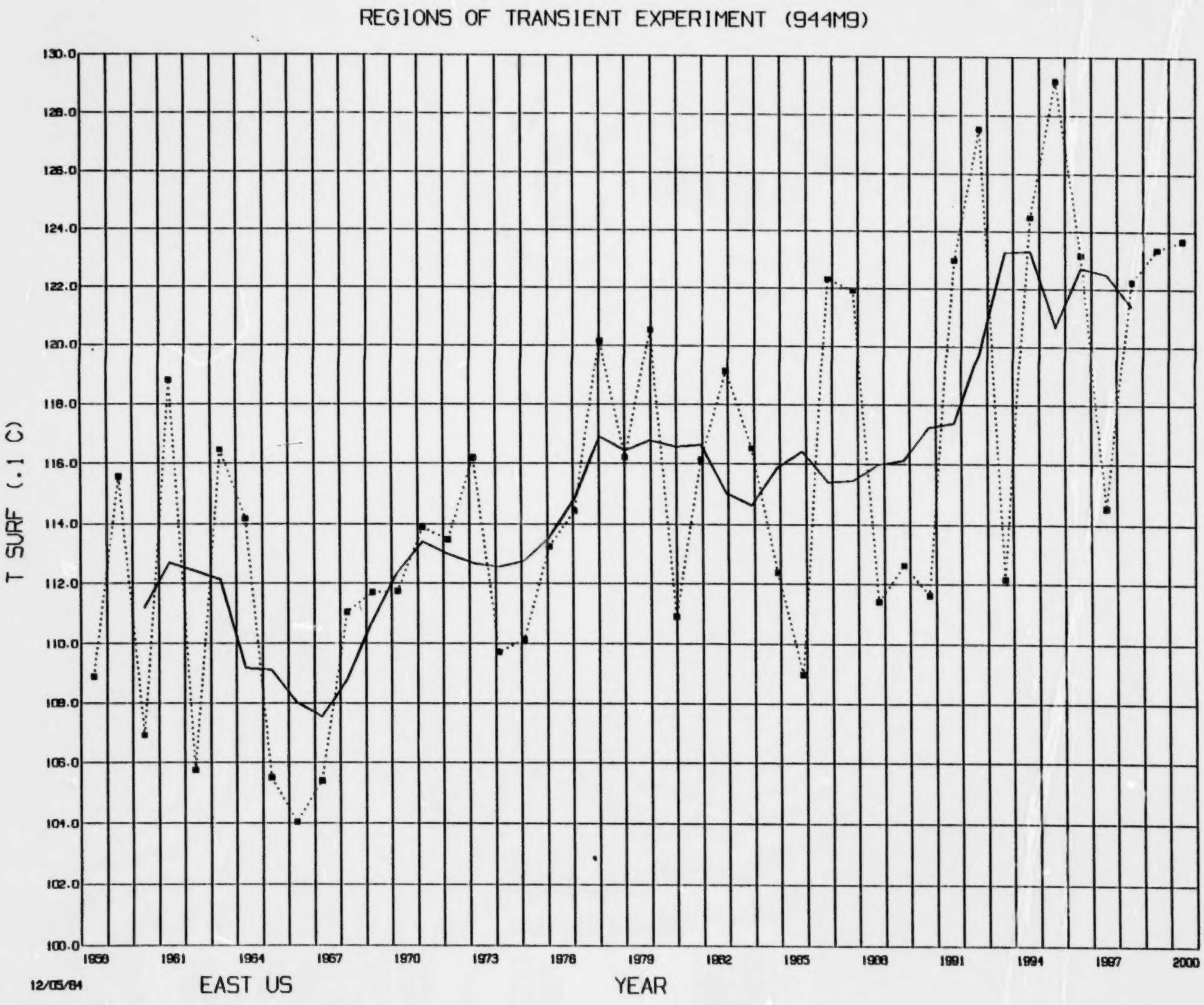

Fig. 15. Model results (as in Fig. 14) for the Eastern United States.

Paper 4

Depletion of Stratospheric Ozone

by

Richard Stolarski
NASA/Goddard Space Flight Center

and

Donald Wuebbles
Lawrence Livermore National Laboratory

This abstract was prepared by Workshop Chairman Harvey Jeffries from a taped recording of the workshop presentation by Richard Stolarski and Donald Wuebbles. The following paper contains information presented at the workshop and has been submitted to *Nature* for publication.

Nimbus 7 SBUV/TOMS Measurements of the Springtime Antarctic Ozone Hole

by

R.S. Stolarski
A.J. Krueger
M.R. Schoeberl
R.D. McPeters
P.A. Newman
J.C. Alpert

Paper 4

Depletion of Stratospheric Ozone

Richard Stolarski and Donald Wuebbles

Abstracted by H. Jeffries
from Taped Meeting Presentation

Richard Stolarski described the fundamental science behind the stratospheric models for ozone (O_3). Donald Wuebbles presented time-dependent predictions of ozone as a function of altitude from his model. The following text was abstracted from a tape recording of their presentations. A paper describing the springtime Antarctic ozone depletion by Stolarski and co-workers follows this abstract.

Ozone Is Both Formed And Lost In The Stratosphere

Ozone is formed by the interaction of UV-radiation from the sun and oxygen (O_2) in the earth's atmosphere. Ozone is also destroyed by UV-radiation, as well, but this produces atomic oxygen that usually re-forms O_3; this cycle occurs many times. Sometimes, the atomic oxygen reacts with O_3 to make two O_2, thus ending a long chain process. The absorption of UV, and the chemical transformations that follow, result in an increase in stratospheric temperature. It also limits the amount of UV-radiation that reaches the earth's surface.

The amount of ozone in the atmosphere is most conveniently measured as the "total column" of ozone in units called Dobson Units (DU). Ozone, however, has tropospheric sources as well as the stratospheric source, and thus its vertical concentration profile varies significantly. The peak O_3 concentration is usually in the stratosphere at 20–30 km. Likewise, total column ozone varies greatly over the surface of the earth, much like weather patterns do. Values are usually between 250–500 DU.

Ozone Cycle Can Be Modified By "Catalyst-like" Compounds

Some chemical compounds have a potential to greatly shorten the cyclic chain that makes O_3 in the stratosphere. The ones with the greatest effect are those that are regenerated in the process, and therefore act much like a catalyst to accelerate the loss of O_3. These compounds result in ozone depletion in the upper stratosphere. That is, the amount of O_3 that would normally be present is decreased. This lower amount of O_3 absorbs less UV-radiation and thus the surface UV-radiation levels can be elevated. In addition, less heating of the upper stratosphere may occur.

Source Of These Compounds Is The Troposphere

All the chemical compounds in the stratosphere come from the troposphere. The compounds must have a long lifetime in the troposphere, that is, they cannot be soluble, must not absorb visible light, and must not react fast with $HO^{\cdot}$. These "un-reactive" compounds can survive long enough to be transported into the stratosphere where they do encounter sufficiently energetic UV-radiation that their chemical bonds are broken and they can then participate in chemistry. A major class of such compounds are the chlorofluorocarbons (CFCs) or Freons, the most common being F12 and F11 (CCl_2F_2 and CCl_3F).

Complex Interactions Require Models

The dynamic processes and the chemistry are so complex and interactive that mathematical simulation models are the only tools available to understand the processes. For example, O_3 concentration determines how much UV-radiation radiation is available; the available UV-radiation radiation determines how rapidly the catalytic compounds are decomposed, which determines how much O_3 is present. Furthermore, reactions and UV-radiation absorption give rise to heat; the heat results in winds that transport material that influences the concentrations of the reactants; in addition, temperature feeds back on the chemical reaction rates that produces the material that is absorbing the UV-radiation to cause the heating, and so on. Often the models tend to concentrate on one aspect of the problem using simple descriptions of the other aspects. For example, one dimensional models tend to have complex chemistry and no horizontal transport. Still, these models predict the *average* concentrations in the hemisphere fairly well. More complex and costly two dimensional models also predict concentrations as a function of latitude as well. These models have to make assumptions about how transport occurs, and different assumptions lead to somewhat different predictions of the temporal and spatial distributions of the O_3.

Some Processes In The Models Result In Non-linear Behavior

Because of the relative competition among various species in the models, there are perturbation scenarios in which the effect of some increasing linear change of inputs results in a very non-linear response. For example, when the total chloride is approximately equal to the total NO_x, there is a a break in the rate of O_3 change. Also, the predicted effects are very different at different altitudes, usually resulting in a decrease in O_3 in the upper stratosphere and an increase in O_3 in the upper troposphere and lower stratosphere. These altitude differences often offset each other so that the total column O_3 is only changed a small amount.

Model Predictions

Model calculations have been made from preindustrial times to 2050. These models predicted that the total column O_3 increased during the 1970s. This, however, was the result of the cancellation of substantial, but opposing, changes in O_3 with altitude. A maximum decrease of 4.4% was predicted at 40 km, largely due to CFC emissions (it was noted that increasing CO_2 emissions reduced the CFC impact!), while an increase of 1% was predicted at 30 km, as well as an increase of 6.7% predicted at 8-9 km due to aircraft and increased CH_4 emissions. The extent to which the model predictions are in agreement with the meager observational data during this time will be described in a later section.

In future scenarios, most models predict a small decrease or increase in total column O_3, mainly due to increasing CH_4 in the troposphere. The vertical distributions of O_3, however, are dramatically modified. For example, one model predicts up to a 36% O_3 increase below 26 km and a 22% O_3 decrease above 26 km.

The two dimensional models with transport predict a distribution of the altitude effect with latitude in which the low latitude results are similar to those quoted above for the low and mid-latitudes, but the predictions for the poles showed a decrease at all altitudes. The total column changes predicted by these models, for an increase of 5 ppb chloride, were about 4% O_3 depletion at the equator and 18% O_3 depletion near the poles.

The Depletion Process Is Occurring Now

British Antarctic Survey Station at Halley

The British have been measuring total column O_3 at Halley, Antarctica (76°S) since the International Geophysical Year in 1956. In 1957 the values were 310–320 DU in the springtime. Now they are 40% lower in October (Antarctic spring). In the winter at Halley, there is no sunlight; in the spring, the sun returns. It is speculated that during the dark, very cold winter, CFCs accumulate, and when the sun does reach the upper stratosphere for the first time in the spring, the CFCs undergo rapid reaction and destroy the ozone. As the CFCs are consumed, the ozone levels gradually increase to higher values, but by autumn the level is still 5-10% lower than it was 10 years ago.

Nimbus-7 Satellite Data

NASA has made a color movie from the Nimbus-7 satellite's TOMS instrument that can measure total O_3. The movie, which was shown at the workshop, shows the pole view of O_3 concentrations on each day in October for the years 1980 to 1985. (A paper describing these data follows this abstract). The images are dramatic: in the beginning of each year, the O_3 is reasonably uniform and then the depletion process starts; it appears as if a large hole is being eaten in the atmosphere and then it begins to recover near the end of the month. Each year, however, the area of O_3 depletion increases and the depth of the central depletion is deeper. In 1984, the value at the pole was down to about 190 DU, and in 1985 it was down to about 180 DU.

Paper 4

NIMBUS 7 SBUV/TOMS MEASUREMENTS OF THE SPRINGTIME ANTARCTIC OZONE HOLE

R. S. Stolarski
A. J. Krueger
M. R. Schoeberl
R. D. McPeters
P. A. Newman
J. C. Alpert*

NASA/Goddard Space Flight Center
Laboratory for Atmospheres
Greenbelt, MD 20771

Submitted to Nature
April 8, 1986

---

*Presently at NOAA/NMC Camp Springs, MD

NIMBUS 7 SBUV/TOMS MEASUREMENTS OF THE SPRINGTIME ANTARCTIC OZONE HOLE

Abstract

Satellite measurements confirm the recent decline of total ozone in successive Octobers reported over Halley Bay Station, Antarctica. The decrease occurs during September as the the Sun rises, reaching a minimum in mid-October. Six years of October monthly means show a 30% decrease in the ozone minimum and a 10% decrease in the surrounding ozone maximum. These are shown to be related.

I. Introduction

Farman et al.[1], in a series of measurements which date back to 1956, report a rapid decrease in the total column amount of ozone over the Halley Bay station in Antarctica at 76°S and 27°W. The decrease was most pronounced in October, early spring in the Southern Hemisphere. They attributed the decrease to the increase in stratospheric chlorine due to chlorofluorocarbon release and proposed that the unique conditions of extreme cold and low sunlight in the Antarctic winter and spring maximized the effect. We report measurements from the Solar Backscatter Ultraviolet (SBUV) instrument and the Total Ozone Mapping Spectrometer (TOMS) onboard the Nimbus 7 satellite. These provide global measurements of ozone from November, 1978 to the present time.

The SBUV is a nadir-viewing instrument which obtains total ozone from measurements of the backscattered solar ultraviolet radiation in the wavelength range 310 nm to 340 nm.[2,3] Measurements in the 250 nm to 310 nm wavelength range by the SBUV instrument provide information on the distribution of ozone with altitude. The TOMS instrument is designed to measure the spatial distribution of total ozone by scanning across the track of the satellite to obtain data between successive satellite orbital tracks. Nimbus 7 is a Sun-synchronous polar-orbiting satellite which passes any given point on the dayside near local noon.

II. Observations

a. Spatial morphology of total ozone in October

One of the major advantages of the TOMS instrument is its ability to map total ozone over the entire globe on a daily basis. Figure 1 (see also cover picture) shows a sequence of daily south polar projections of total ozone for October, 1984. The Halley Bay Station is indicated by a * on the figure and the Greenwich meridian is to the top. The extreme low total ozone over Halley Bay is observed to be part of a larger elliptically shaped minimum region extending out to about 60-70°S. The minimum region, which tends to rotate about the pole with an irregular period of about 7-10 days, is bounded by a steep gradient where total ozone increases to values in excess of 300 milli-atm-cm (Dobson Units or DU). At 50-60°S total ozone goes through a maximum which exhibits larger variability due to travelling planetary waves. The existence of a polar minimum and a mid-latitude maximum in total ozone is a part of the normal, long-term climatology of the Southern Hemisphere.[4] The recent year-to-year changes in these features are the focus of this paper.

The twelve panels in Figure 1 show twelve consecutive days from October 11, 1984 to October 22, 1984. This is the time period for which the lowest values are generally recorded. Each panel is centered about the South Pole and gives data out to 45° latitude. On October 11, Figure 1 shows that the minimum in total ozone is relatively symmetrical about the pole and the maximum in total ozone is located in the lower right between about 90°E and 180°E. On succeeding days the total ozone maximum region rotates clockwise, while the minimum region elongates and begins to corotate with the maximum. On October 16 and 17 the maximum region has reached the lower left corner, between 180°E and 270°E where it seems to dissipate and subsequently reappear in the upper right corner. From there it continues to move around the pole but does not pass over Halley Bay. By October 20 the ozone distribution has returned approximately to the original situation on October 11, giving a rotation period at this time of 9 days. The next 2 days are near repeats of October 12 and 13.

Total ozone is proportional to the pressure weighted integral of the ozone mixing ratio, and fluctuations in the amount of total ozone may indicate a relative lifting of the mixing ratio distribution in altitude, a chemical loss in the lower stratosphere, advection of ozone into a region from other locations or all of the above. Figure 2a shows the temperature distribution for October 3, 1982 at a pressure of 50 mb, a level centered in the lower stratosphere. This map can be compared to the total ozone map for the same day in Figure 2b which shows a high correlation of low temperatures with low total ozone and high temperatures with high total ozone. Superposed on each panel of Figure 2 are heavy lines with arrows indicating the geostrophic wind streamlines and wind direction at the 50 mbar surface. The circulation within the ozone minimum region is closed, thus confining air parcels to this cold region, the polar vortex. At lower latitudes parcel trajectories pass from cold, low total ozone regions through the warm, high total ozone regions on the other side of the pole. Along these trajectories total ozone varies by as much as 150 DU.

An excellent correlation between total ozone and 50 mb temperatures exists on all other days we have examined. This correlation results from the adiabatic temperature changes due to vertical motions which simultaneously produce total ozone changes as the air is advected around the pole. At the point where the ozone column is lifted the highest both total ozone and 50 mb temperatures are minimum.

b. Year-to-year trend in total ozone for October

Evidence that the long term total ozone decrease observed at Halley Bay is not unique to Halley Bay is shown in Table 1 where we give the zonal mean, local minimum, and local maximum total ozone values for the month of October in each year for the 70°-80° latitude band for 1970-72 from BUV and 1979-84 from SBUV. Data from the Nimbus 4 BUV instrument, the predecessor to SBUV, was fairly complete for the 1970-1972 period; in later years coverage of the Antarctic by BUV was reduced. The BUV ozone data have been reprocessed with exactly the same algorithm as SBUV and with compatible instrument characterization functions, so it is reasonable to compare the BUV total ozone with the SBUV total ozone. Antarctic total ozone observed in 1979 appears comparable to that observed in the early 1970's; significant total ozone decreases occurred only after 1979. Thus, the long-term behavior of total ozone reported for Halley Bay appears to reflect the general behavior of total ozone for the Antarctic.

The nature of the decrease is shown more clearly in Figure 3 which gives October monthly mean TOMS total ozone maps for each of the six years from 1979 through 1984 for the Southern Hemisphere. The monthly mean values in the minimum region are seen to decrease from about 250 DU in 1979 to about 180 DU in 1983 and 1984. The three days of October 1985 TOMS total ozone data which we have examined indicate values as low as or slightly lower than in 1984. Table 2 indicates the specific values for the October monthly means over three stations (Halley Bay, Syowa and Amundsen-Scott) as well as the minimum, and maximum values of the monthly mean. The total ozone values for Halley Bay agree closely with those reported by Farman et al.[1] We have examined 4 years (1979-1982) of 50 mbar temperature data. The interannual variations in temperature were similar to the total ozone variations, but no definitive trend could be seen in the temperature data.

Figure 3 also shows the October monthly mean total ozone maximum located at about 60°S latitude. The phase of the maximum shifts from year to year; ranging from about 90° E to 180°E. In 1979 the maximum monthly mean total ozone value exceeds 450 DU. By 1984 the maximum is barely over 400 DU, a decrease of just over 10% in 6 years. Although six years is too short to

132

definitively identify a two-year cycle, there does seem to be some modulation of the decrease in both the maximum and minimum. A quasi-biennial oscillation in total ozone has been previously observed but its magnitude was only about 6-8 DU.[5,6]

The year-to-year downward trend seen in the 50-60°S maximum in total ozone is consistent with the decrease in the high latitude minimum region. The air parcel trajectories shown in Figure 2 indicate that the parcels which form the total ozone maximum have also passed through the periphery of the cold region. The existence of maximum and minimum regions are the result of adiabatic descent and ascent of the column as a whole. Therefore, if some mechanism is chemically removing ozone in the cold region of the parcel orbit, a loss should also appear in the maximum in total ozone as the parcel descends and warms.

c. The annual cycle in total ozone

The data given by Farman et al.[1] for Halley Bay showed total ozone amounts coming out of the polar night beginning on October 1, 1984 which were a few tens of percent lower than those entering the polar night. Sunrise occurs in late August over the station, but the data are limited by the solar zenith angle of the observations. The ozone algorithms for both TOMS and SBUV have been carefully scrutinized for their behavior at high solar zenith angles and found to return accurate results for zenith angles up to 85°.[3,7] We thus have observations back through the month of September for the latitude of Halley Bay (76°S). The results show values of total ozone coming out of polar night very close to those observed entering the polar night. This result is also in agreement with the observations of total ozone taken at Syowa station (69°S) for 1982.[8] However, there is some indication from Lunar Dobson and ozonesonde measurements at Syowa that total ozone increases slowly until winter solstice then decreases again until sunrise with a more rapid decrease thereafter.

Throughout the month of September and the first week in October, a rapid decline is observed in total ozone by both SBUV and TOMS until the previously mentioned low values are obtained. This is shown in Figure 4 with data from the SBUV instrument for the period late August 1983 through April 1984. The data points are the satellite data which are centered within ±2° latitude and ±15° longitude of Halley Bay. The solid lines are the maximum and minimum of values reported at all longitudes within the latitude band 74°S to 78°S. Throughout October and November the data over Halley Bay are consistently near the minimum values for all longitudes for this and other years as well. The decline in the minimum value of ozone column extends from late August through early October at a rate of approximately 0.6%/day. At longitudes on the other side of the pole from Halley Bay the total ozone amount is variable and often very large.

Near the end of November the low values have completely disappeared and the minimum curve goes through a maximum. The jump in total ozone is coincident with the final warming in the Southern Hemisphere and marks the switch from winter to summer circulation. During the final warming process large amounts of ozone are advected into the polar regions from lower latitudes. A similar process occurs in the Northern Hemisphere but usually only three months after the winter solstice rather than the five months seen here.[9] Throughout the Antarctic summer the ozone column decreases and the Halley Bay values oscillate between the maximum and minimum curves as lower stratospheric travelling waves pass over the station.

III. Conclusions and Discussion

The satellite data from the Nimbus 7 TOMS and SBUV instruments significantly extend our view of the growing ozone minimum over the South Polar region. The decrease observed by Farman et al.[1] over Halley Bay has been confirmed and shown to be part of a general decrease over the Antarctic region. Data for 1985 indicate a continuation of the ozone minimum. Our data places significant constraints on possible mechanisms for explaining the decrease. The deep minimum, or hole, follows the polar vortex, and its position is well correlated with the temperature minimum in the lower stratosphere. There also appears to be a smaller but significant decrease (~10%) in the total ozone maximum surrounding the polar region over the 6 years studied. The decrease in the total ozone maximum is related to the decrease in the total ozone minimum in that the air parcels in the maximum region have passed through the periphery of the low temperature region, which is associated with the total ozone minimum.

An important constraint placed on theoretical models by this data is that the decrease in total ozone near the pole appears to largely take place in September during twilight, not in the polar night. The maximum rate of decrease in total ozone occurs after most of the polar region is sunlit and is about 0.6% per day extended over 40-50 days in 1983.

Any explanation of the total ozone change must be consistent with the year-to-year changes both in the polar vortex as well as consistent with the rate of decrease through September. Various ideas have been put forward involving combinations of chlorine chemistry, heterogeneous chemistry taking place in polar stratosphere clouds, bromine chemistry and dynamical lifting of the polar stratosphere.[1,10,11,12]

We estimate that, in order for chlorine chemistry at 1983 concentrations to cause the 0.6%/day decline in September, virtually all of the chlorine must be in its active state, i.e. $C\ell$ and $C\ell O$, with little or no interference from NO_x. Therefore any proposed chemical mechanism must be able to remove most of the chlorine from both the $HC\ell$ and $C\ell ONO_2$ reservoirs and to tie up NO_x, preferably as HNO_3. Such a mechanism could involve the cold temperatures and/or polar stratospheric clouds that form within the polar vortex.[13]

Any conclusions concerning the implications of the observed Antarctic decreases in total ozone on predictions of the effects of chlorine from fluorocarbons must await a definitive mechanism and continued observations to verify the persistence of the phenomenon. Only then will we be able to clearly evaluate the relative roles of chemistry, radiation and dynamics in contributing to the observed decrease.

Acknowledgment

We thank the Nimbus 7 Ozone Processing Team (A. Fleig, Chairman) for making available TOMS data from October 1983 and 1984, and the Real-Time TOMS Project for data for a few days in October of 1985 before regularly scheduled processing. Reggie Galimore was responsible for the image processing which made the data readily available for visual examination. We thank S. Solomon, S. Wofsy and N. D. Sze for discussing and making available preprints of their papers and S. Chandra for useful discussions. We thank Lori Winter and Roberta Duffy for their excellent typing of the many versions of this manuscript.

References

1. Farman, J. C., B. G. Gardiner and J. D. Shanklin, Nature, 35, 207-210, 1985.
2. Heath, D. F., A. J. Krueger, H. A. Roeder and B. D. Henderson, Opt. Eng., 14, 323-330, (1975).
3. Klenk, K. F., P. K. Bhartia, A. J. Fleig, V. G. Kaveeshwar, R. D. McPeters and P. M. Smith, J. Appl. Meteor., 21, 1672-1684, (1982).
4. Sticksel, P. R., Mon. Weather Rev., 98, 787-788 (1970).
5. Hasebe, F., in Dynamics of the Middle Atmosphere, J. R. Holton and T. Matsuno, eds., Terra Scientific Publishing Co., Tokyo Japan, pp. 445-464, (1984).
6. Hilsenrath, E. and B. M. Schlesinger, J. Geophys. Res., 86, 12087-12096, (1981).
7. Bhartia, P. K., personal communication (1985).
8. Chubachi, S., in Atmospheric Ozone, C. S. Zerefos and A. Ghazi, eds., D. Reidel Publishing Co., Dordrecht, pp. 285-299. (1984).
9. Rood, R. B., PAGEOPH, 121, 1049-1064, (1983).
10. Solomon, S. and R. R. Garcia, Submitted to Nature, 1986.
11. McElroy, M. B., R. J. Salawitch, S. C. Wofsy and J. A. Logan, Submitted to Nature, 1986.
12. Tung, K. K., M. K. W. Ko, J. M. Rodriguez, and N. D. Sze, Submitted to Nature, March 1986.
13. Steele, H. M., P. Hamill, M. P. McCormick and T. J. Swissler, J. Atmos. Sci., 40, 2055-2067 (1983.

Table 1. Zonal mean, local minimum, and local maximum total ozone values in DU for the month of October each year for the 70-80°S latitude zone from Nimbus 4 BUV (1970-1972) and from Nimbus 7 SBUV (1979-1984).

Year	Zonal Mean	Local Minimum	Local Maximum
1970	306	240	484
1971	334	249	482
1972	337	237	539
1979	333	235	515
1980	270	212	467
1981	266	206	422
1982	283	186	494
1983	245	166	479
1984	240	162	446

Table 2. October mean ozone column as determined by TOMS from 1979 through 1984 over 3 Antarctic Stations plus the minimum and maximum values of the monthly mean (all in Dobson Units or milli-atmosphere centimeters). Also given are the one-sigma variances of the daily values from the monthly mean for the specific locations.

	Halley Bay	Syowa	South Pole	TOMS Minimum	TOMS Maximum
	76°S 27°W	69°S 39°E	90°S		
October					
1979	273 ± 19	367 ± 47	266 ± 25	259	458
1980	232 ± 11	276 ± 22	218 ± 9	215	433
1981	244 ± 12	312 ± 30	223 ± 9	219	449
1982	221 ± 12	240 ± 49	220 ± 22	205	432
1983	199 ± 13	239 ± 32	182 ± 8	178	414
1984	190 ± 8	245 ± 24	187 ± 14	181	404

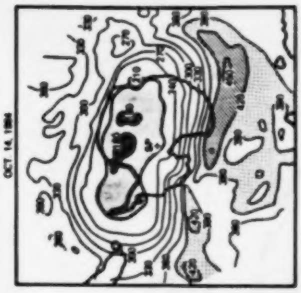
OCT 14, 1984

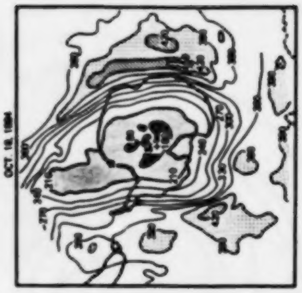
OCT 18, 1984

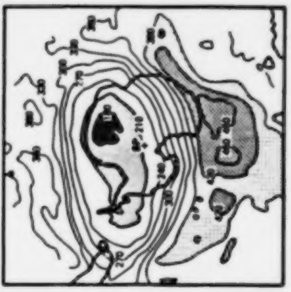
OCT 22, 1984

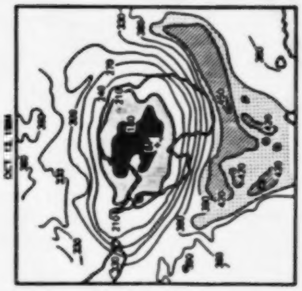
OCT 13, 1984

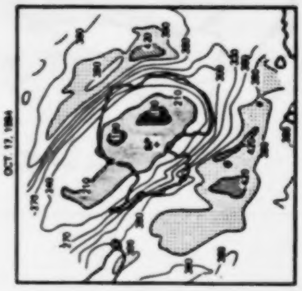
OCT 17, 1984

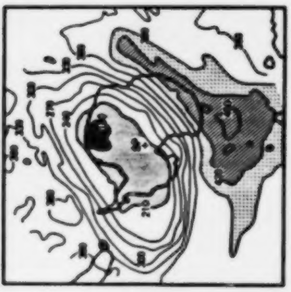
OCT 21, 1984

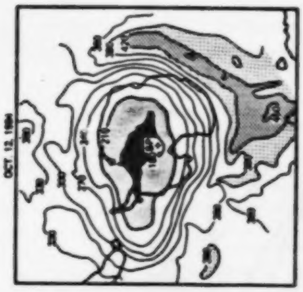
OCT 12, 1984

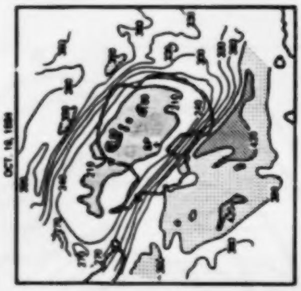
OCT 16, 1984

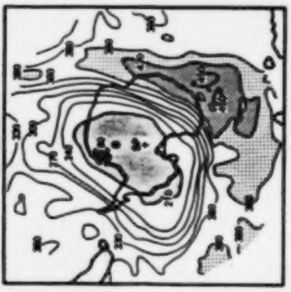
OCT 20, 1984

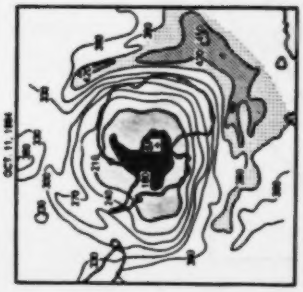
OCT 11, 1984

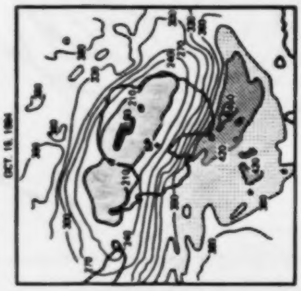
OCT 15, 1984

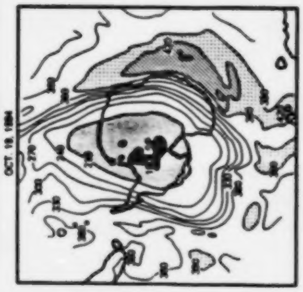
OCT 19, 1984

Figure 1. Twelve day sequence of TOMS data on total ozone content. Shown are south polar projections with the pole indicated by a + and Halley Bay shown by a *. Contours are every 30 Dobson Units (DU). The region shown extends to about 45° latitude and the Greenwich meridian is toward the top of each diagram. Shaded regions indicate total ozone values less than 180 and 210 DU and greater than 390 and 420 DU.

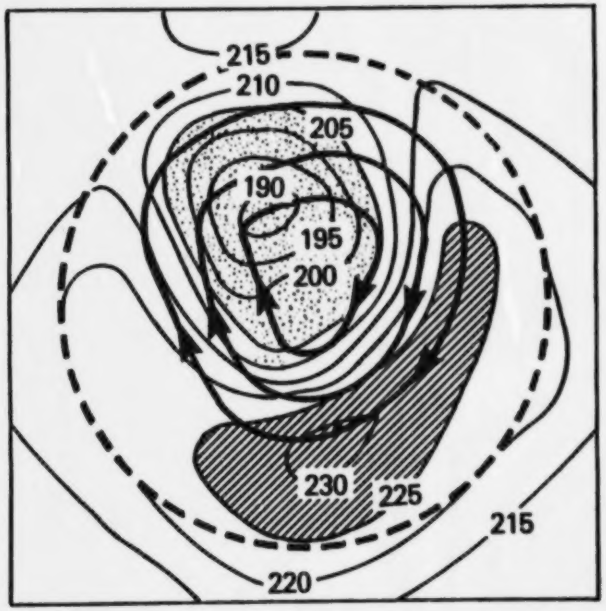
215
210
205
190
195
200
230
225
215
220

(A) TEMPERATURE (50mb)

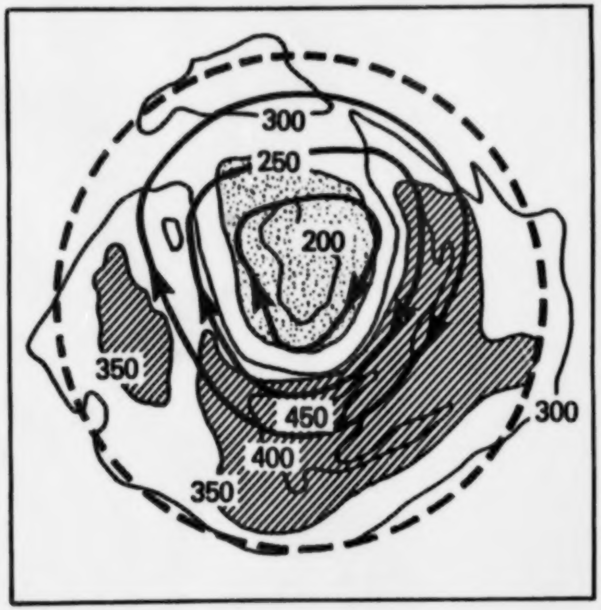
300
250
200
350
450
400
350
300

(B) OZONE

Figure 2a) Contour map of 50 mbar temperature for October 3, 1982. The South Pole is at the center and the dashed circle is 40°S. The shaded regions indicate temperatures of less than 205K and greater than 225K. The heavy lines are the geostrophic streamlines with the arrows indicating wind direction. Contours are every 5 K.

b) Contour map of total ozone for October 3, 1982. Shaded are regions of less than 250 Dobson Units and greater than 350 Dobson Units. Streamlines and wind direction are as in Figure 2a. Contours are every 50 DU.

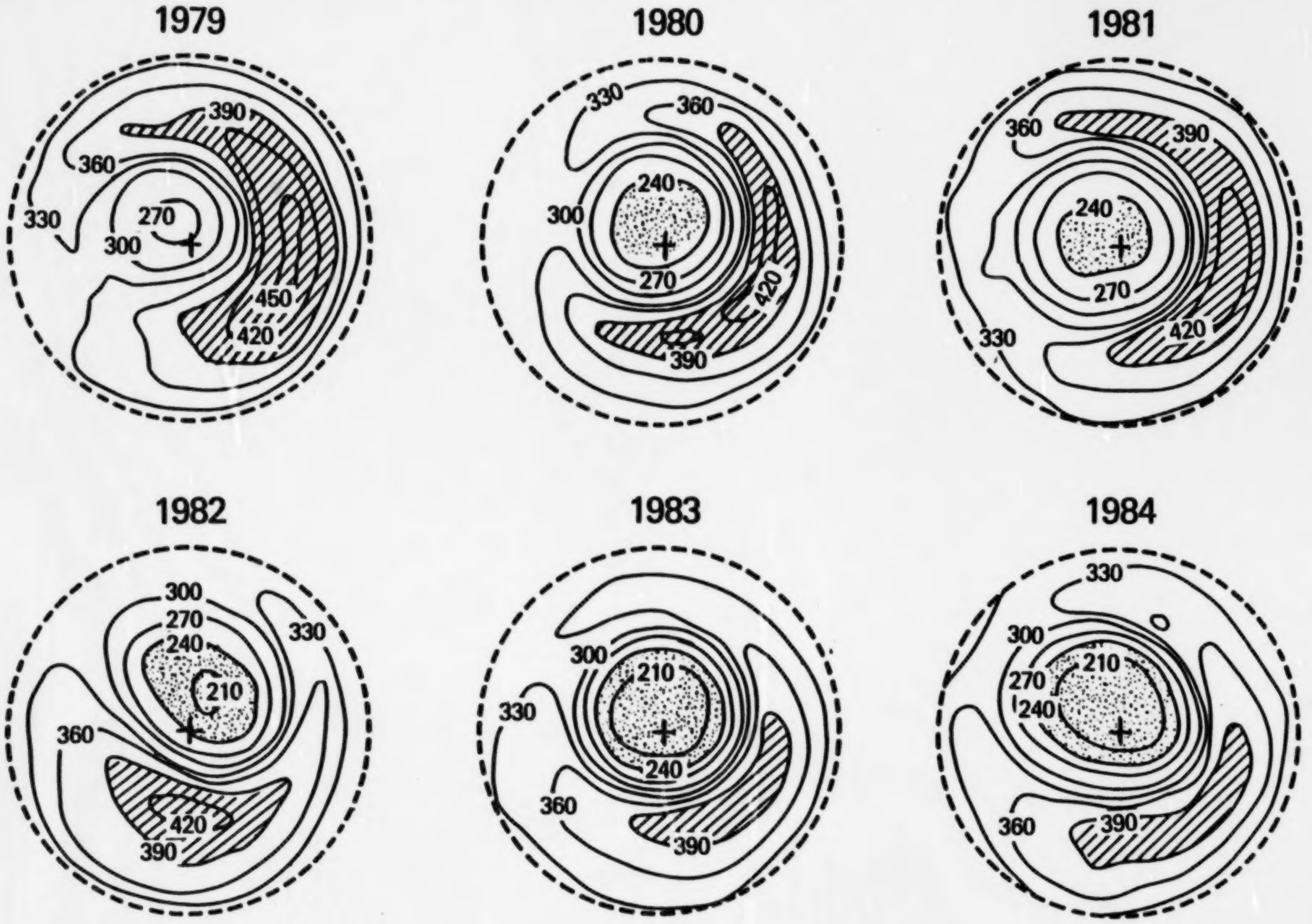
1979
390
360
330
270
300
450
420
1980
330
360
240
300
270
420
390
1981
360
390
240
270
330
420
1982
300
270
240
330
210
360
420
390
1983
300
210
330
240
360
390
1984
330
300
210
270
240
360
390

OCTOBER MONTHLY MEANS

Figure 3. Six year sequence of October monthly mean of total ozone. Shown are south polar projections with the pole indicated by a cross and 30°S latitude by a dashed circle. The Greenwich meridian is toward the top of each panel. Contours are every 30 DU. The shaded regions indicate monthly mean total ozone amounts of less than 240 Dobson Units and greater than 390 Dobson Units.

Paper 4

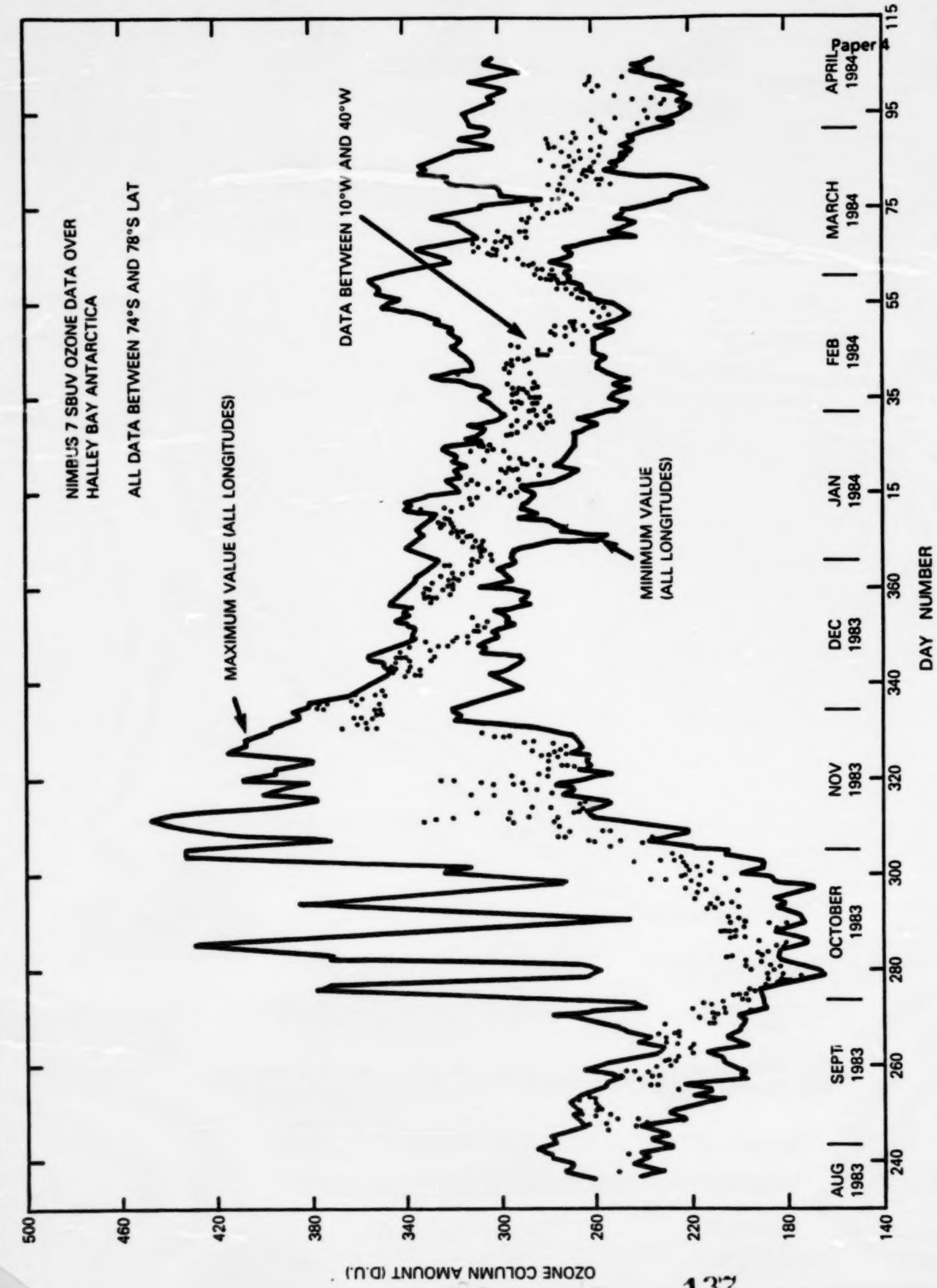
NIMBUS 7 SBUV OZONE DATA OVER
HALLEY BAY ANTARCTICA
ALL DATA BETWEEN 74°S AND 78°S LAT
MAXIMUM VALUE (ALL LONGITUDES)
DATA BETWEEN 10°W AND 40°W
MINIMUM VALUE
(ALL LONGITUDES)
OZONE COLUMN AMOUNT (D.U.)
500
460
420
380
340
300
260
220
180
140
DAY NUMBER
240
260
280
300
320
340
360
15
35
55
75
95
115
AUG
1983
SEPT
1983
OCTOBER
1983
NOV
1983
DEC
1983
JAN
1984
FEB
1984
MARCH
1984
APRIL
1984

Figure 4. Nimbus 7 SBUV data for total ozone content between latitudes of 74°S and 78°S for September 1983 through April 1984. The dots are the data within 15° longitude of Halley Bay. The solid lines are the maximum and minimum values found around the entire latitude circle.

Paper 5

Relationships among CO, NO_X, CH_4, and $HO^{\bullet}$

by

Anne Thompson
Applied Research Corporation

This presentation was based upon the following paper, which has been submitted to the *Journal of Geophysical Reseach* for publication.

Possible Perturbations to Atmospheric CO, CH_4, and OH

by

Anne M. Thompson
Ralph J. Cicerone

ABSTRACT

A photochemical model is used to predict temporal trends in OH, CH_4 and CO over the next fifty years and to assess possible past changes in these trace gases from 1860 to 1985. Various scenarios of perturbed CH_4 and CO levels based on recently reported CH_4 and CO data are simulated at several levels of background NO_x. With low NO_x conditions ($NO + NO_2$=25 pptv) typical of the nonpolluted troposphere we compute a monotonic loss of tropospheric OH from 1860 to 2035 with the magnitude of the decrease dependent on CO and CH_4 increases during the period. If current trends continue (ground level mixing ratios [mole fractions] of CH_4 rising ~1% yr^{-1}), by 2035 northern latitude CH_4 will increase from 1.6 to 2.9 ppmv and CO will double or triple its present day level (to ~250-350 ppbv in the nonpolluted northern hemisphere). The column abundance of OH in the background troposphere will decrease 25-35%, depending on the magnitude of CH_4 and CO increases and assuming that global temperature increases do not raise water vapor levels during that time. Calculations with increased H_2O show a 17-30% decrease in OH.

Under higher NO_x conditions (1 ppbv) OH shows a decline from 1860 to 2035, but only half as much as with low NO_x conditions. In the case of NO_x in a transitional zone (i.e. NO_x increasing from 20 pptv in 1860 to 0.5 ppbv in 2035) CO and CH_4 increases accompany a rise in OH followed by a small decline. The turning point in OH depends on the rate of change in NO_x and O_3. Recently observed upward trends in CO and CH_4 are probably due to increasing emissions of both CH_4 and CO.

We always compute a temporal increase in tropospheric O_3 when CH_4 and CO increase. Typical 1860 values for surface O_3 are 25 ppbv, compared to 30 ppbv (NO_x = 25 pptv) and 40 ppbv (NO_x = 1 ppbv) in 1985. In a transitional NO_x zone we find surface O_3 increasing from 10 ppbv in 1860 to 27 ppbv in 1985.

151

Paper 5

Possible Perturbations to Atmospheric CO, CH_4, and OH

Anne M. Thompson
Applied Research Corporation
Landover, Maryland
and
National Center for Atmospheric Research
and
Ralph J. Cicerone
National Center for Atmospheric Research
Boulder, Colorado

23 May 1986

---

*The National Center for Atmospheric Research is sponsored by the National Science Foundation.

1. INTRODUCTION

The interdependence of atmospheric CO, CH_4, and OH is well known [Levy, 1972; Crutzen, 1973; Wofsy,1976]. The OH radical is centrally important in the photochemistry of the troposphere because it oxidizes many nitrogen-, carbon-, and sulfur-containing species and some halogenated hydrocarbons. The oxidation of methane, for example, starts a chain of processes, eventually forming CO:

$$CH_4 + OH \rightarrow CH_3 + H_2O$$

$$CH_3 + O_2 + M \rightarrow CH_3O_2 + M$$

$$CH_3O_2 + NO \rightarrow CH_3O + NO_2$$

$$CH_3O + O_2 \rightarrow H_2CO + HO_2$$

$$H_2CO + h\nu \rightarrow \begin{cases} H_2 + CO \\ HCO + H \end{cases}$$

$$HCO + O_2 \rightarrow CO + HO_2$$

CO itself reacts with OH; a product is CO_2:

$$CO + OH \rightarrow CO_2 + H.$$

Methane and CO together are the largest consumers of tropospheric OH. Thus, an increase in the background level of either of these species can reduce OH and the oxidizing power of the entire troposphere. This has important implications for the environment, e.g., reduced rates of formation of atmospheric acids, at least in remote regions. The rate at which natural and anthropogenic trace species are oxidized in the boundary layer before passing into the free troposphere and the stratosphere would also be reduced.

Not only are CH_4 and CO the dominant consumers of tropospheric OH, OH is the major sink for CH_4 and CO. Thus, a sort of feedback can be envisioned:

more CO -> less OH; less OH -> more CH_4; more CH_4 -> less OH, and so on. Sustained perturbations to any one of the three species CO, CH_4, OH influence background levels of the other two, possibly with an amplified effect.

Relationships among CH_4, CO and OH and the effects of perturbed CH_4 and CO have been the subject of previous studies [Chameides et al., 1977; Sze, 1977; Hameed et al., 1979; Levine et al, 1985; Crutzen, 1986]. Sze [1977] studied the effects of increased anthropogenic CO production on ground level OH and CH_4. Chameides et al. [1977] described changes in total tropospheric abundances of OH and CH_4. Hameed et al. [1979] pointed out that both magnitude and direction of calculated changes are highly sensitive to ambient NO_x. The current investigation is prompted by newly published evidence for a temporal increase in tropospheric CH_4 [Ehhalt et al., 1983; Rasmussen and Khalil, 1981; Rinsland et al, 1985; Stauffer et al, 1985] and possibly for an increase in CO [Khalil and Rasmussen, 1984; Rinsland and Levine, 1985]. It is similar to the modeling study of Levine et al [1985] in prescribing specific CH_4 and CO changes but it covers a longer time span and wider NO_x and O_3 variations.

Section 2 describes the photochemical model including choice of model inputs and boundary conditions for three cases: low NO_x, midlatitude; high NO_x, midlatitude; low NO_x, low latitude. Basic features of CO and CH_4 perturbation calculations are also presented in Section 2. In Section 3 the model is used to predict CH_4, CO, and OH over the next fifty years and to assess possible CH_4-CO-OH perturbations from 1860 to 1985. Discussion (Section 4) follows. We attempt to discern whether increasing global sources of CO or increasing sources of CH_4 or both are responsible for the recent apparent increases of these gases.

2. CH_4-CO-OH COUPLING

A. Photochemical Model

The coupled photochemical transport model used in these calculations is that of Thompson and Cicerone [1982]. The model solves a set of continuity equations for the time rate of change of species i:

$$\frac{\partial}{\partial z}\left[K(z,t)N(z)\frac{\partial x_i(z,t)}{\partial z}\right] + P_i(z,t) - L_i(z,t) = \frac{\partial c_i(z,t)}{\partial t} \quad (1)$$

where z = altitude; K(z,t) = eddy diffusion coefficient ($cm^2\ s^{-1}$); N(z) = molecular density (cm^{-3}) of background air; $x_i(z,t)$ = mixing ratio or mole fraction of species i; $c_i(z,t)$ is density (cm^{-3}); $P_i(z,t)$, $L_i(z,t)$ = production, loss rates ($cm^{-3}\ s^{-1}$) for chemical reaction of species i. The model domain spans 0-15 km with 24 grid points; vertical transport is simulated by eddy diffusion coefficients as described by Thompson and Cicerone [1982] Fixed profiles for molecular density, H_2, H_2O, and temperature are given in Table 1.

The basic model [Thompson and Cicerone, 1982] solves (1) for 17 radical and gaseous species: O_3, $O(^3P)$, NO, NO_2, NO_3, N_2O_5, HNO_3, HNO_4, H, OH, HO_2, H_2O_2, CH_3, CH_3O, CH_3O_2, CH_3OOH, and H_2CO. In the present study the number of continuity equations is increased to 25 with the addition of CO, CH_4, and six nonmethane hydrocarbon species: C_2H_6, $C_2H_5O_2$, C_2H_5OOH, CH_3CHO, CH_3CO_3, and $CH_3CO_3NO_2$ (peroxyacetylnitrate). Three species are calculated assuming photochemical equilibrium: $O(^1D)$, CHO, C_2H_5O. The NMHC species add eight reactions and three photolyses to the model photochemical scheme (Table 2). One reason for the NMHC additions is to make background hydrocarbon levels more realistic than those obtained if methane is the only hydrocarbon radical precursor. For example, the oxidation of ethane, C_2H_6, produces two moderately long-lived hydrocarbons, CH_3CHO and C_2H_5OOH. The oxidation of CH_3CHO leads to the formation of PAN (peroxyacetylnitrate). PAN may be an important reservoir of odd nitrogen in the troposphere [Crutzen, 1979; Singh and Hanst, 1981; Aikin et al, 1982; Brewer et al, 1983; Kasting and Singh, 1986].

Photolysis rates used in (1) are calculated as described in Thompson [1984] and free radical reactions [Thompson and Cicerone; 1982] appearing in (1) employ rate constants taken from the NASA/JPL [1983] tabulation.

Species boundary conditions (Table 3) used to represent low NO_x conditions (both low and midlatitude) are similar to those used in Thompson and Cicerone [1982]. Two basic low NO_x models are designated LNLL for low latitudes and LNML for midlatitudes. Lower boundary conditions for CO and CH_4 are surface upfluxes prescribed to give appropriate mixing ratios for these species: 1.6 ppmv CH_4, 120 ppbv CO (midlatitude); 85 ppbv CO (low latitude). Ethane at the lower boundary is fixed at 1.5 ppbv, a typical value for the background troposphere [Singh et al, 1979; Rudolph and Ehhalt, 1981]. A transfer velocity upper boundary condition is assumed for CO, CH_4, and C_2H_6.

Boundary conditions for the high NO_x case (~1 ppbv NO_x) are similar to those for the low NO_x model runs (Table 3) except that the high NO_x model uses a surface NO upflux nearly 100 times greater than the flux used for low NO_x model runs. The high NO_x midlatitude model is denoted HNML. Corresponding O_3 is higher in the HNML model than in the LNML case: 41 ppbv O_3 at the surface compared to 30 ppbv. OH is also higher and CO and CH_4 fluxes are adjusted to maintain background surface mixing ratios at typical levels (120 ppbv CO, 1.6 ppmv CH_4). In the HNML model (Table 3) deposition velocities are taken to be higher than in lower NO_x models to reflect the fact that most higher NO_x

environments are in continental areas where surface deposition is faster [Lenschow et al., 1982]. than in the lowest NO_x (marine) environments. In both low NO_x and high NO_x models we neglect lightning-produced NO_x.

For each of the model types LNLL, LNML and HNML, the time dependent equations (1) are integrated until ozone has converged to a time-invariant vertical profile and all other species display periodic 24 hour behavior. Diurnally averaged species concentrations and diurnal factors for reaction and photolysis rates are calculated according to the procedure of Turco and Whitten [1978]. These concentrations and diurnal factors are used as input for a time-independent (steady-state) version of the model, which consists of Eqs (1) with $\partial c_i/\partial t = 0$.

B. Basic Model Results

Calculations to determine the sensitivity of CH_4-CO-OH changes to perturbed CO and CH_4 emissions are carried out with a steady-state model using inputs unchanged except for higher specified fluxes of CO (or CH_4). Perturbation calculations are made for each of the three models LNLL, LNML, HNML. For CH_4 perturbations CH_4 fluxes are adjusted to give methane surface mixing ratios 10-150% higher than present day values. For CO perturbations CO fluxes are modified to give higher surface mixing ratios of CO.

Figure 1 shows vertical profiles (0-15 km) of tropospheric OH (cm^{-3}) with no perturbations (solid lines) and with 50% and 100% CO and CH_4 perturbations. LNML results are illustrated in Figure 1a. Both quantitatively and qualitatively OH responds differently to CO and CH_4 variations. First, in the upper troposphere increasing CO suppresses OH whereas adding CH_4 increases OH. Second, in the mid and lower troposphere addition of CO and CH_4 suppresses OH, but the response is greater for CO because the effective rate of OH removal by CO is shorter.

Figure 1b gives HNML results for OH response to perturbed CO and CH_4. With relatively high background NO_x OH increases rather than decreases near the ground with added CO and methane. This is because in the presence of high NO_x additional CO and CH_4 oxidation forms ozone through smog-type reactions. Additional ozone when photolyzed replenishes OH:

$$O_3 + h\nu \rightarrow O(^1D) + O_2$$
$$O(^1D) + H_2O \rightarrow 2OH.$$

In an environment with higher NO_x, or at least with a high NO_x/hydrocarbon ratio as in the present simulations, adding CO or CH_4 appears to increase oxidant levels. This could affect urban and nonurban atmospheres where NO_x levels are high. Furthermore, enhanced amounts of ozone might be transported from urban to remote (low NO_x) areas where it could increase the potential for forming OH, perhaps offsetting some of the local OH depletion initiated by elevated CO or CH_4 levels (Vukovich et al, 1985).

The high NO_x OH behavior is only a surface phenomenon, however. Total tropospheric OH (column-integrated) in all three models, LNML, LNLL, and HNML, decreases in response to added CO and CH_4. This can be seen in Figure 2 where tropospheric OH is shown as a function of perturbed CH_4 and CO. The effect of high NO_x in the boundary layer is to lessen total column loss.

The effects of perturbed CO and CH_4 fluxes on CO and CH_4 themselves are shown in Figure 3; only results from the LNML model are illustrated but results with HNML and LNLL models are nearly identical. Effects of feedback of CO on CH_4 and vice versa are obvious. For both CO and CH_4 the additional flux required, Δ flux (as a fraction of the initial flux) is less than the desired fractional mixing ratio increase (Δ mixing ratio) and the ratio of the increments, i.e., Δ flux/ Δ mixing ratio, is not constant over the range of perturbations studied. The nonlinearity in the flux/mixing ratio relationship is such that it takes only a 77% increase in the CO emission rate (with no change in CH_4 emissions) to double the CO surface mixing ratio. Methane doubles even more effectively than CO. With fixed CO influx it takes only a 65% increase above the initial CH_4 flux to double surface methane. Similar nonlinearities were noted by Chameides and Davis [1985].

A consequence of the nonlinearity of the response of steady-state mixing ratios to perturbed flux is an infinite number of paths to a given CO or CH_4 increase. For example, a 25% increase in the CO mixing ratio is produced as a result of a 20% increase in CO emissions with no change in the methane flux (Figure 3a). The same CO increase can occur, with no increase in CO emissions, if methane emissions are increased by about 57% (Figure 3b). Clearly, some combination of CO and CH_4 perturbations could also bring about a 25% increase in background CO. From a practical point of view this is very important. Monitoring concentrations of a trace gas that is changing without knowing the source(s) of the change makes meaningful long-term predictions impossible. Should a trend in anthropogenic CH_4 or CO or or of some other gas that is related to changes in OH be deemed undesirable, it would be difficult without knowing cause and effect to devise a control strategy.

3. TRENDS IN ATMOSPHERIC CO, CH_4 AND OH: 1860-2035

A. CH_4, CO, OH Scenarios

We have performed model calculations to predict CH_4, CO and OH changes over the next fifty years and to look backward in time, assessing possible variations in these species since 1860 (chosen as the start of the heavily industrial era). As much as possible observations are used to prescribe model scenarios, although we are limited by sparse data, uneven geographical coverage and a short historical record; i.e. prior to 1950 there are few data for any trace gas.

Perturbations to background CH_4 and CO have been measured or deduced by a number of investigators [Graedel and McRae, 1980; Rasmussen and Khalil, 1981; Blake et al, 1982; Khalil and Rasmussen, 1984; Rinsland et al, 1985], but the magnitude and duration of trends is far from certain. This makes choice of model input for predicting further changes problematic. Extrapolating backward to 1860 is difficult because source budgets are not known accurately and emissions trends must be estimated over the past 125 years. The situation is further complicated by the sensitivity of CH_4 and CO perturbations to NO_x for which no historical data are available and for which the present day record is spotty. Our approach to model runs is to parameterize CH_4 and CO over a range of values in keeping with recently reported data and to combine these with several levels of NO_x. Choices for input are reviewed below.

$\underline{CH_4}$: The weight of evidence favors secular increases in CH_4 of about 1% per year, at least over the past three decades or so [Ehhalt et al, 1983; Blake et al, 1982; Rasmussen and Khalil, 1984; Rinsland et al, 1985], and the long-term record of CH_4 trapped in polar ice cores indicates that CH_4 has been increasing since 1800 [Rasmussen and Khalil, 1984; Stauffer et al, 1985] or even earlier [Craig and Chou, 1982].

For model runs from 1860 to 2035 we have adopted two approaches. The conservative choice assumes no temporal change in CH_4 sources and assigns a constant CH_4 flux at all times. In this case temporal increases in CH_4 occur only in response to perturbed OH caused by altered levels of some other trace gas(es), i.e. in our model, by CO. The second approach specifies the CH_4 mixing ratio at each year of model calculation, following ice core data from 1860 to 1985 [Khalil and Rasmussen, 1985; Stauffer et al, 1985] and assuming a 1% yr^{-1} increase beyond 1.60 ppmv for years after 1985.

CO: The choice of input for CO is complicated because there are large geographical and seasonal variations owing to the relatively short lifetime of CO, a few months in midlatitudes. Also, trends in CO are ambiguous. Khalil and Rasmussen [1984] extracted a 6% yr^{-1} rate of increase from more than 60,000 measurements of CO taken in Oregon over a 3-1/2 year period (1979-1983), but this is probably too high [Seiler, private communication, 1984]. Rinsland and Levine [1985] deduce a 71% increase from 1951 to 1976 from spectroscopic data at one European site. Southern hemisphere CO concentrations may have risen a total of 5-10% between 1971 and 1981 [Seiler et al, 1984].

Three sources of CO are specified in the model and uncertainties in CO budgets and trends are treated by parameterizing relative amounts of natural and anthropogenic sources. Model runs for years other than 1985 assume that anthropogenic inputs scale with population or fossil fuel usage. For year t at altitude z the total source, $S_{total,CO}(z,t)$ consists of:

$$S_{total,CO}(z,t) = Q_{CO}(z,t) + flux_{CO}(t) + S_{NMHC}(z,t) \quad (3)$$

where Q_{CO} is in-situ photochemical formation from CH_4 and C_2H_6 oxidation;

$\mathrm{flux}_{CO}(t)$, the model lower boundary condition, signifies direct boundary layer sources. S_{NMHC} is an explicitly specified term representing in-situ airborne CO sources besides CH_4 and C_2H_6 oxidation, i.e., photooxidation of nonmethane hydrocarbons besides C_2H_6. S_{NMHC} is added to the CO continuity equation with a functional form that follows the product of OH and the altitude dependence of a typical OH and alkane reaction.

For model runs at midlatitude conditions CO is always 120 ppbv at 0 km for 1985 and relative amounts of $S_{NMHC}(1985)$ and $\mathrm{flux}_{CO}(1985)$ are parameterized as shown in Table 4. Type 1-CO (Models 1 and 3) is based on $S^{total,CO}(1985)$ consisting of 35% flux_{CO} and Type 2-CO (Models 2 and 4) is based on 65% of $S^{total,CO}(1985)$ as flux_{CO}. Model runs at years other than 1985 assume that natural sources contributing to S_{NMHC} and flux_{CO} are fixed in time and anthropogenic ones scale with population or fossil fuel usage. The in-situ source is given by:

$$S_{NMHC}(z,t) = S_{NMHC}(z,1985)\ [f_{NMHC,N} + r^{ff}(t)\ f_{NMHC,A}(1985)] \qquad (4)$$

where $f_{NMHC,N}$ (0.82) and $f_{NMHC,A}(1985)=0.18$ are fractions of S_{NMHC} due to oxidation of natural and anthropogenic NMHC [Logan et al, 1981]. $r^{ff}(t)$ is the ratio of fossil fuel usage in year t relative to 1985. We assume that incremental CO emissions follow CO_2 and use Keeling's (1973) values for CO_2 from fossil fuel burning to obtain $r^{ff}(t)$ from 1860 to 1965. After 1965 a 2.5% annual increase in fossil-derived CO_2 is used [NRC, 1983] implying a 30-35 year doubling time for CO from this source. Where combustion CO is mainly from automobiles and is regulated, CO may rise more slowly [Kavanaugh, 1986].

The time dependence of $\mathrm{flux}_{CO}(t)$ is:

$$\mathrm{flux}_{CO}(t) = \mathrm{flux}_{CO}(1985)\ [f_{flux,N} + r^{ff}(t)\ f_A^{ff}(1985) + r^{pop}(t) f_A^{nf}(1985)]$$

with $r^{pop}(t)$ the ratio of population in year t relative to 1985. f's are based on the Logan et al [1981] budget for Northern Hemisphere CO sources; $f_{flux,N} = 0.13$ is the natural fraction of $flux_{CO}$ (oceanic flux, emissions from plants and lightning-induced wildfires); f_A^{ff} and f_A^{nf} are fossil fuel and non-fossil fuel (wood fuel and biomass burning) combustion components of anthropogenic $flux_{CO}$, equal to 0.45 and 0.43, respectively, in 1985.

The time dependence of S_{NMHC} and $flux_{CO}$ are shown in Figure 4. The largely anthropogenic component $flux_{CO}$ displays a large increase -- ~6-fold from 1860 to 2035 -- whereas S_{NMHC}, mostly natural in origin, changes little.

Model runs to simulate the period 1860 to 2035 are based on combinations of the parameterized CH_4 and CO inputs described above. Five scenarios (Models 1-5 in Table 5) are chosen to look at background tropospheric changes assuming constant NO_x. In each case the model is initialized to give 120 ppbv CO and 1.6 ppmv CH_4 for 1985. Calculations are performed with perturbed inputs (CO fluxes, CH_4 mixing ratios or fluxes) at 10 to 30 year intervals. In fact, time-dependent calculations show that CH_4 and CO can exhibit slower transients than would be predicted from their respective steady-state lifetimes. Models 1 and 2 employ constant CH_4 flux at all times, with Model 1 based on a minimum CO change (Type 1-CO) and Model 2 based on a larger CO change (Type 2-CO). Models 3, 4 and 5 simulate scenarios based on large temporal changes in CH_4 (mixing ratios from ice core data with extrapolation to 2035) and varying degrees of change in CO. Model 3 is Type 1-CO and Model 4 is Type 2-CO. Finally, we consider an extreme case in which no CO sources change in time, i.e. constant values of S_{NMHC} and $flux_{CO}$, to look at the effects of perturbed CH_4 on OH and CO (Model 5). This is similar to Models 1 and 2 in assigning all OH changes to only one of the perturbed gases.

$\underline{O_3}$, $\underline{H_2O}$, $\underline{NO_x}$: Besides CH_4 and CO, these trace species and other parameters, e.g. uv radiation, and rainout rates, are critical in determining OH concentrations. Water vapor, radiation fluxes and rainout rates are fixed at constant values (Section 2) for all runs except for the perturbed climate case described later.

Ozone varies so widely in time and space, even on a short term, that there is no way of extracting with certainty historical trends to be followed in calculations. CH_4 and CO perturbations establish self-consistent O_3 levels when O_3 is calculated in model runs with constant boundary conditions: fixed stratospheric input of odd oxygen and surface removal at the lower boundary.

It was shown in Section 2 that NO_x is critical in determining perturbed OH concentrations yet uncertainties in the odd nitrogen budget [Logan, 1983; Liu et al, 1983], introduce some arbitrariness in the selection of appropriate NO_x levels for CH_4 and CO perturbations. There is little doubt that anthropogenic activities exert a large and changing role in NO_x on a local basis, but effects on the background troposphere are less clear. We have taken a simplified approach in choosing three alternate NO_x scenarios to accompany CO/CH_4 perturbation calculations for background midlatitude environments.

Two sets of CH_4/CO perturbations assume nearly constant NO_x. One simulates the nonpolluted marine midlatitude troposphere where we assume low NO_x boundary conditions (LNML, Table 3) at all times. A second NO_x scenario simulates a nonpolluted continental midlatitude environment with ground-level NO_x ~1 ppbv at all times and HNML boundary conditions.

Assuming constant NO_x while CO increases, i.e. CO/NO_x is increasing in time, implies that NMHC and CO emissions increase faster than NO_x. We performed one set of calculations in which NO emissions increase along with CO emissions. Starting with low surface NO_x (20 pptv in 1860) model NO influx at succeeding years increases at the rate given by Brimblecombe and Stedman

[1982] until NO_x is 0.2 ppbv in 1985. Extrapolating forward from 1985, NO_x input follows the pattern of the past two decades with some leveling off due to pollution controls [Kavanaugh, 1986]. We do not know the historical record of NO_x, but this may be a more realistic representation of its temporal evolution in some continental environments than assuming constant 1 ppbv NO_x. We refer to these as "transitional regions."

Model 3 is the only case run with a time-varying NO influx. For consistency with the limits suggested by low and high NO_x scenarios, calculations with changing NO_x are performed with specified O_3, beginning with the Model 3 low NO_x O_3 profile for 1860 and ending with a higher NO_x O_3 profile for 2035. Surface NO_x increases from 20 pptv in 1860 to 480 pptv in 2035.

B. Results

Model results simulating CH_4-CO-OH from 1860 to 2035 are shown in Figures 5 (low NO_x) and 6 (high NO_x). Ground level CH_4 and CO mixing ratios and fractional changes in column-integrated OH for Models 1 and 2 with low NO_x are shown in Figure 5a. With constant CH_4 flux, CO perturbations alone determine CO and OH behavior and CH_4 response. In 1860 CH_4 is 1.2-1.3 ppmv but CO levels are 2-3 times lower than in 1985. From 1985 to 2035 CO is predicted to double or triple at the surface (from 120 to 270 or 355 ppbv). In Models 1 and 2 OH decreases are 22-34% from 1860 to 1985 with an additional 25-34% loss (and a 25% increase in CH_4) projected over the next fifty years. Figure 5a shows that if CO perturbations alone are driving OH changes, then significant changes in background CH_4 have occurred since 1860, but not as great as those deduced from ice core data (Figure 5b).

Figure 5b shows Models 3, 4 and 5 where a steady increase in CH_4 has been specified from 1860 to 2035. Models 3 and 4 correspond to changing scenarios for CO sources (dashed and solid lines respectively). Model 5 (dotted lines) shows CO and OH perturbations responding to increasing CH_4 in the absence of altered CO emissions. When both CO and CH_4 changes are specified (Models 3 and 4), changes for OH are of greater magnitude than when only CH_4 or CO is perturbed. For Model 5 in 1860 CO is ~100 ppbv (probably unrealistically high) and it may increase to 150 ppbv in 2035. The concurrent OH change is a 13% loss from 1860 to 1985 and an additional 13% loss from 1985 to 2035.

Figure 6 shows surface CH_4, CO and total OH for Models 1-5 calculated at ~1 ppbv NO_x at the surface. Because CO and CH_4 are largely controlled by their respective sources, CO and CH_4 patterns are not very different from the low NO_x case (cf Figure 5). However, the OH decrease accompanying each CH_4/CO perturbation is roughly half the magnitude of its low NO_x counterpart. This is because at higher NO_x, CH_4 and CO perturbations cause increases in boundary layer OH that offset mid-tropospheric losses (Figure 1). In Model 5 OH is almost constant from 1860 to the present.

Our CO and CH_4 levels for 1950 are higher than those deduced by Levine et al [1985]. The Levine et al 1950 CO and CH_4 values occur at ~1930 where Figures 5b and 6b show OH 25-35% higher (low NO_x) and 10-15% higher (high NO_x) than in 1985. They estimate 25% higher OH with NO_x and O_3 different from our cases. Although our results are not strictly comparable to Levine et al [1985], we calculate OH changes of similar magnitude.

Figure 7 shows Model 3 type CH_4 and CO with NO_x and OH calculated with the "transitional region" NO_x scenario. OH increases slightly and then decreases slowly. The complexity of NO_x-OH interaction is evident when one compares the boundary layer behavior of OH in the three NO_x cases run with Model 3. Figure 8 shows OH changes in the boundary layer (0-2 km in the model) for the three NO_x scenarios. Vertical profiles of OH are shown for three years, 1970, 2005, 2035, along with a bar graph of total and boundary layer OH column depth. Profile shapes differ sharply among the cases. There is also a pronounced difference in boundary layer OH trend, which at increasing concentrations of NO_x becomes a large fraction of total OH. The relationship between boundary layer and total OH implies that localized and regional scale processes may affect global OH. Even if most of the troposphere is isolated from the urban environment, and OH is decreasing as a whole (as globally increasing CO and CH_4 suggests), transport among various regions needs to be included in a full investigation of the problem. In other words CO and CH_4 perturbations are a problem that is chemically and dynamically more complex than can be treated in a one-dimensional model.

4. DISCUSSION

Changing CH_4-CO-OH levels in the background troposphere imply: (1) changes in tropospheric lifetimes for many trace species; (2) CH_4 and O_3 changes which may affect climate. Since OH controls lifetimes of most terrestrially derived gases, perturbations to atmospheric OH alter rates of photooxidation throughout the troposphere. For example, reduced OH means a slower formation of atmospheric acids, at least in the unpolluted troposphere. As CO increases over time, the ratio OH/HO_2 increases due to $CO + OH \rightarrow CO_2 + HO_2$. This leads to increasing levels of H_2O_2. At low NO_x we calculate a doubling of H_2O_2 from 1860 to the present day.

Changes in atmospheric lifetimes of hundreds of trace gases, e.g. reactive hydrocarbons, sulfur and nitrogen compounds, may have occurred since 1860 as a consequence of OH perturbations. Consider, for example, CH_4 itself. There are two ways in which CH_4 levels can be forced to change: (1) by altering CH_4 emissions; (2) by changing the mean level of atmospheric OH. Looking at Models 1 and 2 where no change in surface CH_4 emissions is assumed, we see that CO increases alone (with OH decreasing) could have caused background level CH_4 to increase 15-20% from 1860 to 1985. From 1985 to 2035 an additional 20% increase in CH_4 is predicted. From the magnitude of CH_4 increases and OH losses shown in Figure 5a, we estimate that ~half the CH_4 increase shown in Models 3 and 4 (Figure 5b) is due to increased lifetime relative to OH (suppressed by CO) and the rest to increased emissions of CH_4. Khalil and Rasmussen [1985] and Levine et al [1985] reached a similar conclusion in analyzing past methane trends.

Changes in CH_4-CO-OH chemistry may affect climate because O_3, CH_4, and CO_2 (to which CO converts by OH oxidation) are greenhouse gases. All of the CH_4 and CO scenarios simulated in our study (Figures 5 and 6) are accompanied by steady increases in tropospheric O_3. Surface O_3 mixing ratios for 1860, 1985, 2035 are given in Table 5. From 1860 to 1985 we calculate an 8-22% increase in O_3 for constant, low NO_x conditions. For high NO_x the increase from 1860 to 1985 is as great as 78% (Model 4). Furthermore, in a set of Model 3 calculations with "transitional NO_x" and O_3 unconstrained (surface deposition instead of fixed mixing ratio) O_3 is only 10 ppbv in 1860 and 27 ppbv in 1985. Dignon and Hameed (1985) have suggested that increasing NO_x emissions probably caused some of the recent increases in tropospheric O_3.

Calculated tropospheric O_3 increases are consistent with observations that tropospheric O_3 has been increasing over the past decade or two [Bojkov, 1984; Logan, 1985] and possibly longer [Volz et al, 1985; Bojkov, 1986]. If tropospheric O_3 increases are part of a long-term trend, then there are continuous perturbations in background chemistry and potentially in global climate, since O_3 is a greenhouse gas [Wang et al, 1976; Fishman et al, 1979;

Ramanathan et al, 1985]. Depending on the altitude dependence of these increases, changes in tropospheric O_3 may be perturbing the earth's radiation field. For example, Ramanathan et al [1985] have shown that a 25% increase in ozone over the past 100 years could have contributed to a modest rise in global temperature and continuing increases in O_3, along with CH_4 and other non-CO_2 greenhouse gases, could have growing effects on global climate.

Secular CO increases over the past century may be influencing global climate through CO_2 because CO contributes to CO_2 through the oxidation $CO + OH \rightarrow H + CO_2$. Atmospheric CO increases also affect radiation by suppressing OH and allowing O_3 and CH_4 to build up, even if CH_4 emissions do not increase.

We note that global climate change would feed back on background CH_4-CO-OH through: (1) altered temperature perturbing chemical reaction rates and tropospheric water vapor; (2) altered precipitation patterns. Since the nature of these changes is not clear [Hansen et al, 1984] we do not know how feedback to trace chemistry would occur. The greatest effect might be modification of average water vapor. We performed a set of calculations (Models 1-5 with high and low NO_x) assuming constant relative humidity [Manabe and Wetherald, 1967] and perturbed temperature from Ramanathan et al [1985]. Higher temperatures imply more water vapor (Table 1), leading to more OH via

$$O(^1D) + H_2O \rightarrow 2OH.$$

In all cases the decline predicted for the next 50 years (Figures 5 and 6) is substantially less than if mean temperature is assumed constant from 1985 to 2035. The fractional OH losses shown in Figures 5 and 6 are reduced 6-8% with higher water vapor. The opposite effect (reinforcement of OH loss) might occur if climate change means increased precipitation and greater removal of OH reservoirs like HNO_3 and H_2O_2. A complete investigation of perturbed photochemical-climate interaction is beyond the scope of this paper.

5. SUMMARY AND CONCLUSIONS

The effects of perturbed CO and CH_4 on tropospheric OH are complex. Total tropospheric OH always decreases when CO or CH_4 is increased, but under certain conditions, surface and upper tropospheric OH may actually increase. The magnitude of OH changes is highly sensitive to local NO_x levels.

CH_4-CO-OH coupling means that a positive perturbation in either CO or CH_4 emissions causes both CO and CH_4 to increase throughout the troposphere. A practical consequence of the coupling is that observed changes in CO or CH_4 cannot be ascribed unambiguously to enhanced CO emissions, CH_4 emissions or to a given combination of the two -- or to changes in OH for other reasons. It is essential to determine sources and emission rates of individual tropospheric gases that show secular changes to distinguish cause effect and to make meaningful long-term predictions.

Recent reports of changing CO and CH_4 form the basis for a series of photochemical model calculations simulating tropospheric trace gases from 1860 to 2035. Several scenarios are considered. In pristine environments (low, constant NO_x) CH_4 will probably continue to increase, reaching a value of 2 ppmv by 2035 (assuming that growing anthropogenic CO emissions perturb OH but CH_4 emissions are unchanged) or 3 ppmv if CH_4 emissions also rise. During that time CO will increase from 20% to two or three times its current level, depending on the intensity of CO emissions. Looking back to 1860 (a reference year for the preindustrial atmosphere) we find CH_4 at 50-80% and CO at 45-85% of present day levels and OH 22-45% higher than at present.

At higher levels of NO_x tropospheric OH may have decreased monotonically since 1860 as in low NO_x environments (although at a smaller rate) or it may have increased to a maximum level then decreased. The complexity of the urban-influenced environment and its potential interaction with remote environments complicates interpretation of CO, CH_4, and OH trends. A more nearly complete treatment of NMHC chemistry and boundary layer dynamics is required than is included in the present modeling study.

There are global consequences of projected CH_4 and CO trends. In all NO_x scenarios considered tropospheric O_3 shows a monotonic increase from 1860 to 2035. In the case of background NO_x in transition from 20 pptv in 1860 to 0.2 ppbv in 1985, surface ozone would have increased from 10 ppbv in 1860 to 27 ppbv in 1985. This compares favorably with recently published O_3 observations taken at a midlatitude continental site. Decreased OH means longer tropospheric lifetimes for hundreds of trace gases, both natural and anthropogenic, and enhanced escape of some of these species to the stratosphere. In the case of CH_4 directly and in the case of CO indirectly (through enhanced formation of O_3 and oxidation of CO to CO_2) there are perturbations in the earth's radiative forcing and possibly climate.

ACKNOWLEDGMENTS

A. M. T. acknowledges support from an NCAR Advanced Study Program Postdoctoral Fellowship and from the NASA Tropospheric Chemistry Program. Thanks to S. Walters and J. Herwehe for programming assistance.

REFERENCES

Aikin, A. C., J. R. Herman, E. J. Maier, and C. J. McQuillan, Atmospheric chemistry of ethane and ethylene, J. Geophys. Res., 87, 3105-3118, 1982.

Atkinson, R. and J. N. Pitts, Jr., Kinetics of the OH radical with HCHO and CH_3CHO over the temperature range 299-466°K, J. Chem. Phys., 60, 3581-3584, 1978.

Blake, D. R., E. W. Mayer, S. C. Tyler, Y. Makide, D. C. Montague, and F. S. Rowland, Global increase in atmospheric methane concentrations between 1978 and 1980, Geophys. Res. Lett., 9, 477-480, 1982.

Bojkov, R., Tropospheric ozone, its changes and possible radiative effects, Spec. Environ. Rep., 16, World Meteor. Org., Geneva, 1984.

Bojkov, R., Surface ozone during the second half of the nineteenth century, J. Clim. Appl. Meteor., 25, 343-352, 1986.

Brewer, D. A., T. R. Augustsson, and J. S. Levine, The photochemistry of anthropogenic nonmethane hydrocarbons in the troposphere, J. Geophys. Res., 88, 6683-6695, 1983.

Brimblecombe, P., and D. H. Stedman, Historical evidence for a dramatic increase in the nitrate component of acid rain, Nature, 298, 460-462, 1982.

Calvert, J. G., and J. N. Pitts, Jr., Photochemistry, Wiley, New York, 1966.

Chameides, W. L., and D. D. Davis, The photochemistry of tropospheric trace species: the central role of radicals and their possible variability, in Chemical Events in the Atmosphere and Their Impact on the Environment, Pontifical Acad. Science, Rome, 1985.

Chameides, W. L., S. C. Liu, and R. J. Cicerone, Possible variations in atmospheric methane, J. Geophys. Res., 82, 1795-1798, 1977.

Cox, R. A., and M. J. Roffey, Thermal decomposition of peroxyacetylnitrate in the presence of nitric oxide, Environ. Sci. Technol., 11, 900-906, 1977.

Craig, H., and C. C. Chou, Methane: The record in polar ice cores, Geophys. Res. Lett., 9, 1221-1224, 1982.

Crutzen, P. J., A discussion of the chemistry of some minor constituents in the stratosphere and troposphere, Pure Appl. Geophys., 106-108, 1385-1399, 1973.

Crutzen, P. J., The role of NO and NO_2 in the chemistry of the troposphere and stratosphere, Ann. Rev. Earth Planet. Sci., 7, 443-472, 1979.

Crutzen, P. J., The role of the Tropics in atmospheric chemistry, in Geophysiology of Amazonica, ed. by R. E. Dickinson, J. Wiley & Sons, N. Y., 1986.

Dignon, J., and S. Hameed, A model investigation of the impact of increases in anthropogenic NO_x emissions between 1967 and 1980 on tropospheric ozone, J. Atmos. Chem., 3, 491-506, 1985.

Ehhalt, D. H., R. J. Zander, and R. A. Lamontagne, On the temporal increase of tropospheric CH_4, J. Geophys. Res., 88, 8442-8446, 1983.

Fishman, J., V. Ramanathan, P. J. Crutzen, and S.-C. Liu, Tropospheric ozone and climate, Nature, 282, 818-820, 1979.

Graedel, T. E., and J. E. McRae, On the possible increase of the atmospheric methane and carbon monoxide concentrations during the last decade, Geophys. Res. Lett., 7, 977-979, 1980.

Greiner, N. R., Hydroxyl radical kinetics by kinetic spectroscopy: V. Reactions with alkanes in the range 300-500 K, J. Chem. Phys., 53, 1070-1076, 1970.

Hameed, S., J. P. Pinto, and R. W. Stewart, Sensitivity of the predicted CO-OH-CH_4 perturbation to tropospheric NO_x concentrations, J. Geophys. Res., 84, 763-768, 1979.

Hansen, J., A. Lacis, D. Rind, G. Russell, I. Fung, and S. Lebedeff, Evidence for future warming: How large and when, CO_2 Conf. of the Natl. Forest Prod. Assoc., 25-27 June 1984, Boulder, CO.

Horowitz, A., and J. G. Calvert, Wavelength dependence of the primary processes in acetaldehyde photolysis, J. Phys. Chem., 86, 3105-3114, 1982.

Kasting, J. F., and H. B. Singh, Nonmethane hydrocarbons in the troposphere: Impact on the odd hydrogen and odd nitrogen chemistry, J. Geophys. Res., submitted, 1986.

Kavanaugh, M., Estimates of future CO, N_2O, and NO_x emissions from energy combustion, Atmos. Environ., submitted for publication, 1986.

Keeling, C. D., Industrial production of carbon dioxide from fossil fuels and limestone, Tellus, 25, 174-198, 1973.

Khalil, M. A. K., and R. A. Rasmussen, Carbon monoxide in the earth's atmosphere: Increasing trend, Science, 224, 54-56, 1984.

Khalil, M. A. K., and R. A. Rasmussen, Causes of increasing atmospheric methane: Depletion of hydroxyl radicals and the rise of emissions, Atmos. Environ., 19, 397-407, 1985.

Lenschow, D. H., R. Pearson, Jr., and B. B. Stankov, Measurements of ozone vertical flux to ocean and forest, J. Geophys. Res., 87, 8833-8838, 1982.

Levine, J. S., C. P. Rinsland, and G. M. Tennille, The photochemistry of methane and carbon monoxide in the troposphere in 1950 and 1985, Nature, 318, 254-257, 1985.

Levy, H., Photochemistry of the lower troposphere, Planet. Space Sci., 20, 919-935, 1972.

Liu, S.-C., M. McFarland, D. Kley, and O. C. Zafiriou, Tropospheric NO_x and O_3 budgets in the Equatorial Pacific, J. Geophys. Res., 88, 1360-1368, 1983.

Logan, J. A., Nitrogen oxides in the troposphere: Global and regional budgets, J. Geophys. Res., 88, 10785-10808, 1983.

Logan, J. A., Tropospheric ozone: Seasonal behavior, trends and anthropogenic influence, J. Geophys. Res., 90, 10463-10482, 1985.

Logan, J. A., M. J. Prather, S. C. Wofsy, and M. B. McElroy, Tropospheric chemistry: A global perspective, J. Geophys. Res., 86, 7210-7254, 1981.

Manabe, S. and R. T. Wetherald, Thermal equilibrium of the atmosphere with a given distribution of relative humidity, J. Atmos. Sci., 24, 241-259, 1967.

NASA/JPL, Chemical kinetics and photochemical data for use in stratospheric modeling, Eval. Number 5, JPL Publ. 82-57, Jet Propul. Lab, Pasadena, Calif., 1982.

NASA/JPL, Chemical kinetics and photochemical data for use in stratospheric modeling, Eval. Number 6, JPL Publ. 83-62, Jet Propul. Lab, Pasadena, Calif., 1983.

NRC (National Research Council), Changing climate: Report of the Carbon Dioxide Assessment Committee, National Academy Press, Washington, D. C., 1982.

Oort, A. H., and E. M. Rasmusson, Atmospheric circulation statistics, NOAA Prof. Paper 5, U. S. Govt. Print. Off., 1971.

Ramanathan, V., R. J. Cicerone, H. B. Singh, and J. T. Kiehl, Trace gas trends and their potential role in climate change, J. Geophys. Res., 90, 5547-5566, 1985.

Rasmussen, R. A., and M. A. K. Khalil, Increases in the concentration of atmospheric methane, Atmos. Environ., 15, 883-886, 1981.

Rasmussen, R. A., and M. A. K. Khalil, Atmospheric methane in the recent and ancient atmospheres: Concerns, trends, and interhemispheric gradient, J. Geophys. Res., 89, 11599-11605, 1984.

Rinsland, C. P., J. S. Levine, and T. Miles, Concentration of methane in the troposphere deduced from 1951 infrared solar spectra, *Nature*, *318*, 245-249, 1985.

Rinsland, C. P. and J. S. Levine, Free tropospheric carbon monoxide concentrations in 1950 and 1951 deduced from infrared total column amount measurements, *Nature* *318*, 250-254, 1985.

Rudolph, J. and D. H. Ehhalt, Measurements of C_2-C_5 hydrocarbons over the North Atlantic, *J. Geophys. Res.*, *86*, 11959-11964, 1981.

Seiler, W., H. Giehl, E.-G. Brunke, and E. Halliday, The seasonality of CO abundance in the Southern Hemisphere, *Tellus*, *36b*, 219-231, 1984.

Singh, H.B., L. J Salas, H. Shigeishi, and E. Scribner, Atmospheric halocarbons, hydrocarbons and sulfur hexafluoride: global distributions, sources and sinks, *Science*, *203*, 899-903, 1979.

Singh, H. B., and P. L. Hanst, Peroxyacetylnitrate (PAN) in the unpolluted atmosphere: An important reservoir for nitrogen oxides, *Geophys. Res. Lett.*, *8*,941-944, 1981.

Stauffer, B., G. Fischer, A. Neftel, and H. Oeschger, Increase of atmospheric methane recorded in Antarctic ice core, *Science*, *229*, 1386-1388, 1985.

Sze, N. D., Anthropogenic CO emissions: Implications for the atmospheric CO-OH-CH_4 cycle, *Science*, *195*, 673-675, 1977.

Thompson, A. M., The effect of clouds on photolysis rates and ozone formation in the unpolluted troposphere, *J. Geophys. Res.*, *89*, 1341-1349, 1984.

Thompson, A. M., and R. J. Cicerone, Clouds and wet removal as causes of variability in the trace-gas composition of the marine troposphere, *J. Geophys. Res.*, *87*, 8811-8826, 1982.

Turco, R. P., and R. C. Whitten, A note on the diurnal averaging of aeronomical models, *J. Atmos. Terr. Phys.*, *40*, 13-20, 1978.

U. S. Standard Atmosphere, 1966, National Oceanic and Atmospheric

Administration, NASA, U. S. Air Force, 1966.

U. S. Standard Atmosphere Supplement, 1976, National Oceanic and Atmospheric Administration, NASA, U. S. Air Force, 1976.

Volz, A., H. G. J. Smit, and D. Kley, Ozone measurements in the 19th century: The Montsouris Series, Eos, 66, 815, 1985.

Vukovich, F. M., J. Fishman, and E. V. Browell, The reservoir of ozone in the boundary layer of the Eastern United States and its potential impact on the global tropospheric ozone budget, J. Geophys. Res., 90, 5687-5698, 1985.

Wang, W., Y. Yung, A. Lacis, T. Mo, and J. Hansen, Greenhouse effects due to manmade perturbations of trace gases, Science, 194, 685-687, 1976.

Wofsy, S. C., Interactions of CH_4 and CO in the earth's atmosphere, Ann. Rev. Earth Planet. Sci., 4, 441-469, 1976.

TABLE 1

FIXED TROPOSPHERE MODEL PARAMETERS

	Mid-Latitude				Low Latitude			
Altitude (km)	Temp. (K)	Molecular Density $N(cm^{-3})$	H_2O Volume Mixing Ratio	Perturbed** H_2O Factors	Temp.† (K)	Molecular Density† $N(cm^{-3})$	H_2O Volume†† Mixing Ratio	H_2 Mixing Ratio
15	216.6	4.05*** (18)	3.10 (-6)	1.48	203.7	4.42 (18)	3.00 (-6)	5.15 (-7)
14	216.6	4.74 (18)	3.50 (-6)	1.48	210.3	5.20 (18)	3.60 (-6)	5.24 (-7)
13	216.6	5.54 (18)	4.00 (-6)	1.48	217.0	6.09 (18)	4.80 (-6)	5.30 (-7)
12	216.6	6.49 (18)	4.80 (-6)	1.48	223.6	7.12 (18)	5.80 (-6)	5.35 (-7)
11	216.8	7.59 (18)	7.00 (-6)	1.48	230.3	8.27 (18)	1.00 (-5)	5.38 (-7)
10	223.3	8.60 (18)	1.20 (-5)	1.45	237.0	9.28 (18)	5.00 (-5)	5.40 (-7)
9	229.7	9.71 (18)	3.30 (-5)	1.40	243.7	1.04 (19)	2.42 (-4)	5.42 (-7)
8	236.2	1.09 (19)	8.00 (-5)	1.39	250.4	1.16 (19)	7.89 (-4)	5.44 (-7)
7	242.7	1.23 (19)	3.00 (-4)	1.36	257.1	1.29 (19)	1.39 (-3)	5.46 (-7)
6	249.2	1.37 (19)	8.86 (-4)	1.29	263.8	1.43 (19)	2.27 (-3)	5.47 (-7)
5	255.7	1.53 (19)	1.37 (-3)	1.27	270.6	1.58 (19)	3.54 (-3)	5.48 (-7)
4	262.2	1.70 (19)	2.03 (-3)	1.25	277.4	1.75 (19)	5.03 (-3)	5.49 (-7)
3	268.7	1.89 (19)	3.25 (-3)	1.24	284.3	1.93 (19)	7.57 (-3)	5.49 (-7)
2	275.2	2.09 (19)	4.55 (-3)	1.22	289.4	2.12 (19)	1.17 (-2)	5.50 (-7)
1 §	281.7	2.31 (19)	5.92 (-3)	1.21	295.9	2.32 (19)	1.85 (-2)	5.50 (-7)
0	288.2	2.55 (19)	7.50 (-3)	1.20	302.6	2.55 (19)	2.53 (-2)	5.50 (-7)

*US Standard Atmosphere (1976)

**Simulation of perturbed climate in the year 2035: midlatitude temperatures are increased 3K at all altitudes. Corresponding H_2O volume mixing ratios, assuming constant relative humidities are obtained by multiplying standard mixing ratios by these factors.

†US Standard Atmosphere Supplements (1966)

††Oort and Rasmusson (1971)

***4.05 (18) signifies 4.05×10^{18}

§Not shown are values for 8 additional grid points between 0 and 1 km which are used for calculations in the boundary layer [Thompson and Cicerone, 1982]

Table 2

Summary of PAN-Related Reactions
(Supplementary to Chemical Reaction Scheme of Thompson and Cicerone, 1982)

Chemical Reaction	Rate ($cm^3\ s^{-1}$)	Reference
$C_2H_6+OH \xrightarrow{O_2} C_2H_5O_2+H_2O$	1.86×10^{-11} exp(-1230/T)	Greiner, 1970
$C_2H_5O_2+NO \rightarrow C_2H_5O+NO_2$	4.2×10^{-12} exp(180/T)	estimated* from rate for CH_3O_2+NO
$C_2H_5O+O_2 \rightarrow CH_3CHO+HO_2$	1.2×10^{-13} exp(-1350/T)	estimated* from rate for CH_3O+O_2
$C_2H_5O_2+HO_2 \rightarrow C_2H_5OOH+O_2$	7.7×10^{-14} exp(1300/T)	estimated* from rate for $CH_3O_2+HO_2$
$CH_3CHO+OH \xrightarrow{O_2} CH_3CO_3+H_2O$	6.87×10^{-12} exp(255/T)	Atkinson and Pitts, 1978
$CH_3CO_3+NO \rightarrow CH_3+CO_2+NO_2$	2.38×10^{-12}	Cox and Roffey, 1977
$CH_3CO_3+NO_2+M \rightarrow CH_3CO_3NO_2$(PAN)+M	5.49×10^{-32} ($cm^6\ s^{-1}$)	Cox and Roffey, 1977
PAN+M $\rightarrow CH_3CO_3+NO_2+M$	3.18×10^{-5} exp(-12540/T)	Cox and Roffey, 1977
Photodissociation Reaction	**Rate (0 km, Diurnally Averaged, s^{-1})**	
$CH_3CHO+h\nu \rightarrow CH_3+HCO$	1.1×10^{-6}	Calvert and Pitts, 1966; Horowitz and Calvert, 1982
$C_2H_5OOH+h\nu \rightarrow C_2H_5O+OH$	1.6×10^{-6}	estimated* from CH_3OOH
PAN+$h\nu \rightarrow CH_3CO_3+NO_2$	7.7×10^{-9}	

*Rate for reference reaction taken from NASA/JPL [1982].

Table 3

Photochemical Model: Trace Gases and Boundary Conditions

Upper Boundary (15 km)

Species	Boundary Condition
O_3	influx: 5×10^{10} cm^{-2} s^{-1}
$O(^3P)$*	influx: 4×10^3 cm^{-2} s^{-1}
CH_3, CH_3O, CH_3O_2, CH_3OOH, $C_2H_5O_2$, H_2O_2, C_2H_5OOH, CH_3CO_3, H, OH, HO_2	photochemical equilibrium
NO_y $(+NO+NO_2+NO_3+HNO_3+HNO_4+2N_2O_5)$	influx: 2.5×10^8 cm^{-2} s^{-1}
H_2CO, PAN, CH_3CHO	zero outflux
CH_4	v† = 0.0003
CO	v = 0.1
C_2H_6	v = 0.013

Lower Boundary (0 km)

	Low NOx (LNLL, LNML)	High NOx (HNML)
O_3	v† = 0.05	v = 0.5
$O(^3P)$	v = 0.5	v = 0.5
CH_3, CH_3O, CH_3O_2 $C_2H_5O_2$, CH_3CO_3 H, OH, HO_2	photochemical equilibrium	photochemical equilibrium
NO	influx=$7.5 \times 10^8 cm^{-2} s^{-1}$	influx=7.5×10^{10} cm^{-2} s^{-1}
NO_2	v = 0.01	v = 0.01
NO_3, N_2O_5	v = 0.5	v = 1.0
PAN	v = 0.1	v = 0.2
H_2CO, CH_3OOH, CH_3CHO, C_2H_5OOH**	v = 0.5	v = 1.0
H_2O_2, HNO_3, HNO_4**	v = 0.5.	v = 1.0
C_2H_6	fixed: 1.5 ppbv	fixed: 1.5 ppbv
CO	influx gives 120-300 ppbv (LNML) 85-214 ppbv (LNLL)	influx gives 120-300 ppbv
CH_4	influx gives 1.6-4 ppmv	influx gives 1.6-4.0 ppmv

Notes:

* Value given is diurnally averaged and is one-half that used in time-dependent calculations.

† Upper boundary: v = troposphere-to-stratosphere transfer velocity ($cm\ s^{-1}$)
Lower boundary: v = surface transfer or deposition velocity ($cm\ s^{-1}$)

** Rainout loss (rate = 1.65×10^{-6} s^{-1} below 6 km) in species continuity equation. Applies to all models.

Table 4: Parameterization of CO Sources -- 1985

$S^{total,CO}$ =	Q_{CO} +	$flux_{CO}$ +	S_{NMHC}
Low NO_x: $S_{total} = 1.9 \times 10^{11}$ cm^{-2} s^{-1}			
Type 1-CO	15%	35%	50%
Type 2-CO	15%	65%	20%
High NO_x: $S_{total} = 4.8 \times 10^{11}$ cm^{-2} s^{-1}			
Type 1-CO	25%	35%	40%
Type 2-CO	25%	65%	10%

Table 5: Model Characteristics.[1]

	Model 1	Model 2	Model 3	Model 4	Model 5
Input					
CH_4	constant CH_4 flux[2]		CH_4 m. ratio from ice core data [Khalil and Rasmussen, 1985]		
CO	Type 1-CO	Type 2-CO	Type 1-CO	Type 2-CO	constant $flux_{CO}$, S_{NMHC}
Output					
O_3 (0 km, low NO_x):					
1860	28 ppbv	26 ppbv	25 ppbv	25 ppbv	27 ppbv
1985[3]	30 ppbv	30 ppbv	30 ppbv	30 ppbv	30 ppbv
2035	34 ppbv	36 ppbv	36 ppbv	37 ppbv	34 ppbv
O_3 (0 km, high NO_x):					
1860	35 ppbv	31 ppbv	26 ppbv	23 ppbv	32 ppbv
1985	41 ppbv	41 ppbv	41 ppbv	41 ppbv	41 ppbv
2035	52 ppbv	57 ppbv	60 ppbv	63 ppbv	53 ppbv

---

[1] Models 1-5 are run at both high and low constant NO_x conditions; a scenario with NO_x driven by increasing NO emissions is run with Model 3.

[2] CH_4 flux: 4.4×10^{10} cm^{-2} s^{-1} (low NO_x); 1.31×10^{11} cm^{-2} s^{-1} (high NO_x).

[3] OH column, 0-15 km (1985): 5.4×10^{11} cm^{-2} (low NO_x); 1.15×10^{12} cm^{-2} (high NO_x).

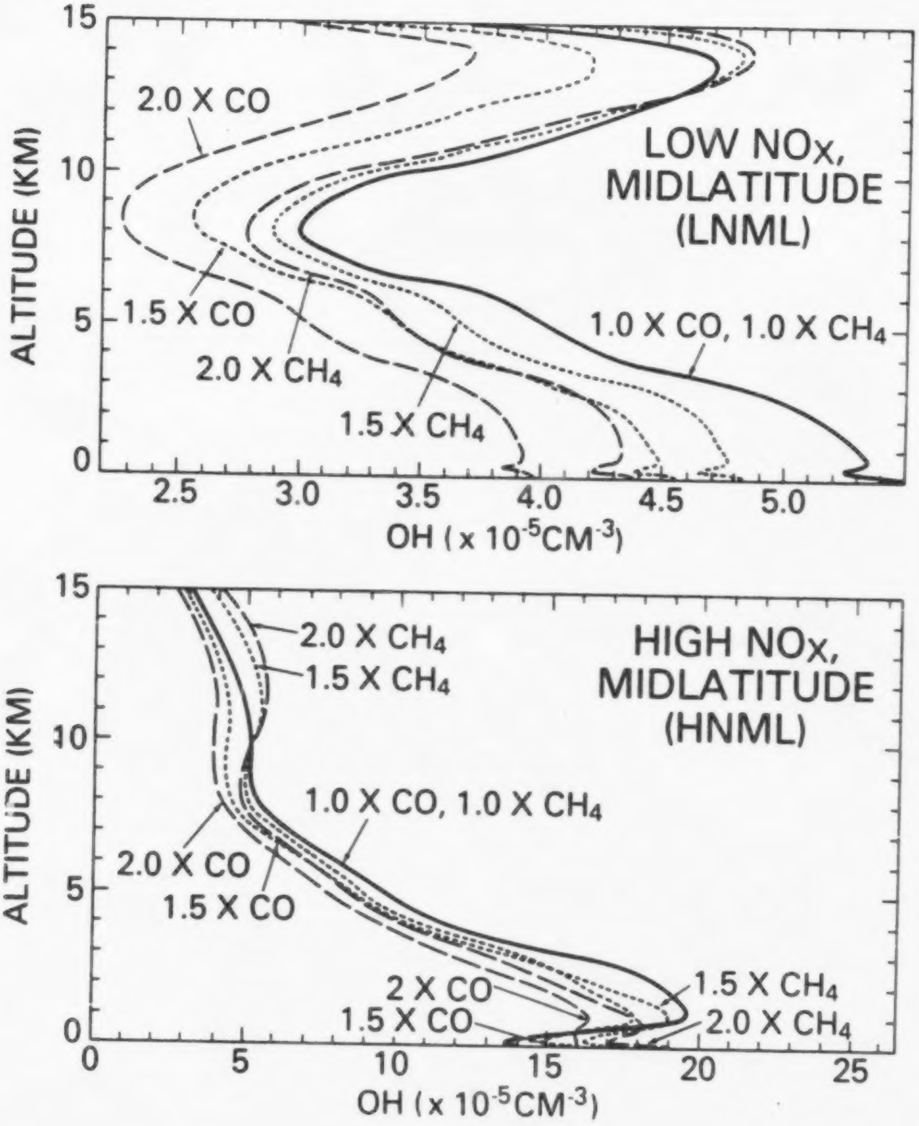

Fig. 1 OH profile (diurnally averaged) from LNML model. Solid line is for unperturbed CO and CH$_4$. Dotted and dashed lines are for perturbed CO or CH$_4$ with fractional increments beyond initial values (1.5 or 2.0) determined at the 0 km level.

EFFECT OF CO AND CH_4 PERTURBATIONS ON OH COLUMN DENSITY, 0-15 KM LOW NO_x (LNML) AND HIGH NO_x (HNML) MODELS

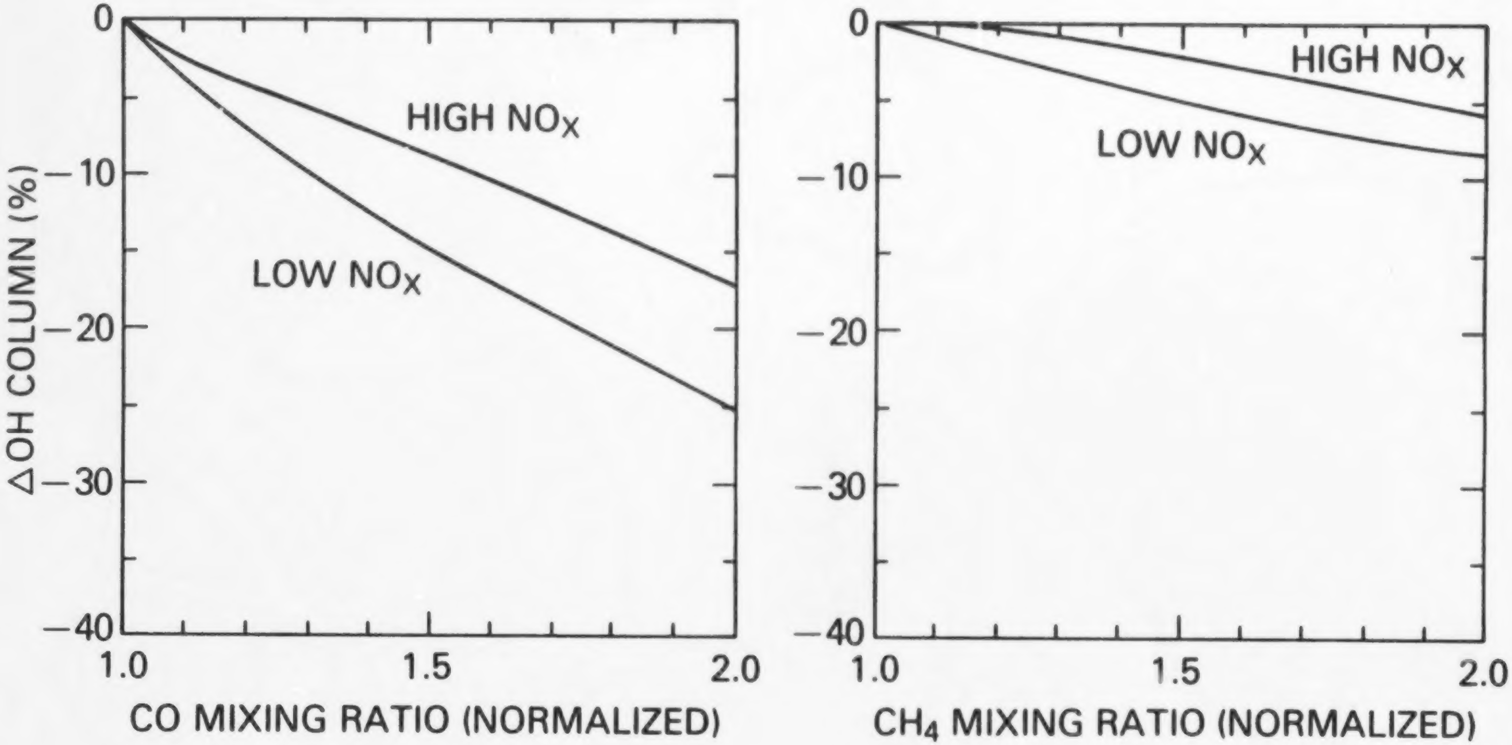

Fig. 2 Tropospheric OH (column-integrated, 0-15 km) as a function of perturbed (a) CO and (b) CH_4. Sensitivity to lower troposphere NO_x is shown: low NO_x model (LNML); high NO_x model (HNML). Identical initial and perturbed ground-level CO and CH_4 mixing ratios are assumed for both models. Reference levels, i.e. corresponding to mixing ratio 1.0, are 120 ppbv CO and 1.6 ppmv CH_4.

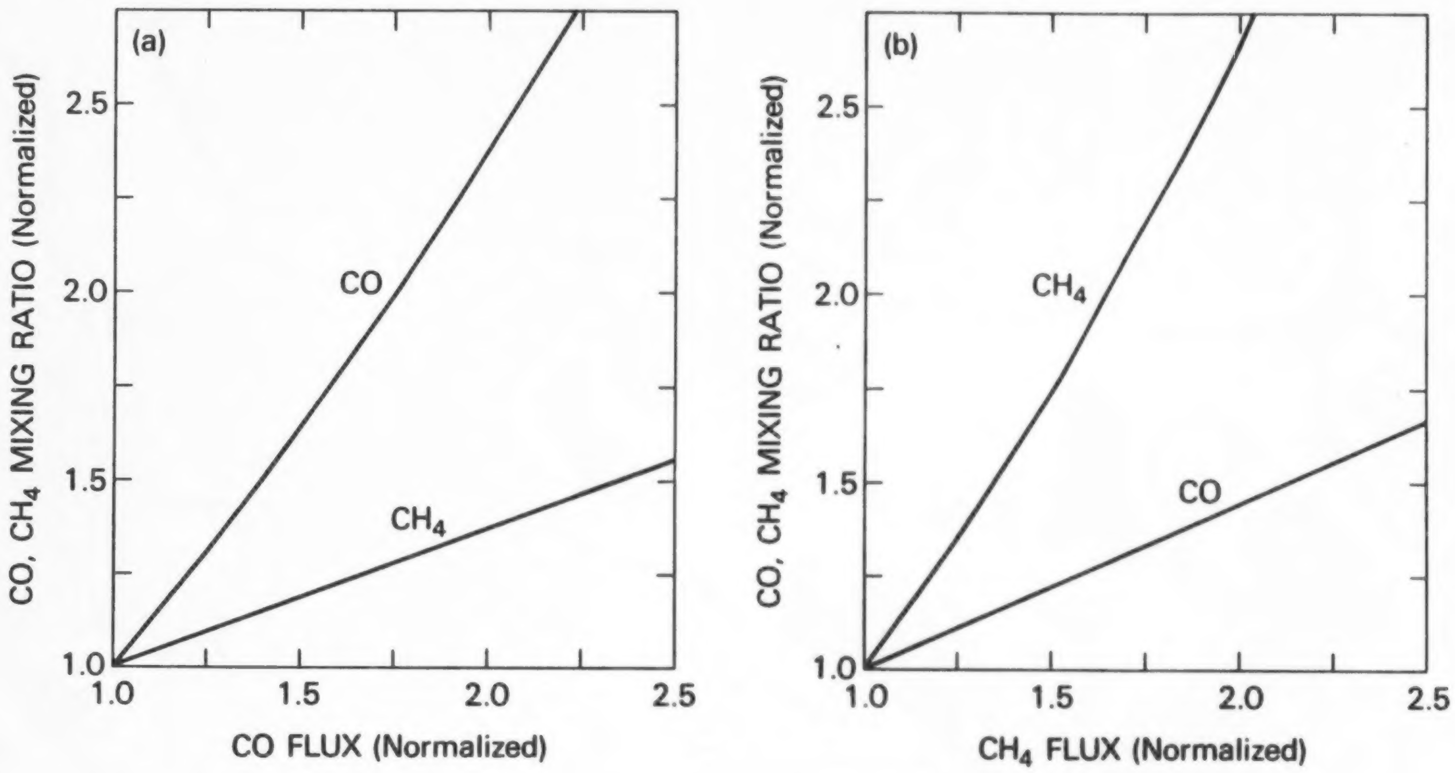

Fig. 3 Fractional increase in mixing ratio (0 km) vs fractional increase in surface flux. Results shown are from LNML model; LNLL and HNML models are similar. (a) specified CO flux varied (1.5-3.8 x 10^{11} cm^{-2} s^{-1}), CH$_4$ flux held constant at 4.4 x 10^{10} cm^{-2} s^{-1}; (b) specified CH$_4$ flux varied (4.4 -11 x 10^{10} cm^{-2} s^{-1}) CO flux held constant at 1.5 x 10^{11} cm^{-2} s^{-1}. Reference CO mixing ratio is 120 ppbv and CH$_4$ mixing ratio is 1.60 ppmv. Note that a given rate of increase for CO or CH$_4$ could be caused by an increased CO flux, by an increase in CH$_4$ sources or by a combination in which both CO and CH$_4$ are perturbed.

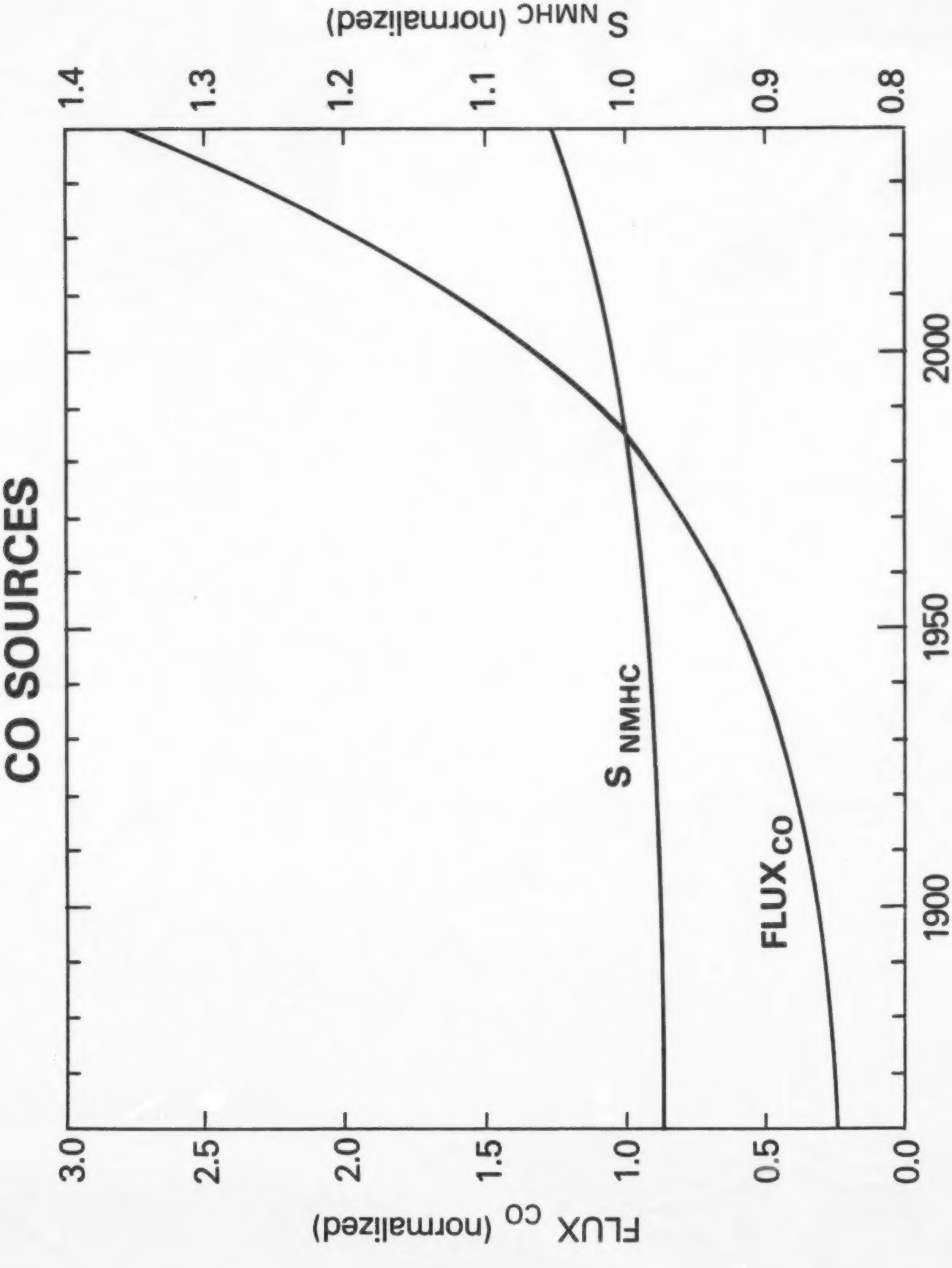
CO SOURCES
FLUX CO (normalized)
3.0
2.5
2.0
1.5
1.0
0.5
0.0
S NMHC (normalized)
1.4
1.3
1.2
1.1
1.0
0.9
0.8
1900
1950
2000
YEAR
S NMHC
FLUX CO

Fig. 4 CO source trends used in Model 1-4 scenarios normalized to 1985. $flux_{CO}$ changes sharply because of anthropogenic inputs, e.g. fossil fuel combustion, biomass burning, wood fuel burning. S_{NMHC} changes more slowly because only a small fraction of the in-situ airborne CO source is assumed to be derived from the oxidation of anthropogenic nonmethane hydrocarbons.

Paper 5

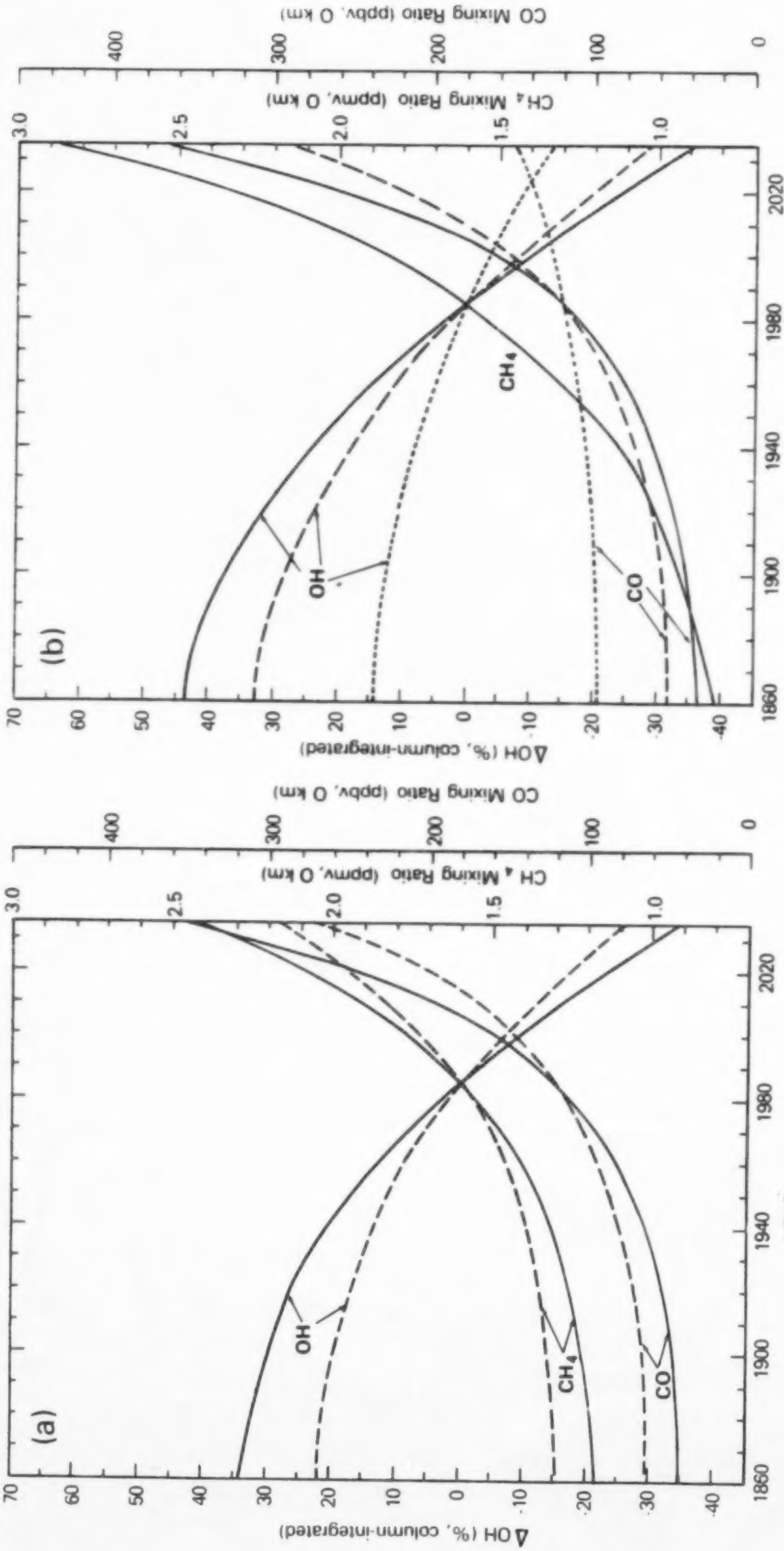
(a)
(b)
ΔOH (%, column-integrated)
70
60
50
40
30
20
10
0
-10
-20
-30
-40
YEAR
1860
1900
1940
1980
2020
CH4 Mixing Ratio (ppmv, 0 km)
3.0
2.5
2.0
1.5
1.0
CO Mixing Ratio (ppbv, 0 km)
400
300
200
100
0
OH
CH4
CO

Fig. 5 Ground level methane and CO mixing ratios and percent changes in column-integrated tropospheric OH from 1860 to 2035. Simulations were carried out with a steady-state model at 10-30 year intervals. Model conditions are appropriate for the midlatitude northern hemisphere with low background NO_x (20-25 pptv). Model calculations for low latitude conditions (higher photolysis rates, lower O_3 and CO mixing ratios) show trends of similar magnitude, implying that OH changes illustrated here are typical of nonpolluted environments. (a) Results from Models 1 and 2 (Table 5). Methane flux is constant at all times; calculated CH_4 increase is due to CO and OH changes. Dashed lines from model runs that set the largely anthropogenic CO upflux at 35% of the CO source in 1985; solid lines assume $flux_{CO}$(1985) produces 65% of present-day CO. Additional CO comes from CH_4 and C_2H_6 oxidation by OH and from an explicitly specified source S_{NMHC} that represents NMHC oxidation. $flux_{CO}$ and S_{NMHC} vary in time as shown in Figure 5. (b) Results from Models 3 (dashed lines), 4 (solid lines) and 5 (dotted lines). Fixed CH_4 mixing ratios follow [Khalil and Rasmussen, 1985; Stauffer et al, 1985]. Model 5 is based on constant CO fluxes and S_{NMHC} at all times.

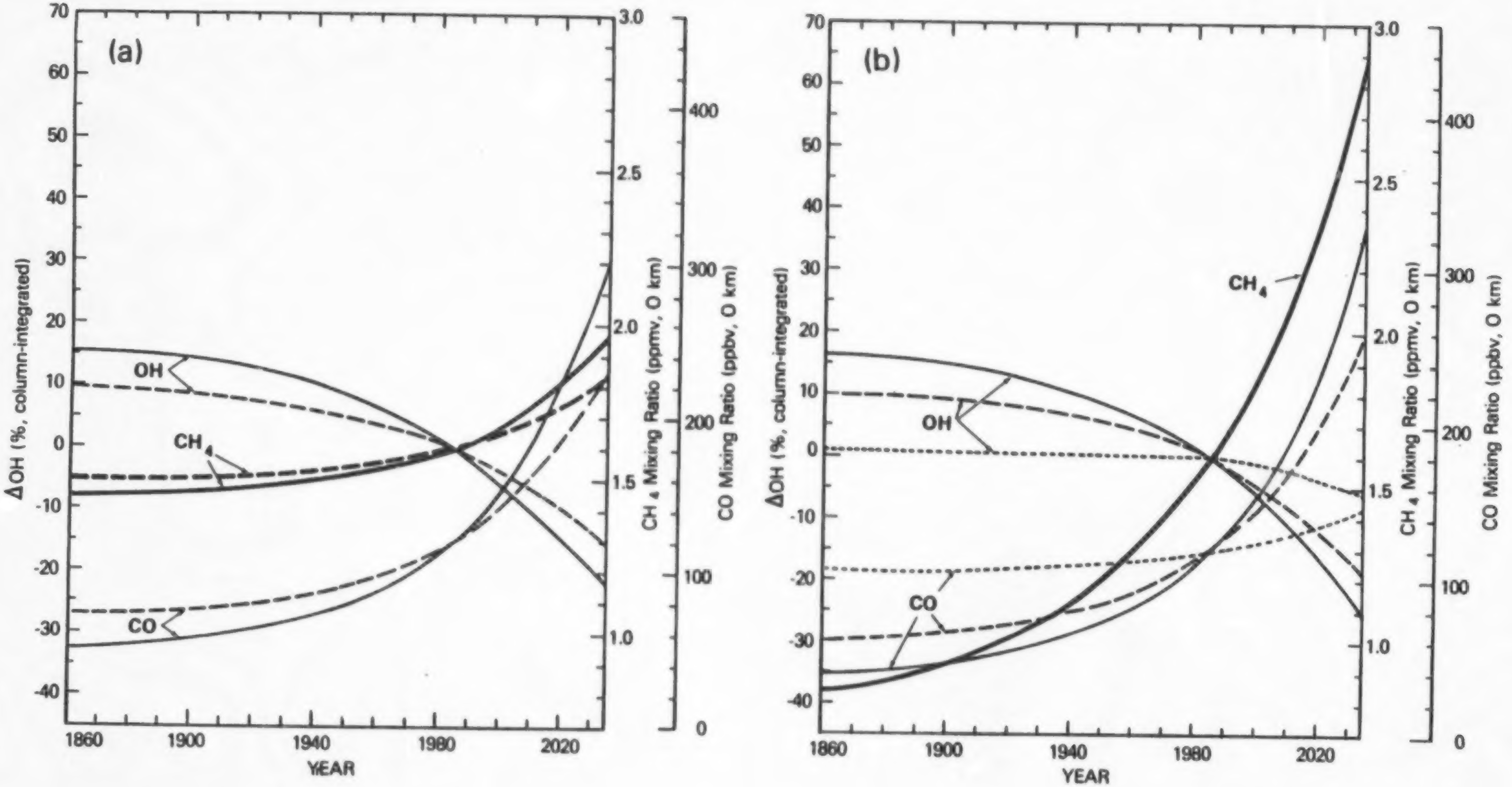

Fig. 6 Ground level methane and CO mixing ratios and percent changes in column-integrated tropospheric OH with background NO_x at 1 ppbv. (a) Results from Models 1 (dashed lines) and 2 (solid lines) as in Figure 5. (b) Results from Models 3, 4 and 5 as in Figure 5.

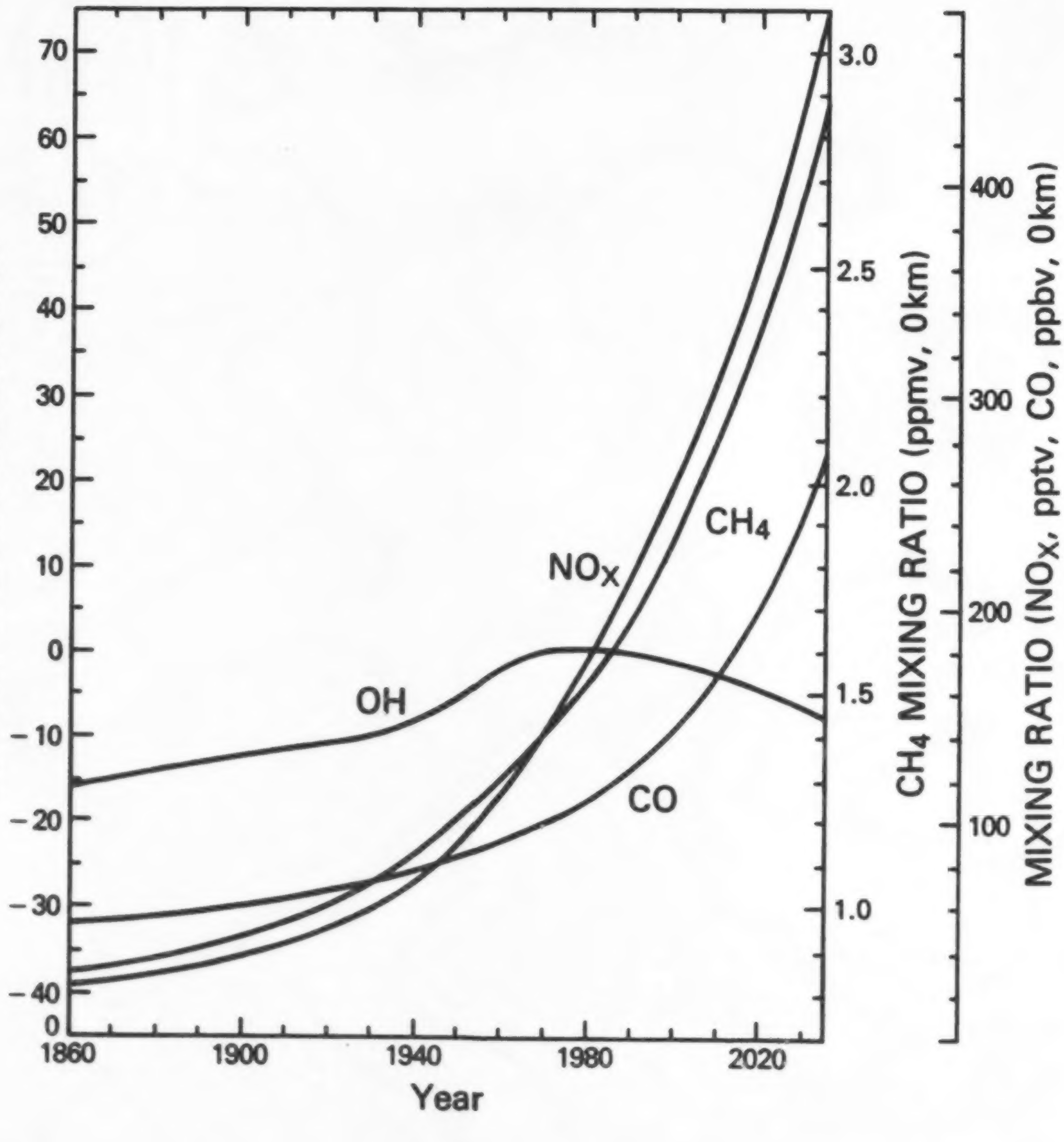

Fig. 7 Ground level CH_4, CO, and NO_x mixing ratios and percent change in tropospheric OH. Model 3 scenario is followed with NO_x increasing from a low (20 pptv in 1860) to moderate level (0.49 ppbv in 2035) in response to increasing NO emissions.

191

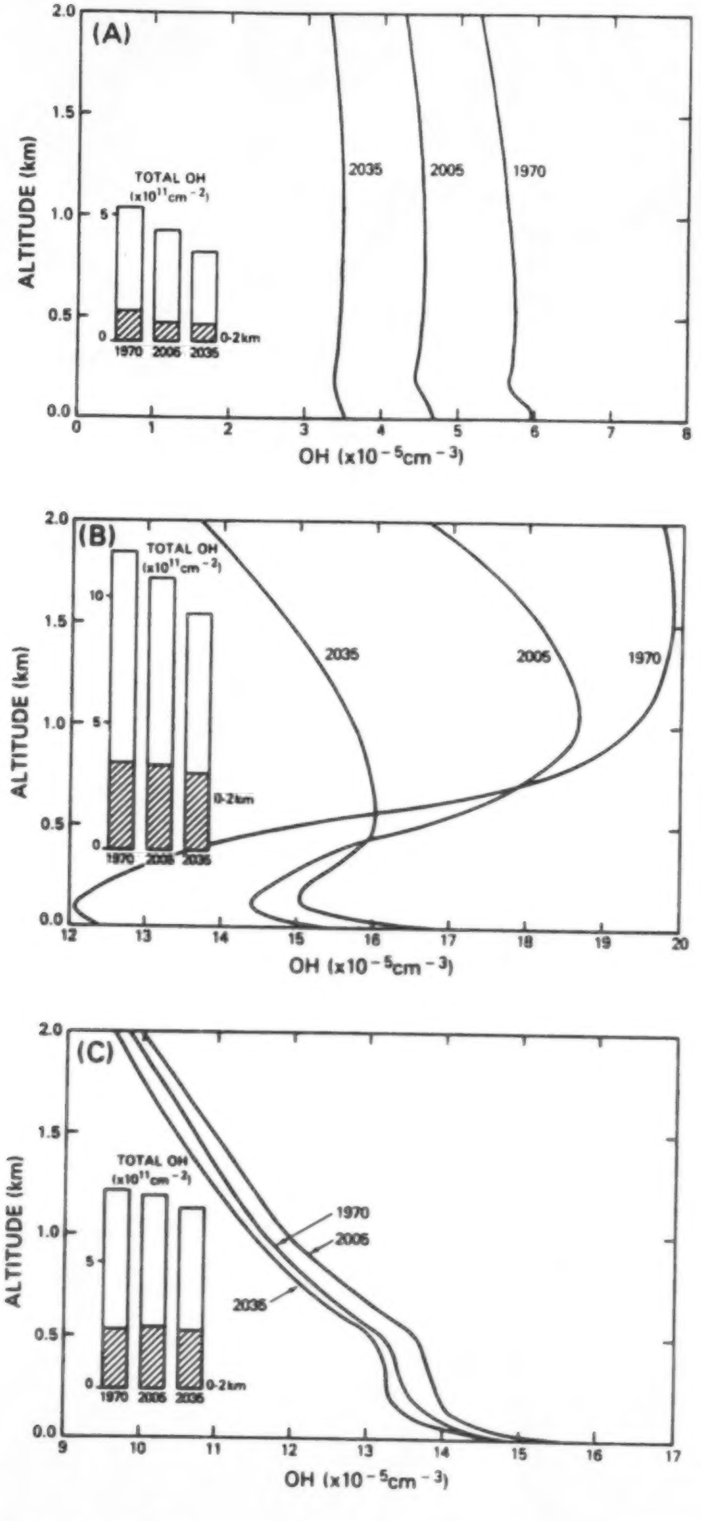

Fig. 8 OH profiles in the boundary layer (0-2 km) for years 1970, 2005, 2035 calculated with Model 3 scenario. Bar graphs give total OH column with shaded part showing the depth of OH from 0 to 2 km. (a) constant low NO_x case; (b) higher NO_x (1 ppbv) case; (c) "transitional region" NO_x.

Paper 6

Tropospheric Ozone

by

Jennifer Logan
Harvard University

This presentation was based upon the following published paper, which has been reproduced with permission of the American Geophysical Union. The author's consent has been obtained.

Tropospheric Ozone: Seasonal Behavior, Trends, and Anthropogenic Influence

by

Jennifer Logan

J. Logan, *Journal of Geophysical Research*, Vol. 90, No. D6, Pages 10,463-10,482, October 20, 1985, copyright by the American Geophysical Union.

NTIS is authorized to reproduce and sell this report. Permission for further reproduction must be obtained from the copyright owner.

Paper 6

JOURNAL OF GEOPHYSICAL RESEARCH, VOL. 90, NO. D6, PAGES 10,463–10,482, OCTOBER 20, 1985

Tropospheric Ozone: Seasonal Behavior, Trends, and Anthropogenic Influence

JENNIFER A. LOGAN

Center for Earth and Planetary Physics, Harvard University, Cambridge, Massachusetts

We present an analysis of data for tropospheric ozone with a focus on spatial and temporal variations. Surface ozone at mid-latitudes displays two modes of seasonal behavior: a broad summer maximum within a few hundred kilometers of populated and industrialized regions in Europe and the United States and a minimum in summer or autumn in sparsely populated regions remote from industrial activity–in Tasmania and Canada for example. The current data base for different regions, in combination with limited historical data, indicates that summertime concentrations of ozone near the surface in rural areas of Europe and the central and eastern United States may have increased by approximately 6–22 ppb (20%–100%) since the 1940's. The seasonal cycle of ozone in the middle troposphere over Europe, the United States, and northern Japan is very similar to that at the surface with a summer maximum, but it is quite different from that at 300 mbar, which is characterized by a maximum in spring. There is good evidence for an increase in ozone in the middle troposphere over Europe during the past 15 years and weaker evidence for a similar increase over North America and Japan. The increase in tropospheric ozone contributes significantly to the trend in the column of ozone and may compensate for 20%–30% of the decrease in ozone in the stratosphere over middle and high latitudes of the northern hemisphere. We argue that the summer maximum in ozone and the observed trends are due to photochemical production associated with anthropogenic emissions of NO_x, hydrocarbons, and CO from combustion of fossil fuels. A strong seasonal variation in ozone observed at Natal, Brazil (6°S), may also result from emissions of NO_x and hydrocarbons, in this case from agricultural burning. Maximum concentrations at Natal are similar to values found at mid-latitudes in summer. Tropical ozone exhibits strong spatial and temporal variability.

1. INTRODUCTION

Ozone plays an important role in controlling the chemical composition of the troposphere. Photolysis of ozone near 300 nm,

$$O_3 + h\nu \rightarrow O(^1D) + O_2 \qquad (1)$$

followed by reaction of the metastable $O(^1D)$ with water,

$$O(^1D) + H_2O \rightarrow OH + OH \qquad (2)$$

leads to producton of OH. A variety of atmospheric species, including CO, CH_4 [*Levy*, 1971], NO_2, and halocarbons are removed from the atmosphere by reaction with OH. Ozone by absorption of thermal radiation at 9.6 μM also plays an important role in the energy budget of the troposphere [*Ramanathan and Dickinson*, 1979; *Fishman et al.*, 1979*a*].

Ozone enters the troposphere from the stratosphere and is destroyed by heterogeneous reactions at the earth's surface [*Regener*, 1949; *Junge*, 1962; *Junge and Czeplak*, 1968; *Pruchniewicz*, 1973]. Ozone is also produced and destroyed within the troposphere by chemical reactions involving free radicals. It is formed during the oxidation of CO, CH_4, and hydrocarbons in the presence of nitrogen oxides and destroyed by reactions with HO_x radicals [*Chameides and Walker*, 1973; *Crutzen*, 1973].

There is a growing body of evidence to suggest that concentrations of ozone in the nonurban troposphere are influenced by human activity. Concentrations of ozone are larger at mid-latitudes in the northern hemisphere than at corresponding southern latitudes [*Pittock*, 1977]. *Fishman and Crutzen* [1978] proposed that the observed excess of ozone in the north may reflect significant photochemical production associated with sources of NO_x and CO from combustion of fossil fuels [see also *Fishman and Seiler*, 1983; *Crutzen and Gidel*, 1983]. Regional-scale pollution episodes, during which ozone concentrations may exceed 100 ppb for several days [e.g., *Cox et al.*, 1975; *Vukovich et al.*, 1977; *Wolff et al.*, 1977; *Guicherit and Van Dop*, 1977; *Wolff and Lioy*, 1980], indicate an extensive anthropogenic influence on ozone near the surface in both Europe and the United States. Measurements from a rural site on the Baltic coast suggest that surface ozone has increased by ~60% since the 1950's [*Warmbt*, 1979]. Concentrations of ozone in the middle troposphere over Europe and North America appear to have increased at a rate of ~1% per year from 1969 to 1981 [*Angell and Korshover*, 1983]. These trends could be due to increasing emissions of ozone precursors such as NO_x, hydrocarbons, and CO.

Increases in ozone are of concern, in part because of the important role ozone plays in controlling the chemical composition and climate of the troposphere and in part because of the deleterious effects of the gas on vegetation and human health. For example, changes in ozone could affect the concentration of OH, which in turn could influence concentrations of the many trace species removed from the atmosphere by reaction with OH. A doubling of tropospheric ozone could increase surface temperatures by 0.9°K, according to model results of *Fishman et al.* [1979*a*]. Ozone is thought to be responsible for most of the crop damage caused by air pollution in the United States. Recent field studies show that the yields of many crops decrease linearly, as ozone is increased, at a rate of 6%–8% per 10 ppb ozone [*Heck et al.*, 1982]. It has been known since 1956 that certain species of trees are susceptible to damage by oxidants, and there is concern at present that ozone may be contributing to the observed decline of forests in Europe and the eastern U.S. [*Skarby and Sellden*, 1984].

This study presents a quantitative assessment of the impact of human activities on the distribution of tropospheric ozone. The assessment relies on systematic measurements of surface ozone in combination with sonde measurements of the vertical distribution. Previous analyses of the sonde data have focused primarily on ozone in the stratosphere [*Dutsch*, 1974, 1978;

Copyright 1985 by the American Geophysical Union.

Paper number 5D0425.

NTIS is authorized to reproduce and sell this report. Permission for further reproduction must be obtained from the copyright owner.

London and Angell, 1982] or have considered the behavior of ozone at a single location [e.g., *Dutsch and Ling*, 1973; *Mattana et al.*, 1973; *DeMuer*, 1976; *Attmanspacher and Hartmannsgruber*, 1976; *Attmanspacher et al.*, 1984; *Pittock*, 1977; *Bojkov*, 1984]. The analysis presented here focuses attention on interesting features in the seasonal behavior of tropospheric ozone that were not apparent in earlier studies [e.g., *Chatfield and Harrison*, 1977*a*, *b*; *Fabian and Pruchniewicz*, 1977; *Fishman et al.*, 1979*b*]. Characterization of the seasonal behavior in different environments, in combination with long-term measurements available for only a few locations, permits useful estimates to be made for the change in ozone resulting from human activities.

Stratosphere-troposphere exchange is most effective during late winter and spring [*Danielsen*, 1968; *Danielsen and Mohnen*, 1977; *Mahlman and Moxim*, 1978], and the lifetime of ozone in the troposphere is only about 1 month. Thus one might expect concentrations of tropospheric ozone to be largest in spring in the absence of a significant photochemical influence on the distribution of the gas. Early measurements at a few sites did show a spring maximum in surface ozone, leading to the hypothesis that the stratosphere provides the dominant source of ozone to the troposphere [*Regener*, 1949; *Junge*, 1962]. More recent data presented here and elsewhere [*Oltmans*, 1981; I. E. Galbally, private communication, 1984] confirm that surface concentrations of ozone at remote locations such as northern Canada, Tasmania, and the Pacific Islands are highest in winter or spring, reflecting the influence of the stratospheric source [cf. *Levy et al.*, 1985]. By contrast, ozone concentrations remain high from spring into late summer at rural locations in Europe and the United States, regions where one might expect significant photochemical production of ozone associated with anthropogenic sources of NO_x, CO, and hydrocarbons. The broad summer maximum extends into the middle troposphere over these regions. Significant increases in ozone are found only in regions with a summer maximum. The data presented here provide evidence for a photochemical influence on large spatial scales.

We present a brief review of the chemistry of tropospheric ozone in section 2. The data analysis is described in section 3, and results are presented in section 4. Implications of these results are discussed in the concluding section.

2. CHEMISTRY OF OZONE IN THE TROPOSPHERE

Ozone is formed by

$$O(^3P) + O_2 + M \rightarrow O_3 + M \qquad (3)$$

and is removed by photolysis

$$h\nu + O_3 \rightarrow O(^1D) + O_2 \qquad (1')$$

$$h\nu + O_3 \rightarrow O(^3P) + O_2 \qquad (1'')$$

The metastable $O(^1D)$ is quenched by O_2 and N_2, though as shown above it can also react with H_2O (reaction (2)). Nitric oxide reacts with ozone to form NO_2

$$NO + O_3 \rightarrow NO_2 + O_2 \qquad (4)$$

with NO_2 removed by photolysis

$$NO_2 + h\nu \rightarrow O(^3P) + NO \qquad (5)$$

Ozone removed by (4) is reconstituted by (5) followed by (3). Because of the cyclic nature of the chemistry, it is convenient to define a family of species undergoing rapid reactions leading to formation or removal of ozone. We identify this family–odd oxygen–with O_3, $O(^1D)$, $O(^3P)$, and NO_2.

Odd oxygen is conserved in reactions (1), (3), (4), and (5). It is formed by reactions of NO with HO_2, CH_3O_2, and RO_2.

$$HO_2 + NO \rightarrow OH + NO_2 \qquad (6)$$

$$CH_3O_2 + NO \rightarrow CH_3O + NO_2 \qquad (7)$$

$$RO_2 + NO \rightarrow RO + NO_2 \qquad (8)$$

The species RO_2 represents a variety of complex organic peroxy radicals. These reactions occur during the photooxidation of CO, CH_4, and hydrocarbons, for example, by

$$OH + CO + O_2 \rightarrow HO_2 + CO_2$$

$$HO_2 + NO \rightarrow NO_2 + OH$$

$$NO_2 + h\nu \rightarrow NO + O$$

$$O + O_2 + M \rightarrow O_3 + M$$

$$\text{Net:} \quad CO + 2O_2 \rightarrow CO_2 + O_3$$

Odd oxygen is removed by reaction of $O(^1D)$ with H_2O, by reaction of O_3 with HO_2 and OH,

$$HO_2 + O_3 \rightarrow OH + 2O_2 \qquad (9)$$

$$OH + O_3 \rightarrow HO_2 + O_2 \qquad (10)$$

by formation of nitrates from NO_2,

$$OH + NO_2 + M \rightarrow HNO_3 + M \qquad (11)$$

and by heterogeneous reactions of O_3 and NO_2 at the earth's surface.

Oxidation of CO, CH_4, and hydrocarbons leads to net production of odd oxygen in the presence of adequate NO_x. The rate for production of ozone is roughly proportional to the concentration of NO, while the rate for loss is almost independent of NO_x ($NO + NO_2$) for concentrations below ~200 ppt [*Fishman et al.*, 1979*b*]. Loss of odd oxygen, primarily by (2) and (9), is balanced by production in (6) and (7) for concentrations of NO near 30 ppt [*Fishman et al.*, 1979*b*; *Logan et al.*, 1981]. Hence regions of the globe characterized by extremely low concentrations of NO, such as the remote Pacific, are likely to provide a net photochemical sink for odd oxygen [*Liu et al.*, 1983], while the continental boundary layer at mid-latitudes, characterized by higher concentrations of NO, is likely to provide a net source. Model studies indicate that, averaged over the globe, chemical sources and sinks for odd oxygen are in approximate balance and are similar in magnitude to the source from the stratosphere and the sink at the ground [*Fishman et al.*, 1979*b*; *Logan et al.*, 1981; *Chameides and Tan*, 1981].

Production of ozone in the troposphere is limited ultimately by supply of CO, CH_4, and hydrocarbons if NO_x is available. One molecule of ozone may be formed for each molecule of CO as shown above, while the yield of ozone from oxidation of CH_4 could be as large as 3.5 [e.g., *Logan et al.*, 1981]. The potential yield of ozone from higher hydrocarbons is larger still, 10–14 for butane and pentane [e.g., *Singh et al.*, 1981].

3. DATA AND ANALYSIS

3.1. *Surface Measurements of Ozone*

Most of the data for near-surface ozone discussed here were obtained with instruments employing one of three techniques: a chemiluminescent analyzer sensitive to light emitted by the reaction of ozone with ethylene, an optical device measuring the absorption of ultraviolet light by ozone, and a variety of wet-chemical sensors in which detection of ozone is based on

TABLE 1. Ozonesonde Data

	Latitude	Longitude	Number	Sonde	Correction Factor	Dates	Notes
				Northern Hemisphere			
Resolute[a]	75°	95°W	597	BM	1.21 ± 0.14 (2%)	January 1966 to November 1979	
			133	ECC	1.03 ± 0.09 (2%)	November 1979 to December 1982	Y
Poker Flat	65°	147°W	51	ECC	—	July 1979 to June 1982	S
Churchill	59°	94°W	282	BM	1.27 ± 0.28 (17%)	October 1973 to August 1979	
			235		1.24 ± 0.15		
			128	ECC	1.04 ± 0.10 (1%)	September 1979 to December 1982	Y
Edmonton	53°	114°W	355	BM	1.25 ± 0.24 (8%)	October 1972 to August 1979	
			327		1.22 ± 0.15 (0%)		
			150	ECC	1.05 ± 0.12 (3%)	August 1979 to December 1982	Y
Goose Bay	53°	60°W	532	BM	1.29 ± 0.22 (8%)	June 1969 to August 1980	
			491		1.26 ± 0.15 (0%)		
			111	ECC	1.04 ± 0.09 (1%)	August 1980 to December 1982	Y
Berlin	52°	13°E	358	B	1.32 ± 0.27 (6%)	November 1966 to January 1973	
			337		1.27 ± 0.14 (0%)		
Lindenberg	52°	14°E	574	GDR	1.26 ± 0.29 (16%)	January 1975 to December 1982	
			483		1.21 ± 0.18 (0%)		
Uccle[b]	51°	4°E	913	BM	1.33	January 1969 to December 1980	
Hohenpeissenberg	48°	11°E	1162	BM	1.09 ± 0.09 (1%)	November 1966 to December 1982	Y
Payerne	47°	7°E	1846	BM	1.24 ± 0.17 (4%)	August 1968 to December 1981	Y
			1769		1.22 ± 0.13 (0%)		
Biscarosse	44°	1°W	343	BM	1.19 ± 0.11 (1%)	March 1976 to December 1982	Y
Sapporo	43°	141°E	261	KC	1.04 ± 0.15 (7%)	December 1968 to December 1982	Y
			245		1.01 ± 0.11 (0%)		
Bedford[c]	42°	71°W	253	BM	—	January 1966 to May 1969	
Boulder[d]	40°	105°W	495	BM	1.16	August 1963 to July 1966	
Cagliari	39°	9°E	219	MB	1.24 ± 0.17 (5%)	July 1968 to August 1976	
			209		1.23 ± 0.14 (0%)		
Wallops Island	38°	76°W	457	ECC	1.00 ± 0.10 (1%)	May 1970 to April 1982	Y
Tateno	36°	140°E	262	KC	1.03 ± 0.15 (4%)	December 1968 to December 1982	Y
			253		1.02 ± 0.12 (0%)		
Palestine	32°	96°W	52	BM/ECC	—	October 1977 to June 1982	S
Kagoshima	32°	131°E	233	KC	0.99 ± 0.14 (1%)	December 1968 to December 1982	Y
Kennedy, Florida[c]	29°	81°W	147	BM	—	February 1966 to February 1969	
New Delhi	29°	77°E	99	I	1.42 ± 0.34 (28%)	January 1969 to December 1976	
			71		1.24 ± 0.17 (0%)		
Grand Turk[c]	21°	71°W	80	BM	—	March 1966 to May 1969	
Poona	19°	74°E	135	I	1.25 ± 0.30 (16%)	February 1966 to December 1975	
			113		1.16 ± 0.17 (0%)		
Ft. Sherman[c]	9°	80°W	43	BM	—	June 1967 to May 1969	
Trivandrum	8°	77°E	32	I	1.26 ± 0.26 (19%)	June 1969 to December 1976	
			26		1.20 ± 0.20 (0%)		
				Southern Hemisphere			
Natal	6°	35°W	40	ECC	—	August 1979 to January 1982	Y
Aspendale	38°	145°E	752	BM	1.23 ± 0.16 (2%)	June 1965 to April 1982	Y
Christchurch	43°	173°E	25	BM	—	March 1965 to December 1965	
Syowa	69°	39°E	135	KC	1.03 ± 0.14 (8%)	November 1969 to November 1980	

All data were obtained on computer tape from the World Ozone Data Center, unless otherwise indicated. The first and second columns give the latitude and longitude of the station. The third column gives the total number of ozone soundings with data in the troposphere during the period given in the sixth column. The fourth column gives the type of ozonesonde used: BM, conventional Brewer-Mast; ECC, electrochemical concentration cell, Kohmyr type; GDR, Brewer, type GDR: KC, carbon-iodine, a version of the electrochemical concentration cell; MB, modified Brewer; I, Brewer, type India. The fifth column gives the average value and the standard deviation of the correction factor (C.F.) at that station and, in parentheses, the percentage of soundings with correction factors outside the range 0.9–1.6 (BM type) and 0.7–1.3 (ECC type). Where two values are given for a particular sonde type at one station, the second value is the average C.F. calculated by excluding all soundings with C.F. outside 0.9–1.6 for BM-type sondes and outside 0.7–1.3 for ECC-type sondes (see text). Measurement programs known to be continuing are indicated by a Y in the seventh column. An S marks stations where measurements are made irregularly in support of other programs. Note that the table does not include a few stations that started operation after 1979.

[a] An estimate of the correction factor is given in Ozone Data for the World for soundings during the winter months when a Dobson measurement of the ozone column cannot be made.

[b] Data taken from *Bulletin Trimestrial* of the Royal Meteorological Institute of Belgium, provided by D. DeMuer.

[c] Data taken from *Chatfield and Harrison* [1977*b*].

[d] Data taken from *Dutsch* [1966].

its reaction with potassium iodide to form molecular iodine. The chemiluminescent and ultraviolet devices are not thought to suffer significantly from interference by other trace gases in nonurban air. The wet-chemical sensor is based on an oxidation reduction reaction that is not specific for ozone. Sulfur dioxide causes a negative interference of 1 mole of O_3 per mole of SO_2, while NO_2 gives a slight positive interference of a few percent [*Katz*, 1977; *Schenkel and Broder*, 1982]. Contamination by NO_2 should be unimportant at rural sites where concentrations of NO_x are 0.2–10 ppb [*Logan*, 1983]. Modern instruments based on the KI reaction employ a filter or scrubber to remove SO_2 from the air being sampled. A field comparison of a chemiluminescent device, an optical device, and three wet-chemical sensors was carried out at Hohenpeissenberg Observatory for 6 months [*Attmanspacher and Hartmansgruber*, 1982]. Results from the three types of instru-

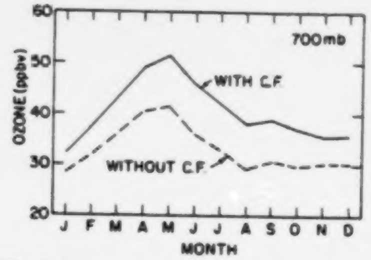

Fig. 1. The influence of seasonal variations in the correction factor on the seasonal distribution derived for ozone. The solid line is an average of monthly mean values for ozone at 700 mbar at Goose Bay, Edmonton, and Churchill, obtained with Brewer-Mast sondes. The dashed line is obtained if results for each sounding are divided by the correction factor before forming monthly means. Concentrations are about 20% lower, since the average correction factor for these stations is ~1.24, but the seasonal pattern is very similar.

ments agreed within about 10% (C. M. Elsworth and I. E. Galbally, unpublished manuscript, 1984).

3.2. *Ozonesonde Measurements*

The two types of ozonesonde in common use, the Brewer Mast (BM) bubbler [*Brewer and Milford*, 1960] and the electrochemical concentration cell (ECC) [*Kohmyr*, 1969; *Kohmyr and Harris*, 1971], are based on the reaction of ozone with KI. The sondes differ in the design of the electrochemical cell. Measurements with Regener sondes have been shown to underestimate concentrations of ozone by 20%–60% below 10 km [*Chatfield and Harrison*, 1977*a*; *Wilcox*, 1978; *Logan et al.*, 1981] and were not considered in this study. We discuss some of the difficulties associated with the electrochemical sondes and argue that the sonde data, with careful analysis, may provide useful information regarding spatial, seasonal, and temporal variations of ozone in the troposphere.

Sulfur dioxide is not removed from air sampled by ozonesondes. Sondes may tend to underestimate ozone in the boundary layer in polluted areas, particularly in winter, when ozone concentrations are lowest (~20–30 ppb) and SO_2 concentrations are highest. Concentrations of SO_2 at rural sites in the eastern United States, for example, are between 5 and 15 ppb in winter but below 5 ppb during other seasons [*Mueller and Hidy*, 1983]. Similar values are observed in southern Germany [*Reiter and Kanter*, 1982]. Concentrations of SO_2 above the boundary layer are generally below 1 ppb [*Blumenthal et al.*, 1981; *Georgii and Meixner*, 1980].

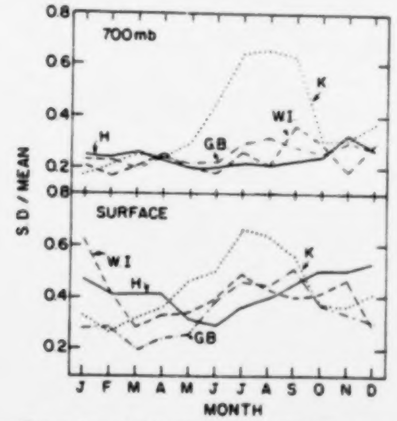

Fig. 2. The ratio of the standard deviation of ozone to the monthly mean concentration of ozone (coefficient of variation) versus season. Results are shown for Hohenpeissenberg (H), Wallops Island (W.I.), Goose Bay (G.B.), and Kagoshima (K) at the surface and at 700 mbar.

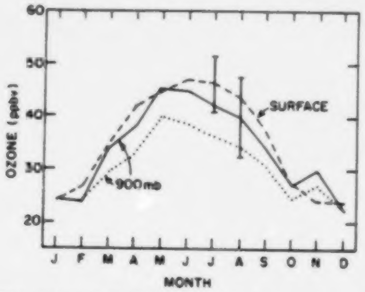

Fig. 3. The seasonal distribution of surface ozone at Hohenpeissenberg. The dashed line shows monthly averages of daily mean surface values, given in Ozone Data for the World (ODW). The dotted line shows monthly averages at 900 mbar (i.e., near surface) obtained from sonde measurements made at ~0800. The solid line shows the sonde data adjusted to daily mean values, using the diurnal behavior of surface ozone as a function of season at Hohenpeissenberg [*Attmanspacher and Hartmansgruber*, 1980]. All results are averages of monthly means for 1976 to 1983. The vertical lines show the year-to-year standard deviation of the monthly mean. The diurnally averaged results estimated from the sonde data are in reasonable agreement with continuous measurements at the surface.

The electrochemical technique does not provide an absolute measure of the ozone concentration. Preliminary studies using a standard ultraviolet photometer showed that concentrations of ozone were overestimated with ECC sondes by 3%–10%, while Brewer Mast sondes gave values too low by 4%–20%. The precision of the sondes in the troposphere was 5%–13% in field tests [*Hilsenrath et al.*, 1984; *Barnes et al.*, 1985]. Comparison of integrated ozone profiles recorded by Brewer Mast sondes with concurrent measurements of the ozone column recorded by a Dobson spectrophotometer indicates that the sonde results are too low by 10%–30% [e.g., *Dutsch*, 1966, see below]. Results from ECC sondes agree more closely with Dobson measurements, largely because the KI solution strength was originally adjusted to give this result [*Kohmyr*, 1969; *Geraci and Luers*, 1978; *Torres and Bandy*, 1978]. In practice, individual soundings are multiplied by a correction factor to ensure that the integrated ozone column is equal to the Dobson measurement of the ozone column. This procedure requires an estimate of the amount of ozone above the altitude reached by the sonde, ~30 km [*Dutsch et al.*, 1970]. The scaling procedure introduces errors caused by uncertainty in the ozone amount above 30 km, errors associated with the Dobson technique, and probably bias resulting from variation of sonde efficiency with altitude. There is evidence to suggest that the response of the sondes to ozone is altitude dependent [*Barnes et al.*, 1985]. Intercomparison flights have shown that ECC sondes give concentrations of tropospheric ozone higher than Brewer Mast sondes by 12%–20% after correction to the Dobson column. Systematic differences are less apparent in the stratosphere [*Attmanspacher and Dutsch*, 1970, 1981; *Hilsenrath et al.*, 1984]. Uncertainties in the response of the sondes to ozone at tropospheric pressures and concentrations should be resolved by further laboratory and field studies. We believe that conclusions presented below are not seriously affected by current uncertainties in absolute concentrations. Our focus is on the seasonal behavior of tropospheric ozone and on temporal changes derived from internally consistent data sets.

3.3. *Analysis of Sonde Data*

Ozonesonde data were obtained for the locations given in Table 1 from the Atmospheric Environment Service of Canada, which coordinates the World Ozone Data Center, and from published reports. These measurements provide the most coherent set of data for tropospheric ozone available at present. The majority of stations use conventional Brewer Mast sondes. The Canadian program changed from Brewer Mast to ECC sondes in ~1979; our analysis employs only BM data. Programs in India and the German Democratic Republic (GDR) use their own version of the Brewer Mast sonde; some difficulties were experienced with the operation of these devices at a recent field intercomparison [*Attmanspacher and Dutsch*, 1981]. The GDR sonde appears to overestimate tropospheric ozone by about 30%, based on comparison of results from Lindenberg and other European stations, as shown below in Figures 18–20. Wallops Island, U. S. A., and Natal, Brazil, employ identical ECC sondes, and their differential response to ozone (~15% compared to the Brewer Mast sonde) was discussed above. The program in Japan uses a version of the ECC sonde, which appeared in field tests to give results similar to the Brewer Mast sonde [*Attmanspacher and Dutsch*, 1981].

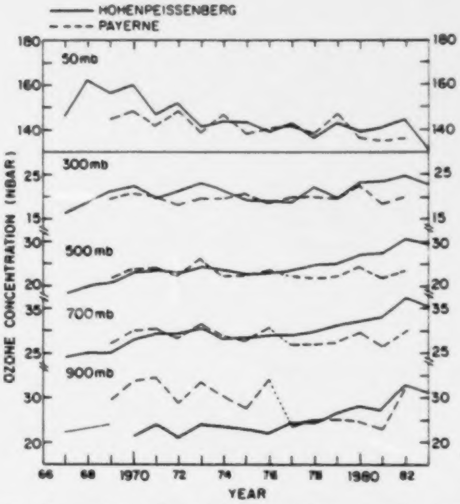

Fig. 5. Comparison of annual mean values of ozone (nbar) at Hohenpeissenberg (solid) and Payerne (dashed) at 900 mbar, 700 mbar, 500 mbar, 300 mbar, and 50 mbar. Measurements were made at ~1600 from 1969 to April 1977, at ~0930 from April 1977 to November 1980, at 1045 from November 1980 to December 1981, and at 1200 thereafter. Results for Hohenpeissenberg for 1967 to 1969 (faint solid line) were given for 850 mbar rather than 900 mbar in ODW.

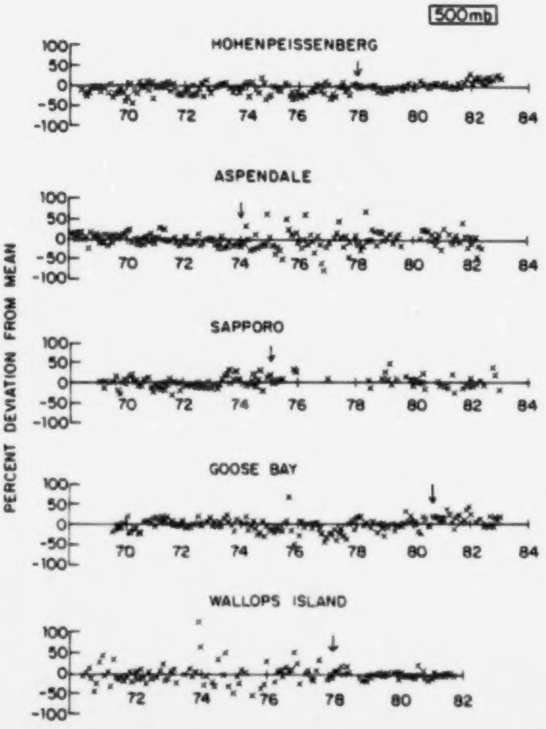

Fig. 4. Time series for ozone at 500 mbar. The seasonal cycle in ozone has been removed from the data as described in the text (see equation (12)); monthly residuals are shown as percent deviations from the monthly means. At Hohenpeissenberg the measurement frequency increased from weekly to three times a week in winter and two times a week in summer in 1978; at Aspendale the frequency decreased from weekly to biweekly in 1974; at Sapporo the frequency changed from weekly to, at most, biweekly in 1975; the influence of these changes on the variance of monthly mean values is evident. At Goose Bay, measurements were made with Brewer-Mast sondes until August 1980 and with ECC sondes thereafter; the latter give ~15% more ozone in the troposphere. At Wallops Island an instrument calibration program was instituted in 1978, and the variance in the data was reduced considerably.

The mean correction factor for each station and its standard deviation are given in Table 1. These factors are about 1.2–1.3(±0.1–0.3) for the Brewer Mast type of sonde and about 1.0(±0.1–0.15) for the ECC type of sonde. The magnitude and variability of the correction factor provide a good indication of the quality of the measurements. A recent World Meteorological Organization (WMO) report recommends that profiles with factors outside the range 0.8–1.4 should be considered unacceptable for BM soundings [*World Meteorological Association*, 1982, hereinafter referred to as WMO 82]. This recommendation is based on results from Hohenpeissenberg where the correction factor is 1.09(±0.09). The low correction factor at this station is attributed to careful preparation and conditioning of the sondes before use (WMO 82). We chose instead to omit from the analysis profiles with correction factors outside the range 0.9–1.6 for BM soundings,

TABLE 2. Ratio of Ozone Concentrations at Payerne and Hohenpeissenberg

Altitude	P/H (1970–1976)	P/H (1977–1980)	$\frac{\text{P/H (1977–1980)}}{\text{P/H (1970–1976)}}$
900 mbar	1.40 ± 0.14	0.96 ± 0.06	0.7
700 mbar	1.02 ± 0.04	0.91 ± 0.02	0.9
500 mbar	1.01 ± 0.04	0.90 ± 0.03	0.9
300 mbar	0.94 ± 0.08	0.99 ± 0.06	~1

At Hohenpeissenberg, ozone was measured at ~0800. At Payerne, ozone was measured at ~1600 from 1970 to April 1977 and at ~0930 from April 1977 to 1980. The second and third columns give the average ratio (and standard deviation) of the annual mean value at Payerne (P) to the annual mean value at Hohenpeissenberg (H) for 1970–1976 and 1977–1980, respectively. The fourth column gives the ratio of P/H for 1977–1980 to P/H for 1970–1976 and provides a measure of the systematic change in ozone concentrations caused by the change in the time of measurement at Payerne.

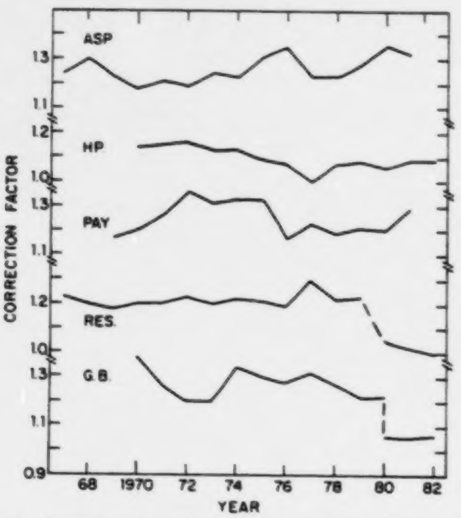

Fig. 6. Annual mean values of the correction factors at Aspendale, Hohenpeissenberg, Payerne, Resolute, and Goose Bay. Values given for Resolute after 1979 and Goose Bay after 1980 are for ECC sondes; all other values are for Brewer-Mast sondes.

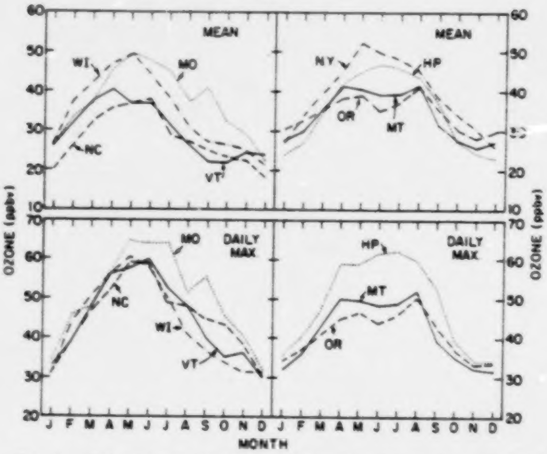

Fig. 8. The seasonal distribution of surface ozone at rural sites in the United States. The upper panels show daily average values; the lower panels show monthly means derived from daily maximum values. The left panels show results for sites in Vermont (VT), coastal North Carolina (NC), Wisconsin (WI), and Missouri (MO) for October 1978 to September 1982; these sites are all below 500-m elevation. The right panels show results for sites in Oregon (OR) and Montana (MT) for October 1979 to December 1983, for Whiteface Mountain (N.Y.) for 1973–1981 (V. Mohnen, private communication, 1984) and for Hohenpeissenberg, Germany (HP), for 1976–1983; these sites are all between 1000-m and 1500-m elevation. The first six sites are part of a rural ozone network maintained by the Environmental Protection Agency from 1976 until 1983 [*Evans et al.*, 1983; G. Evans, private communication, 1985).

since the average correction factor for other stations using these sondes is 1.26. There is a small seasonal variation in the correction factor [*Pittock*, 1977], and use of the WMO criterion would have eliminated many more measurements in summer than in other seasons. We omitted profiles with factors outside the range 0.7–1.3 for ECC soundings. Revised correction factors, after application of these acceptance criteria, are given in Table 1.

We examined the influence of the seasonal variation in the correction factor on the seasonal distribution derived for ozone. Correction factors tend to be highest in late summer and lowest between January and May but are not exactly in phase at each station. The peak-to-peak amplitude of the monthly mean correction factor is <10% at eight stations, 10%–15% at seven stations, and 16%–24% at three stations (Churchill, New Delhi, and Tateno). The peak-to-peak amplitude of the monthly mean ozone concentration in the middle troposphere is 35%–50% of the annual mean value. Consequently, the seasonal variation in the correction factor has little influence on the seasonal distribution of ozone derived from the data, as shown for example in Figure 1.

Monthly mean values and standard deviations were calculated for each station at standard pressure levels (1000 or 900,

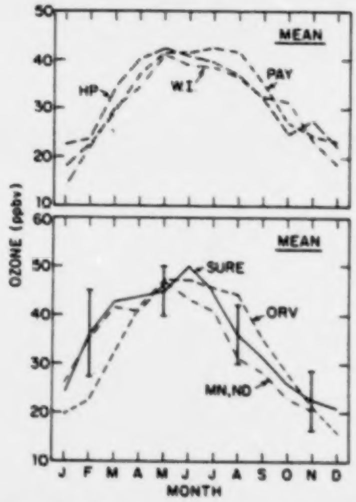

Fig. 7. The seasonal distribution of ozone near the ground at mid-latitudes. The upper panel shows ozonesonde results. Daily average values were derived for Hohenpeissenberg, (HP), 900 mbar as described for Figure 3. Results for Payerne, (PAY), 900 mbar are an average of sonde data at ~0930 and ~1600. Daily average values for Wallops Island (W.I.), 1000 mbar, were derived by using the diurnal variation of rural ozone in the eastern United States as given in *Evans et al.* [1983]. The lower panel shows results from continuous surface measurements at rural sites in the United States. Average values are shown for: two sites in Minnesota and one in North Dakota for 1977 to 1981 (MN, ND; *Pratt et al.* [1983]); nine sites in the northeast quadrant of the United States for August 1977 to July 1978 (SURE; *Mueller et al.* [1983]); and three sites in the Ohio River Valley for May 1980 to August 1981 (ORV; *Shaw and Paur* [1983]). The vertical lines show the standard deviations of the monthly means for the nine SURE sites.

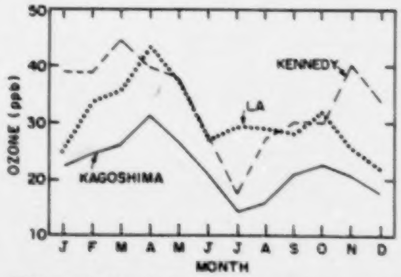

Fig. 9. The seasonal variation of surface ozone near 30°N. Diurnally averaged values are shown for a rural site in Louisiana (LA) (G. Evans, private communication, 1985). Ozonesonde results are shown for Kennedy, Florida, in the morning [*Chatfield and Harrison*, 1977*b*] and for Kagoshima, Japan, for midafternoon.

700, 500, 300, 200, and 150 mbar) for the entire period of observations, unless otherwise stated. The mean value in January, for example, is the arithmetic average of all values obtained in January of any year. Monthly mean values for stations in the North American Ozone Network [*Hering and Borden*, 1967] were taken from *Chatfield and Harrison*, [1977*b*], and results for Boulder are from *Dutsch* [1966]. The coefficient of variation is typically 0.15–0.35 at 500 mbar and 700 mbar and 0.2–0.6 near the ground [*Pittock*, 1977; *Chatfield and Harrison*, 1977*b*], as shown in Figure 2. There does not appear to be a significant seasonal variation in the coefficient of variation in the middle troposphere, except at the Japanese stations.

In section 4 the seasonal variation in tropospheric ozone obtained from sonde measurements is compared with results from ground-based instruments. We demonstrate the compatability of the two techniques with data from Hohenpeissenberg. There is a significant diurnal variation in surface ozone [e.g., *Decker et al.*, 1976; *Evans et al.*, 1983] that first must be taken into account. The diurnal variation of surface ozone at Hohenpeissenberg obtained from continuous measurements [*Attmanspacher and Hartmannsgruber*, 1980] was used to derive diurnal averages from sonde measurements made at 0700–0900. After adjustment to diurnal averages, the sonde data near the ground reproduced the long-term seasonal behavior of ozone derived from ground-based measurements, as shown in Figure 3. This comparison demonstrates that sonde instruments may provide reliable long-term average values for surface ozone and that results from the two techniques may be compared quantitatively with some confidence.

Data from sonde stations with records longer than 10 years were examined for trends. We caution that the quality of these data is rather uneven. The measurement frequency, procedure, time, and sonde type have changed at several stations. Figure 4 illustrates the influence of these changes on time series for ozone at 500 mbar. The seasonal cycle in ozone has been removed from the data by subtracting the average monthly mean value over the entire record from the given monthly mean y(month, year), e.g.,

$$z(\text{month, year}) = y(\text{month, year}) - \bar{y}(\text{month}) \qquad (12)$$

Here, $\bar{y}$(month) is the average of all the monthly means for the particular month: January, for example. Figure 4 shows time series of monthly residuals, z(month, year), expressed as percent deviations from the monthly means, $\bar{y}$(month). The top three panels demonstrate qualitatively that the variance in monthly mean values decreases as the measurement frequency increases. A measurement frequency of three times weekly appears preferable to weekly or biweekly measurements. Almost no measurements were made for 2 years at the Japanese stations and few measurements after 1978; these data are far from ideal for trend detection. Measurements at Goose Bay were made with BM sondes until August 1980 and with ECC sondes thereafter; a discontinuity is evident in the data record. There are, however, similar discontinuities in the data for which there is no apparent rationalization and which could, of course, be real. The data from Wallops Island show the dramatic reduction in data variances that resulted from implementation of a sonde calibration program in 1978.

We found that a change in the time of measurement at Payerne from midafternoon (when ozone near the ground is largest) to dawn (when it is smallest) influences concentrations above the boundary layer. Values for ozone near dawn at 700 mbar and 500 mbar appear to be about 10% smaller than those in the afternoon, based on comparison of results for Payerne and Hohenpeissenberg (see Figure 5 and Table 2). This need not imply a significant diurnal variation in ozone in the middle troposphere. The 10% difference could be an artifact introduced by the change in time of measurement, sonde preparation, etc.

Trends were calculated only for measurements made with a single instrument type, at the same time of day, to ensure that each data set is internally consistent. The seasonal cycle was removed from the time series by using equation (12), and the trend in the monthly residuals, z(month, year), was calculated by linear regression. Results are given in terms of percentage change in ozone per year, with 90% confidence intervals calculated by using the two-sided Students t test. Trends were calculated also for each season, using the series of residuals for the appropriate months, e.g., consecutive residuals for December, January, and February for winter. Sonde data have been scaled to the measured ozone column, and there is considerable variability in the correction factors, as shown in Table 1 and Figure 6. In order to remove any bias introduced by trends in either the ozone column or the correction factor, we repeated the analysis with the correction factor removed from each sounding. The trends in the correction factor and in the ozone column were calculated separately in the same manner as the trend in ozone.

4. RESULTS

4.1. *Ozone at Middle and High Latitudes*

4.1.1. *Ozone near the ground.* The seasonal variation of surface ozone at mid-latitudes of the United States and Europe follows a common pattern. Maximum concentrations occur between March and August, as shown in Figure 7. Results from sonde stations in central Europe and the eastern United States (upper panel) are rather similar to those from rural locations in the United States (lower panel) [*Mueller and Hidy*, 1983; *Shaw and Paur*, 1983; *Pratt et al.*, 1983]. Measurements from a network of rural sites in the United States are displayed in Figure 8, which includes a comparison with results from Germany. Average concentrations in spring and summer are between 30 and 50 ppb (upper panel), while daily maximum concentrations are between 45 and 65 ppb (lower panels). Sites within 100 km of major urban areas (St. Louis (MO) and Munich (HP) exhibit the largest maximum concentrations and the most prolonged summer maxima. Maximum values at sites in less populated and less industrial environments (upper Wisconsin (WI), Vermont (VT), and coastal North Carolina (NC) are lower than values near St. Louis by 5–10 ppb in spring and summer, while maximum values at two remote mountain locations (Montana (MT) and Oregon (OR)) are lower by 10–20 ppb.

The broad summer maximum extending through July or August is found over most of the U. S., from 35°N to 45°N (see Figures 7 and 8) [*Singh et al.*, 1978; *Viezee et al.*, 1982; *Chatfield and Harrison*, 1977*b*; *Mohnen et al.*, 1977; *Mueller and Hidy*, 1983; *Shaw and Paur*, 1983; *Pratt et al.*, 1983]. The same pattern is found in Ontario, Canada (42°–45°) [*Mukammal*, 1984]. In Europe the summer maximum extends to higher latitudes, from 39°N to 55°N [*Fabian and Pruchniewicz*, 1977; *Attmanspacher and Hartmansgruber*, 1980; *Reiter and Kantor*, 1982]. A different seasonal pattern is found at coastal locations near 30°N. Measurements from Florida [*Chatfield and Harrison*, 1977*b*] and Lousiana and preliminary data from Texas [*Viezee et al.*, 1982] show a summer minimum with maxima in spring and late autumn. This pattern is also found in Japan near 30°N (Figure 9).

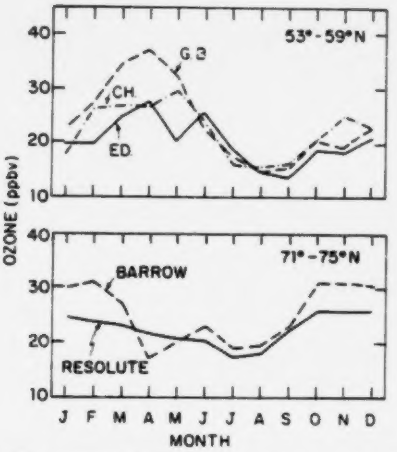

Fig. 10. The seasonal distribution of surface ozone at rural sites in Canada and Alaska. The upper panel shows Brewer-Mast sonde results from Goose Bay (G.B.), Edmonton (ED) and Churchill (CH), while the lower panel shows results for Resolute. All sonde measurements were made near dawn. The lower panel also shows daily average surface data from Barrow, Alaska [*Oltmans*, 1981]; the diurnal variation in ozone at this site is less than 1 ppb.

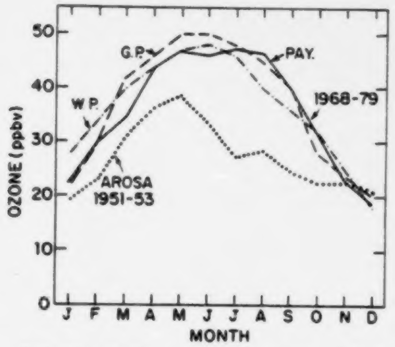

Fig. 12. Seasonal behavior of ozone at mountain locations in Europe. Monthly average values derived from daily maxima are shown for Arosa, Switzerland, 1860 m, for 1951–1953 [*Junge*, 1962] and for Garmisch-Partenkirchen, 740 m (G.P.), and nearby Wank Peak, 1780 m (W.P.), for 1977–1979 [*Reiter and Kantor*, 1982]. Sonde data at 900 mbar for 1968–1976 are given for Payerne, near Arosa (PAY). These measurements were taken at ~1600 hours and should represent daily maxima. The seasonal variation of the correction factor was subtracted out of the Payerne data by dividing results for each sounding by the correction factor before forming monthly means and then multiplying the monthly means by the annual mean correction factor.

The seasonal cycle of ozone near the ground in Canada (53°–59°N) is rather different from that at mid-latitudes in the United States and Europe. Concentrations are highest in spring, while minimum values are found between August and October (Figure 10) (R. Angle, private communication, 1985). Concentrations in summer are very similar at the three sonde stations located in western, central, and eastern Canada. A summer minimum is found also at higher latitudes, Resolute (75°N) and Barrow, Alaska (71°N) [*Oltmans*, 1981], but maximum values occur in winter rather than in spring.

Surface ozone in Canada (53°–59°N) is compared with that in the United States and Europe in Figure 11. The results for the United States and Europe are daily average values, while those for Canada are values measured near dawn. We used recent observations of the diurnal variation of ozone at two rural sites in Alberta to estimate daily average concentrations from the Canadian sonde data, as shown by the hatched area in Figure 11. In summer, daily average values exceed dawn values by ~11 ppb at Ellerslie, near Edmonton, and by ~6 ppb at a more remote site, Bitumount, 57°N (R. Angle, private communication, 1985). We note that daily average values exceed dawn values by ~12 ppb in the eastern United States and by 5–8 ppb in the western United States (G. Evans, private communication, 1985). The results in Figure 11 indicate that average concentrations of ozone in late spring and

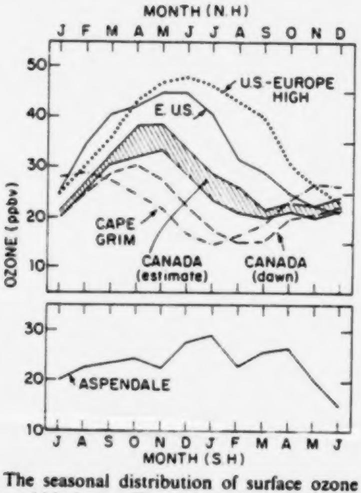

Fig. 11. The seasonal distribution of surface ozone at northern and southern mid-latitudes. The line labeled E. U.S. is an average of results for the nine SURE sites, the three sites in Minnesota and North Dakota, and the four EPA sites in Vermont, North Carolina, Wisconsin, and Missouri (see Figures 7 and 8), with each of the three data sets given equal weighting. Also shown is the average of results for the rural site in Missouri and for Hohenpeissenberg, Germany, the two sites shown in Figure 8 with largest concentrations of ozone (U.S.-Europe, high). These distributions represent daily average values. The results for Canada (dashed line) are an average of measurements from Goose Bay, Edmonton, and Churchill at dawn (Figure 10). The cross-hatched area shows the daily average values estimated from this distribution, using the diurnal variation of ozone at Ellerslie, near Edmonton and Bitumount, Alberta (R. Angle, private communication, 1985). Results for Cape Grim (41°S) represent daily average values (I. E. Galbally, private communications, 1984; C. M. Elsworth and I. E. Galbally, unpublished manuscript, 1984), while results for Aspendale (38°S) are sonde measurements at 1000 mbar made in early afternoon. Measurements from the southern hemisphere are shown 6 months out of phase with respect to the northern hemisphere.

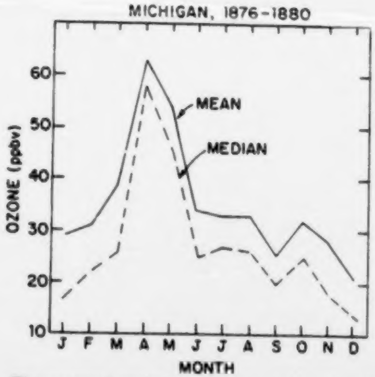

Fig. 13. The seasonal variation of ozone at Lansing, Michigan, in 1876–1880. These results were derived from daily measurements at 0700–1400 made with Schoenbein's test paper (see text) and were taken from *Linvill et al.* [1980].

TABLE 3. Trend in Ozone Near the Ground

	Dates	Scaled to Column	Divided by Correction Factor	Trend in Correction Factor
Hohenpeissenberg	January 1970 to December 1982	2.6 ± 0.7	3.2 ± 0.7	
Sonde[a]	1971–1983	2.8 ± 1.0	—	—
Surface[b]	1971–1983	1.5 ± 0.9	—	—
Payerne	August 1968 to January 1977	(0.8 ± 1.4)	(0.6 ± 1.5)	NS
Resolute	January 1966 to August 1979	(0.1 ± 1.0)	(0.0 ± 1.0)	NS
Goose Bay	June 1969 to August 1980	−1.9 ± 1.1	(−1.1 ± 1.2)	−0.7 ± 0.3
Wallops Island	May 1970 to August 1981	(0.9 ± 1.2)	(0.9 ± 1.2)	NS
Sapporo[c]	January 1969 to December 1982	(1.5 ± 1.7)	(1.3 ± 1.7)	NS
Tateno	January 1969 to December 1982	2.7 ± 1.0	2.3 ± 1.0	0.5 ± 0.3
Kagoshima[d]	January 1969 to December 1982	(−0.5 ± 1.6)	(−0.7 ± 1.5)	NS
Aspendale	June 1965 to April 1982	(0.2 ± 0.8)	(−0.2 ± 0.8)	0.6 ± 0.2

Trend values in this table represent percentage change per year. All trends were calculated from monthly residuals z(month, year) as described in section 3, unless otherwise indicated. Results are shown for 900 mbar for Payerne and Hohenpeissenberg and for ~1000 mbar for the other stations. The third column gives the trend (and 90% confidence intervals) calculated from near-surface ozonesonde measurements that have been scaled to the Dobson measurement of the ozone column. The fourth column gives the trend obtained if results for each sounding are divided by the correction factor for that sounding before forming monthly means. This procedure should remove artifacts introduced by trends in either the correction factor or the ozone column. The fifth column gives the trend in the correction factor. NS indicates that the trend is not statistically significant. Results for Resolute and Goose Bay include only measurements made with Brewer-Mast sondes.

[a] Trend calculated from annual values for ozone at 900 mbar (sonde results).

[b] Trend calculated from annual values for ozone obtained with surface instruments. Data for 1971–1975 were taken from *Attmanspacher and Hartmannsgruber* [1980]. Data for 1976–1983 were taken from Ozone Data for the World.

[c] Sapporo is a major city in northern Japan. Surface ozone concentrations given by the sonde measurements are lower than other mid-latitude stations, probably because of contamination by SO_2. Trends in SO_2 may therefore introduce an artifact in the trend estimated for ozone.

[d] There is a 2-year gap in the data record for Kagoshima, and concentrations after 1978 appear to be systematically smaller than those before 1976.

summer in the rural United States and Europe exceed those in remote regions of Canada by between 6 ppb and 22 ppb or by between 20% and 100%.

Figure 11 includes a comparison between surface ozone at mid-latitudes of the northern and southern hemispheres. Measurements from the clean air site at Cape Grim, Tasmania (41°S), show a summer minimum and winter maximum (I. Galbally, private communication, 1984) and little diurnal variation. Concentrations at Cape Grim in summer are about 20 ppb smaller than typical values in the United States and Europe. Ozone at Aspendale (38°S), 300 km north of Cape Grim, shows a late summer-autumn maximum and a winter minimum, with a much smaller seasonal amplitude than is found at northern mid-latitudes. It is known that ozone at Aspendale is influenced by proximity to the city of Melbourne [*Galbally*, 1971].

There appears to have been a significant change in the seasonal cycle of ozone in Europe over the past 30 years. Concentrations of ozone at Arosa, Switzerland (1780 m), were highest in May in the 1950's [*Junge*, 1962]. Recent measurements from nearby Payerne and from high-altitude stations in Germany [*Reiter and Kantor*, 1982] show the characteristic summer maximum in mid-latitude ozone (see Figure 12). Concentrations of ozone in July and August are now similar to those in May, implying an increase in summertime values in excess of 10 ppb. Data from East Germany provide further evidence for a change in the seasonal cycle of ozone. *Warmbt* [1979] observed increases in both summer and winter values for ozone at Arkona (54°N) on the Baltic coast. Ozone concentrations in summer increased from 18 ppb in 1956–1960 to 31 ppb in 1973–1977, while winter values increased from 11 ppb to 16 ppb. There is no indication of a further increase in ozone since 1977 [*Feister and Warmbt*, 1984].

Measurements of ozone from the 19th century appear to indicate a similar change in the seasonal cycle of ozone in the United States. Ozone was measured on a daily basis in Michigan from 1871 to 1903, using Schoenbein's test paper. The paper, impregnated with starch, changes color in response to the reaction of O_3 with potassium iodide. *Linvill et al.* [1980] calibrated the Schoenbein test results as a function of humidity by using a Dasibi ozone instrument and presented an analysis of the Michigan measurements from 1876 to 1880 in terms of parts per billion ozone (see Figure 13). The Schoenbein results are no doubt less reliable than data obtained with contemporary instrumentation, but the seasonal pattern may be reliable. It appears that ozone was significantly higher in spring than in summer in the 1870's in the midwestern United States, in contrast to results for the present day (compare Figures 7 and 8 with Figure 13).

We performed trend analyses on ozonesonde data near the ground, with results shown in Table 3. Sonde data suggest that ozone increased about 3% yr^{-1} from 1970 to 1982 at Hohenpeissenberg, Germany, while surface data suggest a smaller trend, ~1.5% yr^{-1}. Unfortunately, the sonde data may be contaminated by SO_2, as may surface results prior to 1976 when an SO_2 filter was installed [*Attmanspacher et al.*, 1984]. A negative trend in concentrations of SO_2 could mimic a positive trend in O_3. It appears that the sonde data may exaggerate the magnitude of the trend (Figure 14). Sonde data indicate that the trend is largest in summer, 1.1 ± 0.3 ppb yr^{-1} (Figure 15). Ozone did not change significantly from 1968 to 1977 at Payerne, Switzerland, on an annual basis, but summer values increased by 1.7(± 1.3) ppb yr^{-1}. The change in the time of measurement at Payerne in 1977 precludes accurate assessment of the trend over the entire record. Surface data from Wallops Island, U. S. A., suggest a slight increase in

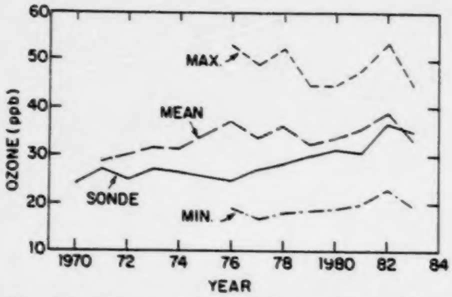

Fig. 14. Annual mean values of surface ozone at Hohenpeissenberg. The solid line shows sonde measurements at 900 mbar made at ~0800. The long dashed line (mean) shows daily average concentrations of ozone measured with surface instruments. Results were taken from *Attmanspacher and Hartmannsgruber* [1980] for 1971–1975 and from Ozone Data for the World for 1976–1983. Annual means of monthly daily maxima (max) and minima (min) are also shown.

ozone during the 1970s', but the trend is not statistically significant; neither is the decrease in ozone at Goose Bay, Canada, once the bias introduced by the trend in the correction factor is removed. It is noteworthy that increases in ozone are found only at stations that show a prolonged summer maximum in the seasonal distribution.

There is no significant trend in ozone at locations that exhibit a summer minimum: Resolute and Goose Bay in Canada (see Table 3); Barrow, Alaska; and the Pacific islands of Hawaii and Samoa [*Oltmans*, 1981, 1984].

4.1.2. *Ozone in the middle troposphere.* The seasonal variation of tropospheric ozone at middle and high latitudes of the northern hemisphere is shown in Figure 16. Results for stations in Europe, the United States, and Japan at latitudes 38°–42° and 43°–48° are shown as composite profiles, as are results for Canada at 53°–59°. The variance of monthly mean values between stations in each group is similar to the variance in the monthly mean at an individual station.

A broad summer maximum is found at 700 mbar over Europe, the United States, and northern Japan, while a late spring maximum is found over Canada. The patterns are similar to those observed at ground level. The seasonal maximum extends from April to August at 48°–53° in Europe but occurs between March and June at 53° in Canada, indicating a longitudinal gradient in ozone at these latitudes. Ozone concentrations in summer over the United States and Europe appear to exceed those over Canada by 5–15 ppb, or between 10% and 40%. The difference in the seasonal cycle of ozone over the two regions is less pronounced at 500 mbar than at 700 mbar.

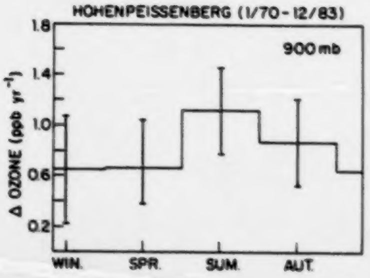

Fig. 15. Trend in ozone in each season at 900 mbar at Hohenpeissenberg (January 1970 to December 1983) derived from ozonesonde data. The horizontal bars give the trend in parts per billion per year, and the vertical bars give the 90% confidence interval for the trend.

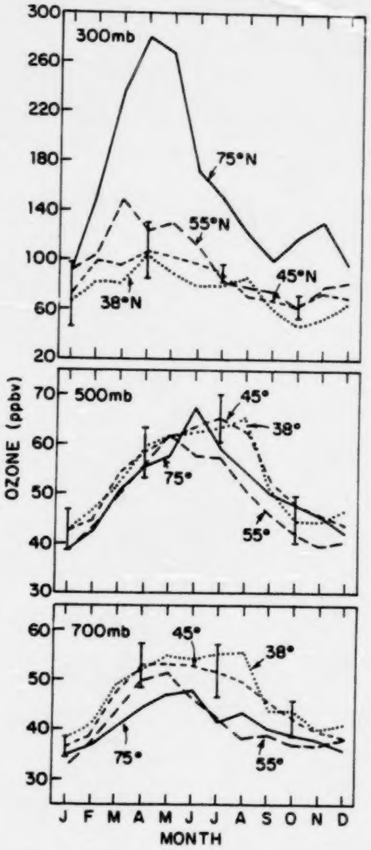

Fig. 16. The seasonal distribution of tropospheric ozone at middle and high latitudes. The solid line (75°) shows results for Resolute; the long dashed line (55°) is an average of monthly mean values for Goose Bay, Edmonton, and Churchill; the short dashed line (45°) is an average for Bedford, Sapporo, Biscarosse, Payerne, and Hohenpeissenberg, and the vertical bars show the standard deviation of the five mean values; the dotted line (38°) is an average for Wallops Island, Cagliari, and Boulder. Results are shown for 300 mbar (upper), 500 mbar (center), and 700 mbar (lower).

Data from Florida and the Bahamas [*Chatfield and Harrison*, 1977*b*] indicate that the summer maximum in ozone at 500 mbar extends as far south as 21°N in the western hemisphere. The summer maximum is not found at lower latitudes over Japan, as shown in Figure 17. Ozone decreases dramatically in early summer over Kagoshima (32°N), and results for Tateno at 36° also indicate the onset of a summer decrease. The decrease appears to be related to seasonal changes in circulation, as discussed below.

Maximum concentrations of ozone occur between March and May at 300 mbar, earlier than in the middle troposphere (Figure 16). The seasonal pattern in the upper troposphere resembles that for ozone in the lower stratosphere. Ozone at 300 mbar shows a steep gradient with latitude which also resembles that for stratospheric ozone, with largest concentrations at high latitudes. This may reflect, in part, the frequency of sampling stratospheric air at 300 mbar, which increases at higher latitudes [*Reiter*, 1975].

The distribution of ozone with latitude in the middle troposphere is very different from that in the upper troposphere–

4

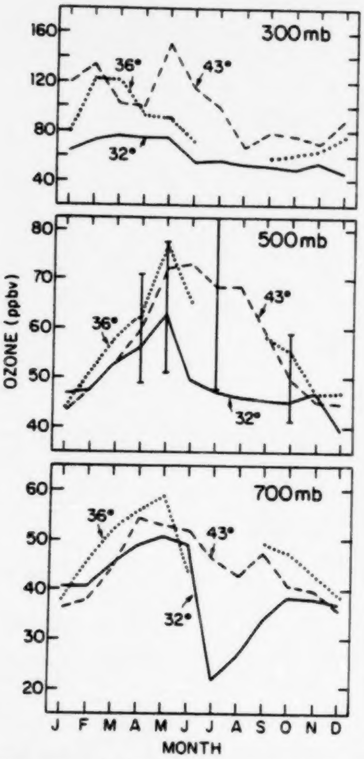

Fig. 17. The seasonal distribution of tropospheric ozone over Japan. Results are shown for Sapporo (43°), Tateno (36°), and Kagoshima (32°). Almost no measurements were made in July and August at Tateno.

lower stratosphere region. Largest concentrations are found at mid-latitudes in the northern hemisphere, between 30° and 50°, as shown in Figures 18–20. The mid-latitude maximum is present in all seasons at 700 mbar, but only in spring and summer at 500 mbar. Figures 18 and 19 give mean concentrations of ozone at sonde stations in January, April, July, and October at 700 mbar and 500 mbar, with supplementary results for August in Figure 20. The solid line indicates a 5° moving average for 20°N to 60°N, while the dashed lines show snapshots of the latitudinal distribution obtained by aircraft sampling.

There is little evidence for a latitudinal gradient in ozone at middle and high latitudes of the southern hemisphere, except in summer (January), but the data are very sparse. Interhemispheric differences at mid-latitudes are shown more clearly in Figure 21. The amplitude of the seasonal cycle in the middle troposphere at 38°S (Aspendale) is much smaller than that at 38°–40°N, as noted previously by *Pittock* [1977] and by *Fishman et al.* [1979*b*], and concentrations are largest in spring in the south in contrast to the broad summer maximum in the north. There is a significant hemispheric asymmetry in the seasonal cycle of ozone at high latitudes also (see Figure 22). Ozone at 700 mbar and 500 mbar is largest in winter and smallest in summer at Syowa (69°S), in agreement with earlier results from Antarctica [*Wisse and Meerburg*, 1969], while ozone is largest in late spring and early summer at Resolute (75°N). There is a summer minimum near the surface in both hemispheres.

Data from sonde stations indicate that tropospheric ozone may be increasing in the northern hemisphere. *Angell and Korshover* [1983] reported an average increase of ~12% from 1970 to 1981 at mid-latitudes; *Bojkov and Reinsel* [1984] reported similar results. We find that the evidence for an increase in ozone at 700–500 mbar is strongest for Europe (~2% yr^{-1} over Hohenpeissenberg, with somewhat smaller increases over Payerne and Uccle) as shown in Table 4. The trends calculated for North America (Wallops Island and Goose Bay) are positive, once the bias introduced by the trend in the correction factor is removed, but are not statistically significant. The trend derived for Wallops Island is significant, 0.9(± 0.6)% per year, only if outliers are first removed from the data record (see Table 4). Angell and Korshover found a larger trend over North America than over Europe. Their analysis included measurements with Brewer Mast and ECC sondes at the Canadian stations and from two times of day at Payerne. These changes in measurement strategy may have introduced inconsistencies in the data they analyzed, as discussed earlier.

Measurements from Resolute indicate that ozone in the middle troposphere is increasing at high northern latitudes also, by ~1% yr^{-1}. The trend is much larger in spring and summer (~1 ppb yr^{-1}) than in other seasons, as shown in Figure 23. There is less seasonal variability in the magnitude of the trend at mid-latitudes, as shown by results for Hohenpeissenberg.

The altitude dependence of the trend in ozone is quite different at locations with a summer maximum in ozone compared to those with a summer minimum. Hohenpeissenberg

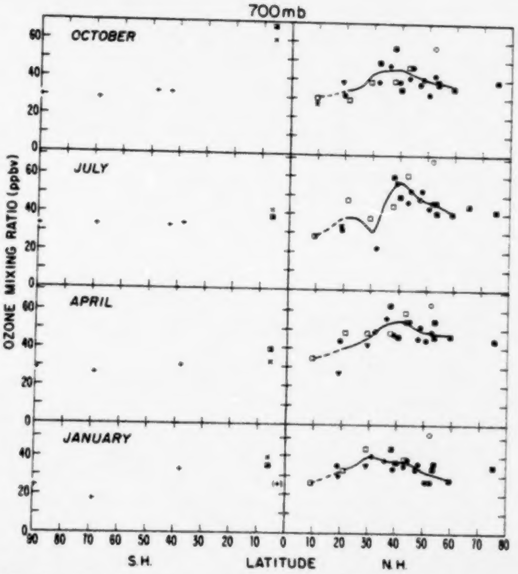

Fig. 18. The distribution of ozone with latitude at 700 mbar. The symbols show monthly mean concentrations for the stations listed in Table 1. The symbols are defined as follows: (solid squares) North America, BM sondes; (open squares) North American Ozonesonde Network, BM [*Chatfield and Harrison*, 1977]; (half-filled square) Americas, ECC; (solid circle) Europe; (open circle) Lindenberg; (triangle) India; (diamond) Japan; (hexagon) Hawaii [*Oltmans*, 1981]; (plus) Australia and the Antarctic, including surface data from the South Pole from *Oltmans* [1981]. Seasonal values are shown for tropical locations (crosses) if they are somewhat different from midseason values because of the small number of tropical measurements. The plus at 2°S shows ECC measurements made at Canton Island (four profiles) in December [*Kohmyr and Sticksel*, 1967]. The solid line is a 5° moving average of sonde results for 20°N to 60°N.

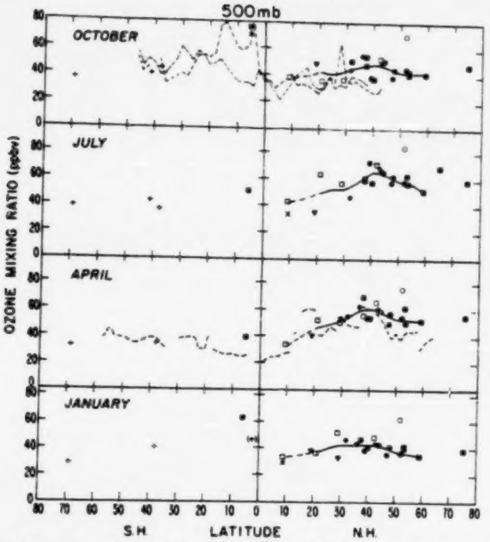

Fig. 19. The distribution of ozone with latitude at 500 mbar. Symbols are defined in Figure 18. The panel for April shows aircraft data from *Routhier et al.* [1980] for the central Pacific south of 40°N and for North America north of 40°N for April and May (dashed lines). The panel for October shows aircraft data from *Gregory et al.* [1984] for a flight from Wallops Island to the west coast of South America. Southbound data are given by the dot-dashed line, northbound data by the dashed line.

(summer maximum) shows the largest increase at the surface and smaller increases at 700 mbar and 500 mbar. Resolute (summer minimum) shows no trend at the surface but a significant increase at 700 mbar and 500 mbar (see Figure 24). Both locations show a switch over from a positive trend in the middle troposphere to a negative trend in the lower stratosphere. This is a feature common to trend results for all the stations in the northern hemisphere (see appendix). At Aspendale, the only sonde station at southern mid-latitudes, there is no significant trend in the middle troposphere, but there is a decrease in ozone in the lower stratosphere (see appendix).

The trend in tropospheric ozone contributes significantly to the trend in the integrated column of ozone. The increase in the troposphere at Hohenpeissenberg appears to compensate for at least 30% of the decrease observed in the stratosphere over the same period and may be of comparable magnitude to the decrease in the stratosphere. The increase in tropopheric ozone at Resolute is about 20% of the decrease in the stratosphere (see appendix).

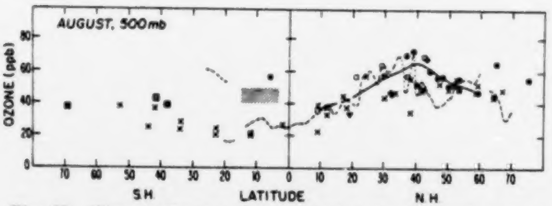

Fig. 20. The distribution of ozone with latitude at 500 mbar in August. Symbols are defined as in Figure 18, except that the sonde data in the southern hemisphere are shown as squares for clarity. The dashed line shows aircraft data of *Routhier et al.* [1980] for the route described in Figure 19. The crosses show the aircraft measurements of *Seiler and Fishman* [1981] taken over both coasts of North America and the west coast of South America. The cross-hatched area shows measurements over central Brazil [*Delany et al.*, 1985; *Crutzen et al.*, 1984].

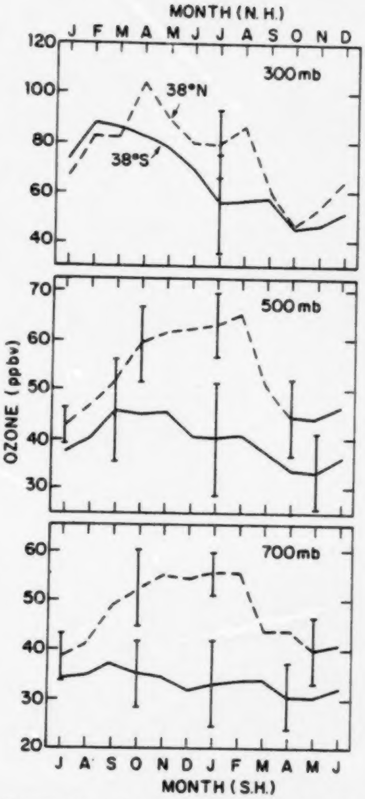

Fig. 21. Comparison of ozone at mid-latitudes of the northern and southern hemispheres. Results are shown for Aspendale, 38°S (solid), and for stations near 38°N (dashed; see Figure 16) for 300 mbar, 500 mbar, and 700 mbar. The vertical lines show the standard deviation of the monthly means.

4.2. *Ozone in the Tropics*

Recent measurements indicate that concentrations of ozone at Natal, Brazil, are much larger than at other tropical locations [*Kirchhoff et al.*, 1983; *Kirchhoff*, 1984]. Figure 25 displays annually averaged concentrations of ozone in the tropics and subtropics (upper panel). The difference between concentrations at Natal (6°S) and Panama (9°N), ~60%, is much too large to be ascribed to the differential response of the ECC and Brewer-Mast sondes to tropospheric ozone, which could account for a difference of about 15%. There is a significant seasonal variation in ozone at Natal, with values in September and October about a factor of 2 higher than in February to April (Figure 25, lower panel). Ozone at Panama shows little seasonal variation [*Chatfield and Harrison*, 1977*b*]. Maximum concentrations in the middle troposphere at Natal are as large as those found at mid-latitudes in summer (compare Figures 16 and 25), while minimum concentrations correspond to those found all year at Panama. The results for Natal in Figure 25 suggest that ozone mixing ratios are almost constant above 600 mbar, but this picture is somewhat misleading. Inspection of individual vertical profiles reveals that high levels of ozone are found in layers above the trade wind inversion, ~800 mbar, as shown in Figure 26. A more detailed analysis of these data and more recent measurements from Natal will be presented elsewhere (V. W. J. H. Kirchhoff and J. A. Logan, unpublished manuscript, 1985). Surface data from Sa Da Bandeira, Angola (15°S), display the same seasonal behavior as ozone at Natal, with a September

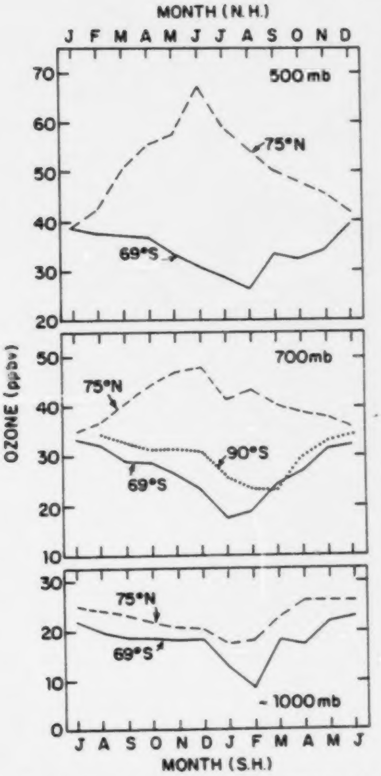

Fig. 22. Comparison of ozone at high latitudes of the northern and southern hemispheres. Results are shown for Syowa (69°S, solid) and Resolute (75°N, dashed) for 500 mbar, 700 mbar, and ~1000 mbar. Surface measurements at the South Pole (90°S, dotted; *Oltmans* [1981]) are also included.

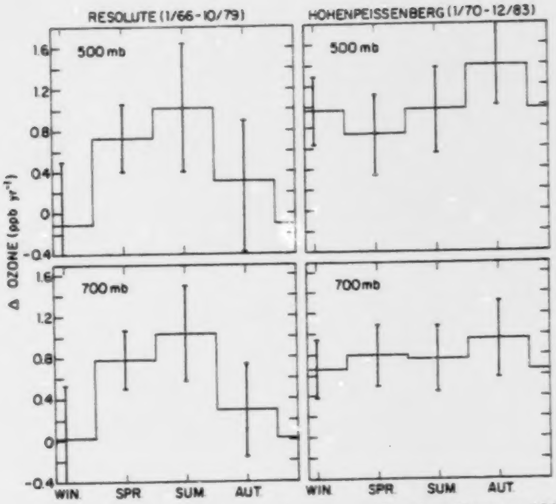

Fig. 23. Trend in ozone in each season at Resolute (January 1966 to October 1979) and Hohenpeissenberg (January 1970 to December 1983) at 700 mbar and 500 mbar. The horizontal bars give the trend in parts per billion per year, and the vertical bars give the 90% confidence interval for the trend.

maximum [*Fabian and Pruchniewicz*, 1977], while ozone at Samoa (14°S) is largest in July and August [*Oltmans*, 1981].

The sonde results suggest significant spatial and temporal inhomogeneities in ozone in the tropics. Recent aircraft measurements, shown in Figures 19 and 20, provide further evidence for inhomogeneities, particularly in the southern tropics. *Routhier et al.* [1980] found concentrations of about 20–30 ppb at 500 mbar over the Pacific Ocean in May and August, while *Seiler and Fishman* [1981] reported similar values for the west coast of South America in August. These

TABLE 4. Trend in Tropospheric Ozone

	Dates	Scaled to Column	Divided by Correction Factor	Trend in Correction Factor
	700 mbar, 500 mbar			
Hohenpeissenberg	January 1969 to December 1982	1.9 ± 0.3	2.2 ± 0.3	−0.4 ± 0.2
Payerne	August 1968 to January 1977	0.9 ± 0.7	(0.7 ± 0.8)	NS
Uccle	January 1969 to December 1980	1.1 ± 0.7[a]	—	—
	January 1969 to March 1981	1.7 ± 0.7[b]	—	—
Resolute	January 1966 to August 1979	1.2 ± 0.5	1.1 ± 0.5	NS
Goose Bay	June 1969 to August 1980	(−0.2 ± 0.7)	(0.5 ± 0.7)	−0.7 ± 0.3
Wallops Island[c]	May 1970 to August 1981	(0.6 ± 0.8)	(0.4 ± 0.9)	NS
Sapporo	January 1969 to December 1982	0.7 ± 0.5	(0.5 ± 0.5)	NS
Tateno	January 1969 to December 1982	0.7 ± 0.5	(0.3 ± 0.5)	0.5 ± 0.3
Kagoshima	January 1969 to December 1982	1.5 ± 1.0	1.5 ± 1.1	NS
Aspendale	June 1965 to April 1982	(0.4 ± 0.5)	(−0.4 ± 0.4)	0.6 ± 0.2
	300 mbar			
Hohenpeissenberg	January 1969 to December 1982	0.8 ± 0.8	1.0 ± 0.8	−0.4 ± 0.2
Goose Bay	June 1969 to August 1980	−4.6 ± 1.7	−3.8 ± 1.7	−0.7 ± 0.3
Kagoshima	January 1969 to December 1982	(1.3 ± 1.3)	(1.4 ± 1.4)	NS

Trends are given as the percentage change per year and are presented in the same format as Table 2. Trends were calculated from monthly residuals z(month, year), as described in section 3. Concentrations at 700 mbar and 500 mbar were averaged before forming monthly means. Results are given for 300 mbar only if statistically significant.

[a] Trend derived from data provided in tabular form by D. DeMuer. Monthly mean values were calculated for soundings with correction factors between 0.8 and 1.4, omitting those flagged as being contaminated in the troposphere.

[b] Trend derived from monthly mean values provided by J. London.

[c] The calculated trend is 0.7 ± 0.6 (scaled to the ozone column) and 0.9 ± 0.6 (divided by C.F.) if ozone values more than 2 standard deviations from the monthly mean are removed from the data set prior to analysis.

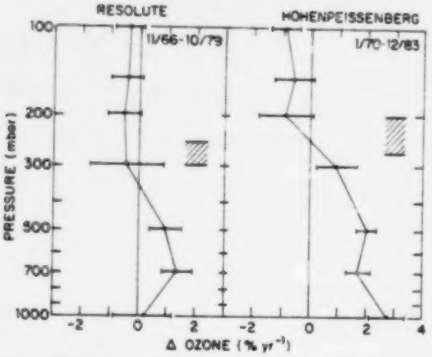

Fig. 24. Vertical distribution of the trend in ozone (in percent per year) at Resolute and Hohenpeissenberg. The horizontal bars give the 90% confidence interval for the trend at each level. The shaded area shows the range of tropopause heights through the year.

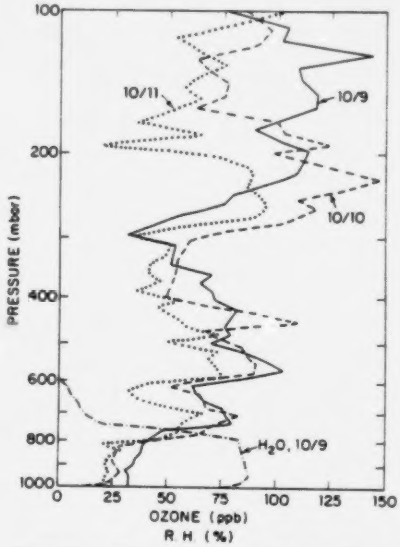

Fig. 26. Vertical profiles of ozone at Natal (6°S). Results are shown for three consecutive days in October 1979. The figure includes the vertical distribution of water vapor, shown in terms of relative humidity, for October 9.

concentrations are about a factor of 2 lower than results for Natal on the east coast of Brazil but are similar to results for Panama. *Crutzen et al.* [1985] reported values of 40–50 ppb over central Brazil in August. A recent expedition over the west coast of South America in October found concentrations of 35–55 ppb from 5°S to 20°S on the southbound flight, but concentrations were even higher, 55–80 ppb, on the northbound flight only a few days later [*Gregory et al.*, 1984]. The high values are similar to results for Natal.

Sonde results from Natal (6°S) and Panama (9°N) in combination with the aircraft measurements indicate that ozone concentrations in the southern tropics are in some cases much greater than those of the northern tropics. The data in Figures 18–20 do not support the previously accepted view [e.g., *Fishman et al.*, 1979*b*] that ozone is more abundant in the northern tropics. The analysis by *Fishman et al.* [1979*b*] may have been confounded by instrumental differences. They compared measurements made with Brewer-Mast sondes at Panama with results from Regener sondes at Canton Island (2°S) and La Paz (10°S).

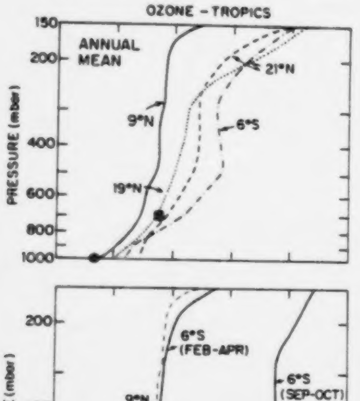

Fig. 25. Average vertical profiles for ozone in the tropics. The upper panel shows annual mean concentrations of ozone at Panama, 9°N (solid); Grand Turk, 21°N (dashes) [*Chatfield and Harrison*, 1977*b*]; Poona, 19°N (dots); and Natal, 6°S (dot-dash). Surface data are from Mauna Loa, 19°N (square), and Samoa, 14°S (circle) [*Oltmans*, 1981]. The lower panel shows average concentrations at Natal (solid) in September and October (11 profiles) and in February-April (10 profiles). Although few profiles are available for each month, the seasonal pattern is reproduced in 3 years of data. Horizontal bars shown one standard deviation based on individual profiles for Natal. Results are compared with the annual mean profile at Panama (dashes) and its standard deviation (based on monthly mean values).

5. DISCUSSION

Daily average concentrations of surface ozone in summer are between 30 ppb and 50 ppb in rural areas of the United States and Europe, while daily maximum concentrations are between 45 ppb and 65 ppb. We argue here that these concentrations are influenced significantly by photochemical production of ozone associated with emissions of NO_x, hydrocarbons, and CO, and we present a quantitative assessment of the magnitude and extent of the anthropogenic influence. The persistence of high ozone concentrations from spring into summer occurs only at continental mid-latitudes of the northern hemisphere. Concentrations appear to be largest in the most densely populated and industrialized regions, the eastern United States and central Europe. The behavior of ozone is quite different in sparsely populated regions remote from industrial activity: for example, Cape Grim and much of

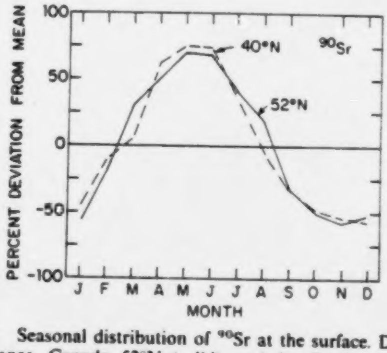

Fig. 27. Seasonal distribution of ^{90}Sr at the surface. Data shown for Moosonee, Canada 52°N (solid), and for Sterling-NYC, 40°N (dashed) are from *Staley* [1982].

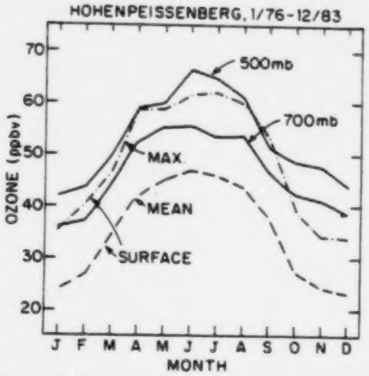

Fig. 28. Seasonal distribution of ozone at Hohenpeissenberg. The solid lines show sonde results for 700 mbar and 500 mbar. The dashed line shows daily mean values, and the dot-dashed line shows daily maximum values at the surface, derived from continuous surface measurements. Results are given for 1976 to 1983.

Canada, where ozone is largest in winter or spring and smallest in summer or autumn (15–25 ppb). The source of ozone from the stratosphere might be expected to give rise to a late winter or spring maximum in tropospheric ozone, since stratosphere-troposphere exchange is most effective during this period [*Danielsen*, 1968; *Danielsen and Mohnen*, 1977; *Mahlman and Moxim*, 1978].

The difference in seasonal behavior of surface ozone cannot be attributed simply to a latitudinal gradient or to differences between the hemispheres. We emphasize in this context first the summer maximum in surface ozone at 53°–55°N in Europe and the late summer-autumn minimum at similar latitudes in Canada. The Canadian sites experience surface air flow from the north in summer [*Bryson and Hare*, 1974] and therefore should represent some of the cleanest continental air in the northern hemisphere. Second, we note that the seasonal cycles of ^{90}Sr, a tracer of stratospheric air, are exactly in phase at 52° and 40° in North America (see Figure 27) [*Staley*, 1982]. This suggests that the different seasonal cycles of ozone at these latitudes cannot be ascribed simply to variations in the source of ozone from the stratosphere. Ozone mixing ratios in rural areas are too large in any event to be supplied by downward transport. Daily maximum mixing ratios of ozone near the ground at Hohenpeissenberg, for example, exceed values at 700 mbar in spring and summer (Figure 28). A similar result was found by *Reiter and Kanter* [1982] at a nearby location. Maximum ozone concentrations at Garmisch (740 m) exceeded those on the neighboring Zugspitze peak (2940 m) by ~10 ppb on sunny summer days. Third, we note the summer-autumn maximum in near-surface ozone at Aspendale (38°S), in contrast to the summer minimum at Cape Grim (41°S). Aspendale is affected by urban air pollution [*Galbally*, 1971], while Cape Grim is usually under the influence of pristine marine air masses. Thus nearly all locations within a few hundred kilometers of anthropogenic sources of NO_x and hydrocarbons exhibit a summer maximum in surface ozone, while very remote sites exhibit a summer or autumn minimum. The principal exceptions to this general behavior are southern coastal sites in the United States near 30°N and similarly situated Japanese stations. During summer, these locations experience tropical marine air flow [*Bryson and Hare*, 1974; *Fukui*, 1977] characterized by low concentrations of ozone (see Figures 18 and 19).

There is good evidence for a change in the seasonal distribution of surface ozone in Europe and the United States. This change implies substantial ozone increases in summer over regions of continental scale between 1950 and 1975. The available long-term measurements, from Arkona on the Baltic coast, show that ozone concentrations in summer increased by ~13 ppb (~70%) from 1958 to 1975, while winter values increased by ~5 ppb (~45%). *Warmbt* [1979] noted that ozone concentrations are highest during years with warm, dry, sunny summers [see also *Attmanspacher et al.*, 1984; *Reiter and Kanter*, 1982]. The measurements from Arosa suggest that ozone has increased by at least 10 ppb (~35%) in summer over the same period, and they imply a larger increase in summer than in other seasons. Measurements from Hohenpeissenberg for 1970 to 1983 indicate an increase in ozone of perhaps 6 ppb (20%), also with evidence for a larger change in summer.

Maximum concentrations of ozone in Michigan occurred in April and May in the 1870's, the same months as they do today in Canada (53°–59°N). If we use as preindustrial values the present-day concentrations of ozone at the relatively remote sites in Canada (Figure 11), we estimate that daily average concentrations of ozone in summer have increased by as much as 6–12 ppb in the Midwest and possibly by as much as 10–22 ppb in highly impacted environments such as the Ohio River Valley. These changes correspond to increases of 20% to 100%. Alternatively, if we adopt ozone concentrations at Cape Grim, Tasmania (15–20 ppb), as representative of the preindustrial atmosphere, we estimate that average concentrations of ozone in summer in the United States and Europe have increased by 15–25 ppb (see Figure 11), consistent with results discussed above.

Increases in ozone of the magnitude discussed here appear to be consistent with current understanding of the photochemistry of rural air. Oxidation mechanisms for hydrocarbons (HC) in the presence of NO_x indicate that several molecules of ozone may be formed for each molecule of NO_x and HC that is released [e.g., *Isaksen et al.*, 1978; *Singh et al.*, 1981], and field observations of O_3, NO_x, and hydrocarbons in rural areas support this view [*Fehsenfeld et al.*, 1983; *Kelly et al.*, 1984; *Parrish et al.*, 1985]. The average emission rate of NO_x from combustion of fossil fuels is $\sim 2 \times 10^{11}$ molecules cm^{-2} s^{-1} in the eastern United States, about a factor of 10 larger than the flux from natural sources [*Logan*, 1983]. Even if only one molecule of ozone were formed for each molecule of NO_x released, the production rate of ozone in the boundary layer in this region would exceed the average flux from the stratosphere $\sim 5\text{–}8 \times 10^{10}$ molecules cm^{-2} s^{-1} [*Danielsen and Mohnen*, 1977; *Mahlman et al.*, 1980; *Gidel and Shapiro*, 1980]. Hence it does not seem unreasonable that ozone concentrations might have increased by as much as a factor of 2 as a result of photochemical production associated with emissions of NO_x and hydrocarbons.

It is likely that much of the increase in ozone occurred between 1940 and the mid-1970's, at least in the United States. Emissions of NO_x from combustion increased by a factor of ~3 during this period, while emissions of hydrocarbons increased by a factor of ~2 [*U.S. Environmental Protection Agency*, 1982]. Emissions of NO_x increased at a slower rate after 1970 and have decreased since 1979, while emissions of HC have decreased since 1970, in part as a result of pollution control measures, in part as a result of energy conservation.

It is more difficult to quantify the possible impact of anthropogenic emissions on concentrations of ozone above the boundary layer. The similarity between the seasonal cycle of ozone in the middle troposphere over Europe, the United States, and northern Japan and that at ground level and the observed increases of ozone in the 1970's in the middle troposphere certainly argue in favor of a significant anthropogenic impact. It is extremely difficult to rationalize the persistence of high concentrations of ozone from April to August at 500 mbar without invoking a photochemical source, largely because of the short lifetime of ozone at mid-latitudes in summer, less than 1 month [*Isaksen et al.*, 1978]. Ozone or its precursors from the boundary layer are most likely to influence the distribution of ozone at higher altitudes in summer, when convective mixing is most effective.

Results from a recent study with a general circulation model also suggest that a photochemical source is required to explain the summer maximum [*Levy et al.*, 1985]. The model allowed for downward transport of ozone from the stratosphere and removal at the surface but did not include photochemical production and loss; it reproduced the observed seasonal cycle at remote locations where ozone concentrations are highest in late winter or spring but failed to simulate the broad summer maximum at mid-latitudes.

The seasonal behavior of ozone and observed increases suggests that the anthropogenic influence extends from about 30°N to 75°N in the middle troposphere and that the latitudinal extent varies with circulation patterns. For example the lack of a summer maximum in ozone over southern Japan (30°N) may be attributed to the onset of the summer monsoon when airflow from the Asian continent is replaced by air from the tropical Pacific [*Fukui*, 1977]. The increase in ozone over Resolute (75°N) at 500 mbar in spring and summer may result from long-range transport of ozone or its precursors from lower latitudes. Measurements of sulfate and particulates indicate that the Canadian Arctic is most likely to be influenced by air masses from mid-latitudes between December and May [*Barrie et al.*, 1981; *Rahn*, 1981], and ozone data near the ground show scant evidence for an anthropogenic impact in summer. The lifetime of ozone in the middle troposphere is expected, however, to be longer than that of SO_2 and sulfate, which are removed from the atmosphere by precipitation scavenging, and hence transport of ozone or its precursors from mid-latitudes may influence high-latitude ozone at 500 mbar in summer.

The increases in tropospheric ozone implied by the sonde data are substantial, 1%–2% yr^{-1} between 30°N and 75°N. It is unfortunate that there are no systematic observations from the period of most rapid growth in emissions of ozone precursors, 1940–1970. The trends in tropospheric ozone since 1967 contribute significantly to the trends in the integrated column of ozone and may compensate for 20%–30% of the decrease in ozone in the stratosphere over middle and high latitudes.

Studies of the influence of tropospheric ozone on climate have shown that surface temperature is most sensitive to changes in ozone near the tropopause [*Wang et al.*, 1980], and the evidence for change in this region is rather weak. Measurements from only two locations, Hohenpeissenberg and Kagoshima, suggest an increase in ozone at 300 mbar, while results for Goose Bay suggest a decrease. However, the variance of ozone concentrations near the tropopause is much larger than in the middle troposphere, and derived trends are less reliable.

Recent observations from Brazil suggest that elevated ozone concentrations in the tropics may result from photochemical synthesis, with combustion of vegetation rather than fossil fuels providing the source of NO_x, HC, and CO [*Crutzen et al.*, 1985]. Concentrations of ozone in the polluted boundary layer in a region of biomass burning in central Brazil, 60–65 ppb [*Delany et al.*, 1985], and values over Natal in September and October, >60 ppb, are similar to concentrations at mid-latitudes of the northern hemisphere in summer. Biomass burning takes place during the dry season, which lasts from June to September to the south and west of Natal [*Ratisbona*, 1976]. The prevailing winds in spring to the south of Natal are westerly above ~500 mbar, but from the ocean below [*Sabral*, 1979; *Oort*, 1983]. High levels of ozone are found above the trade wind inversion (~800 mbar) with much lower concentrations below. We speculate that the enhanced concentrations of ozone over Natal may be due to transport and photochemical degradation of emissions from biomass burning and possibly from biogenic emissions [*Crutzen et al.*, 1985] in the interior of the continent. Stratospheric intrusions could contribute also to the ozone enhancements that occur in the southern spring.

The observations of ozone over Natal in combination with surface data from Samoa, 14°S [*Oltmans*, 1981], and Angola, 15°S [*Fabian and Pruchniewicz*, 1977], indicate a significant seasonal variation in tropical ozone, with highest concentrations in late austral winter or spring. Concentrations of ozone appear to vary significantly with longitude also (see Figures 19 and 20). The lifetime of ozone toward photochemical loss is about 2 weeks in the tropics [*Liu et al.*, 1983; *Logan et al.*, 1981], less than the transit time of air masses around the globe. It is, perhaps, not surprising therefore that the distribution of the gas in the tropics should be quite heterogeneous. The recent data do not support earlier conclusions [e.g., *Fabian and Pruchniewicz*, 1977; *Fishman et al.*, 1979*b*] that ozone is more abundant in the northern tropics than in the south and more abundant at northern mid-latitudes than in the tropics. It is clear that latitudinal gradients in ozone vary significantly with season and with longitude.

Evidence presented here suggests that concentrations of ozone at middle and high latitudes of the northern hemisphere have been influenced significantly by photochemical production associated with emissions of NO_x, hydrocarbons, and CO from combustion of fossil fuels. Ozone over the tropical continents may also be influenced by emissions from combustion, in this case from agricultural burning. At present the seasonal behavior of tropospheric ozone is reasonably well characterized only over continental mid-latitudes of the northern hemisphere. Long-term measurements are sparse, even for Europe and North America. Data for ozone are particularly lacking for the tropics and subtropics. Given the central role of ozone in tropospheric chemistry, it is clear that a concerted effort should be made to determine the global climatology of ozone by establishing a network of suitably placed measurement stations. A serious commitment should also be made to measure ozone on a long-term basis with well-calibrated instruments at selected locations. Measurements of species that affect ozone, such as NO_x, hydrocarbons, and CO, are needed also in order to improve our understanding of the role of photochemistry in determining the distribution of ozone. It will be necessary, in addition, to develop rather sophisticated models for chemistry and dyamics in order to test our concepts about the processes influencing ozone and to evaluate future effects on tropospheric ozone of combustion related emissions. Such models must allow for the transformation and transport of pollutants from urban source regions (or from regions of agricultural burning) to the middle troposphere and must adequately simulate intrusions of stratospheric air and removal of ozone at the surface over varied terrain.

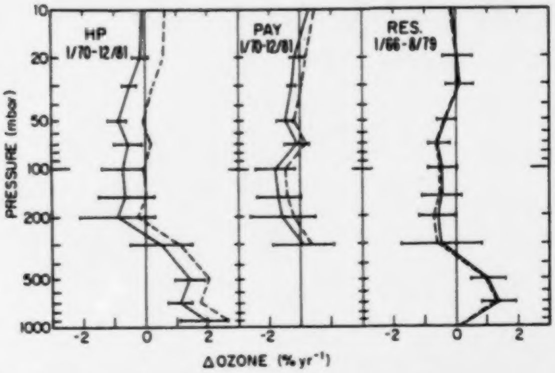

Fig. A1. Vertical distribution of the trend in ozone (in percent per year) at Hohenpeissenberg, Payerne, and Resolute. The solid lines show results for ozone soundings that have been scaled to Dobson measurements of the ozone column. The dashed lines show results that have not been scaled; concentrations were divided by the correction factor before forming monthly means. The horizontal bars give 90% confidence intervals for the trend. Meaningful trends could not be calculated for the troposphere at Payerne because of changes in the time of measurement (see Figure 5).

APPENDIX: THE CONTRIBUTION OF THE TREND IN TROPOSPHERIC OZONE TO THE TREND IN THE OZONE COLUMN

The sonde data permit an evaluation of the contribution of the trend in tropospheric ozone to the trend in the ozone column at those locations where the trends are statistically significant throughout the troposphere and stratosphere. This condition is met most closely at Hohenpeissenberg and Resolute (see Figure A1). Trends in ozone integrated through the troposphere and stratosphere are given in Table A1 in terms of Dobson units. The trend in the ozone column derived from the sonde data is in excellent agreement with the trend derived from concurrent Dobson measurements, but this is not surprising, since the sonde concentrations are normalized to the Dobson data. The increase in the column of ozone in the troposphere is about 20% of the decrease in the column in the stratosphere at Resolute. The results for Hohenpeissenberg are more difficult to interpret. The increase in ozone in the troposphere is ~30% of the decrease in the stratosphere, based on sonde data that have been scaled to the Dobson measurement of the ozone column, but the increase and decrease are of equal magnitude if the conventional scaling procedure is not used. This discrepancy arises because there is a significant trend in the correction factor at Hohenpeissenberg, −0.4% yr^{-1}, of comparable magnitude to the trend in stratospheric ozone (see Tables A1 and A2 and Figure A1). We note that the trend in the ozone column derived from Dobson data at Hohenpeissenberg, −0.28% yr^{-1}, does not agree with the average trend in the ozone column over Europe for 1970–1981, 0.1 ± 0.27% in 12 years. The average trend was derived by *Angell and Korshover* [1983] from 13 Dobson stations. The sonde data that have not been scaled to the Dobson results give no change in the ozone column, in better agreement with the average result for Europe. If the unscaled data provided a better measure of the trend in ozone at Hohenpeissenberg, this could imply that the increase in tropospheric ozone is of similar magnitude to the decrease in stratospheric ozone over Europe.

The results in Table A1 and Figure A1 highlight one of the major difficulties with interpretation of long-term ozonesonde measurements. The procedure of normalizing sonde results to Dobson measurements may introduce a significant bias into

TABLE A1. Trends in Ozone in the Stratosphere and Troposphere

	Hohenpeissenberg, January 1969 to December 1982, D.U. yr^{-1}		Payerne, January 1969 to January 1981, D.U. yr^{-1}		Resolute, January 1966 to August 1970, D.U. yr^{-1}	
Trend	Scaled to Column	Divided by Correction Factor	Scaled to Column	Divided by Correction Factor	Scaled to Column	Divided by Correction Factor
Sonde						
ΔO_3, troposphere	+0.4	+0.5	—	—	+0.2	+0.2
ΔO_3, stratosphere	−1.5	−0.5	−0.9	−0.7	−1.0	−1.3
ΔO_3, total*	−1.1	0.0	—	—	−0.9	−1.1
Dobson						
ΔO_3, column	−0.9 ± 0.5		−0.8 ± 0.5		(−0.6 ± 1.0)	

Ozone Column	Dobson Units	Dobson Units	Dobson Units
Sonde			
O_3, troposphere	26	24	19
O_3, stratosphere	284	281	360
O_3, total*	310	305	379
Dobson			
O_3, column	339	335	392

The upper portion of the table gives trends in ozone derived from ozonesonde measurements and from Dobson measurements made on the same day. Integrated trends in the stratosphere and troposphere were obtained from trend results for the standard pressure levels (see Figure A1) and are given in Dobson units per year (one D.U. = 2.69×10^{16} molecules cm^{-2}). The left-hand columns give results from sonde data that have been scaled to the Dobson measurements of the column; the right-hand columns give results from data that have not been scaled in this manner (see Table 3 footnotes). The lower portion of the table shows the integrated amount of ozone recorded by the sondes and by the Dobson instruments.

*Column of ozone below 10 mbar.

TABLE A2. Trend in Stratospheric Ozone, 100–50 mbar

	Scaled to Column	Divided by Correction Factor	Trend in Correction Factor	Trend in Column
Hohenpeissenberg	−0.7 ± 0.3	−0.4 ± 0.3	−0.4 ± 0.2	−0.28 ± 0.15
Payerne (January 1969 to December 1981)	−0.5 ± 0.3	−0.4 ± 0.4	NS	−0.23 ± 0.14
Uccle (January 1969 to March 1981)	−0.4 ± 0.4	—	—	—
Resolute	−0.7 ± 0.3	—	a	−0.35 ± 0.24
Goose Bay (June 1969 to December 1982)	−0.5 ± 0.3	—	b	−0.20 ± 0.18
Wallops Island (May 1970 to August 1981)	NS	NS	NS	NS
Sapporo	NS	NS	NS	NS
Tateno	−1.2 ± 0.5	−1.6 ± 0.5	0.5 ± 0.3	NS
Kagoshima	NS	NS	NS	0.36 ± 0.21
Aspendale (January 1969 to April 1982)	−0.5 ± 0.4	−1.1 ± 0.4	0.8 ± 0.3	NS

Trends are given as the percentage change per year for average concentrations at 100, 70, and 50 mbar. Trends were calculated as described in section 3 and are presented in the same format as Table 2. Results are given for January 1969 to December 1982, unless otherwise indicated. The trend in the ozone column was calculated from Dobson measurements made on the same days as the ozone soundings.

[a] The trend in the correction factor for January 1969 to January 1979 was 0.5(±0.3)% per year. The change from Brewer-Mast to ECC sondes in 1979 precludes meaningful interpretation of the trend in the C.F. thereafter.

[b] The trend in the C.F. for June 1969 to August 1980 was −0.7(±0.3)% per year. ECC sondes were used after August 1980.

trend results. There are trends in the normalization factors of similar magnitude to the trends derived for ozone in the lower stratosphere at over half the ozonesonde stations, as shown in Table A2. The problem seems to be less serious for the troposphere simply because the derived trends in ozone are much larger. These difficulties arise because the sonde technique, in its present form of implementation, does not provide adequately well-calibrated or internally self-consistent measurements of the concentration of ozone (see section 3).

Acknowledgments. This analysis would not have been possible without the dedicated efforts of the research groups who initiated and maintained the long-term measurement programs that formed the basis for this study. To them I extend my sincere appreciation. I am indebted to S. C. Wofsy for many enlightening discussions and would like to thank him and M. B. McElroy for their constructive comments on this paper. Special thanks are due to R. Yevich and C. S. Spivakovsky for their invaluable assistance with analysis of the ozonesonde data. I would like to acknowledge useful discussions with H. Levy II and I. Galbally and to thank R. Angle, D. DeMuer, G. Evans, I. Galbally, V. Kirchhoff, and V. Mohnen for kindly providing unpublished measurements of ozone. L. Morrison of Atmospheric Environment Service was most cooperative in supplying computer tapes of the sonde data. R. Bojkov brought to my attention the change in the time of measurements at Payerne. Finally, I would like to thank C. Demore for her expert editorial assistance and M. Burrell for her patience and skill in drafting the many figures. This work was supported by NSF grant ATM-81-17009, NASA grant NSG-2031 and CRC contract CAPA-22-83 to Harvard University.

REFERENCES

Angell, J. K., and J. Korshover, Global variation in total ozone and layer mean ozone: An update through 1981, *J. Climate Appl. Meteorol., 22*, 1611–1626, 1983.

Attmanspacher, W., and H. U. Dutsch, International ozonesonde intercomparison at the Observatory Hohenpeissenberg, January 19 to February 5, 1970, *Ber. Dtsch. Wetterdienstes, 16*(120), 1970.

Attmanspacher, W., and H. U. Dutsch, Second international ozonesonde intercomparison at the Observatory Hohenpeissenberg, April 5–20 1978, *Ber. Dtsch. Wetterdienstes*, 157, 1981.

Attmanspacher, W., and R. Hartmannsgruber, Some results of 6 years (1967-1972) of regular ozone soundings at the Meteorological Observatory Hohenpeissenberg, FRG, *Contrib. Atmos. Phys., 49*, 18–33, 1976.

Attmanspacher, W., and R. Hartmannsgruber, Trend and extreme value of 8 years continuous measurements of ozone near the surface at the Meteorological Observatory Hohenpeissenberg, FRG, in *Proceedings of the Quadrennial International Ozone Symposium, 4–9 August, 1980, Boulder, Colorado*, National Center for Atmospheric Research, Boulder, Colo., 1980.

Attmanspacher, W., and R. Hartmannsgruber, Intercomparison of instruments measuring ozone near the ground at the Hohenpeissenberg Observatory, October 1, 1978 to April 30, 1979, *Ber. Dtsch. Wetterdienstes*, 161, 1982.

Attmanspacher, W., R. Hartmannsgruber, and P. Lang, Long period tendencies of atmospheric ozone based on ozone measurements started in 1967 at the Hohenpeissenberg Meteorological Observatory, *Meteorol. Rundsch., 37*, 193–199, 1984.

Barnes, R. A., A. R. Bandy, and A. L. Torres, Electrochemical concentration cell ozonesonde accuracy and precision, *J. Geophys. Res., 90*(D5), 7881–7888, 1985.

Barrie, L. A., R. M. Hoff, and S. M. Daggupaty, The influence of mid-latitudinal pollution sources on haze in the Canadian Arctic, *Atmos. Environ., 15*, 1407–1419, 1981.

Blumenthal, D. L., W. S. Keifer, and J. A. McDonald, Aircraft measurements of pollutants and meteorological parameters during the Sulphate Regional Experiment Program (SURE): Meteorological Research, Inc., *Rep. EA-1909*, Electr. Power Res. Inst., Palo Alto, Calif., 1981.

Bojkov, R. D., Tropospheric ozone, its changes and possible radiative effects, *Spec. Environ. Rep. 16*, World Meteorol. Org., Geneva, 1984.

Bojkov, R. D., and G. C. Reinsel, Trends in tropospheric ozone concentrations, *Proceedings of the Quadrennial Ozone Symposium, Greece, September 3–7, 1984*, edited by C. S. Zerefos and A. Ghazi, D. Reidel, Hingham, Mass., 1984.

Brewer, A. W., and J. R. Milford, The Oxford-Kew ozone sonde, *Proc. R. Soc., A256*, 470–495, 1960.

Bryson, R. A., and F. K. Hare, The climates of North America, in *World Survey of Climatology*, vol. *11*, chap. 1, edited by R. A. Bryson and F. K. Hare, Elsevier, New York, 1974.

Chameides, W. L., and A. Tan, The two-dimensional diagnostic model for tropospheric OH: An uncertainty analysis, *J. Geophys. Res., 86*, 5209–5223, 1981.

Chameides, W., and J. C. G. Walker, A photochemical theory of tropospheric ozone, *J. Geophys. Res., 78*, 8751, 1973.

Chatfield, R., and H. Harrison, Tropospheric ozone, 1, Evidence for higher background values, *J. Geophys. Res., 82*, 5965–5968, 1977*a*.

Chatfield, R., and H. Harrison, Tropospheric ozone, 2, Variations along a meridional band, *J. Geophys. Res., 82*, 5969–5976, 1977*b*.

Cox, R. A., A. E. J. Eggleton, R. G. Derwent, J. E. Lovelock, and D. H. Pack, Large range transport of photochemical ozone in northwestern Europe, *Nature, 225*, 118–121, 1975.

Crutzen, P. J., A discussion of the chemistry of some minor constituents in the stratosphere and troposphere, *Pure Appl. Geophys., 106–108*, 1385, 1973.

Crutzen, P. J., and L. T. Gidel, A two-dimensional photochemical model of the atmosphere, 2, The tropospheric budgets of the anthropogenic chlorocarbons, CO, CH_4, CH_3C, and the effect of various NO_x sources on tropospheric ozone, *J. Geophys. Res.*, *88*, 6641–6661, 1983.

Crutzen, P. J., A. C. Delaney, J. Greenberg, P. Haagenson, L. Heidt, R. Lueb, W. Pollock, W. Seiler, A. Wartburg, and P. Zimmerman, Tropospheric chemical composition measurements in Brazil during the dry season, *J. Atmos. Chem.*, *2*, 233–256, 1985.

Danielsen, E. F., Stratosphere-troposphere exchange based on radioactivity, ozone and potential vorticity, *J. Atmos. Sci. 25*, 502–518, 1968.

Danielsen, E. F., and V. Mohnen, Project Duststorm: Ozone transport in situ measurements, and meteorological analysis of tropopause folding, *J. Geophys. Res.*, *82*, 5867–5877, 1977.

Decker, C. E., L. A. Ripperton, J. J. B. Worth, F. M. Vukovich, W. D. Bach, J. B. Tommerdahl, F. Smith, D. E. Wagoner, Formation and transport of oxidants along Gulf Coast and in northern U. S., *Rep. EPA-450/3-76-033*, U.S. Environ. Prot. Agency, Research Triangle Park, N. C., 1976.

Delany, A. C., P. J. Crutzen, P. Haagenson, S. Walters, and A. F. Wartburg, Photochemically produced ozone in the emissions from large-scale tropical vegetation fires, *J. Geophys. Res.*, *90*, 2425–2429, 1985.

DeMuer, D., Vertical ozone distribution over Uccle, Belgium, from six years of soundings, *Contrib. Atmos. Phys.*, *49*, 1–16, 1976.

Dutsch, H. U., Two years of regular ozone soundings over Boulder, *Tech. Note. 10*, Natl. Center Atmos. Res., Boulder, Colo., 1966.

Dutsch, H. U., The ozone distribution in the atmosphere, *Can. J. Chem.*, *52*, 1491–1504, 1974.

Dutsch, H. U., Vertical ozone distribution on a global scale, *Pure Appl. Geophys.*, *116*, 512–529, 1978.

Dutsch, H. U., and C. C. Ling, Six years of regular ozone soundings over Switzerland, *Pure Appl. Geophys.*, *106–108*, 1151–1168, 1973.

Dutsch, H. U., W. Zulig, and C. C. Ling, Regular ozone observations at Thalwill, Switzerland and at Boulder, Colordao, *Rep. LAPETH 1*, Lab. Atmospharenphys. Eidgenoss. Tech. Hochsch., Zurich, 1970.

Evans, G., P. Finkelstein, B. Martin, N. Possiel, and M. Graves, Ozone measurements from a network of remote sites, *J. Air Pollut. Contr. Assoc.*, *33*, 291–296, 1983.

Fabian, P., and P. G. Pruchniewicz, Meridional distribution of ozone in the troposphere and its seasonal variation, *J. Geophys. Res.*, *82*, 2063–2073, 1977.

Fehsenfeld, F. C., M. J. Bollinger, S. C. Liu, D. D. Parrish, M. McFarland, M. Trainer, D. Kley, P. C. Murphy, and D. L. Albritton, A study of ozone in the Colordao mountains, *J. Atmos. Chem.*, *1*, 87–105, 1983.

Feister, U., and W. Warmbt, Long term surface ozone increase at Arkona, *Proceedings of Quadrennial Ozone Symposium, Greece, September 3–7, 1984*, edited by C. S. Zerefos and A. Ghazi, D. Reidel, Hingham, Mass., 1984.

Fishman, J., and P. J. Crutzen, The origin of ozone in the troposphere, *Nature*, *274*, 855–857, 1978.

Fishman, J., and W. Seiler, Correlative nature of ozone and carbon monoxide in the troposphere: Implications for the tropospheric ozone budget, *J. Geophys. Res.*, *88*, 3662–3670, 1983.

Fishman, J., V. Ramanathan, P. J. Crutzen, and S. C. Liu, Tropospheric ozone and climate, *Nature*, *282*, 818–820, 1979*a*.

Fishman, J., S. Solomon, and P. J. Crutzen, Observational and theoretical evidence in support of a significant in-situ photochemical source of tropospheric ozone, *Tellus*, *31*, 432–446, 1979*b*.

Fukui, E. (Ed.), *The Climate of Japan*, Elsevier, New York, 1977.

Galbally, I. E., Surface ozone observations at Aspendale, Victoria, 1964–1970, *Atmos. Environ.*, *5*, 15–25, 1971.

Georgii, H.-W., and F. X. Meixner, Measurement of the tropospheric and stratospheric SO_2 distribution, *J. Geophys. Res.*, *85*, 7433–7438, 1980.

Geraci, M. J., and J. K. Luers, An evaluation of electrochemical concentration cell sonde measurements of atmospheric ozone, *J. Appl. Meteorol.*, *17*, 1521–1527, 1978.

Gidel, L. T., and M. A. Shapiro, General circulation model estimates of the net vertical flux of ozone in the lower stratosphere and the implications for the tropospheric ozone budget, *J. Geophys. Res.*, *85*, 4049–4058, 1980.

Gregory, G. L., S. M. Beck, and J. A. Williams, Measurements of free tropospheric ozone: An aircraft survey from 44°N to 46°S latitude, *J. Geophys. Res.*, *89*, 9642–9648, 1984.

Guicherit, R., and H. Van Dop, Photochemical production of ozone in Western Europe (1971–1978) and its relation to meteorology, *Atmos. Environ.*, *11*, 145–155, 1977.

Heck, W. W., O. C. Taylor, R. Adams, G. Bingham, J. Miller, E. Preston, and L. Weinstein, Assessment of crop loss from ozone, *J. Air Pollut. Contr. Assoc.*, *32*, 353–361, 1982.

Hering, W. S., and T. R. Borden, Ozonesonde Observations Over North America, vol. 4., *Environ. Res. Pap. 279, AFCRL-64-30(IV)*, Air Force Cambridge Res. Lab., Cambridge, Mass., 1967.

Hilsenrath, E., et al., Results from the balloon ozone intercomparison campaign (BOIC), in *Proceedings of the Quadrennial Ozone Symposium, Greece, 3–7, September 1984*, edited by C. S. Zerefos and A. Ghazi, D. Reidel, Hingham, Mass., 1984.

Isaksen, I. S. A., O. Hov, and E. Hesstvelt, Ozone generation over rural areas, *Environ. Sci. Technol.*, *12*, 1279–1284, 1978.

Junge, C. E., Global ozone budget and exchange between stratosphere and troposphere, *Tellus*, *14*, 363–377, 1962.

Junge, C. E., and G. Czeplak, Some aspects of the seasonal variation of carbon dioxide and ozone, *Tellus*, *20*, 422–434, 1968.

Katz, M., *Methods of Air Sampling and Analysis*, edited by M. Katz, pp. 549–555, American Public Health Association, Washington, D. C., 1977.

Kelly, N. A., G. T. Wolff, M. A. Ferman, Sources and sinks of ozone in rural areas, *Atmos. Environ.*, *18*, 1251–1266, 1984.

Kirchhoff, V. W. J. H., Are northern hemisphere tropospheric ozone densities larger?, *Eos Trans. AGU*, *65*, 449–450, 1984.

Kirchhoff, V. W. J. H., E. Hilsenrath, A. G. Motta, Y. Sahai, and R. A. Medrano, Equatorial ozone characteristics as measured at Natal, *J. Geophys. Res.*, *88*, 6812–6818, 1983.

Kohmyr, W. D., Electrochemical concentration cells for gas analysis, *Ann. Geophys.*, *25*, 203–210, 1969.

Kohmyr, W. D., and T. B. Harris, Development of an ECC ozonesonde, *NOAA Tech. Rep. ERL 200-APCL18*, U.S. Dep. Commer., Boulder, Colo., 1971.

Kohmyr, W. D., and P. R. Sticksel, Ozonesonde Observations 1962–1966, vol. 1, *ESSA Tech. Rep. IER 51-IAS 1*, U.S. Dep. Commer., Boulder, Colo., 1967.

Levy, H., II, Normal atmosphere: Large radical and formaldehyde concentrations predicted, *Science*, *173*, 141–143, 1971.

Levy, H., II, J. D. Mahlman, W. J. Moxim, and S. C. Liu, Tropospheric ozone: The role of transport, *J. Geophys. Res.*, *90*, 3753–3772, 1985.

Linvill, D. E., W. J. Hooker, and B. Olson, Ozone in Michigan's environment 1876–1880, *Mon. Weather Rev.*, *108*, 1883–1891, 1980.

Liu, S. C., M. McFarland, D. Kley, O. Zafiriou, and B. J. Huebert, Tropospheric NO_x and O_3 budgets in the Equatorial Pacific, *J. Geophys. Res.*, *88*, 1360–1368, 1983.

Logan, J. A., Nitrogen oxides in the troposphere: Global and regional budgets, *J. Geophys. Res.*, *88*, 10,785–10,807, 1983.

Logan, J. A., M. J. Prather, S. C. Wofsy, and M. B. McElroy, Tropospheric chemistry: A global perspective, *J. Geophys. Res.*, *86*, 7210–7254, 1981.

London, J., and J. K. Angell, The observed distribution of ozone and its variations, *Stratospheric Ozone and Man*, vol. 1, edited by F. A. Bauer and R. B. Ward, pp. 7–42, CRC Press, Boca Raton, Fla., 1982.

Mahlman, J. D., and W. J. Moxim, Tracer simulation using a global general circulation model: Results from a mid-latitude instantaneous source experiment, *J. Atmos. Sci.*, *35*, 1340–1374, 1978.

Mattana, N., G. P. Porra, and A. Serra, Cinq annees de sondages ozone sur Cagliari (Sardaigne), *Pure Appl. Geophys.*, *106–108*, 1169–1179, 1973.

Mohnen, V. A., A. Hogan, and P. Coffey, Ozone measurements in rural areas, *J. Geophys. Res.*, *82*, 5889–5895, 1977.

Mueller, P. K., and G. M. Hidy, The sulfate regional experiment: Report of findings, *Rep. 1901* (3 vols.), Electr. Power Res. Inst., Palo Alto, Calif., 1983.

Mukammal, E., Report on Oxidant Climatology of Ontario, Atmos. Environ. Serv., Toronto, Canada, 1984.

Oltmans, S. J., Surface ozone measurements in clean air, *J. Geophys. Res.*, *86*, 1174–1180, 1981.

Oltmans, S. J., Tropospheric ozone at four remote observatories, *Proceedings of the Quadrennial Ozone Symposium, Greece, 3–7 September, 1984*, edited by C. S. Zerefos and A. Ghazi, D. Reidel, Hingham, Mass., 1984.

Oort, A. H., Global atmospheric circulation statistics, 1958–1973, *NOAA Prof. Pap. 14*, 1983.

Parrish, D. D., D. W. Fahey, E. J. Williams, S. C. Liu, M. Trainer, P. C. Murphy, D. L. Albritton, and F. C. Fehsenfeld, Background ozone and anthropogenic ozone enhancements at Niwot Ridge, Colorado, *J. Atmos. Chem.*, in press, 1985.

Pittock, A. B., Climatology of the vertical distribution of ozone over Aspendale, *Q. J. R. Meteorol. Soc.*, *103*, 575–584, 1977.

Pratt, G. C., R. C. Hendrickson, B. I. Chevone, D. A. Christopherson, M. V. O'Brien, and S. V. Krupa, Ozone and oxides of nitrogen in the rural upper midwestern U. S. A., *Atmos. Environ.*, *17*, 2013–2023, 1983.

Pruchniewicz, P. G., The average tropospheric ozone content and its variation with season and latitude as a result of the global ozone circulation, *Pure Appl. Geophys.*, *106–108*, 1058–1073, 1973.

Rahn, K. A., The Mn/V ratio as a tracer of large scale sources of polluttion aerosol for the Arctic, *Atmos. Environ.*, *15*, 1457–1464, 1981.

Ramanathan, V., and R. E. Dickinson, The role of stratospheric ozone in the zonal and seasonal radiation energy balance of the earth troposphere system, *J. Atmos. Sci.*, *36*, 1084–1104, 1979.

Ratisbona, L. R., The climate of Brazil, in *World Survey of Climatology*, vol. 12, chap. 5, edited by W. Schwerdtfeger, Elsevier, New York, 1976.

Regener, E., Ozonschicht und atmospharische turbulenz, *Ber. Dsch. Wetterdienstes*, *11*, 45–57, 1949.

Reiter, E. R., Stratospheric-tropospheric exchange processes, *Rev. Geophys. Space Phys.*, *13*, 459–474, 1975.

Reiter, R., and H. J. Kanter, Time behavior of CO_2 and O_3 in the lower troposphere based on recordings from neighboring mountain stations between 0.7 and 3.0 km ASL including the effects of meteorological parameters, *Arch. Meteorol. Geophys. Bioklimatol., Ser. B*, *30*, 191–225, 1982.

Routhier, F., R. Dennett, D. D. Davis, A. Wartburg, P. Haagenson, and A. C. Delaney, Free tropospheric and boundary-layer airborne measurements of ozone over the latitude range of 58°S to 70°N, *J. Geophys. Res.*, *85*, 7307–7321, 1980.

Sabral, Z. R., Um estudo climatologico dos campos de vento e de temperatura nos nivers superiores sobre a America do Sul, M. Sc. dissertation, Sao Jose dos Campos, Inst. Pesq. Espacais., Sao dos Campos, Brazil, 1979.

Schenkel, A., and B. Broder, Interference of some trace gases with ozone measurements by the KI method, *Atmos. Environ.*, *16*, 2187–2190, 1982.

Seiler, W., and J. Fishman, The distribution of carbon monoxide and ozone in the free troposphere, *J. Geophys. Res.*, *86*, 7255–7265, 1981.

Shaw, R. W., and R. J. Paur, Measurements of sulfur in gases and particles during sixteen months in the Ohio River Valley, *Atmos. Environ.*, *17*, 1431–1438, 1983.

Singh, H. B., F. L. Ludwig, and W. B. Johnson, Tropospheric ozone: Concentrations and variabilities in clean remote atmospheres, *Atmos. Environ.*, *12*, 2185–2196, 1978.

Singh, H. B., J. R. Martinez, D. G. Hendry, R. J. Jaffe, and W. B. Johnson, Assessment of the oxidant forming potential of light saturated hydrocarbons in the atmosphere, *Environ. Sci. Technol.*, *15*, 113–119, 1981.

Skarby, L., and G. Sellden, The effects of ozone on crops and forests, *Ambio*, *13*, 68–72, 1984.

Staley, D. O., Strontium-90 in surface air and the stratosphere: Some interpretations of the 1963-1975 data, *J. Atmos. Sci.*, *39*, 1571–1590, 1982.

Torres, A. L., and A. R. Bandy, Performance characteristics of the electrochemical concentration cell ozonesonde, *J. Geophys. Res.*, *83*, 5501–5504, 1978.

U.S. Environmental Protection Agency, National air pollutant emission estimates, 1940–1980, *Rep. EPA-450/4-82-001*, Research Triangle Park, N. C., 1982.

Viezee, W., H. B. Singh, and H. Shigeishi, The impact of stratospheric ozone on tropospheric air quality: Implications from analysis of existing field data, report, *Proj 1140*, SRI Int., Menlo Park, Calif., 1982.

Vukovich, F. M., W. D. Bach, B. W. Crissman, and W. J. King, On the relationship between high ozone in the rural surface layer and high pressure systems, *Atmos. Environ.*, *11*, 967–983, 1977.

Wang, W-C., J. P. Pinto, and Y. L. Yung, Climatic effects due to halogenated compounds in the earth's atmosphere, *J. Atmos. Sci.*, *37*, 333–338, 1980.

Warmbt, W., Results of long term measurements of near surface ozone in the GDR, *Z. Meteorol.*, *29*, 24–31, 1979.

Wilcox, R. W., Comments on "Tropospheric ozone, 1, Evidence of higher background values" by R. Chatfield and H. Harrison, *J. Geophys. Res.*, 6263–6264, 1978.

Wisse, J. A., and A. J. Meerburg, Ozone observations at Base King Baudouin in 1965 and 1966, *Arch. Meteorol. Geophys. Bioklimatol., Ser. A*, *18*, 41–54, 1969.

Wolff, G. T., and P. J. Lioy, Development of an ozone river associated with synoptic scale episodes in the eastern United States, *Environ. Sci. Technol.*, *14*, 1257–1261, 1980.

Wolff, G. T., P. J. Lioy, G. D. Wight, R. E. Meyers, and R. T. Cederwall, An investigation of long range transport of ozone across the mid western and eastern United States, *Atmos. Environ.*, *11*, 797–802, 1977.

World Meteorological Organization, Report of the meeting of experts on sources of errors in detection of ozone trends, *Rep. 12*, WMO Global Ozone Res. Monit. Proj., Geneva, 1982.

J. A. Logan, Center for Earth and Planetary Physics, 108 Pierce Hall, 29 Oxford Street, Harvard University, Cambridge, MA 02138.

(Received February 25, 1985;
revised May 17, 1985;
accepted May 17, 1985.)

Paper 7

Effects of Increased UV Radiation on Urban Ozone

by

Gary Whitten
Systems Applications, Inc.

This presentation was based upon the following paper prepared for the workshop.

Effects on Urban Smog Resulting From Changes in the Stratospheric Ozone Layer and in Global Temperature

by

G.Z. Whitten
M.W. Gery

Paper 7

EFFECTS ON URBAN SMOG RESULTING FROM CHANGES IN THE STRATOSPHERIC OZONE LAYER AND IN GLOBAL TEMPERATURE

by

G. Z. Whitten
M. W. Gery

Systems Applications, Inc.
101 Lucas Valley Road
San Rafael, CA 94903

Presented at the U.S. Environmental Protection Agency Workshop on
"Global Atmospheric Change and EPA Planning"
Raleigh, North Carolina

11-12 November 1985

Paper 7

EFFECTS ON URBAN SMOG RESULTING FROM CHANGES IN THE STRATOSPHERIC OZONE LAYER AND IN GLOBAL TEMPERATURE

As part of ongoing research into the nature and causes of photochemical smog, Systems Applications, Inc. has conducted a preliminary investigation into the potential changes in urban ozone levels due to an increase in solar ultraviolet (UV) radiation resulting from reductions in the stratospheric ozone layer. Estimates were also made of the effects on urban ozone chemistry resulting from a general warming of the lower atmosphere. Hence, the focus of this study was on the effect of reductions in stratospheric ozone by as much as 30 percent on (1) peak ozone concentrations in urban areas and (2) the attendant control requirements predicted by a modified version of the Empirical Kinetics Modeling Approach (EKMA). The model used in this study was the simple trajectory model used in the EKMA. This model was developed by the U.S. Environmental Protection Agency (EPA) and is widely used to assess the effectiveness of emissions control scenarios to abate urban ozone. Because these investigations were intended as the first phase of a more thorough study of these potential effects, only simple modeling techniques were applied to a limited number of situations.

PHOTOLYSIS RATE RELATIONSHIPS

A reduction of the atmospheric ozone column is known to allow more ultraviolet radiation to reach the global surface in the wavelength region between 280 and 330 nm (Bahe et al., 1979). In addition to causing biological effects as skin cancer, radiation in this region plays a major role in smog chemistry. We began by investigating the ozone formation processes in the lower troposphere that would be affected by increased UV transmission through the atmosphere. From this preliminary work, it is evident that the photolysis channel of formaldehyde that leads to radical products is selectively enhanced at a higher UV flux. Formaldehyde emissions are products of incomplete combustion, and formaldehyde is a major intermediate oxidation product from virtually all organic molecules. Since radicals from formaldehyde photolysis are the main source of radicals needed to drive the chain reactions that generate photochemical smog (Whitten, 1983), an increase in rate of photolysis would have a bearing on the design of future control strategies.

The photolysis of ozone to electronically excited oxygen atoms is thought to be the second most important source of the radicals that drive smog formation. However, the role of ozone photolysis is different from that of formaldehyde because ozone is the principal ingredient of photochemical smog. At low levels of oxidation potential, the excited oxygen atoms tend to accelerate smog reactions, making the atmospheric chemistry more efficient in generating ozone from minimal precursor emissions. However, at the highest or most severe ozone levels, the excess radicals can partially suppress the ozone peak, making the precursors seem less efficient in generating ozone. Other photolysis rates can also be affected, but their contribution to smog formation is less important.

A specific increase in formaldehyde photolysis to radical products is difficult to determine accurately for a number of reasons. Atmospheric photolysis rates have often been calculated in 10 nm wavelength intervals. However, the accurate calculation of formaldehyde photolysis requires fine spectral resolution for both the formaldehyde absorption cross-section and the surface solar flux (related to the ozone absorption cross-section). Only in this manner can a comparison of the respective fine structures be performed. Near-ground solar flux data of high resolution and known stratospheric ozone abundance have not been readily available. Although we have obtained high-resolution absorption cross-section data, we are currently estimating surface solar fluxes using low-resolution information provided by the National Aeronautics and Space Administration. Figure 1 shows two different determinations of the UV absorption spectra of formaldehyde. Figure 2 shows a high-resolution spectrum of surface solar flux data.

The necessary photolysis rate parameter, commonly refered to as the "J value" is obtained from integration of the product of absorption cross-section, light flux, and quantum yield over all relevant wavelengths. Figure 3 shows the product function for the two formaldehyde cross sections given in Figure 1. Plots of the product functions against wavelength are often referred to as the "photoaction spectrum." The J-value is the area under this photoaction curve. Figure 3 was generated from a NASA computer program for the UV flux (which has only a 5 μm resolution) and quantum yield data from NASA (1983). The 1 nm values in the figure were determined by linear interpolation of the solar radiation data. The photoaction spectrum using high-resolution UV data has not yet been generated. However, a comparison of Figures 1 and 2 shows that there can be several overlaps in fine structure. At this time, we have determined that a minimum resolution of 0.25 μm is required. Coarser resolutions

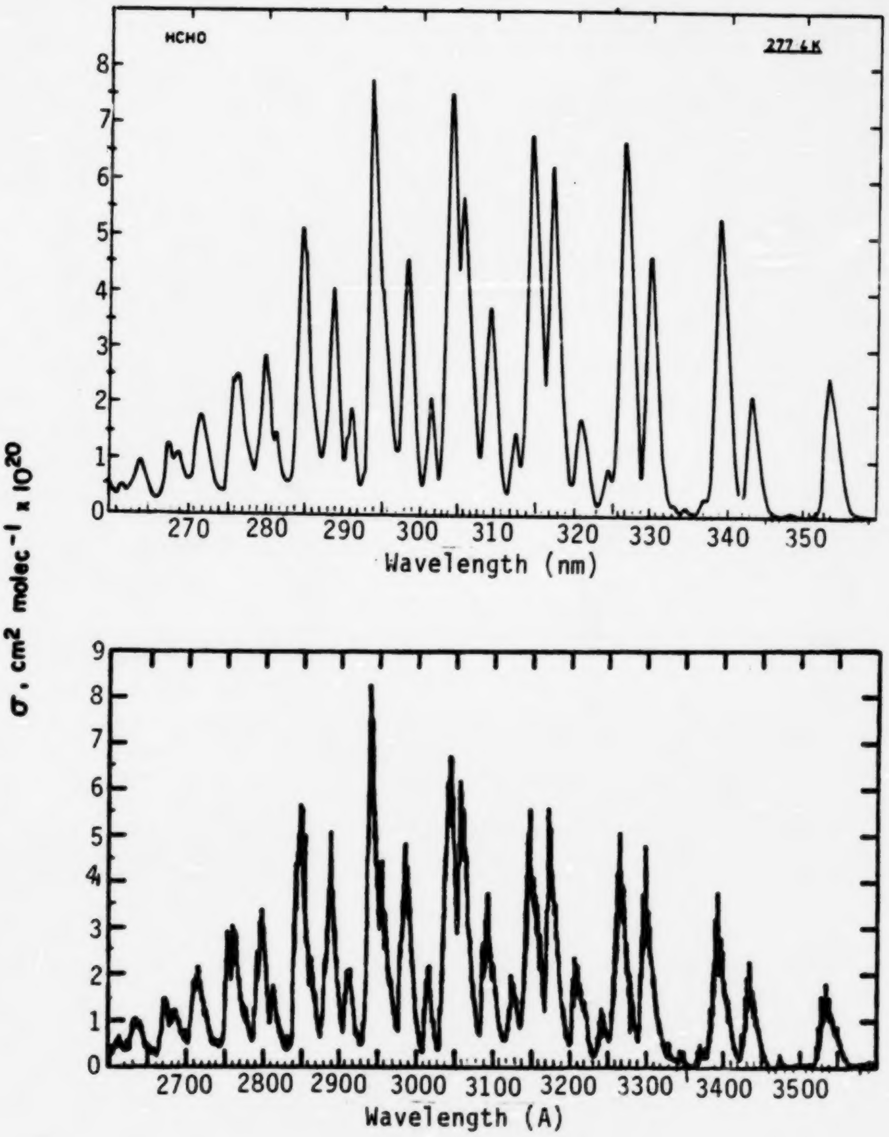

FIGURE 1. Formaldehyde absorption cross sections from Moortgat (1985) and Bass et al. (1980).

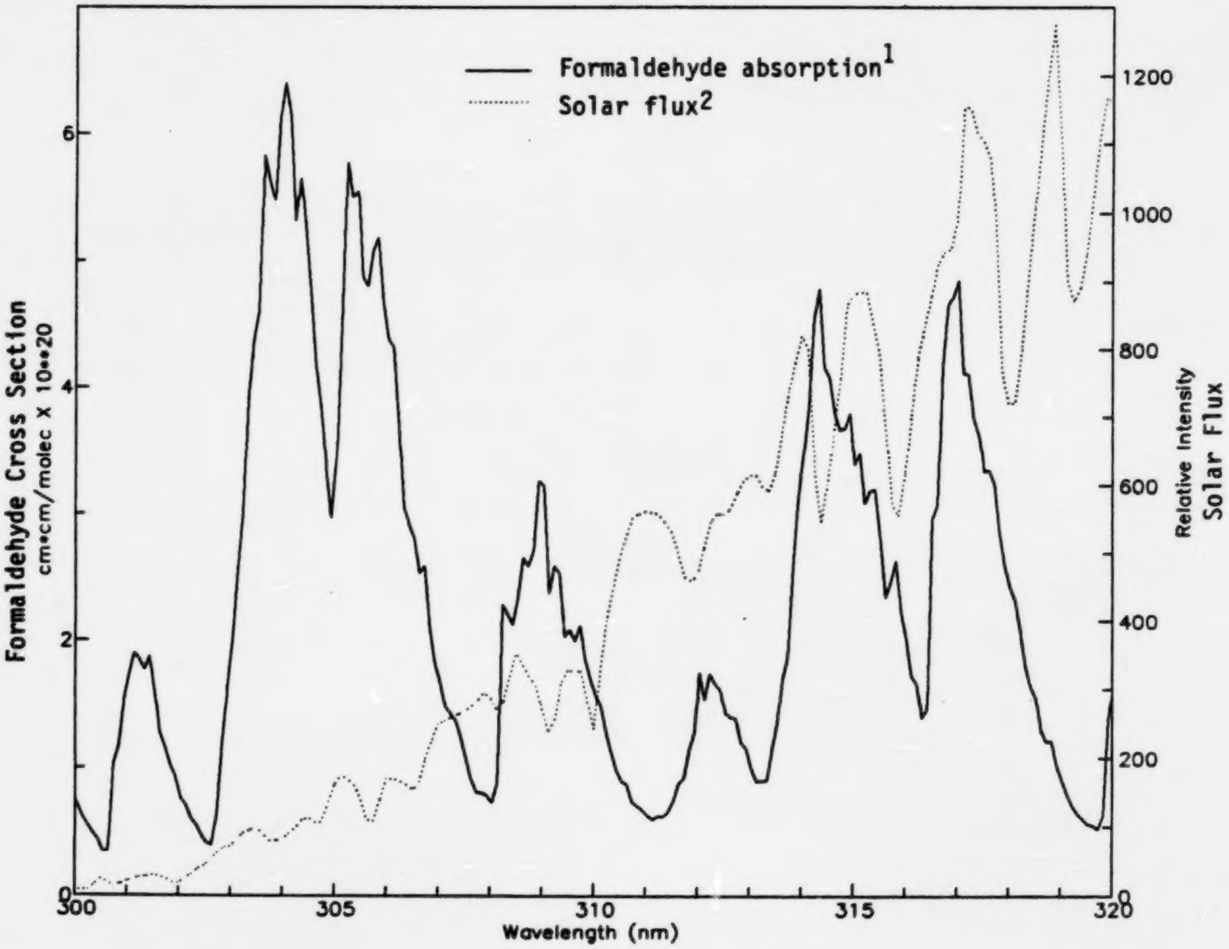

FIGURE 2. Matched high-resolution spectra for formaldehyde cross section and solar flux. 1. Source: Bass (private communication 1985). 2. Source: Bahe et al (1979).

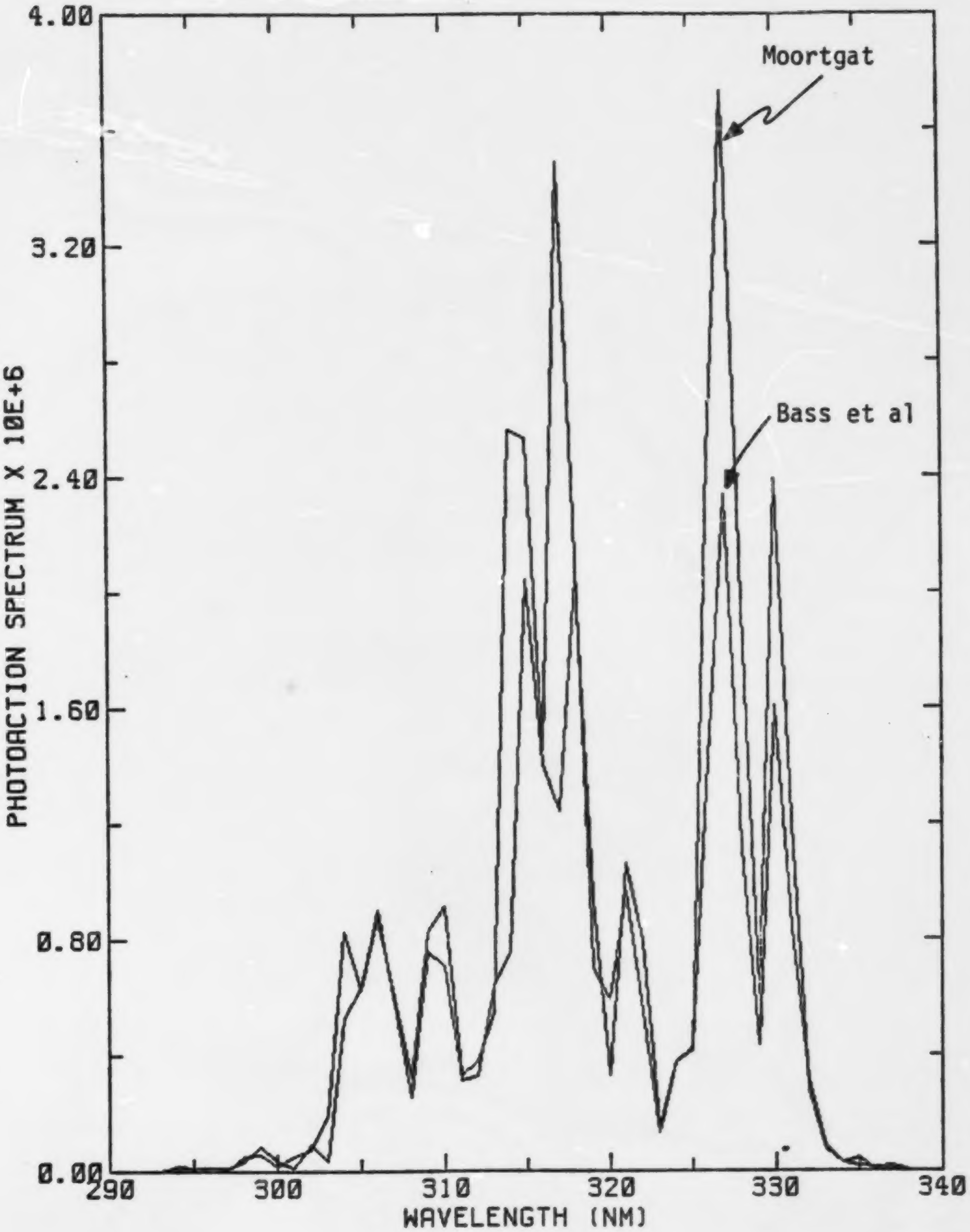

FIGURE 3. Formaldehyde photoaction spectrum using the absorption cross sections of Moortgat (1985) and Bass et al. (1980).

would miss the overlaps in fine structure, whereas finer resolutions should not affect the calculated J-values.

Figure 2 also shows a correspondence between the peaks of the formaldehyde absorption spectrum and dips in the solar flux. This correspondence suggests that formaldehyde in the troposphere is affecting the photolysis rate of formaldehyde at the surface. This finding is consistent with observations of tropospheric formaldehyde in the 0.2-0.5 ppb range and indicates that theoretical calculations of the J-values for formaldehyde must take tropospheric formaldehyde absorption into account along with high-resolution UV data.

Figure 4 shows a high resolution photoaction spectrum for ozone derived from the surface solar data of Bahe et al. (1983). This data was collected with a Dobson Unit (DU) of 300.* The figure also shows a 200 DU curve, which was calculated by applying the 300-to-200 DU ratios of the calculated NASA solar data to the measured 300 DU solar data of Bahe et al. (1983). The increase in UV to the short wavelength side is evident in the plot.

MODEL PREDICTIONS

Using the spectral data, we estimated formaldehyde and ozone photolysis rates as a function of zenith angle and ultraviolet flux changes due to stratospheric ozone depletion. The estimated photolysis rates for formaldehyde, coupled with the information compiled for surface ozone photolysis, provide the inputs needed to calculate diurnal photolysis rates for projected future ozone column densities. This information is then used to evaluate the future impact of stratospheric ozone changes on near-surface smog formation.

The preliminary results of the possible effects of increased ultraviolet radiation on urban smog are based on simulation of atmospheric conditions for three urban cities:

(1) Nashville--because it is nearly in compliance with the 0.12 ppm federal ozone standard.

---

* This unit of measure is the height (in 10^{-3} cm) that all ozone molecules above the earth's surface would attain if all those molecules were compressed to pure ozone at 1 atmosphere pressure and 298 K.

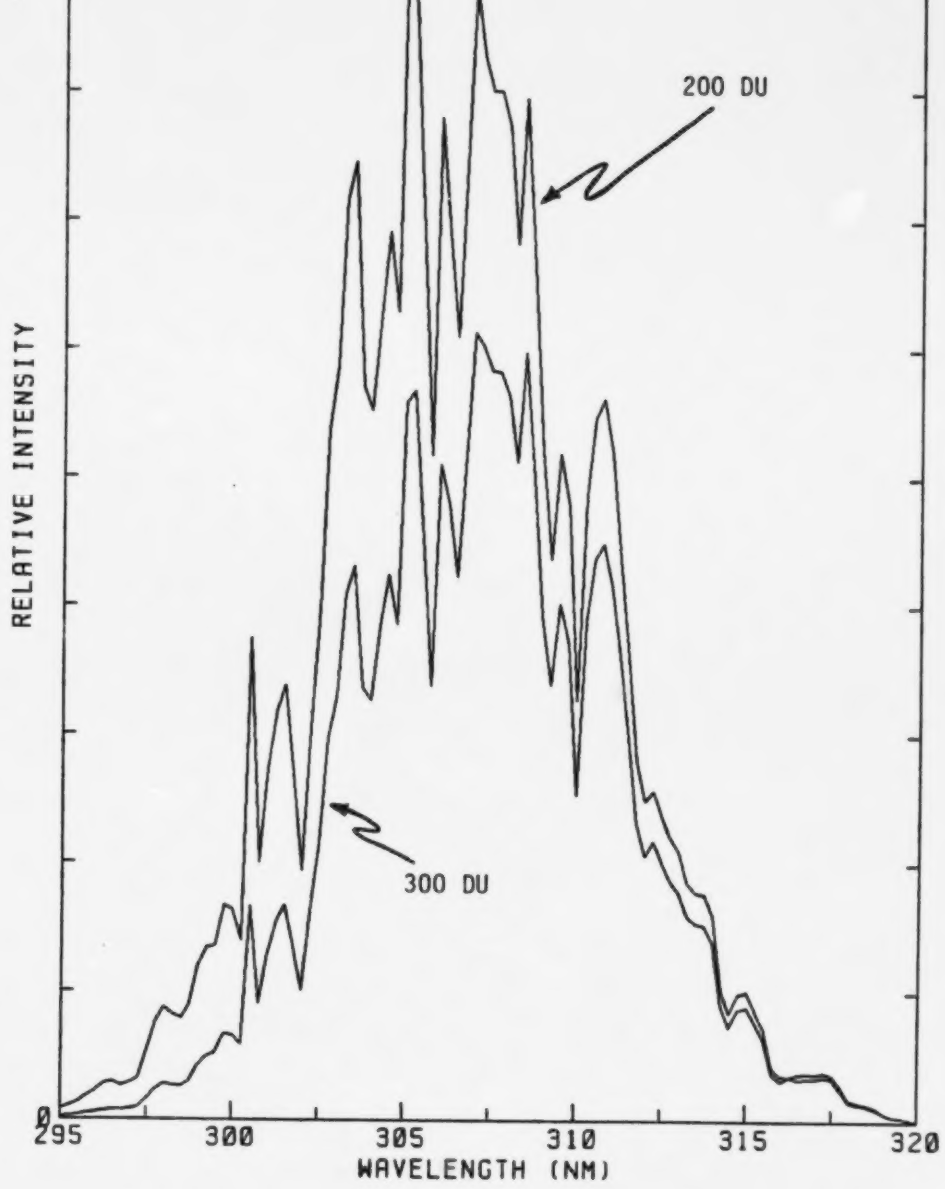

FIGURE 4. Photoaction spectra for ozone using the measured solar radiation of Bahe et al. (1979) at 300 Dobson, and a 200 Dobson estimate from information provided by NASA-Goddard.

(2) Philadelphia--to represent cities that require moderate control (30-50 percent reduction in organic precursors) to achieve the 0.12 ppm standard.

(3) Los Angeles--because of the severity of the exceedance of the ozone standard in that region.

Present-day predictions are based on a total ozone column of 300 DU and future predictions are based on a total ozone column of 250 and 200 DU. A 33 percent decrease in total ozone column would increase ozone photolysis by nearly a factor of two, and increase formaldehyde photolysis to radical products by nearly 20 percent. Both of these increases are still somewhat uncertain because of uncertainties regarding the spectral fine structure and other factors.

The effects of these photolysis rate increases are given in Table 1 for 298 K and 302 K. For all three cities, the model predicts higher ozone concentrations resulting either from increases in temperature or decreases in the Dobson number. The magnitude of the increases in ozone is apparently a function of local hydrocarbon-to-nitrogen oxide ratio, reactivity, meteorology, and emission distribution. The linearity of the response to stratospheric ozone depletion is not general. For the Los Angeles case, the increases in ozone are moderate and quite linear with decreasing Dobson number. For the Philadelphia case, ozone is predicted to increase progressively as the Dobson number declines; that is, only a modest increase in ozone is seen for a decline in Dobson number from 300 to 250 units, but a more dramatic increase in ozone is seen when the Dobson number declines from 250 to 200 units. For the Nashville case, the increases are all very dramatic and the linearity is a function of temperature. At the more normal temperature of 298 K, the simulated urban ozone tends to increase linearly with Dobson number decrease; but at the warmer 302 K temperature, the simulated ozone increases more for the first 50-unit Dobson change than for the second 50-unit change, down to the 200 unit limit studied.

The effects of a 4 K increase in temperature are most pronounced in the Los Angeles and Nashville simulations where 14 to 23 ppb increases in simulated ozone peaks are predicted. The effects of a combined temperature increase and reduced Dobson number appear to be always additive, if not synergistic, especially for the Nashville simulations. When a 4 K temperature increase is combined with only a 50-unit Dobson reduction, the simulated peak ozone jumps from a base value of 0.13 ppm to over 0.18 ppm ozone.

The EKMA isopleth diagram for Nashville shown in Figure 5 indicates that peak ozone is nearly independent of total precursor loading (for 300 DU,

TABLE 1. Ozone concentrations (ppm) predicted for changes in Dobson number and temperature for three cities.

	Ozone Concentrations					
Temperature (K)	298K			302K		
Dobson Number	300	250	200	300	250	200
City						
Los Angeles*	0.288	0.301	0.315	0.306	0.318	0.331
Philadelphia	0.112	0.127	0.149	0.122	0.134	0.159
Nashville	0.130	0.161	0.195	0.146	0.184	0.215

* For Los Angeles, values under 298 K used actual hourly temperatures and values under 302 K are from simulations using those temperatures increased by 5 K.

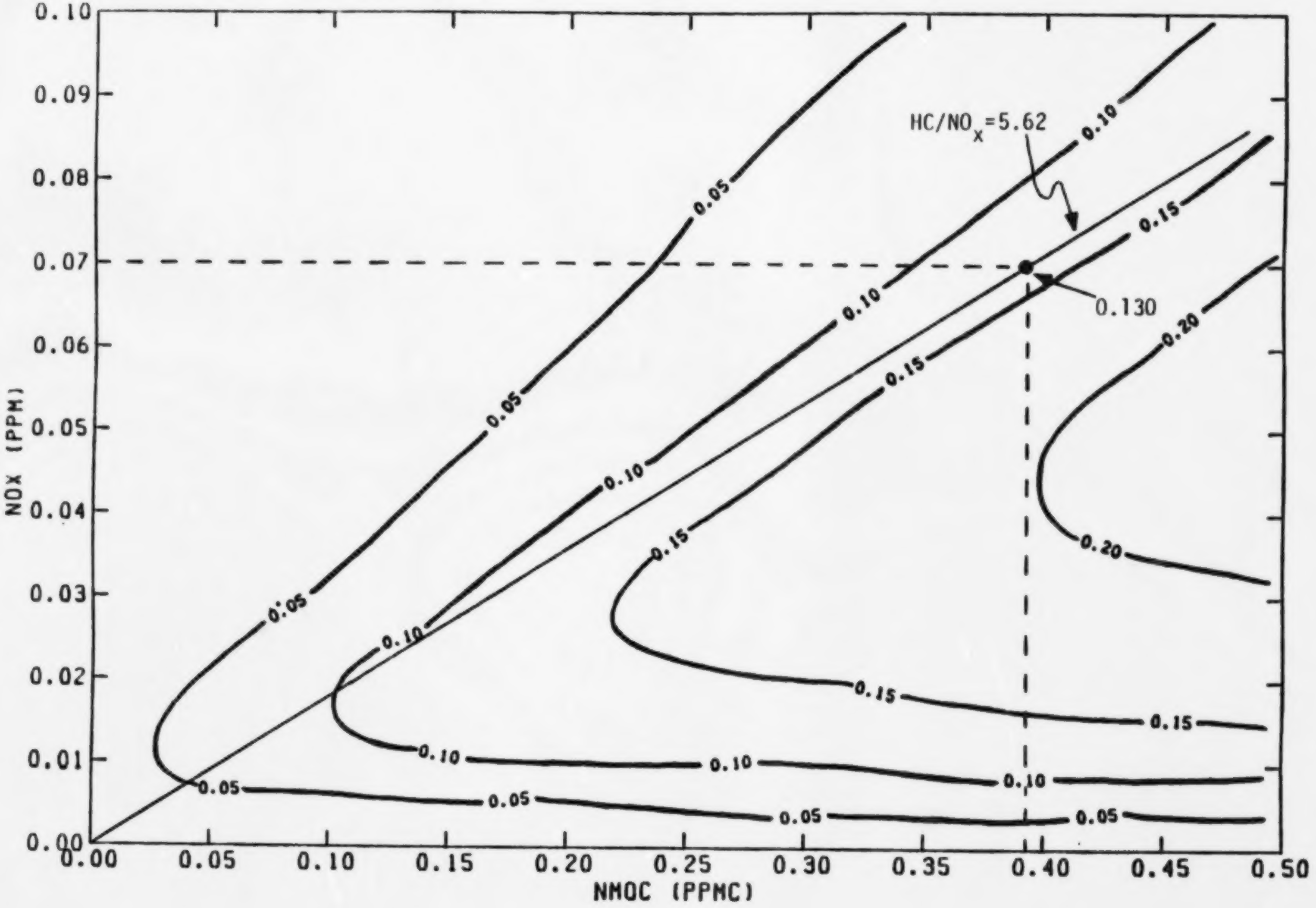

FIGURE 5. EKMA isopleth diagram for Nashville case with 300 DU at 298 K.

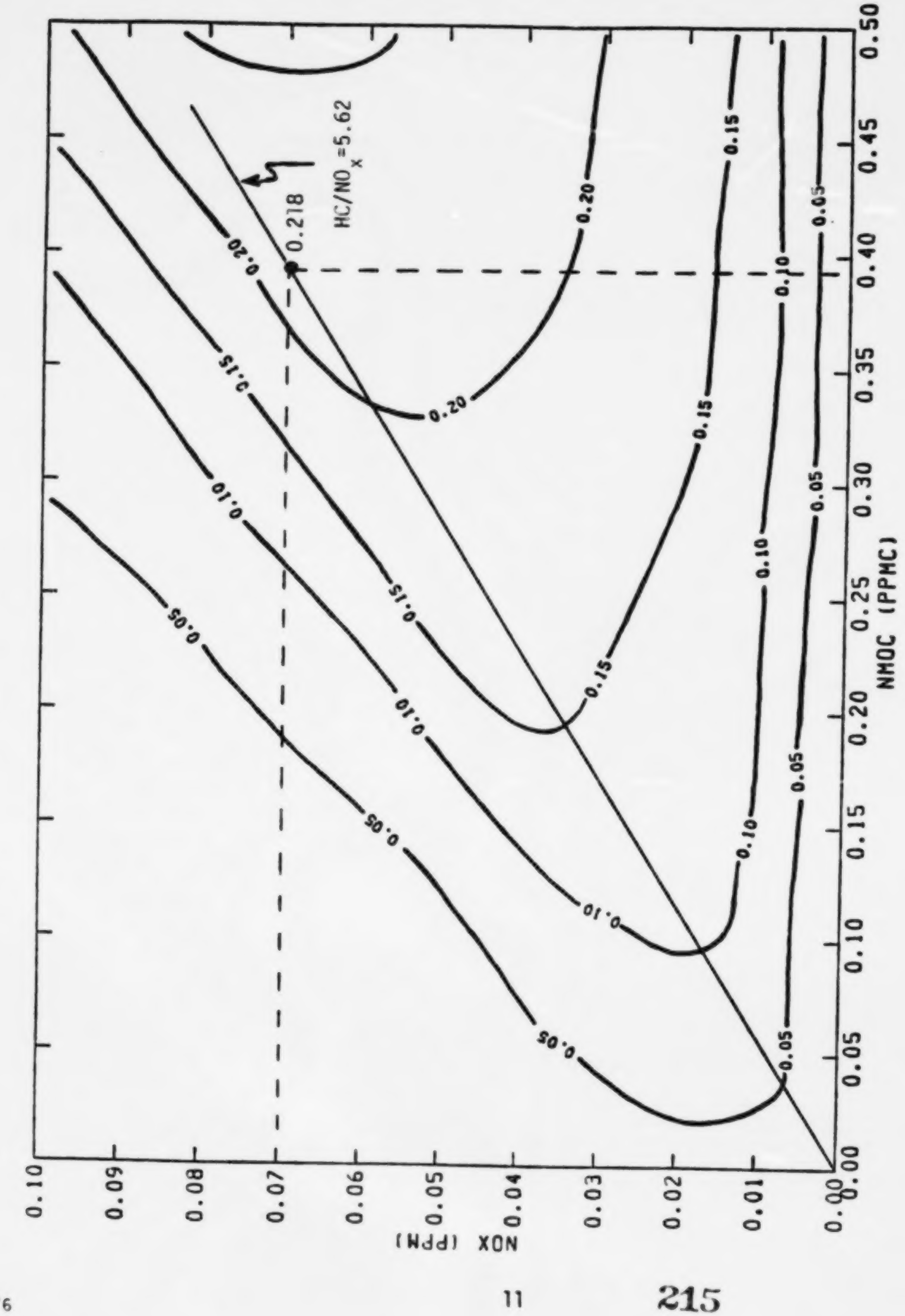

FIGURE 6. EKMA isopleth diagram for Nashville case with 200 DU at 302 K.

298 K), but rather strongly defined by the ratio of organic-to-nitrogen oxide precursors. Thus, substantial changes in emissions of volatile organics (VOC) and nitrogen oxide (NO_x) might occur without affecting peak ozone as long as the ratio of VOC/NO_x is held constant. An increase in temperature or ultraviolet flux evidently alters the ratio of VOC/NO_x, which results in 0.13 ppm ozone.

The isopleth diagram shown in Figure 6 corresponds to the 200 Dobson number/302 K case shown in Table 1 for Nashville. The difference isopleth for Figures 5 and 6 is shown in Figure 7. From this difference isopleth we see that the sensitivity to UV and temperature perturbations is both a function of VOC/NO_x ratio and overall concentration. Hence, control strategies aimed at lowering the VOC/NO_x ratio (by emphasizing VOC control over NO_x control) may be undermined by either decreases in the Dobson number or increases in tropospheric temperature, but control strategies that reduce the total VOC and NO_x loading (even at the optimum VOC/NO_x ratio for generating ozone) will probably be little affected by such global effects.

Another way of describing the simulated effects of increased UV radiation is to say that the extra UV flux is equivalent to increasing the reactivity of the VOC mix. Figure 8 shows the diurnal curves of NO_2 and ozone in the Philadelphia simulations. Although the ultimate ozone peaks increase from about 0.11 ppb to only about 0.15 ppm, the shape of the ozone curve shows that ozone above or near the 0.12 ppm standard is reached much earlier in the day. Trajectory models such as that used here imply an equivalence in distance with time. Therefore, an occurrence of high ozone concentrations earlier in the day implies that more people will be exposed to episodic levels of ozone. Often the population density increases as the distance from the high initial sources of precursors decreases. Hence, the number of people exposed to episodic ozone levels may increase dramatically if the ozone peak occurs earlier in the day.

RECOMMENDATIONS

The results of our preliminary investigation suggest the following recommendations:

> The appropriate type of model for assessing effects on population exposure would be a grid model rather than a trajectory model. In addition to providing estimates of the increased number and hours of exposure, a grid model could provide estimates of changes in the horizontal spread of an episodic cloud that might result from global effects.

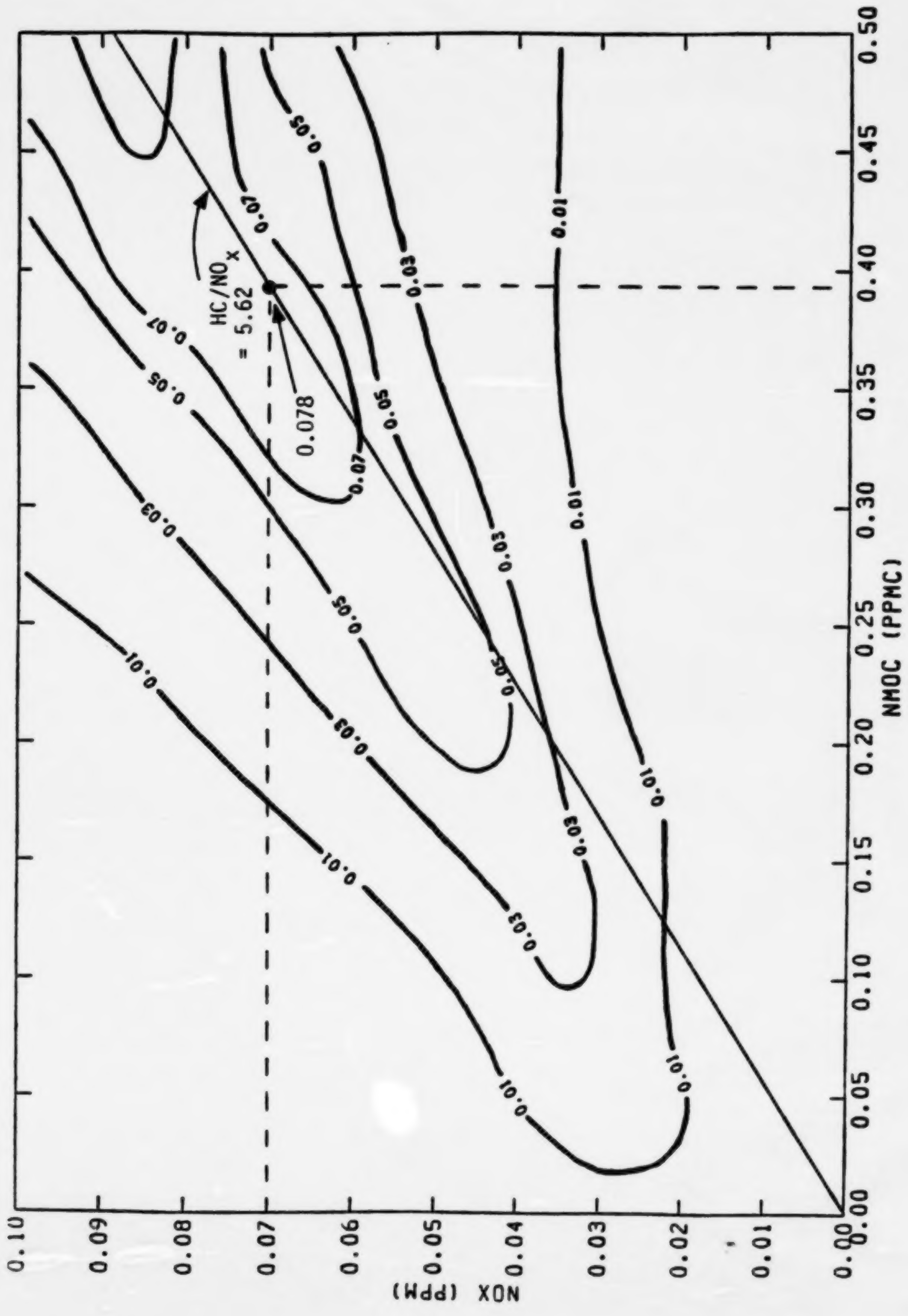

FIGURE 7. Difference isopleth for Nashville case (200 DU and 302 K minus 300 DU and 298 K).

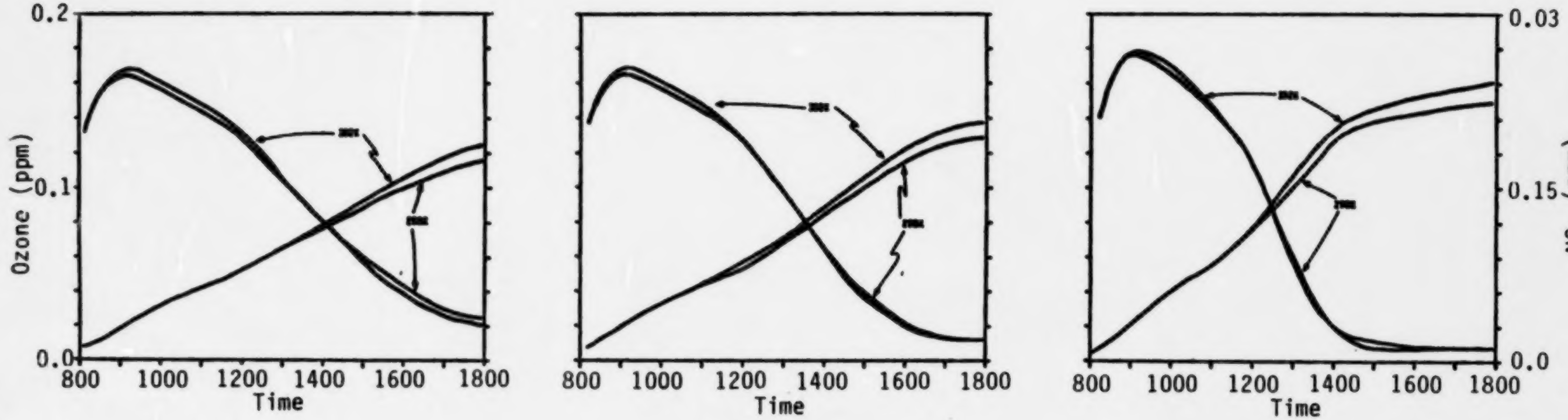

FIGURE 8. Diurnal ozone (increasing) and NO_2 (decreasing) traces for Philadelphia trajectory at 300, 250, and 200 DU.

Since the processes we have discussed represent different types of processes than those previously investigated (e.g. projected future increases in rates of reaction, rather than in emissions or boundary conditions), a larger number of test cases than have been thus far performed should be investigated. The study of future changes for additional urban scenarios should provide a clearer understanding of the atmospheric consequences of these processes and indicate a clearer range of expected changes in future control strategies.

In addition to the simulation of various single-day urban episodes, multi-day and long-term scenarios should be investigated. Increases in the urban photochemical production of ozone, combined with variations in the concentrations of species above the mixing layer due to global effects, could cause changes in nocturnal and next-day chemistry that are not obvious from single-day simulations. Species above the mixing layer can come from the free troposphere as well as from carryover from the same or upwind urban areas. Both free-troposphere and carryover species would likely be affected by changes in the stratospheric ozone layer or by global warming.

Also, since the calculations that should be performed for these simulations are relative to the Dobson number, differences in seasonal extremes of photochemical ozone production with respect to measured Dobson variation can be investigated for present and future scenarios. Present-day smog episodes may occur more frequently in the fall than in the spring, due to the seasonal shift in Dobson number.

Our investigation of the key reactions involved in the temperature effect indicated that PAN chemistry explains most of this effect; that is, increased ozone at the higher temperatures is offset by reductions in PAN concentrations. Since this preliminary study of the effect of temperature involved only the effect on chemistry, follow-on work should include the possible effects of increased temperature on emission rates and meteorology. Emissions from evaportive sources and emission sources related to additional use of air conditioning would obviously increase. Also, the frequency and intensity of smog episode meteorology would require further study to elucidate the effects of global warming on smog intensity.

REFERENCES

Bass, A. M., L. C. Glasgow, C. Miller, J. P., Jesson and D. L. Filken. 1980. Planet. Space Sci., 28:675.

Bahe, F. C., W. N. Marx, U. Schurath, and E. P. Roth. 1979. Determination of the absolute photolysis rate of ozone by sunlight, $O_3 + h\nu \rightarrow O(^1D) + O_2 (^1\Delta_g)$, at ground level. Atmos. Environ., 13:1515.

Bahe, F. C., H. Illner, W. N. Marx, U. Schurath, and P. Roth. 1979. "Messung der von Veränderungen der Ozonschicht stark abhängigen kurzwelligen Sonnenstrahlung. Gesellschaft für Strahlen- und Umweltforschung MBH, January 1979.

NASA. 1983. "Chemical Kinetics and Photochemical Data for Use in Stratospheric Modeling." National Aeronautics and Space Administration, Jet Propulsion Laboratory, California Institute of Technology, Pasadena, California.

Whitten, G. Z. 1983. The chemistry of smog formation: A review of current knowledge. Environ. International, 9:447-463.

Paper 8

Linkages between Climate Change and Acid Rain

by

Dennis Tirpak
U.S. Environmental Protection Agency

This paper was based upon the presentation made at the workshop.

Paper 8

Linkages Between
Global Climate Change
and Acid Rain

Dennis A. Tirpak

February, 1986

[The views expressed are those of the author.
They do not represent official views of the
U.S. Environmental Protection Agency.]

Linkages Between Global Climate Change and Acid Rain

Introduction

Two important problems facing the atmospheric and ecological science communities and government policy analysts are changes in the global atmosphere from increased CO_2 and trace gases and the acid rain phenomenon.

Acid rain and climate change from the greenhouse effect have independently evoked considerable attention and concern as issues of public policy, but the circumstances that have shaped the issues are quite similar. For example, in both cases the scientific community recognizes that large uncertainties in atmospheric modeling and complex chemical and physical interactions present challenges limiting their ability to provide answers to questions of causality, magnitude, and implications. Faced with the absence of clear signals, the policy community has walked a tightrope between the scientific uncertainties surrounding these issues on one side and the potentially large economic and environmental risks on the other side.

The Federal government has two separate programs to address these issues: i.e., the National Climate Program (NCP) and the National Acid Precipitation Assessment Program (NAPAP). While these programs have largely evolved along independent paths, they have in fact many scientific and policy issues in common which have not been heretofore explicity recognized. For example, will climate change enhance or negate the impacts of potential SO_2 controls?

Could natural source emissions of SO_2 and NO_x resulting from climate change partially offset potential anthropogenic source reductions? Could increased precipitation resulting from climate change alter the rainout of pollutants before they reach ecologically critical receptor areas? Will total deposition change? What will be the combined effects of changes in carbon, nitrogen and sulfur on forests, aquatic systems and materials? How will proposed solutions to the acid rain problem affect long-term climate trends.

The purpose of this paper is to examine some of the scientific connections between these problems and to speculate about their implications. It will also briefly explore the management and policy styles that have shaped the approach to these problems. The implications formed in this paper are that much more must be done to develop appropriate research and to assess the implications of climate change on acid rain policy. We must begin to chart a national research course that fully links these two issues.

FORCES SHAPING APPROACHES TO THE PROBLEMS

The National Climate Program (NCP) and the National Acid Precipitation Assessment Program (NAPAP) have their origins in different Congressional authorities. The former program was initiated as a result of the "National Climate Program Act of 1976 - Public Law 95-367" and the latter program had its origin in Public Law 96-294, "The Energy Security Act of 1980". As a result of these different laws, two distinct and independent management structures have evolved with different relationships within the Federal research establishment and the university community.

In the evolution of these programs, there has been an implicit assumption that the problems involve different time scales. The acid rain problem has been viewed as a problem that must be solved in the 1990's. This target date has evolved because of the perception that current ecological evidence suggests that a rapid solution is required and because of the implication that a major new control program would take at least a decade to implement. Beyond the 2000 - 2010 period, the emission modeling community has typically forecast that the number of older electric utility and industrial sources would decline thereby reducing emissions. In contrast the climate change problem has been viewed as a problem of the mid twenty-first century. This impression grows out of the manner in which large Global Circulation Models (GCMs) have been utilized to predict climate change. In many cases, scientists have used a doubled CO_2 atmosphere as a reference case when running Global Climate Models (GCMs). The general prediction for when CO_2 will double is the year 2050, plus or minus 20 years. This date often appears in the literature and the popular press as the target date for significant climate changes.

In addition, to temporal differences, the problems have generally been seen to have different spatial scales. Acid rain is recognized as a regional or subcontinental scale problem and climate change as a global issue. Model development activities have relected this difference in the specification of grid scales, boundary conditions and input data. For example, typical GCM's have grid scales of hundreds of miles, while long range transport models developed for source receptor studies have grids under 100 miles.

Finally, the nature of the effects have been perceived to be significantly different. For example, the principal concerns associated with acid rain are effects on aquatic ecosystems, forests and materials in sensitive regions or in areas with high deposition levels. The effects of changing climate touch all of the above plus impacts from sea level rise, on crop productivity, hydrology, and human health indeed almost every aspect of society.

The Time Dimension

There is uncertainty over how and when the earth will respond to increases in atmospheric carbon dioxide, CFCs and other trace gases. However, the "greenhouse" effect, i.e., the process by which these gases trap heat in the lower atmosphere, is one of the most well analyzed of the potential responses. This effect has been of interest because for several decades, scientists have measured the increases in atmospheric CO_2 at Mauna Loa Observatory. The steady rise in the annual average concentration of CO_2 from 316 ppm in 1959 to over 345 ppm in 1984 has generally been accepted as a global trend Keeling (1,2). For comparative purposes, various reports by Brewer (3), Raynaud (4) and Bojkov (5) have estimated CO_2 levels to be in the range of 260 to 280 ppm in the late nineteenth century.

The present rate of increase of atmospheric CO_2 (about 1.5 ppm per year), suggests that it will take more than 150 years for CO_2 to approximately double the preindustrial concentrations. But emission rates for CO_2 have not remained constant in the past and most assuredly will not in the future. The most important factors influencing emissions are the rate of population growth, the rate of worldwide energy consumption, and the fraction of total energy supplied by fossil fuel. For example, world energy consumption prior to 1973 grew at about 5 percent per year, but in response to rising energy prices, the growth of energy consumption has been reduced to about half the earlier rate according to a report of the World Energy Conference (6). A complete summary of CO_2 emission scenarios is presented by Perry (7) and by Ausbuel and Nordhaus (8). The most reasonable estimates of energy forecasts, suggest that growth rates for carbon releases to the year 2030 will most likely range between one and half to three percent per year. Wuebbles (9) described the corresponding atmospheric CO_2 concentrations in ppm empirically to be:

$$[CO_2] = 341.4 + 1.539 (t-to) \exp [0.00917 (t-to)]$$

where t is the time in years beyond 1983. This suggests that atmospheric CO_2 will double from preindustrial levels in the period between 2050 to 2060.

However, CO_2 is not the only gas capable of modifying future climate. Other trace gases, including the chlorofluorocarbons, nitrous oxides, methane, and carbon tetrachloride were first noted to be increasing in the atmosphere according to Lovelock, Singh, and Rasmussen as summarized by the World Meteorological Organization (10). For example, production of CFC-11 (CCl_3F) and CFC-12 (CCl_2F) is projected by Quinn (11) to increase by 7.2 percent and 3.6 percent annually while atmospheric concentrations are increasing by approximately 10 percent per year according to Cunnold (12, 13). The rate of increase in atmospheric methane has been estimated to be between one and two percent. The impact of these trace gases on mean global temperatures has been estimated by Ramanathan et. al. (14) to be roughly equivalent to that of CO_2. Predicting growth rates for all of these compounds beyond the year 2000 is difficult, but conservative estimates suggest that the result of changes in these gases will be to shift the equivalent impact of CO_2 doubling to the time period between 2030 and 2050. This perception of the new equivalent doubling time is recognized in a recent conference statement by the United Nations Environment Program, World Meteorological Organization and the International Committee of Scientific Unions (15) which notes that, "The role of greenhouse gases other than CO_2 in changing the climate is already about as important as that CO_2. If present trends continue, the combined concentrations of atmospheric CO_2 and other greenhouse gases would be equivalent to a doubling of CO_2 from pre-industrial levels possibly as early as the 2030's".

What then is the significance of a doubled CO_2 world and how is it related to the timeframe associated with the acid rain problem? In responding to these questions it must be recognized that a doubled CO_2 world has been fabricated and utilized by the climate research community as a bench mark for comparing results and estimating climate effects. Typically global climate models are run by initializing the models with a doubled CO_2 atmosphere, because simulations with small increases in CO_2 provide results which are difficult to interpret. The doubled CO_2 silulations, while often dramatic, provide only a snapshot of what the climate might be like at some future date. However, climatological changes resulting from increased emissions of CO_2, CFCs and other trace gases are taking place today, although not readily apparent. These changes will become increasingly evident according to Hansen (16), in the next 10-30 years, depending upon the degree of buffering provided by the oceans, the extent to which changes in cloud cover amplify or retard the warming and other factors. Thus significant climate changes are likely to occur in the time frame under consideration by Congress and other governments for implementing an acid rain strategy.

Second, there is a growing recognition that at least some aspects of the acid rain problem are long term processes. For example, acid deposition impacts on various soil systems and materials are most likely to have long term impacts which may not be easily quantified for decades. Impacts on many lake systems are described as extensive according to the results of recent surveys by the Environmental Protection Agency (17). In some cases, e.g., lakes in the southeast, the acidification process is thought to be associated with long term natural acid producing processes, while in other cases e.g. high elevation lakes, acidification may take place more rapidly. The acidity of individual watersheds appears to be a function of lake elevation, physical and geologic features and the percent of watershed covered with coniferous vegation. In contrast, current hypotheses on forest damage have not yet permitted a clear understanding about the rate or causes of forest decline in Germany and the United States. While the rate of damage appears to be high in Germany, one or more phenomenan, including air pollution and climate, may ultimately be proven to be the cause. The differences between the U.S. and German forest problems make guesses about the rate of decline speculative.

A third factor influencing current thinking about the time dimension of the two problems is the perception that the potential need for acid rain controls will diminish sometime between 2010-20 because older, more nonpolluting, utility and industrial sources will be replaced by lower emission sources of SO_2 and NO_x. However, there is a growing recognition that difficulties in obtaining suitable new sites, in raising capital, and in obtaining permits now make it more likely that utlities wil extend the lives of existing plants.

Recently, the Congressional Office of Technology Assessment (18) found that by the year 2000, nearly a third of the existing U.S. fossil generating capacity will be more than 30 years old, including about 700 coal fired units totaling nearly 40,000 MW. In the past, the benefits of new technology outweighed the benefits of plant improvements, but plants reaching 30 years of age over the next decade have attractive unit sizes (100 MW or larger) and performance (heat rates of 10,000 Btus/KWh). Extending the lives of such units at an anticipated capital of cost $200-400/KW is an extremely attractive opportunity for many utilities. In many instances plant improvements can also include up to 5 percent efficiency improvements and/or capacity upgrades of 5-10 percent. Current research efforts by the Electric Power Research

Institute and individual utilities may soon make it economically attractive to extend the lifetime of many plants from 40 to 60 years or more. In theory, there are few obstacles to extending the life of an existing plant almost indefinitely. As a result of this process, it is possible as shown in Figure (1) that many existing sources will continue to operate well beyond the 2010-20 time period.

In summary, some aspects of the acid rain problem are increasingly likely to be viewed as a long term ecological issue, rather than a problem requiring an "emergency response". It is also probable that efforts to extend the life of many existing utility plants will inadvertently extend the time period of concern about acid rain well into the next century. Hence, as shown in Figure (1) the sensitive timeframe for acid rain is sliding forward into the next century, while perceptions about when climate change will be important are shifting backward in the direction of the early decades of the next century.

CLIMATE IMPACTS ON ACID RAIN PROCESSES

The National Academy of Sciences reports that a doubling of the concentration of atmospheric CO_2 will raise the earth's global temperature by $3° \pm 1.5°C$. This estimate is based on predictions from different atmospheric models with the most complex being the general circulation models (GCMs). These models predict climate from first principles. They break the atmosphere into several layers which are represented by energy equations and components

FIGURE 1.

THE TIME DIMENSION

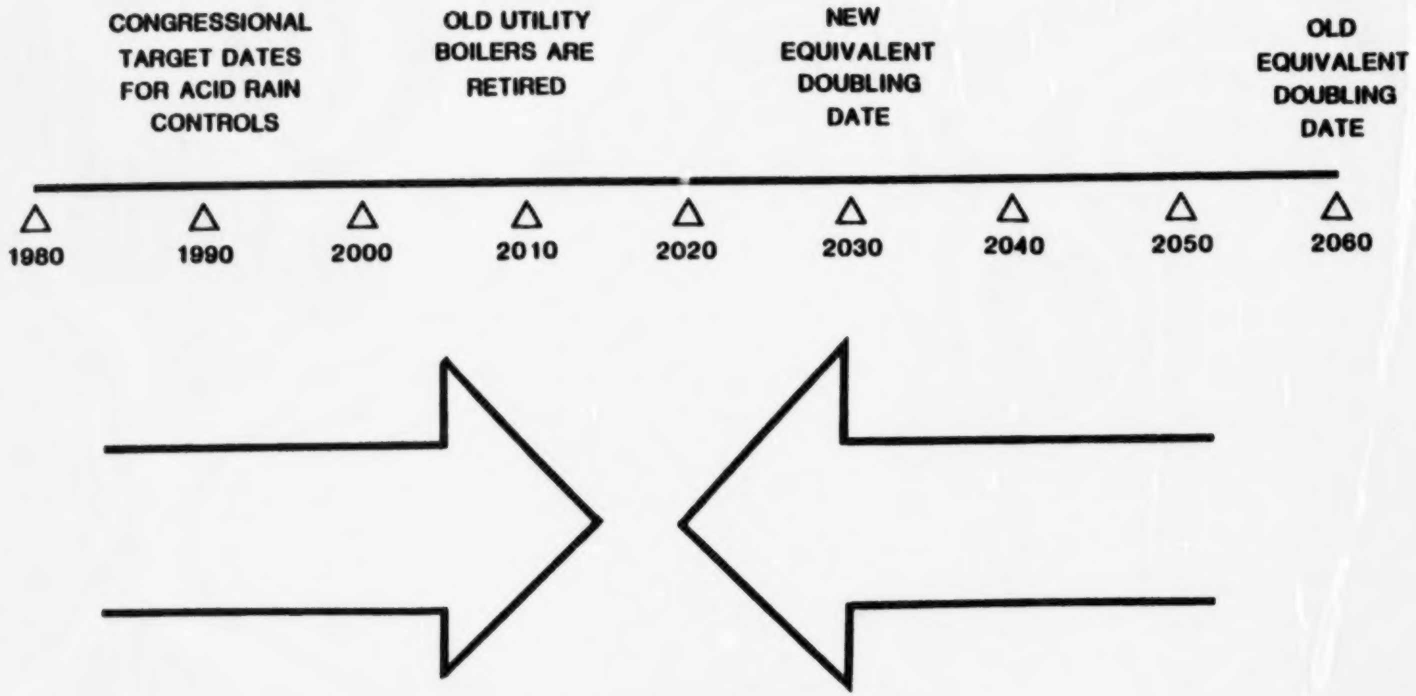
CONGRESSIONAL TARGET DATES FOR ACID RAIN CONTROLS
OLD UTILITY BOILERS ARE RETIRED
NEW EQUIVALENT DOUBLING DATE
OLD EQUIVALENT DOUBLING DATE
1980
1990
2000
2010
2020
2030
2040
2050
2060

THE ISSUES CONVERGE.....

- Plant Extensions Keep Emissions High Longer
- Trace Gases Bring About Climate Change Sooner
- Some Acidification Impacts May Take Longer

of the wind velocity. GCMs also solve radiation and transport equations to obtain heating or cooling in each layer. A review of modeling studies is provided in several reports including reports by the National Research Council (19) and Schlesinger (20).

The results of various modeling studies generally agree on two conclusions: (1) that the atmospheric surface air temperature will rise and that this temperature increase will be much greater in the polar regions than at equatorial latitudes, and (2) that there will be alterations in the hydrologic cycle including changes in regional precipitation and evaporation. Current models cannot predict with great specificity parameters such as humidity, groundwetness, cloud cover, windfields, and snow cover, but preliminary numerical experiments and sensitivity analyses yield insights into these topics.

For example, the work of Hansen (21) and Washington (22) suggest that there will be:

- Increases in zonal mean precipitation at all latitudes due to increases of available moisture evaporated from warmer oceans.
- Decreases in soil moisture in tropical and subtropical continental areas and increases at higher latitudes. At the mid latitudes the change depend on the season, for example, soils may be drier.

Table 1

Climate Change	Acid Rain Related Impact	Potential Implications
Increased Air Temperatures	Increased emissions of S, H^+ and NH_3, from soils	Anthropogenic emission reduction partially nullified
	More rapid oxidation of SO_2 and NO_x particularly in northern latitude	Decreased importance of long range transport of SO_4 and NO_3 ions
Increased Water Temperatures	Increased S emissions from oceans	Increased importance of marine sulfur emissions along coastal areas
Changed Precipitation	Changed scavenging rates for average deposition of SO^4 and NO_3	Altered importance of long-range sources
	Changed seasonal and annual average deposition of SO_4, NO_3, and H^+	Altered impacts on aquatic system and forests
	Changed winter snow pack	Altered vulnerability of aquatic life during spring snow melt
	Altered frequency of wet days	Changed degradation rates for materials
Increased Ground Wetness	Increased emissions of S, N, NH_3, from soils	Anthropogenic emission reductions partially nullified

Climate Change	Acid Rain Related Impacts	Potential Implication
Increased Humdity	Increased production of lightning generated NO_x	Anthropogenic NO_x emissions decreases partially nullified
Changed Cloud Cover at Different	Increased natural NO_x emissions from lightning	Changes in fertilization of high forests altitude

Table 1 (Cont'd)

Altitudes	Changes in cloudwater impaction at high altitudes	
	Changes in aqueous phase oxidation rates for SO_2 and NO_x	Altered significance of long range trans-changes
Increased Number of Days with Temperatures Above 0°C	Increased natural emissions Lengthened growing season	Changed food production
Increased number of days without frost	Changed significance of frost as a mechanism for forest damage	Potential decrease in forest impacts associated with forest and overfertilization by atmospheric nitrogen
Increased Dryness in interior U.S. and Seasonal Changes and Frequency of Drought	Increased importance of dry deposition	Altered impacts on aquatic systems and forests
	Increased amount of Ca and Mg dust/particles	
	Increased pH of rainfall	
Increased Atmospheric CO_2	Increased fertilization of forest and crops - potential changes in demand for other nutrients including S and N	May negate possible forest productivity declines in some areas

- Increases in humidity at most latitudes because of more evaporation.
- Increases in clouds depending on altitude in the mid latitudes.
- Changes in the strength and direction of major wind patterns because of decreases in the mid- and lower troposphere equator-to-pole temperature gradients.
- Increases in precipitation in the northern hemisphere during the winter.
- More persistent droughts in some areas of the south and eastern U.S. and more sequences of wetter than normal months in the northwest.
- Decreases in the number of days that the surface temperatures drops below 0°C

These results, while not a forecast, can be used to speculate about how climate change can affect acid deposition in the future. For this purpose, a representative list of potential climate changes and the associated acid deposition implications is presented in Table 1. While not comprehensive, it is apparent from Table 1 that climatological shifts have the potential to both enhance and negate the impacts of potential acid rain policies. In the following discussion, consideration is given to two climate parameters where there is agreement that significant changes will occur, namely temperature and precipitation.

TEMPERATURE EFFECTS ON ACID RAIN

The temperature increases projected to occur because of rises in CO2 and other trace gases will have significant atmospheric and ecological effects related to the acid rain problem. Among these effects are those associated with shifts in global wind patterns, changes chemical reaction rates in the troposphere and changes natural emission rates. Still other important changes related to future temperature increases are alterations in cloud cover and humidity and an extension of the growing season.

1) WIND PATTERNS

Winds are generated around the world because radiation from the sun is not equally distributed over the globe. As a result, temperature and pressure gradients are created between the equator and the poles and winds act to reduce these gradients. Changes in temperature at the equator and the poles associated with increased CO_2 and trace gases will alter these winds. For example, according to one GCM experiment by Washington, at the equivalent of doubled CO_2, there is a decrease in the strength of the mid-latitiude westerlies in the summer between 30°-60° latitude. It was also demonstrated that westerlies north of 60° latitude increase in strength in the winter because the greatest relative increases of lower tropospheric warming for doubled CO2 occur near the sea ice margins. While these results are not precise enough for decision making, there appear to be two kinds of implications which are important.

First, if windfields shifted significantly, the manner in which current source-receptor models are used to analyze the transport and deposition of sulfur species would have to be altered. Because current models are pretuned to historical data, their applicabilty to the 2010-2020 time period will be limited. To determine the importance of such changes a series of sensitivity studies using a range of windfields and other climatological parameters generated by several GMC's could be conducted.

Second, summertime stagnation episodes with elevated temperature and pollution levels have always been a focus of concern to the the air pollution community because of their important health and ecological impacts. For example, Altshuller (23) and others have demonstrated the relationship between increased sulfate concentrations and the summer months. He noted that increased summer sulfate concentrations appeared to be related to increases in regional emissions of SOx, to photochemically induced reaction processes and to a higher frequency of summer regional scale sulfate episodes. In the future, changes in the frequency and duration of these blocking events appear to be likely as demonstrated by Mearns, Katz and Schneider (24) who examined historical temperature data to determine that the number high temperature episodes was likely to increase with even a modest 1.9°C change in global temperature. If changes in the frequency and length of these epsiodes is demonstrated with additional analyses to be correct, traditional air pollution strategies for ozone, SO_2 and other pollutants will need to be reexamined.

2) ATMOSPHERIC REACTION RATES

A second important impact of elevated surface air temperatures concerns changes in the reaction rates of sulfur, nitrogen, and other compounds. It is generally known that these rates are a function of temperature, solar radiation, humidity, and cloud cover. However, the precise influence of changes in temperature on important reaction rates has been difficult to ascertain because smog chamber experiments are often conducted with a constant radiation flux and temperature. To overcome this difficulty, scientists have examined the net result of all these variables in both summer and winter field studies. The Environmental Protection Agency's Critical Assessment Review Papers (25) reports on such field studies. They indicate that upper level oxidation rates for SO_2 are over 12 percent hr-1 for midday, summer conditions and that average conversion rates are in the range of 3 to 5 percent hr-1 for summertime conditions. Other data indicate that wintertime conversion rates are less than 1 percent hr-1. This suggests that temperature along with other parameters plays an important role in the conversion of SO_2 to SO_4.

Another relationship between temperature and clouds is also important in determining reaction rates. It is known from the cloud physics literature that there is a tendency for cloud liquid water content to increase with temperture over a broad range of cloud types. There is also some evidence that clouds will increase with increases in CO_2 and trace gases, but there remains uncertainty about the net climate forcing induced by clouds. For example, Somerville and Remer (26) suggest the possibility that increased optical thickness may provide a negative feedback to stablize climate against other radiation forcings. However, it has been demonstrated by Gilliami and Wilson (27) that in-cloud conversion rates of SO_2 and SO_4 were on the order of 10 percent hr-1, a very significant rate compound to the average winter and summer rates. Moreover, when clouds come in contact with mountains, the net deposition of pollutants through direct interception is significant. For example, Scherbatskoy and Bliss (28), have shown that 82% of the total water available to three mountains (900-1200m) in Vermont came from clouds with a mean pH of 3.7 compared to 4.2 for rainfall. Assuming that climate change is accompanied by increasing cloud cover, aqueous conversion rates will increase, the potential for long range transport will diminish and the net wet deposition in high elevation forests will change. If the summertime is viewed as a surrogate for temperature, cloud cover, and other climate variables, then it can be postulated that climate change has a high potential to alter the transport, transformation and deposition of acidic species.

3) EMISSIONS

It is well recognized that fossil fuel combustion sources particularly oil and coal, are yet another important link between climate change and acid rain. Reductions in emissions from such sources through increased efficiency, energy conservation and use of alternative technologies have the potential to slow the rate of climate change and reduce acid rain concentrations. Natural sources of sulfur, however are generally considered to be small. Robinson (29) has characterized these emission to be less than ten percent of the estimated 12 to 15 Tg yr-1 of anthropogenic sulfur emissions. Among the important natural sources, sulfur from soils is estimated to be 0.23 Tg S yr-1. The basis for these estimates is derived from the work of Adams (30,31) who also points out that sulfur emission rates in tropical areas are probably at least an order of magnitude higher along areas such as the U.S. Gulf Coast than at 25°N. Adams noted that gaseous sulfur emissions from soils are generally considered to be related to temperature, moist climate, the fraction of high organic soils and latitude.

Climate change can alter these emission rates by changing temperature, soil moisture, percent of coastal marsh area, type of vegetation and the time period between frosts. Based on the results from Hansen, it can be assumed that the average daily temperature maximum for many locations in the U.S. will increase 5-7°F in a doubled CO_2 climate. Such a shift may be viewed as the equivalent of shifting the climate in current U.S. Gulf Coast States approximate 10° North. Using the results of Adam's latitudinal relationship, it is estimated that soil emission rates may increase nearly 10 times for the states in the southern third of the country. Even a conservative estimate of a fivefold increase in emission rates, taking into consideration the arid soil in the west, would mean that sulfur emissions from soils alone would be approximately 1.15 Tg S yr-1 or nearly ten percent of anthropogenic emissions. Moreover, most other natural emission sources of sulfur, nitrogen, and ammonia, e.g., oceanic sources and lightning are directly related to the changes in climate variables.

Precipitation

Climate forecasts, as generated by current GCM's, replicate measured precipitation at very aggregated levels. For example, Hansen states that the GISS model represents dry areas in the Sahara desert, off the west coast of North and South America and southwest Africa and in the lee of mountain chains such as the Andes and Himalayas. Similarly, regions of high rainfall are successfully reproduced along the equator, in the Amazon and African rainforests. Seasonal precipitation patterns reproduced by the model are also generally consistent although the poleward movement of precipitation in the summer over the U.S. was somewhat higher than measured.

Nonetheless, when current GCMs are utilized to predict precipitation patterns resulting from increased levels of CO_2, the results are less certain because of the coarse resolution of the modeling grids and because of the manner of parameterizing key processes. However, all the GCMs suggest substantial changes throughout the hydrologic cycle and even generally agree on impacts at a few locations i.e., a dryer interior of the U.S. particulary during the summer. For several locations in the U.S., the model of Hansen et. al., predicts changes in precipitation which vary from today's conditions by approximately +25% to -5% for doubled CO_2. Improvements to these models, will be forthcoming over the next decade as improved data sets are generated for clouds and the oceans and as more vigorous methods are developed to more accurately represent important processes.

Other investigators including Williams (32), Pittock and Salinger (33), and Jager and Kellogg (34) have studied the influence of global warming on regional precipitation patterns by comparing historical precipitation records in warm and cold years. An analysis of long-term temperature and precipatation data over the United States was conducted by Diaz and Qualye (35). More recently Rind and Libedeff (36) compared temperature and precipitation over the U.S. for the cold period of 1990 to 1920 and the warm period of 1940 to 1960. The global temperature difference between the two periods was about 0.3°C. They compared their results to those of Diaz and Quayle and the results were shown to be generally similar. Both analyses show a precipitation increase in the Southeast and Northwest and a precipitation decrease over the Midwest. Rind and Libedeff show a broad increase of approximately 10% over the eastern U.S. for a .27°C increase in global temperature. To assess these relationships in the acid sensitive Adirondack Park area, temperatures and precipitation were analyzed. The results in Figure 2, show the relationship between the ten year mean temperature and changes in precipitation for the period 1930 through 1980.

These temperature differences are relatively small compared to those projected for increased CO_2 and trace gases, but the results provide insights about the type of changes that may take place over the next few decades. Together with the results from GCM models these analyses

FIGURE 2.

Ten Year Mean
Temperature - Precipitation
Relationship for Adirondack Park Area

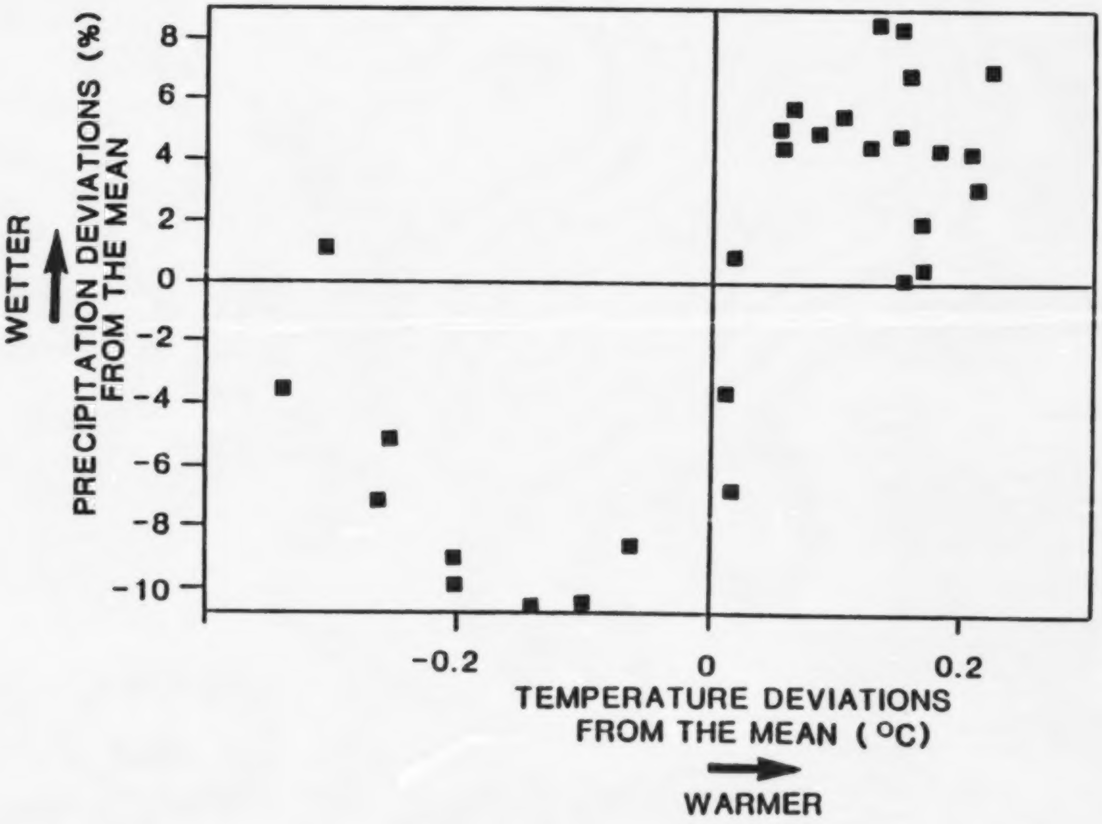

suggest that shifts in mean precipitation of ±10 percent or greater may easily be possible in the Northeast over the next few decades as wind patterns and other climate variables shift due to global warming. Changes in extreme precipitation events may even be greater.

RELATIONSHIP TO ACID DEPOSITION

These changes in annual precipitation could play a significant role in determining the form and amount of sulfur, nitrogen, hydrogen ions and other substances deposited in regions sensitive to acid rain. Changes in precipitation would affect the the concentration and total quantity of deposited acidic material and the ratio of wet to dry deposition. We know, for example, from work by Scott (37) that scavenging of sulfate aerosol is a function of precipitation rate and of storm type i.e. convective, warm/nonconvective, and cold storms. Still other investigators have conducted field studies at different distances from pollution sources and found that while very little scavenging takes place directly adjacent to plumes, an enhancement of sulfate and nitrate precipitation seems to occur at distances up to 200km presumably because precursors have more of an opportunity to react with atmospheric water vapor. Also from Likens (38), we know that when precipitation does occur, the highest concentrations of acidity generally occur with the lowest amounts of precipitation, while total deposition generally increases with increasing amounts of precipitation.

In summary, changes in the location and quantity of precipitation likely to be induced by global warming will affect the chemical composition of important substances deposited in sensitive regions. The potential also exists, if regional precipitation patterns shift relative to major source regions, to washout pollutants before reaching sensitive areas or to increase the chance that pollutants will be dry deposited. However, total deposition of acidic material may not be reduced in sensitive regions, if increases due to changes in the frequency and intensity of precipitation balance out losses due to increased scavenging between sources and receptors.

Impacts of Precipitation on Sensitive Lakes

The potential impact of changes in precipitation on sensitive lakes can be examined by utilizing a model to predict changes in alkalinity. For this purpose, the Adirondack Lakes Region was analyzed using assumed changes in precipitation as suggested by historical climate relationships and forecasts. The model was developed by Schnoor (39) and modified by Hoogendyke and Kaplan (40) to support analyses of how changes in runoff, evapotranspiration, and sulfur deposition would effect future lake chemistry. The Schnoor model is represented by the equation:

$$\text{akalinity} = \frac{I}{Q}\;\frac{k_h\left(\frac{L_{acy}}{L_{ref}}\right)^m + k_o}{R\cdot 0.1} - L_{acy}$$

$\frac{I}{Q}$ = inflow to outflow ratio (evapotranspiration concentration factor)

k_h = weathering rate constant for acid hydrolysis

k_o = weathering rate constant in the absence of free acidity

L_{acy} = total acidity input

L_{ref} = reference acidity

m = fractional reaction order constant

R = precipitation rate

0.1 = units conversion factor

The application of this model requires various assumptions about baseline conditions and the processes of acidification. For example, in this application, an Adirondack Lake data set of approximately 600 lakes was utilized and assumed to apply to all 2,865 lakes in the region, although the applicability of the model is limited for brown colored water with high organic acid concentrations. According to Baker and Harvey (40), approximately 37 percent of the high elevation Adirondack lakes may be in this category.

Other key assumptions include the selection of the existing mean annual precipitation to be 100 cm/yr, a reference acidity level corresponding to a natural background of 5 kg/HA and a current acidity of 40 Kg/HA. The evapotranspiration factor was held constant at 1.2 although it can be expected that it may vary with wind, temperature, rainfall, vegetation and soil moisture. Hence, the analysis should be viewed with caution and should not be considered a forecast of future lake status.

With these caveats in mind, it is useful to examine the results depicted in Table 2. The results demonstrate that rainfall is an important variable which must be accounted for in order to assure the efficacy of future acid rain policies. The results for existing deposition and rainfall suggest that up to 1,019 lakes or (35 percent) are currently below a pH 5.5. This is in close agreement with Baker and Harvey who provide lake survey data indicating that 34 percent of the lakes are below pH 5.5. Table 2 also notes that the number of lakes with a pH of less than 5.5 changes from 1,019 to 724 when sulfur deposition is decreased and from 40 Kg/HA to 30 Kg/HA and rainfall is constant. When rainfall is increased by 25 cm/yr and sulfur held constant the number of lakes less than pH 5.5 change from 1,019 to 787. Finally, if rainfall is increased by 25 cm and deposition increased to 50 Kg/HA, the number of lakes less than 5.5 pH is constant at 1,019.

Table 2

Estimated Number of Adirondack Lakes with pH < 5.5 for Alternative Amounts of Rainfall and Sulfur Deposition

Projected Mean Annual Rainfall (cm)	Alternative Future Sulfur Deposition Levels (Kg/HA)	No of Lakes <5.5 pH
95	40	1076
100	40	1019
110	40	920
125	40	787
95	30	774
100	30	724
110	30	637
125	30	544
95	50	1308
100	50	1254
110	50	1156
125	50	1019

While simplified these results suggest that uncertainties in future climate may be an important factor in attempting to predict the impact of acid rain control strategies on lake systems. Moreover, it can be anticipated that forest and material effects will also be a function of climate variables. How significant a factor climatology will be in altering acid rain impacts must await the development of improved lake, forest and material models. However, it is apparent that current efforts to reduce uncertainty in long range transport models, air pollution data bases and lake models may be of little value, in the absense of corresponding efforts to understand the impact of future climate.

THE MANAGEMENT STYLES

The NCP and NAPAP programs had very different origins and consequently evolved significantly different budgetary and management processes. Table 3 presents the funding history for both programs (41). The National Climate Program was assembled from then existing programs in several agencies particularly NOAA, NSF, DOE and NASA. It was conceived at a time when CO_2 emissions from energy sources were viewed as a significant source of climate change. The NCPO was given a mandate to develop an integrated budget, but the traditionally has acted simply to provide coordination among the Federal agencies. It has developed broad guidance while leaving

Table 3

Funding history
for the National Climate Program (NCP)
and the National Acid Precipitation Assessment Program (NAPAP)

(Million $)

Fiscal Year	NCP	NAPAP
1980	121	11
1981	134	13
1982	141	18
1983	140	23
1984	145	27
1985	145	62
1986*	145	80

Estimated

individual agencies to prepare and defend specific parts of their programs. The NCP has also avoided direct management of the program, preferring to serve in a coordinating role when key issues of importance warranted attention, such as whether to support major programs to measure clouds or develop improved data on oceanographic parameters.

In contrast, the National Acid Precipitation Assessment Program began with very limited resources, but has grown considerably, i.e., from approximately $11 million in 1980 to over $80 million in the FY-86 budget. The program has three cochairmen from NOAA, DOA and EPA. The NAPAP had few of the traditions that marked climate research activities and as a result developed an independent budget and research planning process. The Office of Management and Budget encouraged and supported this process as a means of obtaining advice to supplement the normal agency budget processes. Consequently, the NAPAP made vigorous attempts from its inception to establish budget priorities and to ensure that all agencies adhered to budgeting decisions. Finally, the Executive Committee of NAPAP closely manages activities on a week to week basis. Program decisions are continously reviewed to correspond to newly emerging scientific information. NAPAP's coordinating activities have generally focused on other air pollution programs.

As a result of these different beginnings and contrasting management approaches the programs have developed significantly different approaches for planning research, conducting business and supporting participants. From the discussion above it is apparent that increased coordination between the NCP and NAPAP will become increasingly important in the future. The scientific links between the programs and the need to optimize resources for tropospheric chemistry and climatological research will lead this process. The challenge before the federal agencies is to assess how this need can be accommodated in an innovative manner and without losing sight of the framework and specific objectives that have shaped each program.

SUMMARY

An examination of the time horizons of importance to both the acid rain and climate change problems suggests that these two issues can no longer be viewed in isolation. This paper, has demonstrated that our understanding of emissions, atmospheric reaction rates, pollutant transport and acid lake effects are likely to be influenced by long term changes in climate. Moreover, it is very likely that as we attempt to unravel the causes of forest and material damage that additional links between climate and acid rain will probably become apparent. The outgrowth of this recognition must not only be a more holistic approach to the conduct of acid rain and global climate research, but also other troposheric and stratospheric programs. In a broader context. These issues are only symbolic of the broader relationship between general air pollution problems and changes in the global atmosphere. For example, there are important reactions between CO, NO_x, CH_4, OH, and other oxidizing agents that control local tropospheric ozone levels and directly or indirectly affect the radiation balance of the globe. Similarly, fine particulates affect regional visibility and may influence global climate change.

In fifty years, the earth will be very different from what it is today. Most likely, it will have higher CO_2 concentrations, different precipitation patterns, higher temperatures and probably higher concentrations of other atmospheric chemicals. Any single one of these changes may be of little concern, but in combination it is safe to say that the atmosphere and climate of the next century may make the world a very different place. How can we prepare for this future? First, we can begin to plan long term experiments that will assess the synergistic impacts on the atmosphere and climate. Second, we can conduct studies of future atmospheric effects on health, ecology and welfare.

In the near term, several steps specific to acid rain and climate should be considered:

1) A detailed assessment of both the ecological and atmospheric impacts of climate change on acid rain should be

undertaken to precisely define the synergistic links between these issues. Ultimately other pollution problems could be added to this analysis.

2) The acid rain and the climate change science communities should join together to define and develop potential climate change scenarios with significance to the acid rain community. Once developed these scenarios should be used in long range transport models to further our understanding of source-receptor relationships and in the design of acid rain effect studies.

3) The global climate community must begin to generate and make available data which is useful to acid rain researchers. It is suggested that climate models be run with 1 1/4 x CO_2 and 1 1/2 x CO_2, and that greater attention be paid to the use of smaller grid sizes in order to improve regional predictions. Ultimately, as technology and computational techniques improve, it may be possible to nestle improved chemistry models within global circulation models.

4) Finally, the managements of both NAPAP and NCP should join together to integrate these two important national programs and where appropriate conduct joint experiments. The managements must assure that the resources are allocated in a mutually supportive manner and that the appropriate institutional mechanisms exist to foster cooperation between scientists in both programs.

ACKNOWLEDGEMENTS: The author wishes to acknowledge the cooperation of M. Gibbs, and C. Hoogendyk in the preparation of this paper and the many useful suggestions made by colleagues on the Acid Deposition Assessment Staff and Strategic Studies Staff of the U.S. Environmental Protection Agency in Washington, D.C. The author appreciates the assistance of Deloris Swann in the preparation of this manuscript.

REFERENCES

1. C.D. Keeling, R.B. Bascaston, A.E. Bainbridge, C.A. Ekdahl, P.R. Guenther, L.S. Waterman, and J.F.S. Chin, "Atmospheric Carbon Dioxide Variation at Mauna Loa Observatory, Hawaii," Tellus 28:538-551, 1976.

2. R.B. Bascaston and C.D. Keeling, "Atmospheric Carbon Dioxide Concentration and Observed Airborne Fraction," pp. 103-112 in B. Bolin, ed., Carbon Cycle Modeling, Scope 16, John Wiley and Sons, New York, 1981.

3. P.G. Brewer, 1983," Past and Future Atmospheric Concentrations of Carbon Dioxide," p. 186-188 in "Changing Climate" National Academy Press, Washington, D.C.

4. D. Raynaud and J.M. Barnola, "An Antararctic Ice Core Reveals CO_2 variations over the Past Few Centuries," p. 309 Nature Vol 315, May 23, 1985.

5. R.J. Bojkov, ed., World Meteorological Organization, p. 42 Report No. 10. Project on Research and Monitoring of Atmospheric CO_2. 1983, Geneva.

6. World Energy Conference, World Energy Resources, 1985-2020. (New York: IPC Science and Technology Press), 1978.

7. A.M. Perry, "Carbon Dioxide Production Scenarios," pp. 337-363 in W.C. Clark, ed., Carbon Dioxide Review: Oxford University Press, New York, 1982.

8. J. Ausbuel and W.D. Nordaus, "A Review of Estimates of Future Carbon Dioxide Emissions", p. 153-185, in Changing Climate, National Academy Press, Washington, D.C., 1983.

9. D. Wuebbles, M. MacCracken and F. Luther, "A Proposed Reference Set of Scenarios for Radiatively Active Atmospheric Constituents", U.S. Department of Energy Report TR015, October, 1984.

10. World Meteorological Organization - Global Ozone Research and Monitoring Project - Report No. 11, "The Stratosphere, 1981, Theory and Measurements", Geneva, 1981.

11. T.H. Quinn, et. al. "Projected Use, Emissions, and Banks of Potential Ozone Dupleting Substances", Rand, Inc., Draft Report August, 1985.

12. Cunnold, D.M., et. al., 1983a. "The Atmospheric Lifetime Experiment. 3. Lifetime Methodology and Application to Three Years of $CFCl_3$ Data." Journal of Geophysical Research, 88:C13:8401-14.

13. Cunnold, D.M. et. al., 1983b. "The Atmospheric Lifetime Experiment. 4. Results for CF_2Cl_2 based on three years data." Journal of Geophysical Research, 88:C13:8401-14.

14. Ramanathan, V. et. al., 1985 "Trace Gas Trends and Their Potential Role in Climate Change," Journal of Geophysical Research, 85:D3:5547-66.

15. United Nations Environment Program, World Meteorological Organization and International Committee of Scientitic Unions, Conference Statement, Villach, Austria, 1985.

16. Hansen, et. al., "Evidence for Future Warnming: How Larger and When", Presented at "CO_2 Conference of the National Forest Products Association", June 25-27, 1984, Boulder, CO.

17. R.A. Linthurst et. al. "Chemical Characteristics of Lake Populations the Eastern United States", U.S. Environment Protection Agency, 1986 (In Press).

18. "New Electric Power Technologies," July 1985, Congress of the United States, Office of Technology Assessment, Report OTA-E-247, Washington, D.C.

19. National Research Council, Carbon Dioxide and Climate: A Second Assessment, p. 72, National Academy of Sciences, Washington, D.C. 1982.

20. M.E. Schlesinger, "A Review of Climate Model Simulations of CO_2-Induced Climate Change," Report No. 41, Climate Research Institute and Department of Atmospheric Sciences, Oregon State University, 1983.

21. J. Hansen, G. Russell, D. Rind, P. Stone, A Lacis, S. Lebedeff, R. Ruedy and L. Travis, "Efficient Three-Demensional Global Models for Climate Studies: Models I and II, pp. 609-662, Monthly Weather Review, Vol. III, 1983.

22. W. M. Washington, and G. A. Meehl, "Seasonal Cycle Experiment on the Climate Sensitivity Due to Doubling of CO_2 with an Atmospheric General Ciruclation Model Coupled to a Simple Mixed Layer Ocean Model", National Center for Atomspheric Research, March 1984.

23. A.P. Altshuller, "Seasonal and Episodic Trents in Sulfate Concentrations (1963-1978) in the Eastern United States", p. 1337-48, Environmental Science and Technology, Vol. 14, No. 11, November 1980.

24. L. Mearns, R. Katz and S. Schneider, "Extreme High Temperature Events: Changes in their Probabilities with Changes in Mean Temperature", Journal of Climate and Applied Meteorology

25. E. Robinson and J. B. Homalya, 1983. "Natural and Anthropogenic Emission Sources, Chapter A-2, in A. P. Altshuller and R. A. Linthurst, "The Acidic Deposition Phenomenon and its Effects: Critical Assessment Review Papers," Washington, D.C., U.S. EPA, No. 600/8-84-016AF, July, 1984.

26. R.C. Somerville and L.A. Remer, "Cloud Optical Thickness Feedback in the CO_2 Climate Problem", p. 9668-72, Journal of Geophysical Research, Vol. 89, No. D6, October 20, 1984.

27. N.V. Gilliani, Transport Processes", Chapter A-3, in "The Acidic Deposition Phenomenon and Its Effects: Critical Assessment Review Papers", Washington, D.C. U.S. EPA No. 600/8-84-016 AF, July, 1984.

28. T. Scherbatskoy and M. Bliss, "Occurence of Acidic Rain and Cloud Water in High - Elevation Ecosystems in The Green Mountains of Vermont", p. 449-463, in P.J. Samson editor. The Meteorology of Acidic Deposition "Proceeding of APCA Specialty Conference Hartford, Conn. 16-19 Oct. 1983 p. 449-463.

29. E. Robinson, "National and Anthropogemic Emission Sources" in Chapter A-2, in "The Acidic Deposition Phenomenon and Its Effects - Critical Assessment Review Papers", U.S. Environmental Protection Agency, No. 600/8-83-016AF, July, 1984.

30. D.F. Adams, et. al., "Bigenic Sulfur Source Strengths", Presented of 74th Annual Meeting of the Air Pollution Control Association, Philadelphia, PA., June, 1981.

31. D.F. Adams, et. al." Biogenic Sulfur Source Strengths", p. 1493-98, Environmental Science and Technology. No. 15, 1981.

32. J. Williams, "Anomalies in Temperature and Rain During Warm Arctic Seasons as a Guide to the Formulation of Climate Scenarios", p. 249-60, Climate Change, Vol. 2, 1980.

33. A. Pittock and M. Salinger, "Towards Regional Scenarios for a CO_2-Warmed Earth", p. 23-39. Climate Change Vol. 4, 1982.

34. J. Jager and W. Kellogg, "Anomalies in Temperature and Rainfall During Warm Arctic Seasons," p. 39-60, Climate Change Vol. 15, 1983.

35. M.F. Diaz and R.G. Qualye, "The Climate in the United States since 1995: Spatial and Temporal Changes p. 246-66, Monthly Weather

36. Rind and S. Libedeff," Potential climate Impacts of Increasing Atmospheric CO_2 with Emphasis on Water Availability and Hydrology in the United Stated", U.S. Environmental Protection Agency, Office of Policy Analysis April, 1984.

37. B.C. Scott, "Parameterization of sulfate Removal by Precipitation", p. 1375-89, Journal of Applied Meteorology, No. 17, 1978.

38. G.E. Likens, et.al. "Long-Term Trends in Precipitation Chemistry at Hubbard Brook, New Hampshire, p. 2641-47, Atmospheric Environmental Vol. 18. No. 12, 1984.

39. J. L. Schnoor and W. Stumm, "Acidification of Aquatic and Terrestrial Systems", in Chemical Processes in Lakes. Wiley Interscience, New York, 1984.

40. C. Hoogendyk and E. Kaplan, "Aquaffects: Aquatic Effects Simulator", Brookhaven National Laboratory, February, 1985.

41. J. Baker and T.B. Harvey, "Critique of Acid Lakes and Fish Polulation Status in the Adirondack Region of New York State", NSPAS Project E3-25 North Carolina State University, December, 1984.

42. "National Climate Program - FY 1984-1986, Interim Plan" Prepared by National Climate Program Office, NOAA, June 1985.

APPENDICES

Appendix A: Workshop Agenda
Appendix B: Workshop Attendees

Global Atmospheric Change and EPA Planning

November 13–14, 1985

Agenda

Day 1 : 10:00 - 5:30

Morning

10:00–10:05	Welcome and Introduction	A. Ellison, EPA/ASRL
10:05–10:10	Meeting Purpose	H. Jeffries, UNC
10:15–10:20	OAQPS Overview	J. Weigold, EPA/OAQPS
10:20–10:30	Office of Policy Analysis Overview	R. Morgenstern, EPA/OPA
10:30–11:00	Atmospheric Change Overview	J. Hoffman, EPA/OPPE
11:00–11:30	Emissions and Atmospheric Concentrations	R. Cicerone, NCAR
11:30–12:00	Evidence for a Greenhouse Effect	J. Perry, NAS

Lunch : 12:00 - 1:30

Afternoon

1:30–2:15	OAQPS Perspective	G. Emison, OQAPS
2:15–3:00	Past and Future Changes in Climate	D. Rind, GISS

Break : 3:00 - 3:15

3:15–4:00	Depletion of Stratospheric Ozone	R. Stolarski, NASA/GSFC
4:00–4:45	Relationships among CO, NO_x, CH_4, and HO	A. Thompson, NASA/GSFC
4:45–5:30	Tropospheric Ozone	J. Logan, Harvard

Dinner

Day 2 : 8:00 - 12:30

Morning

8:00– 8:30	Discussion	
8:30– 9:00	Stratospheric/Tropospheric Ozone	D. Wuebbles, LLNL
9:00– 9:45	Effects of Increased UV on Urban Ozone	G. Whitten, SAI

Break : 9:45 - 10:15

10:15–10:45	Linkages Between Climate Change and Acid Rain	D. Tirpak, EPA/OPPE
10:45–11:00	Overview of Stratospheric Ozone Activities	J. Hoffman, EPA/OPPE
11:00–12:30	Science/Policy Panel Discussion	Leader: M. McElroy, Harvard

Main Meeting Adjourned

Afternoon : 2:00 - 4:00

Steering Committee Meeting

APPENDIX B

EPA Workshop on Global Atmospheric Changes and EPA Planning Workshop Attendees

Mr. Frederick Allen
Office of Policy, Planning, and Evaluation (PM-221)
U.S. Environmental Protection Agency
401 M Street, SW
Washington, DC 20460
(202) 382-4012

Mr. John D. Bachmann
Office of Air Quality Planning and Standards (MD-12)
U.S. Environmental Protection Agency
Research Triangle Park, NC 27711
(919) 541-5531

Mr. Charles Brunot
Office of Research and Development (RD-680)
U.S. Environmental Protection Agency
401 M Street, SW
Washington, DC 20460
(202) 382-5776

Dr. Joseph J. Bufalini
Atmospheric Sciences Research Laboratory (MD-84)
U.S. Environmental Protection Agency
Research Triangle Park, NC 27711
(919) 541-2422

Mr. Frank Camm
The Rand Corporation
2100 M Street, NW
Washington, DC 20037-1270
(202) 296-5000

Dr. Ralph Cicerone
National Center for Atmospheric Research
P.O. Box 3000
Boulder, CO 80307
(303) 497-1434

Mr. Roger Cortesi
Office of Research and Development (RD-675)
U.S. Environmental Protection Agency
401 M Street, SW
Washington, DC 20460
(202) 382-5750

Mr. Alexander Cristofaro
Office of Policy, Planning, and Evaluation (PM-221)
U.S. Environmental Protection Agency
401 M Street, SW
Washington, DC 20460
(202) 382-5490

Dr. Larry T. Cupitt
Atmospheric Sciences Research Laboratory (MD-84)
U.S. Environmental Protection Agency
Research Triangle Park, NC 27711
(919) 541-2878

Dr. Basil Dimitriades
Atmospheric Sciences Research Laboratory (MD-59)
U.S. Environmental Protection Agency
Research Triangle Park, NC 27711
(919) 541-2706

Dr. Marcia C. Dodge
Atmospheric Sciences Research Laboratory (MD-84)
U.S. Environmental Protection Agency
Research Triangle Park, NC 27711
(919) 541-2374

Dr. Alfred H. Ellison, Director
Atmospheric Sciences Research Laboratory (MD-59)
U.S. Environmental Protection Agency
Research Triangle Park, NC 27711
(919) 541-2191

Mr. Gary Evans
Environmental Monitoring and Support Laboratory
(MD-56)
U.S. Environmental Protection Agency
Research Triangle Park, NC 27711
(919) 541-3124

Mr. Gerald Emison, Director
Office of Air Quality Planning and Standards (MD-10)
U.S. Environmental Protection Agency
Research Triangle Park, NC 27711
(919) 541-5615

Mr. Bruce W. Gay, Jr.
Atmospheric Sciences Research Laboratory (MD-84)
U.S. Environmental Protection Agency
Research Triangle Park, NC 27711
(919) 541-2830

Dr. Lester D. Grant, Director
Environmental Criteria and Assessment Office (MD-52)
U.S. Environmental Protection Agency
Research Triangle Park, NC 27711
(919) 541-4173

Mr. Mark Greenberg
Environmental Criteria and Assessment Office (MD-52)
U.S. Environmental Protection Agency
Research Triangle Park, NC 27711
(919) 541-4156

Mr. John S. Hoffman
Office of Policy, Planning, and Evaluation (PM-219)
U.S. Environmental Protection Agency
401 M Street, SW
Washington, DC 20460
(202) 382-4036

Dr. Harvey Jeffries, Professor
Room 120, Rosenau Hall 201-H
The School of Public Health
University of North Carolina
Chapel Hill, NC 27514
(919) 966-5451

Mr. Bruce Jordan
Office of Air Quality Planning and Standards (MD-12)
U.S. Environmental Protection Agency
Research Triangle Park, NC 27711
(919) 541-5655

Mr. William H. Keith
Office of Research and Development (RD-680)
U.S. Environmental Protection Agency
401 M Street, SW
Washington, DC 20460
(202) 382-5716

Dr. Robert E. Lee
Environmental Monitoring and Support Laboratory
(MD-78A)
U.S. Enviromental Protection Agency
Research Triangle Park, NC 27711
(919) 541-2454

Dr. Jennifer Logan
Harvard University
108 Pierce Hall
29 Oxford Street
Cambridge, MA 02138
(617) 495-4582

Mr. James Losey
Office of International Activities (A-106)
U.S. Environmental Protection Agency
401 M Street, SW
Washington, DC 20460
(202) 382-4894

Dr. Michael McElroy
Harvard University
Room 100-E Pierce Hall
29 Oxford Street
Cambridge, MA 02138
(617) 495-4359

Dr. Joe McSorley
Air & Energy Engineering Research Laboratory
(MD-65)
U.S. Environmental Protection Agency
Research Triangle Park, NC 27711
(919) 541-2920

Mr. Richard D. Morgenstern
Office of Policy, Planning, and Evaluation (PM-221)
U.S. Environmental Protection Agency
401 M Street, SW
Washington, DC 20460
(202) 382-4034

Dr. Deran Pashayan
Office of Research and Development (RD-680)
U.S. Environmental Protection Agency
401 M Street, SW
Washington, DC 20460
(202) 382-5776

Dr. John S. Perry (JH-810)
Board on Atmospheric Sciences and Climate
National Academy of Sciences
2101 Constitution Avenue, NW
Washington, DC 20418-0001
(202) 334-3517

Dr. Francis Pooler
Atmospheric Sciences Research Laboratory (MD-80)
U.S. Environmental Protection Agency
Research Triangle Park, NC 27711
(919) 541-4551

Dr. David Rind
Goddard Institute for Space Studies
2880 Broadway
New York, NY 10025
(212) 678-5593

Mr. Steve Seidel
Office of Policy, Planning, and Evaluation (PM-220)
U.S. Environmental Protection Agency
401 M Street, SW
Washington, DC 20460
(202) 475-8825

Dr. Jack H. Shreffler
Atmospheric Sciences Research Laboratory (MD-59)
U.S. Environmental Protection Agency
Research Triangle Park, NC 27711
(919) 541-2191

Dr. Bernard J. Steigerwald
Office of Air Quality Planning and Standards (MD-10)
U.S. Environmental Protection Agency
Research Triangle Park, NC 27711
(919) 541-5555

Dr. Richard Stolarski
NASA/GSFC
Code 616
Greenbelt, MD 20771
(301) 344-9111

Dr. Anne Thompson
NASA/GSFC
Code 616
Greenbelt, MD 20771
(301) 344-0834

Mr. Joseph Tikvart
Office of Air Quality Planning and Standards (MD-14)
U.S. Environmental Protection Agency
Research Triangle Park, NC 27711
(919) 541-5512

Mr. Dennis Tirpak
Office of Policy, Planning, and Evaluation (PM-220)
U.S. Environmental Protection Agency
401 M Street, SW
Washington, DC 20460
(202) 382-2724

Mr. John C. Topping
Office of Air and Radiation (ANR-443)
U.S. Environmental Protection Agency
401 M Street, SW
Washington, DC 20460
(202) 382-7403

Mr. James Weigold
Office of Air Quality Planning and Standards (MD-11)
U.S. Environmental Protection Agency
Research Triangle Park, NC 27711
(919) 541-5641

Mr. Stephen Weil
Office of Policy, Planning, and Evaluation (PM-223)
U.S. Environmental Protection Agency
401 M Street, SW
Washington, DC 20460
(202) 475-8661

Dr. Gary Whitten
Systems Applications, Inc.
101 Lucas Valley Road
San Rafael, CA 94903
(415) 472-4011

Dr. William E. Wilson
Atmospheric Sciences Research Laboratory (MD-84)
U.S. Environmental Protection Agency
Research Triangle Park, NC 27711
(919) 541-2251

Mr. Dwain L. Winters
Office of Air and Radiation (ANR-445)
U.S. Environmental Protection Agency
401 M Street, SW
Washington, DC 20460
(202) 382-7407

Dr. Herbert L. Wiser
Office of Air and Radiation (ANR-443)
U.S. Environmental Protection Agency
401 M Street, SW
Washington, DC 20460
(202) 382-5750

Dr. Don Wuebbles
Lawrence Livermore National Laboratory
P.O. Box 808
Mail Code L-262
Livermore, CA 94550
(415) 422-1845

Dr. Larry J. Zaragoza
Office of Air Quality Planning and Standards (MD-12)
U.S. Environmental Protection Agency
Research Triangle Park, NC 27711
(919) 541-5519